Development studies based on Kampo theories for new treatment strategies and drug discoveries

(漢方薬の理論に立脚した新しい治療戦略と薬開発に関する研究)

2022 年度

富山大学

生体情報システム科学専攻

趙　慶峰

Content

Introduction

In traditional medicine, both Chinese traditional medicine and Japanese Kampo medicine share the same basic ideas. " Huangdi Neijing (皇帝内経)" describes the health cure lesson, the "Shanghan Lun (傷寒論): SL" discusses medical treatments for extrinsic pathogenesis (viruses and bacteria; the possibility of adaptation for COVID-19), and the "Jingui Yaolüe (金匱要略): JY" shows medical treatment for intrinsic pathogenesis. What both Chinese medicine and Kampo medicine have in common is that they all use "herbal medicines" obtained from the natural world and combine herbal medicines to bring therapeutic effects. There are many classical writings on crude drugs starting with "Shin-nou Honzou Kyo; Shennong Ben Cao Jing (神農本草経)" is the basis of these medicines. Furthermore, it is also common that the diagnosis is based on individual medical conditions.

Through research-based modern medical analysis methods, many active compounds from herbal medicine have been discovered and used as clinical drugs. It can be said that traditional medicine has made great contributions in this regard. However, in these results, the efficacy of various prescriptions is sought in the effective compound in crude drugs, but it has deviated from the concept of traditional medicine. In addition, unlike modern medicine which takes medicines for the treatment of “diseases”, in these traditional medicines, the individualities of physiological conditions and the healing power are first diagnosed, and then an appropriate prescription is made. In other words, although the current research has achieved results, it lacks the viewpoints of traditional medicine's "effects-based on a combination of crude drugs" and "effects-based on biological reactions". Research based on these unique views of traditional medicine may produce new discoveries and developments in the future.

Therefore, we conducted various experiments based on the "unique perspective of traditional medicine"

Chapter 1: Acquisition of basic data on 120 kinds of crude drugs in the Kampo medicine, construction of a library for studying on neuronal/glial cell function and expressed genes, and study on changes expression levels of a depression-related factor[1, 2].

All the component profiles of 120 kinds of crude drug extracts, which were supplied from the Institute of Natural Medicine, University of Toyama, were obtained by 3D-HPLC. After that, cells of the nervous system (N18TG2) and glial system (C6Bu-1) were treated at two concentrations, and a total of 480 morphological photographs were obtained. In addition, RNA was extracted from each treated cell and converted to cDNA to create a library. Using the library, I investigated the expression level of BNIP-3 mRNA, which was previously reported by our laboratory as an antidepressant-related factor, by PCR. As a result, many of the herbal medicines that make up "Hochuekkito (補中益気湯:HET)" show an increase the expression, while the herbal medicines that make up "Sanou-shashin-to (三黄瀉心湯:SST)" and "Orengedokuto (黄連解毒湯:OGT)" that calm the mind show downregulation.

Chapter 2: Inhibitory effect of each cytotoxicity caused by the combined extraction of Coptidis Rhizoma and Rhei Rhizoma: An example of "herb pair" theory[3].

During the research related to SST and OGT, both have an inhibiting the abnormal rise of Qi as described above, it was found that the co-existence of Coptidis Rhizoma (CR) and Rhei Rhizoma (RR), which include in OGT, inhibited each other's cytotoxicity. Since the color of the solution when CR and RR were extracted together was lighter than that when each was extracted, components were analyzed by 3D-HPLC. At least, the amount of CR-derived berberine in co-extraction was

dramatically educed than in CR alone extract. When the CR and CC extracts were combined in vitro, a new precipitate was formed. However, when cytotoxicity was determined by the MTT assay, elimination of toxicity was only observed in co-extraction, not in vitro mixing. The details of the mechanism are still under consideration, but this result will be noted as embodying the idea of "herb pair" in Chinese medicine theory.

Chapter 3: Stepwise detection of trace agonistic components in HET by electrophysiological techniques[4)]

Most antidepressants are inhibitors of the serotonin 2C receptor (5-HT2CR), but HET shows a stimulant of 5-HT2CR. In this study, the analysis of active compounds was carried out by electrophysiological methods, without skipping any intermediate steps of separation. It was found that the molecule with 283.14 has strong physiological activity, but the structure itself has not been determined because it may be an ultra-trace component. These results are conceivable that a trace amount of a component having high activity is likely to be involved in the action of Chinese herbal medicine. And because of the trace amount, it may have many components that are still not yet known.

Chapter 4: Attempt to develop a new Kampo prescription aiming at "prevention of heart disease caused by drug side effects" based on the theory and its molecular action mechanism[5)]

Based on the Kampo medicine theory, it is possible to develop a new prescription. In fact, numerous prescriptions have been reported and are actually used in China to prevent the aggravation of COVID-19. From that point of view, we started basic research aiming at the development of prescriptions to prevent heart failure caused by side effects of anticancer drugs. As the basic prescription, I focused on Shenfu

Decoction (人参附子湯: SFD) and searched for genes involved in its action and analyzed its association. Myoblast cell line H9C2 cells, which were differentiated to cadiac type by decreasing the serum and retinoic acid supplementation, were treated in doxorubicin and SFD. The gene chip analysis method was firstly used followed by network pharmacology and protein-protein network/module analysis. The results indicated that SFD can significantly affect the expression of ubiquitination-related genes to play an important role in treating heart failure. Also, the findings of hub genes' information could help us to understand molecular mechanisms and to make further effective novel Kampo prescriptions.

The above research results gave us 1) the basic knowledge of the crude drugs that make up Chinese herbal medicine in Chapter 1, 2) the knowledge of the "herbal pair" effect in Chapter 2, 3) the knowledge of the effect of a ultra-trace agonistic component that induces the physiological action in Chapter 3, and 4) the findings on the attempt to develop new Kampo prescriptions by new combinations and on depending the molecular mechanisms in Chapter 4. Conducting research based on the basic idea of classical Chinese medicine may lead to discover of new concepts and therapeutic drugs. The results of this study describe examples of this possibility.

Chapter #1

Profiling of 120 types of herbal extracts and their effects on morphology in cultured neuronal or glial cell lines, followed by RNA extraction for a cDNA library: Effects of BNIP-3 mRNA expression, a virtually considered for anti-depression

1.1 Introduction

Experimental methods for the direct addition of crude drugs or "Kampo" prescriptions to cultured cells often produce unexpectedly useful information, which may be applied in research. We previously reported the significant up-regulation of BNIP-3 mRNA expression when Hochuekkito (Bu Zhong Yi Qi Tang)[1], as well as many antidepressant[2], was added to a culture medium of NG108-15 cells, which is a hybrid cell of neuroblastoma N18TG-2 and glioma cell C6-Bu-1. Starting from that results, we also found that the BNIP-3 mRNA expression was also detected in brain regions with highly active nerves[3], suggesting the functional significance of BNIP-3 in the brain. As in the case of BNIP-3 described above, studying the effects of crude drugs and Kampo prescriptions on cultured cell lines makes it possible to obtain new findings triggered by them.

Hochuekkito is composed of 10 kinds of crude drugs. The experiment about the effects of each crude drug would be planed. As samples to be used for that purpose, the total 120 kinds of herbal extracts were supplied by the Institute of Natural Medicine (INM), University of Toyama, to facilitate joint research as part of a national project. Therefore, not only hochuekkito, but all 120 kinds of crude drug extracts were examined in order to obtain information that will be the basis for studying the effects of many Kampo and Wakan-yaku prescriptions in the future. After obtaining these extracts and conducting original profiling using three-dimensional high-performance liquid chromatography (3D-HPLC), they were added to cultured cells, and their effects on cell morphology were assessed. RNA was extracted from each sample and a cDNA library applicable to real-time PCR was prepared. Further research using this cDNA library is expected. As a result, although the experimental number for individual crude drugs is

reduced due to the large number of samples, that may be limited to rudimentary knowledge, it obtained the interesting data that could be used for future crude drug and Kampo prescription research. Then we decided to open all in this article.

When considering the effects in the brain, it seems to be important to consider the effects on neuron and glia separately. In that case, it may be best to use primary cultured cells. Differences in isolation technique, however, may carry problems and the questioned stabilities of the results. In that respect, established cell lines are not so seriously concerned. Based on these points, in this study, neuroblastoma cell line N18TG2 and glioma cell line C6Bu-1 were treated by each of 120 basic crude drugs that make up Kampo-prescriptions and Wakan-yaku. Firstly, their proliferative properties and morphological changes were examined. After the observation, RNA was extracted to prepare cDNA libraries. Using the library, as an example of gene expression change analysis, the effect of BNIP-3 mRNA expression by each crude drug treatment was examined.

A Kampo prescription, Hochuekkito (HET), along with Juzentaihoto (JTT) and Hangekoubokuto, have been clinically applied to compensate for feelings of depression. From this point, these prescriptions are expected to have a function as an antidepressant. The authors show that HET has an antidepressant effect in behavioral pharmacology[4], and that HET and some antidepressants increases BNIP-3 mRNA expression in neuronal cultured cells[1] and in stressed mice[2]. Based on these facts, BNIP-3 is considered to be a candidate for a factor in the brain related to antidepressant effect. Studies have been conducted by us on changes in the expression at the stage of neuronal growth[5] and on analysis of the site of expression in the brain[3].

BNIP-3 was firstly found and established as a factor associated with mitophagy[6,7].

Mitophagy is a function that maintains the stability of the whole cell by removing dysfunctional mitochondria[8]. In that respect, BNIP-3 has been a certain type of programmed death function. Recently, it has been reported that ginsenoside Rb1, a main ingredient in Panacis Ginseng Radix, has been shown to suppress H_2O_2-induced cell death in cultured endothelial cells, and BNIP-3 is involved in its mechanism through a small RNA miR210 concerning its RNA expression[9]. However, in addition to our report on the contribution to the antidepressant effect, it has also been shown to be involved in synaptic activity[10].

Based on these points, in this study, neuroblastoma cell line N18TG2 and glioma cell line C6Bu-1 were treated by each of 120 basic crude drugs that make up Kampo-prescriptions and Wakan-yaku. Firstly, their proliferative properties and morphological changes were examined. After the observation, RNA was extracted to prepare cDNA libraries. Using the library, as an example of gene expression change analysis, the effect of BNIP-3 mRNA expression by each crude drug treatment was examined. Based on the results of the primary screening, we selected 24 kinds of herbal medicines, including 10 kinds of herbal medicines forming HET, and further examined BNIP-3 mRNA expression.

1.2 Materials and Methods

1.2.1 Crude hot water extract of herbal medicine

The crude drug extracts used in the present study were supplied by INM (http://www.inm.u-toyama.ac.jp/jp/collabo/). All extracts were made in 2015 at a concentration of 10 mg/ml. Since yield information was not provided, all experiments

were performed at a final extract concentration of 10 or 100 μg/ml. All extracts were filtered through a sterile filter with a pore size of 0.22 μm.

1.2.2 3D-HPLC

Each extract solution (1 mg/ml) was centrifuged to remove insoluble substances followed by filtering through a membrane filter (0.22 μm) and then used for HPLC (20 μl). The HPLC apparatus (Hitachi Ltd., Japan) consisted of a pump (L-2130) with analysis system software (Elite LaChrom); it was equipped with a photodiode array detector (UV 230-400 nm, L-2455), system controller, auto-injector (L-2200), and column oven (L-2300). HPLC conditions were as follows: column, LaChrom Ultra C18 (5 μm, Lot No. 21D5-011; Hitachi Ltd., Japan) with 150 × 4.6 mm I.D.; eluant, (A) H_2O containing 0.1% formic acid and (B) CH_3CN containing 0.1% formic acid (a linear gradient was used from '95% A and 5% B' to '30% A and 70% B' for 90 min); temperature, 20 °C; and flow rate, 0.2 ml/min.

1.2.3 Cell culture and morphological observations

N18 and C6 cells were both continuously cultured using our previously described methods with slight modifications[10]. Briefly, cells were cultured in DMEM supplemented with 10% FBS. All cultures were maintained at 37 °C under 10% CO_2. Thirty microliters of the filtrated crude drug solution were added to 3 ml of medium in a 35-mm dish to prepare sample-treated cells at 100 μg/ml. In the case of the 10 μg/ml treatment, the above sterilized crude drug extract was used after diluting it 10 times with sterile water. All drug treatments were performed at the same time as the start of cultivation. Forty-eight hours later, the drug treatment was also performed after exchanging the culture solution. The same treatment was conducted again after another

48 hours. Morphological observations with photography were conducted approximately 24 hours after the final drug treatment and followed by RNA extraction.

1.2.4 RNA isolation and cDNA construction

The acidic phenol method was used to extract RNA according to the manufacturer's instructions (Trisure: Bioline, Germany). RNA concentrations and the certification of its quality were spectrophotometrically assessed at 230～320 nm. Each RNA concentration was calculated from the value obtained at 260 nm. Total RNA (1 μg) was isolated and incubated with 5 μM of a random 6 mer primer and 0.5 μl of PrimeScript RT Enzyme Mix I (Takara, Japan) in 20 μl of solution at 37°C for 15 min to make single-stranded complementary DNA (cDNA). The cDNAs obtained were kept at -80°C as a cDNA library.

1.2.5 Real-time PCR

After the 10-fold dilution of each cDNA solution by EASY dilution solution (Takara No. 9160, Otsu, Japan), 1 μl was used as a real-time PCR template. Specific primers for BNIP-3 (Accession No.NM_053420), i.e. TTAAACACCCGAAGCGCACA (forward) and CAGGAACACCGCATTTACAG (backward), were used to produce a 318-bp product. The PCR mixture contained cDNA solution (1 μl) and 0.5 μM of each primer in the reaction solution, with a premix of Taq DNA polymerase and SYBR Green (Cat. No. RR307A, Takara). PCR was performed using a real-time PCR machine (Takara Thermal Cycler Dice TP600, Takara, Otsu, Japan), with the following conditions: (1) 95 °C for 30 s; (2) 50 cycles at 95 °C for 5 s, 55 °C for 10 s, and 72 °C for 20 s. A linear calibration standard line was obtained using cDNA from non-treated cells at 4 concentrations.

1.3 Results

Table 1 shows the 120 crude extracts used in the present study. Individual results are shown in “All data on profiling of 120 herbal extracts”. Crude extracts were numbered according to Japanese alphabetical order. Therefore, the list in “All data on profiling of 120 herbal extracts” is in this order to avoid confusion due to deviations from basic information in INM. In Table 1, the order is rearranged alphabetically by Latin names and displayed as L1 to L120. The number in the adjacent column is notation according to the Japanese order, and corresponds to the number in “All data on profiling of 120 herbal extracts”. For example, Glycyrrhizae Radix, L62 in the Table, is displayed as No. 18 in “All data on profiling of 120 herbal extracts”. Table 1 shows the relationship between two types of numbers. A, B, and C in the third column in Table 1 indicate the ranking of herbal medicines in “Shennong Ben Cao Jing”, an important classical book on Chinese medicine. In this book, crude drugs were divided into three categories: Johon (high quality material; 120) = nourishes life, Chuhon (middle quality material; 120) = nourishes physicality, and Gehon (lower quality material; 125) = therapeutic drug, which are highly toxic. In the Table, A = Johon, B = Chuhon, and C = vulnerable. Columns 4 and 5 show cytotoxicity in C6 and N18 cells. Please refer to the photographic results shown in “All data on profiling of 120 herbal extracts”. ▲: moderate toxicity and **X**: strong toxicity (cell deah)

Individual results in “All data on profiling of 120 herbal extracts” are explained in Fig. 1 using L62 (No. 18), *Glycyrrhizae Radix*, as an example. Fig. 1A shows 3D-HPLC results. Changes in color indicate the height of the signal at that wavelength and outflow time. Fig. 1B indicates the concentration of extracted RNA. Fig. 1C shows cell morphology after a treatment with an extract of RNA.

As shown in Fig. 2, individual data represent the results obtained at various wavelengths (Fig. 2B) as well as the absorption spectrum at each outflow time (Fig. 2C). The absorption spectrum in Fig. 2 shows glycyrrhizin (Fig. 2C), which is generally eluted last in the HPLC detection of "Kampo" prescriptions under these conditions.

Table 2 shows the top 30 species extracted from all the information shown in "All data on profiling of 120 herbal extracts" in order of increasing or decreasing BNIP-3 mRNA expression. In the table, the top shows the results from C6 and the bottom shows the results from N18. The circle mark on the left side of Latin No. shows the crude drug that was subjected to the secondary assay described later. The crude drugs subjected to secondary assay were selected, in principle, in which the frequency of use is high (No. of use is 10 or more) is based on the first results. In addition, if a herbal medicine can make up a Kampo prescription, that herbal extract was also added to the list of the secondary assay. As a result, secondary assayed extracts contain herbal medicines that makeup HET, JJT, Sanoushashinto (SST), and Ourengedokuto (OGT).

Fig. 3 shows the results of the crude drugs that make up HET, SST, and OGT. The open column shows the results for N18, and the Shadow column shows the results for C6.

Table 1　List of 120 herbal extracts (10 μg/ml) used in the present study

Latin No.	Jpn No.	Shen	toxic		No. use	HET	BNIP-3		Latin name	Japanses Name
			C6	N18			C6	N18		
L1	35	A			3		49	43	Achyranthis Radix	Goshitu （牛膝）
L2	105	C			-		129	99	Aconiti Tuber Radix	Houbushi（炮附子）
L3	31	B	×	▲	-		50	35	Albizziae Cortex	Goukanhi （合歓皮）
L4	73	A			14		93	117	Alismatis Rhizoma	Takusha （沢瀉）
L5	114		▲	▲	-		64	66	Alpiniae Fructus	Yakuchi （益智）
L6	118		▲	▲	1		46	20	Alpiniae Officinari Rhizoma	Ryoukyou （良姜）
L7	58		▲	×	1		63	86	Amomi Semen	Shukusha （縮砂）
L8	77	B			6		64	224	Anemarrhenae Rhizoma	Chimo （知母）
L9	97	B			5		242	100	Angelicae Dahuricae Rhizoma	Byakushi （白芷）
L10	85	B			37	#	93	66	Angelicae Radix	Touki （当帰）
L11	88	A			1		75	82	Araliae Cordatae Rhizoma	Dokkatu （独活）
L12	37		▲	▲	2		36	48	Arctii Fructus	Goboushi （牛蒡子）
L13	100	B	×	×	1		24	65	Arecae Semen	Binrouji （檳榔子）
L14	23	C			9		132	138	Armeniacae Semen	Kyounin （杏仁）
L15	2	A	▲	×	2		121	139	Artemisiae Capillari Flos	Inchinkou（茵陳蒿）
L16	12		▲	×	1		79	76	Artemisiae Folium	Gaiyou （艾葉）
L17	41	A		▲	5		96	110	Asiasari Radix	Saishin （細辛）
L18	83	A			2		80	93	Asparagi Radix	Tenmondou （天門冬）
L19	6	B			14	#	171	123	Astragali Radix	Ougi （黄耆）

L20	66	A			34	#	80	36	Atractylodis Lanceae	Soujutu （蒼朮）
L21	98	A			8		77	114	Atractylodis Rhizoma	Byakujutu （白朮）
L22	21	B			14		78	71	Aurantii Fructus Immaturus	Kijitu （枳実）
L23	81	A			24	#	25	78	Aurantii Nobilis Pericarpium	Chinpi （陳皮）
L24	75			▲	2		83	24	Bambusae Caulis	Chikujo（竹茹）
L25	84				1		99	57	Benincasae Semen	Tougashi （冬瓜子）
L26	40	A			22	#	147	72	Bupleuri Radix	Saiko（柴胡）
L27	110	A			3		34	178	Cannabis Fructus	Mashinin （麻子仁）
L28	30			▲	2		79	61	Carthami Flos	Kouka （紅花）
L29	78		×	×	2		42	270	Caryophylli Flos	Chouji （丁子）
L30	20	A			1		84	162	Chrysanthemi Flos	Kikuka （菊花）
L31	60	A	▲	×	5	#	134	135	Cimicifugae Rhizoma	Shouma （升麻）
L32	28	A	▲	×	39		84	84	Cinnamomi Cortex	Keihi （桂皮）
L33	90	A			-		26	98	Cistanchis Herba	Nikujuyou （肉蓯蓉）
L34	1				2		131	76	Clematidis Radix	Ireisen （威霊仙）
L35	64	B			25		167	36	Cnidii Rhizoma	Senkyu （川芎）
L36	86				-		91	84	Codonopsitis Radix	Toujin （党参）
L37	116	A			3		53	48	Coicis Semen	Yokuinin （薏苡仁）
L38	10	B	▲	×	11		69	62	Coptidis Rhizoma	Ooren （黄連）
L39	46	B	▲	×	3		46	77	Corni Fructus	Sanshuyu （山茱萸）
L40	5				1		137	59	Corydalis Tuber	Engosaku （延胡索）
L41	42				-		49	125	Crocus	Safuran

L42	3				-		174	146	Curcumae Rhizoma	Ukon （鬱金）
L43	14			▲	-		161	82	Curcumae Rhizoma	Gajutu （莪朮）
L44	33				-		83	78	Cyperi Rhizoma	Koubushi （香附子）
L45	93	B			-		268	135	Dictamni Radicis Cortex	Hakusenpi （白鮮皮）
L46	49	A			4		88	152	Dioscoreae Rhizoma	Sanyaku （山薬）
L47	69	B			-		120	94	Dipsaci Radix	Zokudan （続断）
L48	52	A		▲	-		91	86	Eleutherococci Senticosi Rhizoma	Shigoka （刺五加）
L49	109	B	×	×	13		28	80	Ephedrae Herba	Maou （麻黄）
L50	99		▲	▲	1		122	89	Eriobotryae Folium	Biwayou （枇杷葉）
L51	89	A			1		82	38	Eucommiae Cortex	Tochu （杜仲）
L52	36	B	▲	×	3		146	47	Euodiae Fructus	Goshuyu （呉茱萸）
L53	120	C	▲	×	5		51	24	Forsythiae Fructus	Rengyou （連翹）
L54	92	B			2		235	143	Fritillariae Bulbus	Baimo （貝母）
L55	119				-		51	35	Ganoderma	Reishi （霊芝）
L56	44	B			13		55	107	Gardeniae Fructus	Sanshishi （山梔子）
L57	82	A			1		23	31	Gastrodiae Rhizoma	Tenma （天麻）
L58	62				-		112	239	Gentianae Macrophyllae Radix	Shingyou （秦艽）
L59	117	A			3		79	87	Gentianae Scabrae Radix	Ryutan （竜胆）
L60	65	A			-		244	9	Ginseng Radix	Ninjin （生干人参）
L61	32	A			-		71	86	Ginseng Radix Rubra	Koujin （紅参）
L62	18	A			93	#	121	147	Glycyrrhizae Radix	Kanzou （甘草）
L63	103	B			-		147	184	Imperatae Rhizoma	Boukon （茅根）

L64	115	A			-		81	84	Leonuri Herba	Yakumosou （益母草）
L65	4				-		127	104	Linderae Radix	Uyaku （烏薬）
L66	53		×	×	2		204	102	Lycii Cortex	Jikoppi （地骨皮）
L67	34	B	××	×	12		65	1	Magnoliae Cortex	Kouboku （厚朴）
L68	61	A		▲	2		123	7	Magnoliae Flos	Shini （辛夷）
L69	95			▲	7		144	96	Menthae Herba	Hakka （薄荷）
L70	67	B			2		76	183	Mori Cortex	Souhakuhi （桑白皮）
L71	68		▲	▲	-		103	42	Mori Folium	Soyou （桑葉）
L72	108	B	×	×	8		46	69	Moutan Cortex	Botanpi （牡丹皮）
L73	113		▲	▲	-		66	92	Myrrha	Motuyaku （没薬）
L74	22				3		204	101	Notopterygii Rhizoma	Gyoukatu （羌活）
L75	94	A			11		134	111	Ophiopogonis Tuber	Bakumontou （麦門冬）
L76	55	B	▲	×	44		114	327	Paeoniae Radix	Shakuyaku （芍薬）
L77	63		×	×	-		153	103	Paeoniae Radix Rubra	Sekishaku （赤芍）
L78	91	A			37	#	141	176	Panacis Ginseng Radix	Ninnjinn（人参、湯通し）
L79	76				-		77	241	Panacis Japonici Rhizoma	Chikusetu-ninjin （竹節人参）
L80	45	A			-		52	55	Panax Pseudoginseng	Sanshichi-ninjin （三七人参）
L81	70			▲	6		88	160	Perillae Herba	Soyou （蘇葉）
L82	87	C			6		75	62	Persicae Semen	Tounin （桃仁）
L83	8	B	▲	×	8		64	34	Phellodendri Cortex	Oubaku （黄柏）
L84	96	C			27		145	111	Pinelliae Tuber	Hange （半夏）
L85	56	C		▲	4		75	81	Plantaginis Semen	Shazenshi （車前子）

L86	19	B		▲	12		82	151	Platycodi Radix	Kikyou （桔梗）
L87	11	A	▲		3		106	106	Polygalae Radix	Onji （遠志）
L88	13		▲	×	1		84	76	Polygoni Multiflori Radix	Kashu （何首烏）
L89	80	B			6		133	129	Polyporus	Chorei （猪苓）
L90	101	A			46		109	134	Poria	Bukuryou （茯苓）
L91	9		▲	×	-		104	190	Pruni Cortex	Ouhi （桜皮）
L92	107		×	×	-		97	178	Psoraleae Semen	Hokosshi （補骨脂）
L93	15	B			4		143	82	Puerariae Radix	Kakkon （葛根）
L94	106		×	×	2		25	68	Quercus Cortex	Bokusoku （樸樕）
L95	51	B			22		69	171	Rehmanniae Radix	Jiou （地黄）
L96	57	A			-		73	179	Rehmanniae Radix	Jukujiou （熟地黄）
L97	71	C	×	×	16		158	101	Rhei Rhizoma	Daiou （大黄）
L98	74	B	▲	×	-		76	91	Salviae Miltiorhizae Radix	Tanjin （丹参）
L99	104	B			11		87	111	Saposhnikoviae Radix	Boufu （防風）
L100	25				-		113	60	Sasa Folium	Kumazasa （隈笹）
L101	112	A			3		111	81	Saussureae Radix	Mokkou （木香）
L102	39	B			5		68	57	Schisandrae Fructus	Gomishi （五味子）
L103	26	B		×	8		60	76	Schizonepetae Spica	Keigai （荊芥）
L104	29	B			-		98	69	Scrophulariae Radix	Genijin （玄参）
L105	7	B	▲	▲	27		96	31	Scutellariae Radix	Ougon （黄芩）
L106	38	A	×	×	1		64	138	Sesami Semen	Goma （胡麻）
L107	102	C			3		125	146	Sinomeni Caulis et Rhizoma	Boui （防已）

L108	43				-		49	101	Smilacis Rhizoma	Sankirai （山帰来）
L109	24	B			2		129	99	Sophorae Radix	Kujin （苦参）
L110	50				-		96	94	Sparganii Rhizoma	Sanryou （三稜）
L111	27		×	×	-		21	16	Spatholobi Caulis	Keikettou （鶏血藤）
L112	54	A			1		154	103	Tribuli Fructus	Shiturishi （蒺藜子）
L113	16	B			4		146	165	Trichosanthis Radix	Karokon （栝楼根）
L114	79		▲	▲	4		119	52	Uncariae Uncis Cum Ramulus	Choutoukou （釣藤鉤）
L115	111	A	▲	×	-		104	76	Viticis Fructus	Mankeishi （蔓荊子）
L116	47	B	▲	×	2		44	72	Zanthoxyli Fructus	Sanshou （山椒）
L117	59				51	#	70	121	Zingiberis Rhizoma	Shoukyou （生姜）
L118	17	B		▲	12		140	213	Zingiberis Siccatum Rhizoma	Kankyou （乾姜）
L119	72	A			39	#	197	145	Zizyphi Fructus	Taisou （大棗）
L120	48	A			3		71	109	Zizyphi Spinosi Semen	Sansounin （酸棗仁）

Detailed results are provided in “All data on profiling of 120 herbal extracts”. Briefly, each column has the following contents in order from the left: numbered alphabetically by Latin names, numbered according to the Japanese order that corresponds to the number in Supplementary Materials, ranking of herbal medicines in “Shennong Ben Cao Jing”, cell toxicity in C6 and N18 cells, Latin names, and Japanese names. “Shennong Ben Cao Jing” is a classical book on Chinese medicine that was written around AC200. In the book, crude drugs were divided into three categories: A) Johon (high quality material; 120) = nourishes life, B) Chuhon (middle quality material; 120) = nourishes physicality, and C) Gehon (lower quality material; 125) = therapeutic drug, but with high toxicity. Regarding cytotoxicity, the state was subjectively judged from observations of cell morphology; the mark “X” indicates that cells were dead or dying, and “▲” indicates that either some cells remain viable or cells are undergoing transformation or differentiation. The information is shown in the“No. of use” indicates the number of the corresponding crude drug used in 138 kinds of Kampo prescriptions that are sold by Japan's largest Kampo medicine company (Tsumura). For example, Glycyrrhizae Radix (L62: Jpn No. 18) is the most frequently used crude drug in 93 of 138 Kampo prescriptions (67.4%). The mark “#” in the fourth column indicates that crude drugs are members of HET. The fifth and sixth columns show the results of these experiments, showing the BNIP-3 mRNA expression level in C6 and N18 cells as a percentage of that in vehicle-treated cells cultured at the same time.

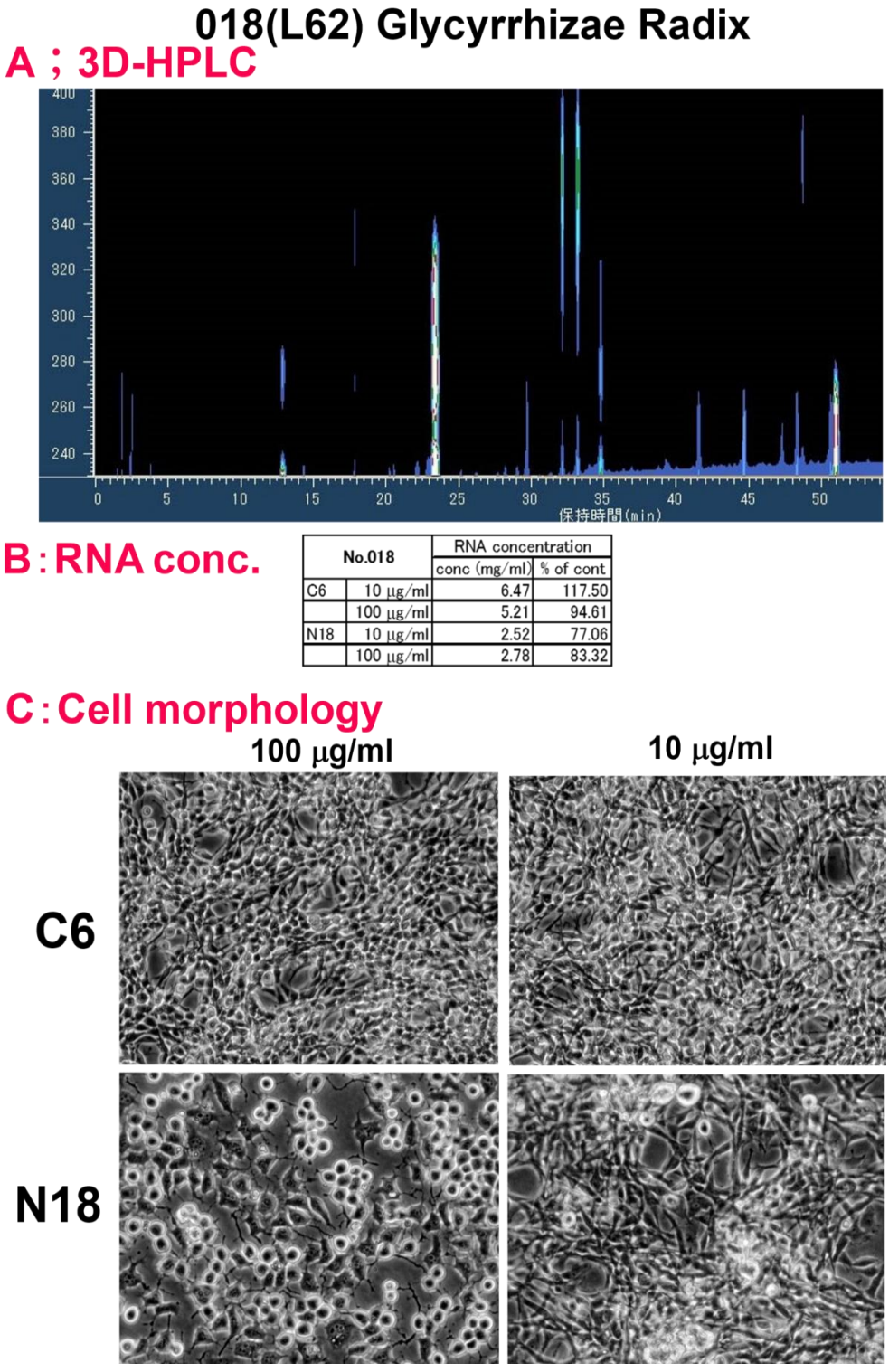

Fig. 1 An example data sheet (*Glycyrrhizae Radix*) included in "All data on profiling of 120 herbal extracts" to explain how to interpret results.

A: 3D-HPLC chart, B: RNA concentration as percentage of vehicle-treated sample, and C: morphological photographs.

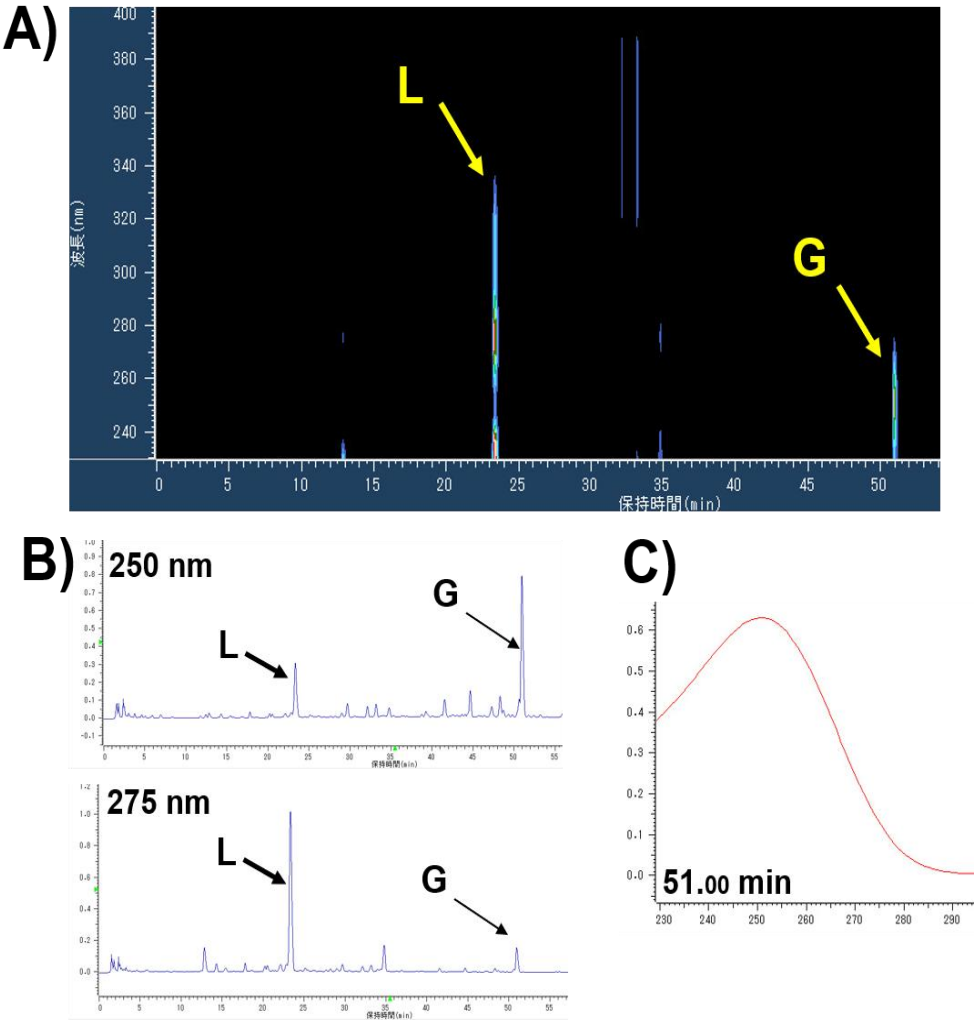

Fig. 2 Example of data for 3D-HPLC

Regarding the results for *Glycyrrhizae Radix* shown in this figure, the 250 and 275 nm charts indicated in Fig 2B are the optimum wavelengths for quantifying glycyrrhizin and liquiritin, respectively. C shows the absorption spectrum of glycyrrhizin from 3D-HPLC. G = glycyrrhizin, L = Liquiritin.

Table 2 The top 30 crude drug about the BNIP-3 expression in order of increasing or decreasing BNIP-3 mRNA expression.

C6 (30 from the lowest expression level)

	Latin No.	Jpn No.	No. use	BNIP3(%) C6	BNIP3(%) N18	Latin name
	L111	27	-	21	16	Spatholobi Caulis
	L57	82	1	23	31	Gastrodiae Rhizoma
	L13	100	1	24	65	Arecae Semen
◎	L23	81	24	25	78	Aurantii Nobilis Pericarpium
	L94	106	2	25	68	Quercus Cortex
	L33	90	-	26	98	Cistanchis Herba
◎	L49	109	13	28	80	Ephedrae Herba
	L27	110	3	34	178	Cannabis Fructus
	L12	37	2	36	48	Arctii Fructus
	L29	78	2	42	270	Caryophylli Flos
	L116	47	2	44	72	Zanthoxyli Fructus
	L6	118	1	46	20	Alpiniae Officinari Rhizoma
	L39	46	3	46	77	Corni Fructus
◎	L72	108	8	46	69	Moutan Cortex
	L1	35	3	49	43	Achyranthis Radix
	L41	42	-	49	125	Crocus
	L108	43	-	49	101	Smilacis Rhizoma
	L3	31	-	50	35	Albizziae Cortex
	L53	120	5	51	24	Forsythiae Fructus
	L55	119	-	51	35	Ganoderma
	L80	45	-	52	55	Panax Pseudoginseng
	L37	116	3	53	48	Coicis Semen
◎	L56	44	13	55	107	Gardeniae Fructus
	L103	26	8	60	76	Schizonepetae Spica
	L7	58	1	63	86	Amomi Semen
	L5	114	-	64	66	Alpiniae Fructus
	L8	77	6	64	224	Anemarrhenae Rhizoma
◎	L83	8	8	64	34	Phellodendri Cortex
	L106	38	1	64	138	Sesami Semen
	L67	34	12	65	1	Magnoliae Cortex

C6 (30 from the highest expression level)

	Latin No.	Jpn No.	No. use	BNIP3(%) C6	BNIP3(%) N18	Latin name
◎	L21	98	8	359	114	Atractylodis Rhizoma
	L45	93	-	268	135	Dictamni Radicis Cortex
	L60	65	-	244	9	Ginseng Radix
	L9	97	5	242	100	Angelicae Dahuricae Rhizoma
	L54	92	2	235	143	Fritillariae Bulbus
	L66	53	2	204	102	Lycii Cortex
	L74	22	3	204	101	Notopterygii Rhizoma
◎	L119	72	39	197	145	Zizyphi Fructus
	L42	3	-	174	146	Curcumae Rhizoma
◎	L19	6	14	171	123	Astragali Radix
◎	L35	64	25	167	36	Cnidii Rhizoma
	L43	14	-	161	82	Curcumae Rhizoma
◎	L97	71	16	158	101	Rhei Rhizoma
	L112	54	1	154	103	Tribuli Fructus
	L77	63	-	153	103	Paeoniae Radix Rubra
◎	L26	40	22	147	72	Bupleuri Radix
	L63	103	-	147	184	Imperatae Rhizoma
	L52	36	3	146	47	Euodiae Fructus
	L113	16	4	146	165	Trichosanthis Radix
	L84	96	27	145	111	Pinelliae Tuber
	L69	95	7	144	96	Menthae Herba
	L93	15	4	143	82	Puerariae Radix
◎	L78	91	37	141	176	Panacis Ginseng Radix
◎	L118	17	12	140	213	Zingiberis Siccatum Rhizoma
	L40	5	1	137	59	Corydalis Tuber
	L31	60	5	134	135	Cimicifugae Rhizoma
	L75	94	11	134	111	Ophiopogonis Tuber
	L89	80	6	133	129	Polyporus
	L14	23	9	132	138	Armeniacae Semen
	L34	1	2	131	76	Clematidis Radix

N18 (30 from the lowest expression level)

	Latin No.	Jpn No.	No. use	BNIP3(%) C6	BNIP3(%) N18	Latin name
	L67	34	12	65	1	Magnoliae Cortex
	L68	61	2	123	7	Magnoliae Flos
	L60	65	-	244	9	Ginseng Radix
	L111	27	-	21	16	Spatholobi Caulis
	L6	118	1	46	20	Alpiniae Officinari Rhizoma
	L53	120	5	51	24	Forsythiae Fructus
	L24	75	2	83	24	Bambusae Caulis
	L57	82	1	23	31	Gastrodiae Rhizoma
◎	L105	7	27	96	31	Scutellariae Radix
◎	L83	8	8	64	34	Phellodendri Cortex
	L3	31	-	50	35	Albizziae Cortex
	L55	119	-	51	35	Ganoderma
	L20	66	34	80	36	Atractylodis Lanceae
◎	L35	64	25	167	36	Cnidii Rhizoma
	L51	89	1	82	38	Eucommiae Cortex
	L71	68	-	103	42	Mori Folium
	L1	35	3	49	43	Achyranthis Radix
	L52	36	3	146	47	Euodiae Fructus
	L12	37	2	36	48	Arctii Fructus
	L37	116	3	53	48	Coicis Semen
◎	L114	79	4	119	52	Uncariae Uncis Cum Ramulus
	L80	45	-	52	55	Panax Pseudoginseng
	L102	39	5	68	57	Schisandrae Fructus
	L25	84	1	99	57	Benincasae Semen
	L40	5	1	137	59	Corydalis Tuber
	L100	25	-	113	60	Sasa Folium
	L28	30	2	79	61	Carthami Flos
◎	L38	10	11	69	62	Coptidis Rhizoma
	L82	87	6	75	62	Persicae Semen
	L13	100	1	24	65	Arecae Semen

N18 (30 from the highest expression level)

	Latin No.	Jpn No.	No. use	BNIP3(%) C6	BNIP3(%) N18	Latin name
	L47	69	-	120	2250	Dipsaci Radix
◎	L76	55	44	114	327	Paeoniae Radix
	L29	78	2	42	270	Caryophylli Flos
	L79	76	-	77	241	Panacis Japonici Rhizoma
	L58	62	-	112	239	Gentianae Macrophyllae Radix
	L8	77	6	64	224	Anemarrhenae Rhizoma
◎	L118	17	12	140	213	Zingiberis Siccatum Rhizoma
	L91	9	-	104	190	Pruni Cortex
	L63	103	-	147	184	Imperatae Rhizoma
	L70	67	2	76	183	Mori Cortex
	L96	57	-	73	179	Rehmanniae Radix
	L27	110	3	34	178	Cannabis Fructus
	L92	107	-	97	178	Psoraleae Semen
◎	L78	91	37	141	176	Panacis Ginseng Radix
◎	L95	51	22	69	171	Rehmanniae Radix
	L113	16	4	146	165	Trichosanthis Radix
	L30	20	1	84	162	Chrysanthemi Flos
	L81	70	6	88	160	Perillae Herba
	L46	49	4	88	152	Dioscoreae Rhizoma
	L86	19	12	82	151	Platycodi Radix
◎	L62	18	93	121	147	Glycyrrhizae Radix
	L42	3	-	174	146	Curcumae Rhizoma
	L107	102	3	125	146	Sinomeni Caulis et Rhizoma
◎	L119	72	39	197	145	Zizyphi Fructus
	L54	92	2	235	143	Fritillariae Bulbus
	L15	2	2	121	139	Artemisiae Capillari Flos
	L14	23	9	132	138	Armeniacae Semen
	L106	38	1	64	138	Sesami Semen
◎	L31	60	5	134	135	Cimicifugae Rhizoma
	L45	93	-	268	135	Dictamni Radicis Cortex

The top shows the results from C6 and the bottom from N18. The circle mark on the left side of Latin No. shows the crude drug that was subjected to the secondary assay.

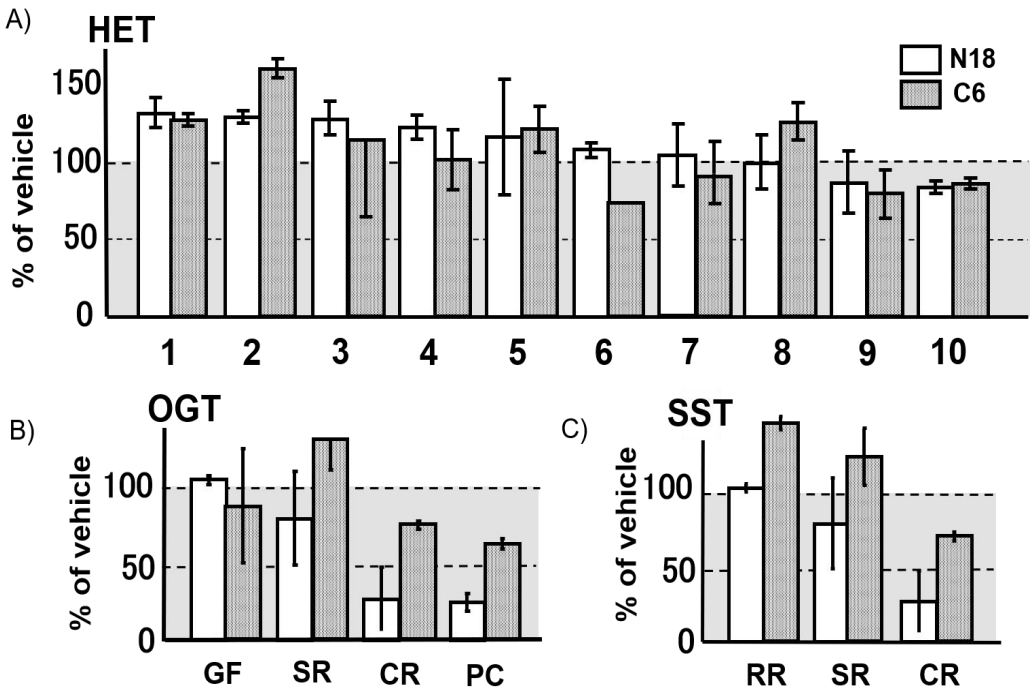

Fig. 3 Effects of the herbal extracts contained in HET, OGT and SST on BNIP-3 mRNA expression

Values show mean ± SEM (n=3) compared with vehicle-treated cells. The top figure shows the effects of crude drugs contained in HET. The results are arranged in the order of large values in N18TG-2 cells. The open column shows the results for N18, and the Shadow column shows the results for C6. 1) Glycyrrhizae Radix, 2) Astragali Radix, 3) Zizyphi Fructus, 4) Cimicifugae Rhizoma, 5) Panacis Ginseng Radix, 6) Atractylodis Rhizoma, 7) Angelicae Radix, 8) Bupleuri Radix, 9) Zingiberis Rhizoma, 10) Aurantii Nobilis Pericarpium. Bottom results were obtained from the crude drugs treated cells contained in OGT (left) and SST (right). GF: Gardeniae Fructus, SR: Scutellariae Radix, CR: Coptidis Rhizoma, PC: Phellodendri Cortex, RR: Rhei Rhizoma

1.4 Discussion

Each of the 120 crude drug extracts provided by INM was added to a culture medium with N18 or C6 cells at a concentration of 10 or 100 μg/ml. Morphological changes were observed followed by RNA isolation to construct cDNA libraries using random primers. All data obtained were added to "All data on profiling of 120 herbal extracts". Morphological data with the amount of RNA obtained from treated cells provide a number of research options.

Several crude extracts exhibited strong toxicity in N18 and C6 cells (Table 1). Toxic effects were more frequently observed in N18 cells than in C6 cells, indicating differences in toxicities between these cell lines, which may be due to differences in the sensitivities of neuronal and glial cells to drugs. Proliferative activity was greater in glial cells. On the other hand, neuronal cells possess the potential to act with functional activity after differentiation; however, the N18 cells used in the present study were in the undifferentiated stage. Therefore, the same factors involved in the activity and/or expression of biological factors with proliferation, for example, BDNF[11], the STAT-3 pathway[12], caspase-3[13], and small RNA 124/Smad4[14], may function in crude extract treatments to inhibit the proliferation of C6 and N18 cells. Neuronal differentiation factors and/or drivers, such as BDNF[15], Plag1[16], and small RNA miR-200[17], may also be present in crude extracts that more strongly inhibited the proliferation of N18 cells than C6 cells. This result may have been predicted solely from morphological images. For example, L103 (26) appeared to only exert effects on N18 cells. In N18 cells, even if L103 causes the same proliferative inhibition, it can be observed to be in the direction of neural differentiation or only in proliferative inhibition. Low concentrations of L26 (40) and L52 (36) were previously suggested to be responsible for axonal growth and neuronal differentiation, whereas only the inhibition of proliferation or dendritic growth was observed with low concentrations of L28 (30). Further studies using antibodies may provide more detailed insights. As discussed above, simple observations of the morphological effects of crude herbal extracts with RNA quantification can give us insight into

effective compounds based on their physiological mechanisms on cell proliferation/death, neuronal differentiation, and other processes. Much information can be obtained from very simple photos: ① Cells were rounded and dead, ② adhesion was maintained and only proliferation was suppressed, and ③ the proliferation of neuronal cells was stopped by differentiation and neurite outgrowth. Based on such morphological information, I plan to conduct various studies in the future. For example, crude drugs A and B both exhibited toxicity when used alone, but inhibited the toxicity of the other when administered together. Many prescriptions combine crude drugs A and B. Furthermore, differentiation-inducing factors may function well under conditions.

The relationship between the classes of herbal medicine in "Shennong Ben Cao Jing " and cytotoxicity was examined. Among the 120 herbal medicines used in the present study, there were 38 Johon types, 35 Chuhon types, and 8 Gehon types. Five out of the 38 Johon types (13%) and 13 (37%) out of the 35 Chuhon types exhibited strong toxicity. Therefore, Johon-type medicines appear to be less toxic than Chuhon-type medicines, as described in the classical reference book. However, from the viewpoint of long-term toxicity, such as the inclusion of mercury, which is listed as Johon in the "Shennong Ben Cao Jing", the classical reference cannot be completely accepted without scientific evidence.

In the present study, filter-sterilized crude drug extracts were directly applied to cells at 10 and 100 μg/ml. The direct application of crude extracts to cultured cells is not always accepted by some researchers. Oral administration is considered the most suitable approach for research on "Kampo" medicine and crude drugs. However, direct application to living cells may provide molecular and pharmacological assay-like information on crude drugs. This approach, in combination with other techniques, such as electrophysiology, may be useful for obtaining information on active ingredients that are only available in small amounts. Many active unknown compounds present at very small amounts in crude galenical drugs have been suggested to exert agonistic effects[18], similar to the secretome of a conditioned medium in differentiated PC12 cells, which induced neuronal differentiation in human

stem cells[19]. For example, ephedrine in *Ephedra Herba* acts as an agonist in the noradrenergic system.

Crude drugs may vary due to different lots and the duration for which they are stored. Therefore, 3D-HPLC data needs to be acquired immediately before an experiment is conducted when possible. Even if bioactivities from the same crude drugs with different backgrounds differ, comparisons of differences in components by HPLC may identify useful active ingredient candidates. 3D-HPLC data shown in "All data on profiling of 120 herbal extracts" are in Table S1; however, original data are unchanged and may be reanalyzed at any wavelength, time point, or using other factors. If the reader is interested in any data, I can provide more detailed information and/or analysis and compare these with the reader's own extracts.

"Kampo" medicine is generally prescribed in combination with crude herbal drugs. There are cases where the combination is simply unrelated, or opposing effects may be obtained depending on the combination, as in the case of *Ephedrae Herba* described above. In the "Kampo" theory, prescriptions are often based on a combination of two types of herbal medicines called "paired drugs". In the present study, combinations were not examined. However, we focused on the potential for a reversal phenomenon in both cell morphology and RNA levels (L1(35), L26(40), and L110(50)) according to the concentrations applied. When the concentration is low, component(s) may exhibit high efficacy, whereas when the concentration is high, the efficacy may be reduced.

To date, research on "Kampo" medicine has focused on the main compounds in herbal medicines, that is, a large number of ingredients. However, a more detailed analysis of compounds at low amounts that produce high efficacy is needed. By using herbal medicine with "paired drugs" to search for active compounds, trace amounts of active components with physiological effects may be discovered. Molecular pharmacological research methods using cell cultures will be indispensable in research on trace components. Even if the reaction *in vivo* does not directly show crude drug effects, future developmental potential cannot be excluded.

As an example of the use of this library, we examined changes in the expression

levels of BNIP-3 mRNA. As described in the Introduction, we previously demonstrated that HET, as well as an antidepressant treatment, increased the expression levels of BNIP-3 in NG108-15 cells.[1, 2] Previous studies also examined the function of BNIP-3[20].

The findings obtained are shown in Table 2, and 10 crude drugs comprising HET are shown with "#" in the HET column. Five out of the 10 types of crude drugs increased expression levels in the N18 and C6 cell lines and three types in one of the cell lines, while two types decreased expression levels in both cell lines. From the results, we selected 20 extracts from the top of each standard, and in addition to adding 2 kinds of herbal medicines to make up HET. Totally 24 kinds of herbal extracts were tested as a secondary assay. Among these 24 species, herbal medicines comprising SST and OGT were also included.

As shown in Fig. 3, many herbal extracts which are included in HET had an increasing effect on BNIP-3 mRNA expression. OGT showed the opposite effect. In SST, there was a difference between the results with N18 and C6. In clinical use of Kampo medicine, HET is used to treat feeling depression, while OGT and SST are used when feeling upset or feeling uncomfortable. In other words, HET and OGT/SST are clinically applied with the expectation of the opposite effect on mood. Regarding HET, the increase of BNIP-3 mRNA reportedly shows by our previous studies using NG108-15 cells. Although OGT and SST are both used for almost the same therapeutic purpose, Jin Gui Yao Lue (Kinkiyouryaku), a classical important reference book of Kampo medicine, shows that SST use a taking medicine with short extraction time in some case. The difference in the direction of BNIP-3 mRNA action between N18 and C6 of SST, and the difference from OGT in that point, may indirectly reflect the above-mentioned differences in clinical objectives. Moreover, the difference might be controlled by Rehmanniae Radix. It is also possible that differences in responsiveness due to differences in receptors and reaction mechanisms between C6 and N18 cells.

As mentioned in the introduction, BNIP-3 has been considered a kind of apoptotic factor. BNIP-3 is known to be involved in the bi-directional association between

mTOR and NF-kB by forming a dimer to be activated by oxidative stress[21]. The activity is suppressed by small RNA miR-210 which binds to the 3'-non coding region[22]. It has also been shown that ginsenoside Rb1, the main component of Panacis Ginseng Radix, suppresses the peroxidative stress-induced cell damage through the increase of miR-210 and subsequent suppression of BNIP-3 expression. Of the herbal medicines examined this time it may be possible to include ingredients with similar actions. The authors are particularly interested in Astragali Radix.

In the future, we will also examine the changes in effectiveness in the process from a combination of herbal medicines to prescription, from one of the classical Kampo theories of “herb pairs”. The effects and the mechanisms of herbal medicines and the active ingredients, and the supplementary effects by other combined herbal drugs from the viewpoint of “herb pairs” are necessary for further experiments in the future.

Chapter #2

Examination of the molecular mechanism of the mutual inhibitory effect of each cytotoxicity caused by the combined extraction of *Coptidis Rhizoma* and *Rhei Rhizoma*: An example of providing evidence to "herb pair" theory

2.1 Introduction

Traditional Japanese medicine, "Kampo medicine," has been systematized in the 18th century by Tohdou Yoshimatsu as the ancestor, based on Traditional Chinese medicine. After a period of decline, its usefulness has been reviewed today and its position as complementary medicine has been established. However, the scientific evidence for its effectiveness is not yet sufficient.

Evidence studies on the efficacy of Kampo herbs have been achieved through the isolation and proof of their active compounds and the elucidation of the physiological mechanism of efficacy. However, these “element reductionism”-like analysis methods have a gap in proving the original action of Kampo herbs. In that regard, one of the authors has written a review in this journal[23]. In modern science, research on crude drugs that are effective is being studied in the direction of analyzing their components, but from the perspective of integrated pharmacology in Traditional Chinese medicines and Kampo medicines, it is possible to combine crude drugs that further emphasize their effectiveness or to suppress the side effects. This is called "herbal pair", and in the basic phenomenon, it has the same foundation as modern pharmacology.

"Orengedoku-to (OGT)" and "Sanoshashin-to (SST)" are known as typical Kampo prescriptions that suppress the state of excitement. It is also used for mental anxiety and insomnia, but it cannot be shown that the distinction between the two is clear. OGT consists of four herbal medicines, *Coptidis Rhizoma* (CR), *Scutellariae Radix* (SR), *Phellodendron Cortex* (PC), and *Gardeniae Fructus* (GF). Of these, CR contains a large amount of berberine. Berberine is also used in clinical treatment as an antidiarrheal and intestinal regulator. SST is composed of three herbal medicines, *Rhei Rhizoma* (RR), CR and SR. CR and SR are common with OGT, but RR, which has a strong action as a laxative, is added to it.

The original action of RR is heat regulation and the laxative action is an unfavorable action in this case. If OGT and SST are used properly in anticipation with the opposite action on the digestive system, it is doubtful that CR and RR,

which have the opposite effect, are mixed in SST. Furthermore, the prescription consists of only three crude drugs. It will be a point to be clarified.

The authors have created a cDNA library for the purpose of examining the gene expression effect of 120 kinds of crude drugs alone[24], and are proceeding with various experiments on the components, cytotoxicity, function, and gene expression. In the process, we observed a mysterious phenomenon related to CR and RR. When both were extracted with hot water, it was observed that the color of the extract was lighter than that of each of them alone. It was also observed that simple mixing of each crude drug extracted individually causes precipitation. With this as a starting point, the purpose of this study was to consider the significance of Kampo medicine prescription, especially from the viewpoint of "herbal pair"

2.2 Materials and Methods

2.2.1 Extraction of galenicals

Approximately 20 g of each prescription or galenical was added to 500 ml of boiling water for 60 min. Galenicals were removed while the solution was still hot, and the extract was frozen using liquid nitrogen. The frozen extract obtained was freeze-dried.CR and RR were purchased from Tochimoto Tenkai-do (Osaka, Japan).

2.2.2 Three-dimensional high-performance liquid chromatography analysis of extracts (3D-HPLC)

Each extract solution (1 mg/ml) was centrifuged to remove insoluble substances followed by filtering through a membrane filter (0.22 μm) and then used for HPLC analysis (20 μl). The HPLC apparatus (Hitachi Ltd., Japan) consisted of a pump (L-2130) with analysis system software (Elite LaChrom); it was equipped with a photodiode array detector (UV 230-400 nm, L-2455), a system controller, an auto-injector (L-2200), and a column oven (L-2300). The HPLC conditions were as follows: column, LaChrom Ultra C18 (5 μm, Lot No. 21D5-011; Hitachi Ltd., Japan) with 150 × 4.6 mm I.D.; eluant, (A) H_2O containing 0.1% formic acid and (B)

CH3CN containing 0.1% formic acid (a linear gradient was used from ‘95% A and 5% B’ to ‘30% A and 70% B’ for 90 min); temperature, 20 °C; and flow rate, 0.2 ml/min.

2.2.3 Cell culture and morphological observations

N18TG-2 cells were continuously cultured using our previously described methods[25] with slight modifications. Briefly, the cells were cultured in DMEM supplemented with 10% FBS. All cultures were maintained at 37°C under 10% CO_2. The filtrated crude drug solution was added to a 3 ml medium in a 35 mm dish at 30 µl to prepare a sample treated cells. Drug treatments were performed at the same time as the start of cultivation. The morphological observation to take photos was done by Nikon.

2.2.4 3-(4,5-di-methylthiazol-2-yl)-2,5-diphenyltetrazolium bromide, yellow tetrazole (MTT) assay

The MTT assay for quantifying cell viability was performed according to common methods. The cells were cultured in a 24-well plate. Drug treatment was performed at the same time of starting culture and at after 48 hrs. The assay was performed when non-treated control cells reached near confluent, usually 4 days after. In the assay, after the culture medium was removed, 300 µl of 0.5 mg/ml MTT in HBS solution was added, and the cells were further cultured for 3 to 4 h. Then, after removing the MTT solution, adding 300 µl DMSO, and leaving it for 10 min or more, a part (50 µl) of each solution was transferred to a 96-well plate, and the absorbance at 570 nm was measured by a microplate reader. The results were displayed as a percentage compared with the control cell value after subtracting the values for DMSO only from all the values.

2.3 Results

Figure 4 shows the color of the 10 mg/ml hot water extracted solution. The concentration of the solution was calculated by the recovery rate of the crude drug(s).

Tube 1) is CR, 2) is RR, and 3) is the solution when both are extracted together. All solutions were removed from the impurities by centrifugation followed by filtration (0.22 μm). Tube 4) is a mixture of equal amounts with 20 mg/ml solution of CR and RR after centrifugally filtered. The recovery rates were 1) 30%, 2) 20%, and 3) 20%. It was shown that the color of the solution was clearly lighter when mixed extraction at the crude drug stage, as compared with the color of the solution when CR and RR were extracted individually. It was also found that when the separately extracted solutions were mixed *in vitro*, a large amount of precipitate was generated and the color of the solution faded.

The 3D-HPLC spectrum of the solution is shown in Fig. 5. On the right side, the spectra isolated at 280 nm are shown with the same intensity for each solution for comparison. The strong peak seen at about 25 min in the CR is berberine. This peak disappeared almost completely when co-extracted with RR (Fig.5 (3)). In the case of post-mixing, the peak was significantly attenuated, although it remained slightly. Some of the peaks seen in RR alone (Fig. 5 (2)) also disappeared by mixed extraction. However, some peaks that disappeared by mixed extraction were not affected by post-mixing. Since the precipitate formed by the post-mixing could not be dissolved by various solvents, HPLC data could not be obtained.

Fig. 6 shows the morphological changes in N18-TG2 cells treated with each extract at three concentrations. Each extract was treated at the same time as the start of culture. Although it is a little bit difficult to know the real morphological change by the photograph, it was observed that CR and RR cause growth suppression or cell death depending on the concentration. The effect was not observed when both were extracted at the same time, but rather the simultaneous extracted solution treatment seemed to promote proliferation. The results of treating the supernatant and the precipitate obtained by mixing the CR and RR after extraction are shown in 4) and 5), respectively. In morphological observation, a morphology similar to RR alone was observed in the supernatant treatment, while when the precipitate was suspended and added (not dissolved), an effect similar to that of CR treatment alone was observed.

The MTT assay was performed for the purpose of quantifying the findings

obtained from morphological observation. A concentration of 10 μg/ml was used for the assay. Fig. 7 shows the results of evaluation when the drug was treated at the same time as the starting cultivation. The results observed in the morphological observation were supported by these data. Interestingly, it was found that cell proliferation was slightly promoted in the extract obtained by extracting CR and RR at the same time. On the other hand, when both were extracted separately and then remixed, data showing cytotoxicity or proliferation inhibition similar to that in the case of the single treatment of CR or RR was obtained. Thus, it was considered that some kind of chemical modification might have occurred only by simultaneous extraction.

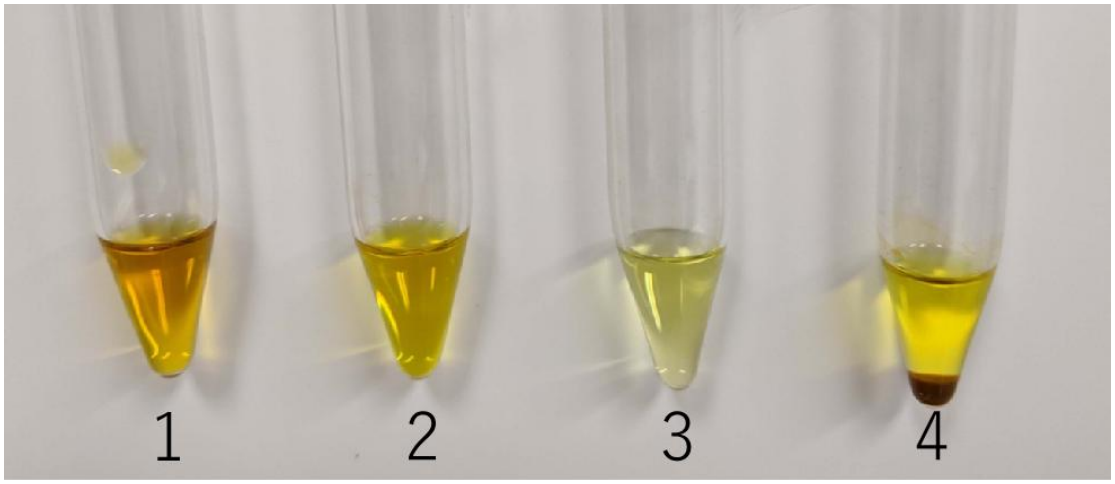

Fig. 4 Colors of hot water extracts of crude drugs

Each crude drug was extracted by hot water for 60 min and freeze-dried. They are dissolved at 10 mg/ml (estimated galenical) and sterilized with a 0.22 μm sterile filter after centrifugation (1-3). 1) *Coptidis Rhizoma* (CR), 2) *Rhei Rhizoma* (RR), 3) CR and RR co-extraction, 4) 20 mg/ml sterilized solution of CR and RR was prepared in the same manner as above, and then the equal amounts were mixed.

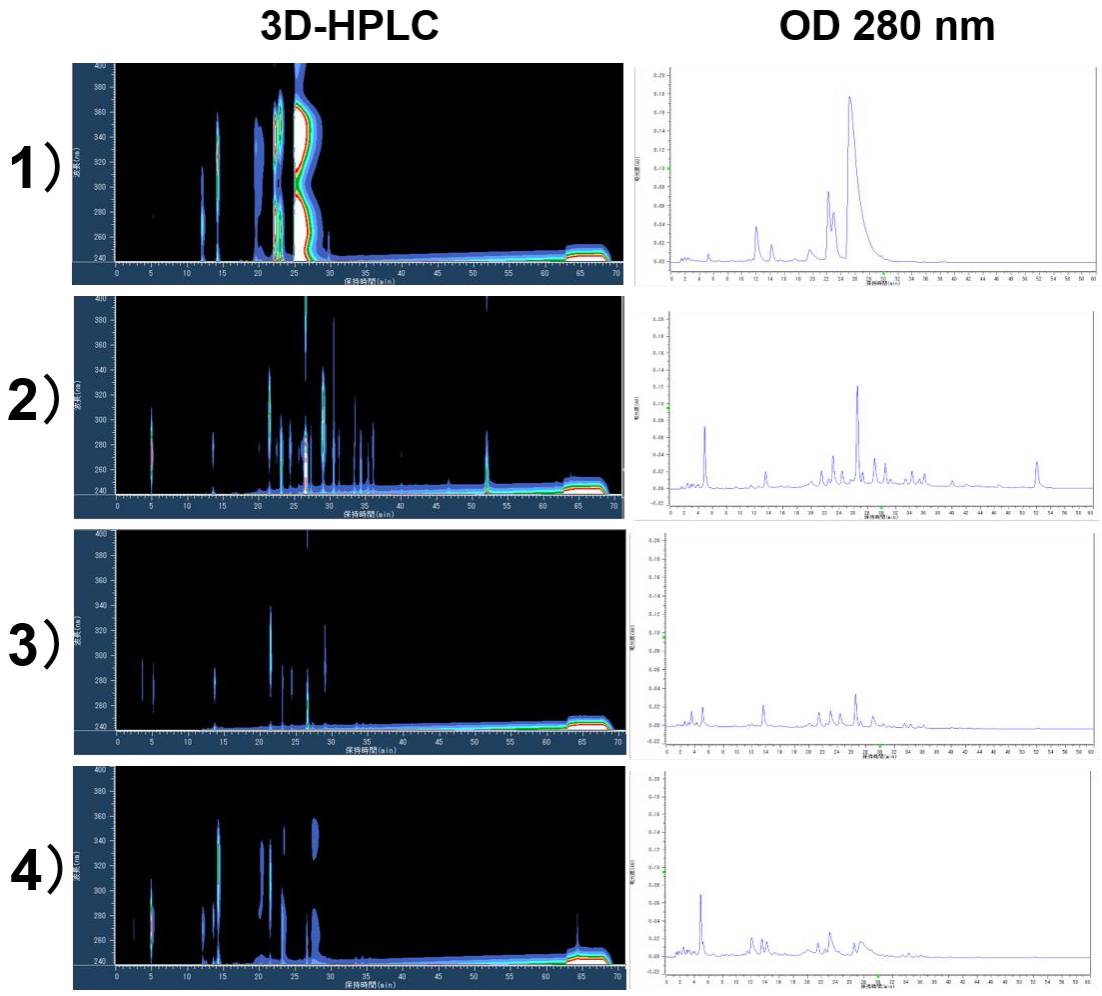

Fig.5 The 3D-HPLC charts of each extract

After diluting each solution shown in Fig. 1 to 1 mg / ml, the 3D-HPLC spectrum was obtained. 1) *Coptidis Rhizoma* (CR), 2) *Rhei Rhizoma* (RR), 3) CR and RR co-extraction, 4) the supernatant of post-mixed CR and RR.

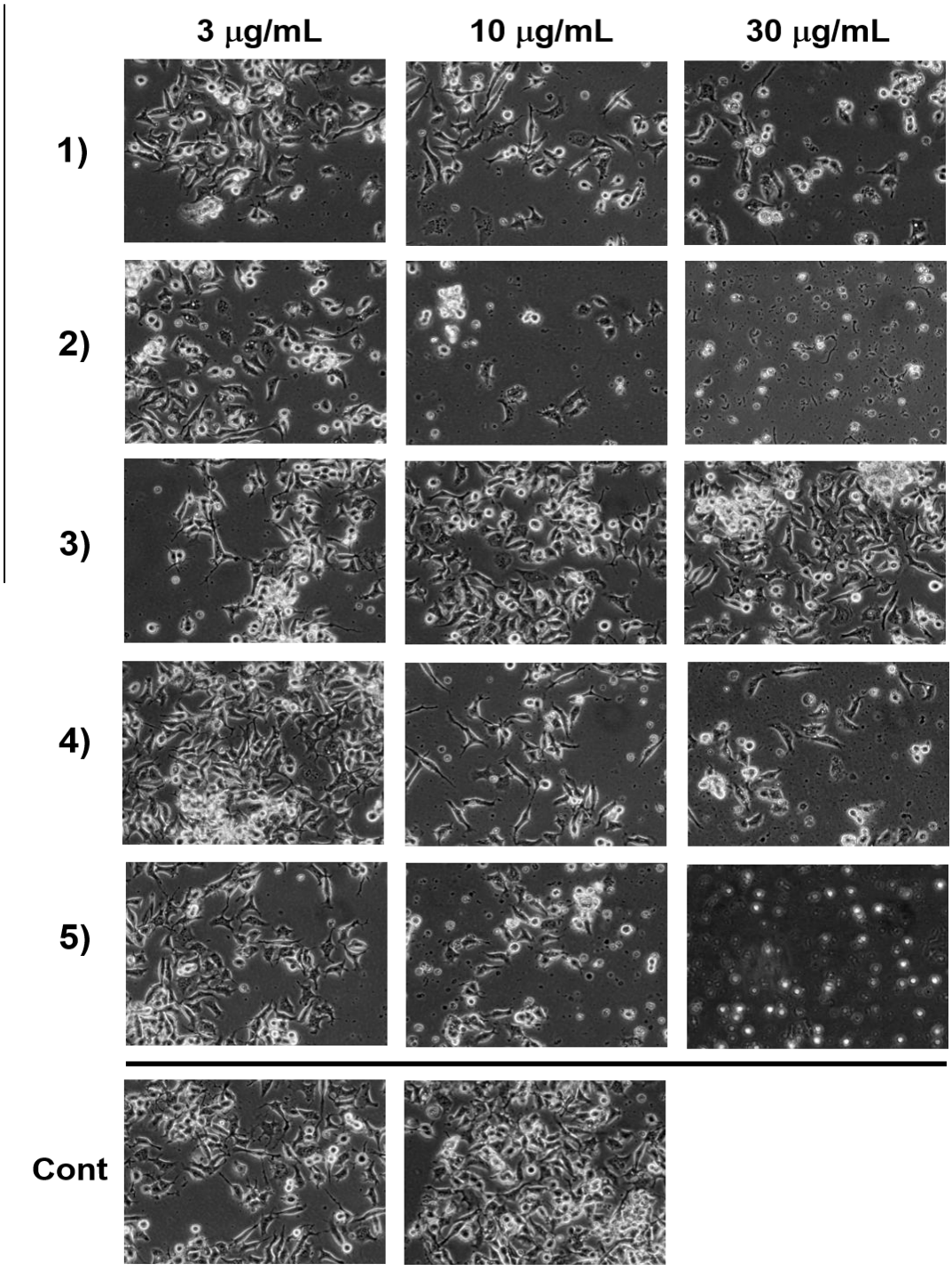

Fig. 6 Survival and proliferative changes by each extract treatment in N18TG2 cells (morphological photograph)

Each crude drug extract was treated at a concentration of 3 10, 30 μg/ml at the same time as the starting the culture. 1) *Coptidis Rhizoma* (CR), 2) *Rhei Rhizoma* (RR), 3) CR and RR co-extraction, 4) re-suspension of the precipitate of post-mixed CR and RR, and 5) the supernatant of post-mixed CR and RR. Control pictures showed both the dense and sparse areas (since it is difficult to ensure objectivity in morphological photographs, the results shown in Fig. 4 below quantified information on cell proliferation and survival by MTT assay).

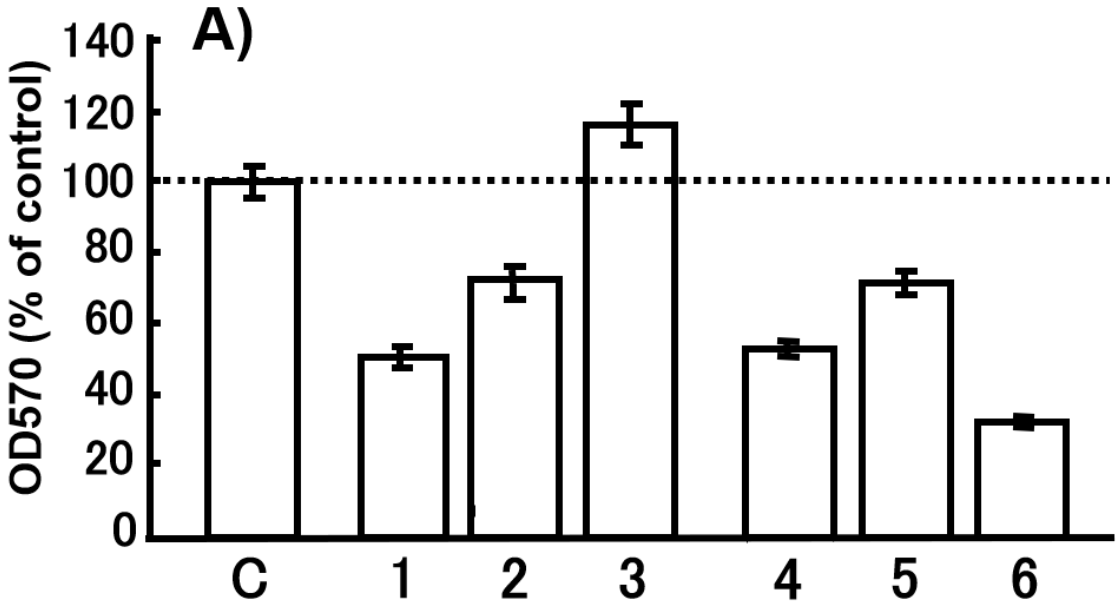

Fig. 7 Survival and proliferative changes by each extract treatment in N18TG2 cells (MTT assay)

Each herbal extract was treated at a concentration of 10 mg/ml at the same time as the start of cell culture. 1) *Coptidis Rhizoma* (CR), 2) *Rhei Rhizoma* (RR), 3) CR and RR co-extraction, 4) re-suspension of the precipitate of post-mixed CR and RR, 5) the supernatant of post-mixed CR and RR, and 6) the re-mixed of the supernatant and the precipitate which were obtained by post-mixing.

2.4 Discussion

These findings indicate the following possibilities.

1) Simultaneous extraction of RR and CR suppresses the cytotoxicity of each individual, and the resulting changes in the components of the mixture extract are involved in the background.

2) When the extracts of RR and CR are mixed after extraction, a precipitate is produced probably due to a physicochemical reaction. It is presumed that the precipitate contains berberine of CR, but it could not be confirmed because it could not be dissolved.

3) When the precipitate was resuspended and added to the culture medium, CR-like cell death was observed. On the other hand, in the supernatant after removal of the precipitate of the post-mixing, RR-like cell death was continuously observed, unlike the extract of simultaneous extraction. These results were also supported by the results of the MTT assay, although the experimental conditions were slightly different.

4) From the above results, it is considered that the composition of the components in the co-extract (A) is different from that of the supernatant obtained by mixing after individual extraction (B). There are two kinds of possibilities; one is a new component that suppresses the toxic factor of both may be synthesized in A during the reaction, and another is that the toxic component in B may have been removed in A during the not extraction. It will be an issue for future study to consider which one.

When studying the mechanism of action and evidence of Traditional Kampo Medicine/Wakan-Yaku (TKM) consisting of a combination of multiple herbal medicines, usually the prescription itself is regarded as one drug and research is conducted in model animals, etc., or an effective herbal medicine in an effective herbal prescription is used. Many studies have been also conducted so far by searching for the active compound in herbal medicine or by biochemically assaying the action of the main compound. However, in the search study of active compound, it is often the case that the effectiveness sometimes becomes invisible during the

sorting. In the classical theory of TKM, there is the idea of "herbal pair". The idea is that the combination of two crude drugs is the minimum unit of action. For example, the idea is that the combination strengthens or suppresses each other's actions, but there is still little evidence of research on that theory. The phenomenon caused by the combination of RR and CR reported here could be an example of experimentally proving the "herbal pair" theory.

It has been well known that RR alone has laxative and a kind of sedative effects (*Seinetsu* in Japanese). As for the active ingredient as a laxative, it has long been known that sennosides are decomposed into rhein by intestinal bacteria[26]. The difference in the intestinal bacterial flora of each individual person affects the RR action. Sennosides are also used as laxative medicines. Regarding the sedative effect, although it is known in animal experiments as the effect of the extract in Japanese references, the active components are not always clear. On the other hand, as for the action of CR, it is determined that berberine is contained in 4.2% or more as its main component according to the regulations of the Japanese Pharmacopoeia. And berberine itself is commercially available as an intestinal regulator. From the results of the HPLC in this article, the peak of berberine has almost completely disappeared due to the mixture of RR. It is highly possible that the effect of berberine is weakened when RR is present in the formulation.

As a TKM prescription in which RR and CR coexist, there is SST which consists of 3 crude drugs, these 2 and SR. SST is effective against bleeding (nosebleeds, hematemesis, etc.), and is also used for headaches, tinnitus, and increased blood pressure. OGT is also known to have the same effect. It is composed of 4 crude drugs, CR, SR, PC, and GF. RR is not contained. Since the classical references are different between these two (SST is in Kinki-Youryaku (Jin Gui Yao Lue) and OGT is in Gedai-Hiyou (Wai tai mi yao)), it can be interpreted that the prescriptions with almost the same treatment purpose were made by different classical authors and/or doctors. But, since OGT contains GF which has an effect on the digestive system, it can also be considered that the emphasis is on the action on the system. On the other hand, although SST contains RR, which is recognized as a laxative, the expected effect is

limited to the upper part of the body (in the Kampo concept, "JouShou"). It may be possible to think that CR is added to isolate it, and by forming a precipitate, the side effects of each other are reduced.

Regarding the effect of RR on cell molecular physiology, the effect of promoting BDNF gene expression has been reported[27]. Those findings, like this one on the base, are shown as the result of series of experiments on the effects of many herbal medicines using a cell system. The primary cultured neuronal cells from the brain of the transgenic mouse having the gene in which luciferase sequence is inserted downstream of the BDNF expression control sequence are used.

The report of the official paper shows that *Ginseng Radix* (GR) promotes BDNF expression[27], but the well-known ingredients of GR, many ginsenosides, did no effect, suggesting that the active ingredient is an unknown compound. Similarly, the action of RR and the additive/synergistic effect when combined with crude drugs also have been reported. Whereas this paper examines the possibility of component changes in the disappearance of RR/CR cytotoxicity when combined with, Fukuchi's report focuses on the fact that RR activates nerve cells through BDNF expression. In this study as well, the extract after simultaneous extraction of RR/CR tends to promote cell proliferation. It is also interested in the direction of activity and changes in the active compounds by mixing the two, including on changes in BDNF expression.

In present, this study includes multiple complex possibilities as summarized in the first part of the discussion, and in order to clarify them, further studies such as gene expression changes , related to cell death should be conducted. It is also necessary to clarify the difference between the physicochemical phenomena that occur between crude drug extracts and the biochemical reactions as an evaluation system. Anyway, this report may at least show that studies based on "herbal pair" in Kampo theory may bring interesting results that have never been seen before.

Chapter #3

Use of an electrophysiological technique for Stepwise detection of trace agonistic components of Hochuekkito in *Xenopus* oocytes injected with serotonin 2C receptor mRNA

3.1 Introduction

Kampo medicine is a Japanese variant of Chinese traditional medicine that involves the extensive use of herbs. Many prescriptions effect “mood”, and since they are prescribed according to the symptoms of a patient and individual body condition differences, they are considered to be a pioneer in “tailor-made medicine”. Studies on the mechanisms of action of each Kampo prescription will contribute to the discovery of novel concepts related to depression and the development of new and efficient antidepressants.

Kampo medicine has its systematic theory[28]. To date, studies on new drug development based on Kampo medicine have been based on analytical methods of modern science, achieved significant advances, and provided extensive evidence for the effectiveness of each Kampo prescription. However, the effectiveness of herbal medicine is markedly reduced by the process of fractionation, or the main components of active herbal medicine are replaced by research targets.

In the present study, based on the theories of Kampo and Wakan-Yaku, experiments were conducted using modern scientific techniques. The results obtained may provide novel hypotheses for *in vivo* anti-depressive mechanisms; however, further detailed studies are needed. Several Kampo prescriptions may exert anti-depressive effects, with each being prescribed based on unique theories. Typical prescriptions of Kampo medicine that may exert anti-depressive effects are “Huchuekki-to (HET): Bu Zhong Yi Qi Tang” and “Juzentaiho-to (JTT): Shi Quan Da Bu Tang”. We previously demonstrated that HET exerted anti-depressive effects in mice using a behavioral pharmacological method[29]. HET and JTT are composed of 10 herbal crude medicines, 5 of which are common to both. The 5 shared herbal medicines (abbreviated as Com5) do not have prescription names and are also included in “Kihito: Gui Pi Tang”. Kihito is known to exert effects on the brain and has the potential as an anti-dementia drug[30]. In the present study, we investigated the mechanisms underlying the stimulatory effects of HET on 5-HT2CR using electrophysiological techniques. We previously reported that HET exerted 5-HT2CR stimulatory effects[31]. Many antidepressants function as inhibitors of 5-HT2CR[32]. In

contrast, HET exerts agonistic effects on 5-HT2CR[31]. We previously proposed that the desensitization of 5-HT2CR is involved in the effects of HET on the serotonergic system to induce anti-depressive effects[33]. However, the present results suggest that this hypothesis is incorrect. The 5HT2CR stimulatory effects of HET were detected in extracts of the five herbal medicines that are present in HET only (Hoc5). Instead of following the hypothesis, we analyzed the contribution of each effective crude drug and its components by performing bioassays to assess electrophysiological activity. Although other trace active components may exist that were not examined in the present study, we identified a particular "trace component" that exerted stimulatory effects. Based on the present results and the mechanism of action of HET, we also considered this relationship according to the theory of Kampo medicine.

3.2 Materials and Methods

3.2.1 Extraction of Kampo prescriptions and galenicals

Approximately 50 g of each prescription or galenical was added to 900 ml of boiling water for 60 min. Galenicals were removed while the solution was still hot, and the extract was frozen using liquid nitrogen. The frozen extract obtained was freeze-dried.

All galenicals were purchased from Tochimoto Tenkai-do (Osaka, Japan). The contents of extracted prescriptions and galenicals as well as the Lot No. of each galenical and extracted yields are shown in Table 3. The weight values of each galenical, which constituted prescriptions, are listed on the left side of Table 3.

Table 3　Galenical list that make up the Kampo prescription used in this study

g	g	Name	Lot.No	yiels(%)	Producted Area	
2		Citrus unshiu Markovich (CM)*	007807004	34.5	Japan	Shikoku
2		Zizyphi Fructus (ZF)	007108004	56.0	China	
2		Zingiberis Rhizoma (ZR)	005808001	10.5		
2		Bupleuri Radix (BR)	004208001	12.8	Japan	Nara
1		Cimicifugae Rhizoma (CR)	006007001	26.1		
		(all 5 of above (Hoc5))		25.2		
4	3	Ginseng Radix	008607037	20.0	Korea	
4	3	Atractylodes Rhizoma	009307015	37.8	China	
3	3	Astragali Radix	001007006	22.8	Japan	
3	3	Angelicae Radix	008007016	41.3	Japan	Yamato
1.5	1.5	Glycyrrhiza Radix	002007034	28.6	China	Northwest
		(all 5 of above (Com5))		33.3		
	3	Poria	009508003	*	Korea	
	3	Rehmanniae Radix	005007023	*		
	3	Cnidii Rhizoma	006207005	*		
	3	Paeoniae Radix	005308002	*	Japan	
	3	Cinnamomi Cortex	002807017	*	Vietnam	
		(all 5 of above)				
Hochuekkito (HET)				27.9		
	Juzentaohoto (JTT)			25.2		

Lot number at the place of production and source, and the recovery rate is shown in this table. In this article, all extract concentrations are shown in herbal equivalents based on these recover rate. Individual extraction was not performed for the five herbal medicines specific to JTT. Citrus unshiu Markovich (CM) is actually the mixture of Citrus unshiu Markovich and Citrus reticulate Bianoco. This table will also help readers to understand the abbreviations in the text.

HET and JTT are combinations of 10 galenicals, with five out of the 10 galenicals being common to both (Com5). Com5 and the other 5 galenicals in HET (Hoc5) were extracted and freeze-dried. The gross galenical weights of the extracts for HET, JTT, Com5, and Hoc5 were 49, 57, 46.5, and 45 g, respectively. The weight of Com5 was assessed based on the ratio that constitutes HET.

Before the extract was applied to the oocytes that expressed 5-HT2CR on the cell surface, the freeze-dried extract was resolved using the buffer for the electrophysiological experiment and then centrifuged to remove insoluble matter.

3.2.2 Three-dimensional high-performance liquid chromatography (3D-HPLC) analysis of extracts.

Each extract solution (10 mg/ml) of the supernatant obtained by centrifugation followed by filtration through a 0.22-μm membrane filter was subjected to a 3D-HPLC analysis (20 μl). The HPLC apparatus (Hitachi Ltd., Japan) consisted of a pump (L-2130) with analysis system software (Elite LaChrom), a photodiode array detector (UV 230-400 nm, L-2455), system controller, auto-injector (L-2200), and column oven (L-2300). HPLC conditions were as follows: column, LaChrom Ultra C18 (5 μm, Lot No. 21D5-011; Hitachi Ltd., Japan) with 150 × 4.6 mm I.D.; eluant, (A) H_2O containing 0.1% formic acid and (B) CH_3CN containing 0.1% formic acid. A linear gradient was used from '95% A and 5% B' to '30% A and 70% B' for 90 min. The temperature of the column was controlled at 20°C. The flow rate was 0.2 ml/min.

3.2.3 Synthesis of 5-HT2CR mRNA and injection into Xenopus oocytes.

pBluescript II KS(-) vectors (approximately 3.0 kbp) with a rat 5-HT2CR cDNA insert (approximately 3.0 kb) were used as a template to make in vitro synthesized mRNA. The vector was transformed into DH5 Escherichia coli to enhance the amount of mRNA by the estimated method. The vector obtained with 5-HT2CR cDNA was linearized with XhoI at 37°C for 60 min. The linearized vector (250 ng) was incubated with T7 RNA polymerase and the mCAP analog in the reaction buffer of the transcription kit (Stratagene) to make 5-HT2CR mRNA in vitro. Products were extracted with phenol/chloroform and precipitated in ethanol and sodium acetate.

Synthesized 5-HT2CR mRNA (100 ng) was injected into Xenopus oocytes isolated from female Xenopus laevis. X. laevis were anesthetized in ice water, and a lobe of the ovary was dissected and placed in sterile modified Barth's solution (MBS: 88 mM NaCl, 1 mM KCl, 0.41 mM $CaCl_2$, 0.33 mM $Ca(NO_3)_2$, 0.82 mM $MgSO_4$, 2.4 mM $NaHCO_3$, and 7.5 mM HEPES-NaOH, pH 7.6). Oocytes were then isolated manually and defolliculated by incubation in 1.5 mg/ml collagenase (type IA; Sigma,

St. Louis, MO, USA) at 20°C in a calcium-free MBS solution. Synthetic mRNA was injected into oocytes using a microinjector (Drummond, Broomall, PA, USA), which were then incubated in MBS containing 2.5 units/ml penicillin and 2.5 μg/ml streptomycin at 18°C.

It has long been confirmed that Xenopus oocytes do not naturally express 5-HT2CR, ion channels, or many receptors[8]. Muscarinic receptors are only expressed in the follicular cells and if the follicle cannot be removed, oocytes react to acetylcholine[35]. In addition, Xenopus oocytes are classically used for cloning and functional analysis of ion channels and receptors because it efficiently translates injected mRNA[36]. In the case of 5-HT2CR expression, responsiveness to 5-HT appears about 18 hours later from injected mRNA, and the responsiveness usually continues until 3 to 4 days[34].

Since Xenopus is a poikilotherm, it becomes completely anesthetized by soaking it in ice water. After confirming the reflex reaction has disappeared, open the base of the foot about 1-2 cm and remove the oocytes. Xenopus then sews the open area with a suture and uses surgical adhesive to waterproof the wound. Xenopus awakens when it is placed in ice-free water overnight during the water temperature gradually returns to room temperature. After confirming that Xenopus behaves perfectly, return it to the aquarium. One Xenopus can use several times. From the above, the burden of Xenopus surgery is extremely light, and normal behavior is restored immediately after surgery. In light of the Code of Ethics for Animals, it can be evaluated as a very minor burden, however, Xenopus is equivalent to fish and is not subject to the "Animal Experiment Code of Ethics"

3.2.4 Electrophysiological recording

Responses to 5-HT were recorded using a two-electrode voltage-clamp amplifier at a holding potential of −60 mV. Oocytes were positioned in a 50-μl chamber and continuously perfused with MBS solution at approximately 1 ml/min at room temperature (less than 25°C). Drugs were applied by changing the perfusing solution to the drug-containing buffer in the case of extracts of the Kampo prescription or

galenicals. When an isolated compound was applied, one drop of the MBS solution (approximately 20 μl) was directly dropped from the micropipette into the chamber. Data were recorded and digitized for analyses (MacLab, AD Instruments, Castle Hill, NSW, Australia).

3.2.5 LC-MS analyses

LC-MS analyses were performed with a Shimadzu LC-IT-TOF mass spectrometer equipped with an ESI interface. The following ESI parameters were used: source voltage 3.5 kV (negative mode), capillary temperature 200ºC, and nebulizer gas 1.5 l/min. The mass spectrometer was operated in the negative ion mode scanning from m/z 100 to 2000. A Waters Atlantis dC18 column (2.0 mm i.d. × 150 mm) was used and the column temperature was maintained at 40ºC. The mobile phase was a binary eluent of (A) 5 mM ammonium acetate solution and (B) CH_3CN under the following gradient conditions: 0-30 min linear gradient from 10 to 100% B, 30-40 min isocratic gradient at 100% B. The flow rate was 0.2 ml/min.

3.3 Results

We previously reported that many types of antidepressants inhibit 5-HT2CR, and based on these findings, Kampo medicine that exerts anti-depressive effects is anticipated to exhibit similar inhibitory activity. Contrary to expectations, HET, the anti-depressive effects of which were experimentally demonstrated in a depressive model animal, exerted significant stimulatory, not inhibitory effects. Similarly, in this experiment, HET at 3 mg/ml generated a strong activation signal in *Xenopus* oocytes expressing 5-HT2CR (Fig. 8). HET is composed of 10 types of herbal medicines, 5 of which are common to JTT and Kihito. The five types specific to HET (Hoc5) exerted strong 5-HT2CR stimulatory effects, whereas Com5 and JTT did not (Fig. 8). The stimulatory effects of Hoc5 were dependent on its concentration (Fig. 8 inset).

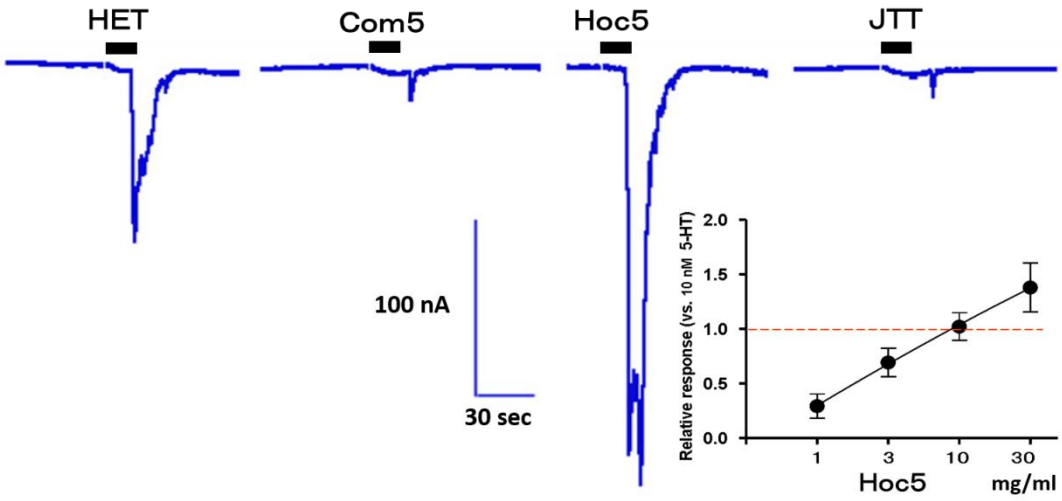

Fig. 8 Effects of HET, JTT, and component crude drugs, Com5 and Hoc5, on 5-HT2CR-induced current responses in *Xenopus* oocytes injected with synthetic 5-HT2CR mRNA.

Xenopus oocytes were injected with 5-HT2CR mRNA and the voltage was clamped at -60 mV. Each extract was added to perfusing solution. The concentration of each extract was 3 mg/ml (estimated galenical weight). The inset shows the concentration dependency of the Hoc5 application relative to the current intensity induced by 10 nM 5-HT. Refer to Table 1 for each abbreviation.

Since Hoc5 exerted strong 5-HT2CR stimulatory effects, the activities of each of the five herbal medicines were examined. Fig. 9 shows the current responses of each herbal medicine at 3 mg/ml. Cimicifuga Rhizoma (CR) exerted strong stimulatory effects with an EC50 value of 0.9 mg/ml and a confidence interval (CI) value of 0.48–1.65 mg/mL. Stimulatory effects were also observed with Citrus unshiu Markovich (CM) but were weaker with an EC50 value of 4.0 mg/ml and CI value of 1.73–9.29 mg/mL. Significant activation was not observed for the three other crude extracts.

Since CR activated 5-HT2CR, its components were separated by 3D-HPLC, and activity was examined by direct application to oocytes. The 3D-HPLC chart of CR is shown in Fig. 10A, and that extracted at 274 nm in Fig. 10B. The fraction showing large peaks under these HPLC conditions was purified. After the HPLC solvent was removed by evaporation, CR was newly dissolved in a small amount of HBS buffer and applied to cells. Therefore, it was not possible to quantify its exact concentration. Strong activation was observed in fraction No. 12. There was no activity in the large peak after an elution time of 20 min (data not shown).

The molecular weight of the substance of peak No. 12 was assessed by LC/MS. The LC results on CR at 280 nm are shown in Fig. 11A. The absorption wavelength of peak P2 in Fig. 11A is shown in Fig. 11B and was similar to the spectrum in Fig. 10. The molecular weight of the substance was estimated to be 283.1393 (Fig. 11C); however, it was not possible to estimate the material from that value. Although identification by NMR was attempted, it was not successful because the required amount with sufficient purity was not obtained.

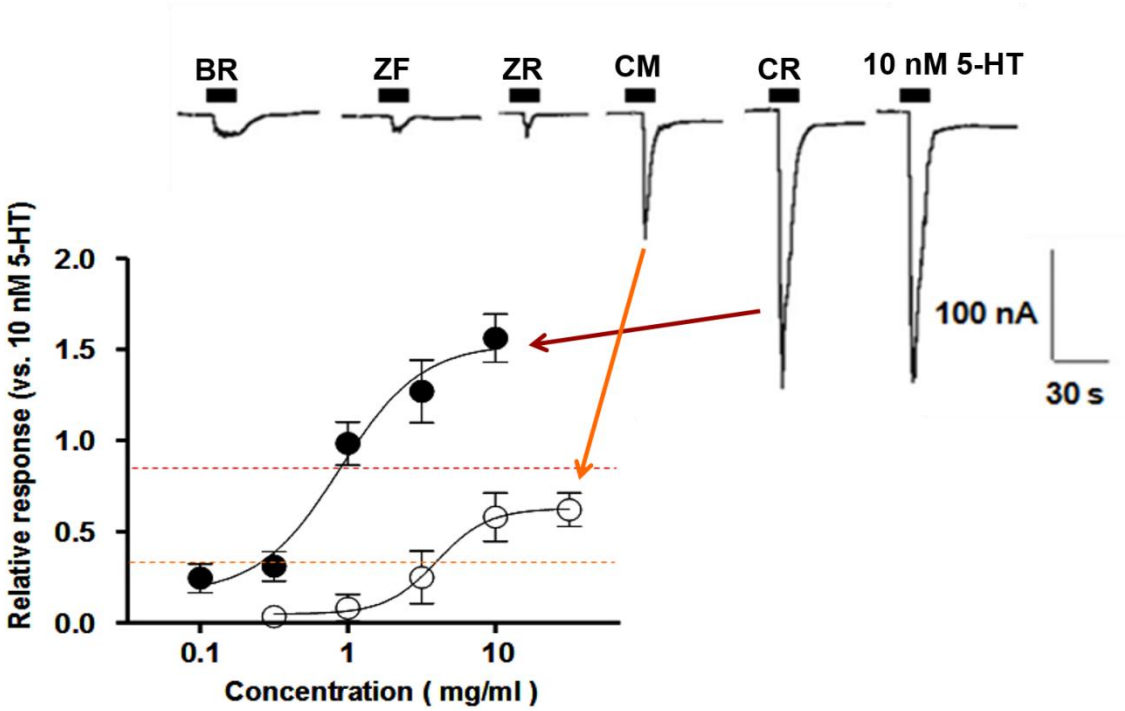

Fig. 9 Effects of each extract of Hoc5 component crude drugs on 5-HT current responses in Xenopus oocytes injected with synthetic 5-HT2CR mRNA.

Xenopus oocytes were injected with 5-HT2CR mRNA and the voltage was clamped at -60 mV. Each extract was added to perfusing solution. The concentration of each extract was 3 mg/ml (estimated galenical weight) in the current response figure. The lower figure shows the concentration dependency of CR and CM relative to the current intensity induced by 10 nM 5-HT. The EC50 values of CR and CM were 0.9 and 4.0 mg/ml, respectively. Refer to Table 1 for each abbreviation.

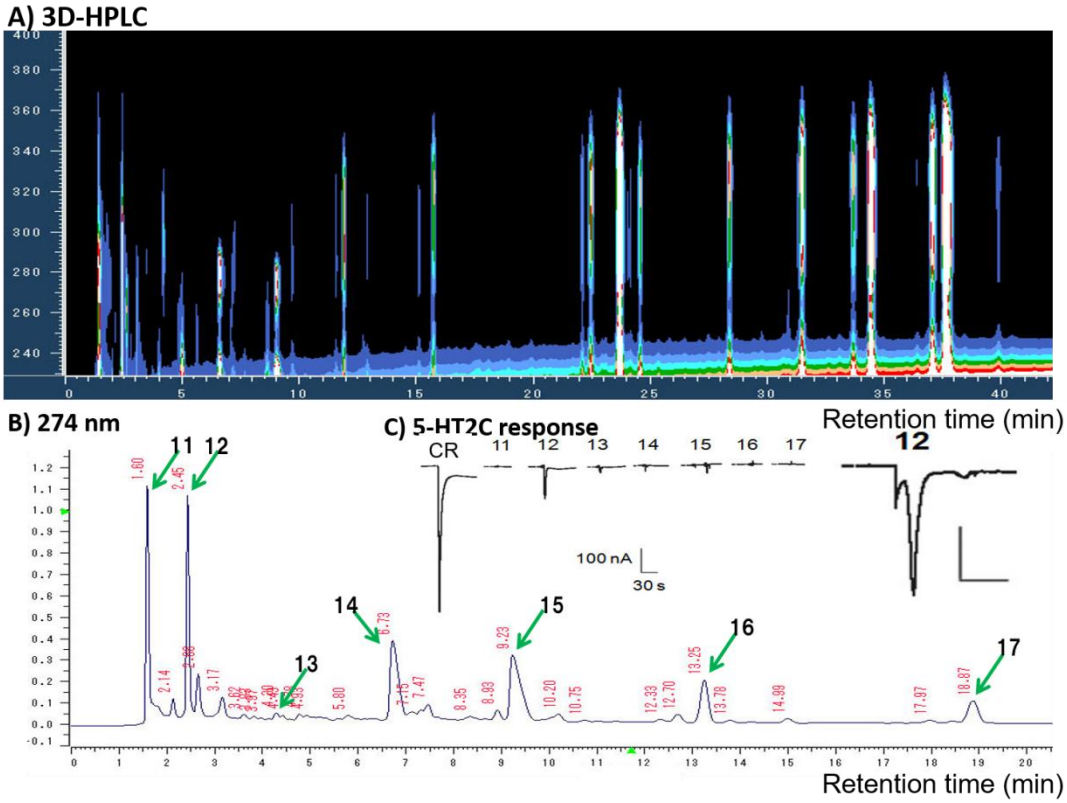

Fig. 10 Component analysis and fractionation of the CR extract by 3D-HPLC and 5-HT2CR current responses by each fraction

A) 3D-HPLC chart using the *Elite LaChrom* system (Hitachi, Japan); a color change indicates the height of the signal at that wavelength and outflow time. B) An isolated chart at 274 nm from 3D-HPLC and C) electrophysiological experiments for each isolated fraction using the same system described in Figs. 8 & 9.

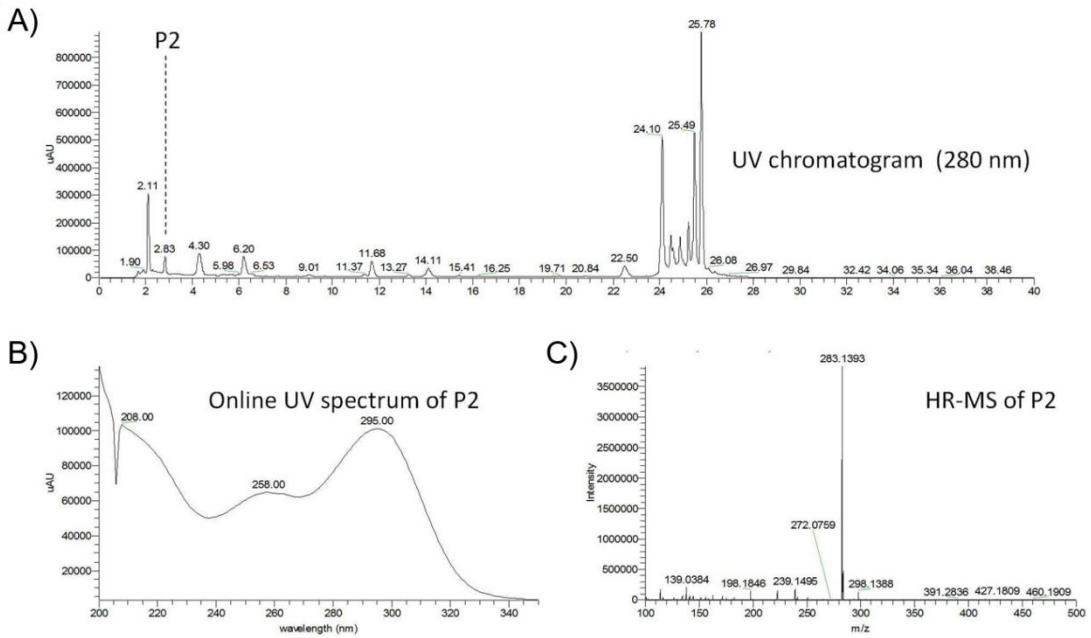

Fig. 11 LC-MS analyses of peak No. 12 in Fig. 3

A: The chromatogram at 280 of CR; the UV spectrum of peak P2 in Fig. 11A was equivalent to peak No. 12 in Fig. 10. B: The UV spectrum of peak P2. C: A MS analysis of the molecular weight of peak P2.

3.4 Discussion

The active component responsible for the 5-HT2CR stimulatory effects of HET was examined, and a trace amount of a component with a molecular weight of 283.1393 was obtained. Since the amount of the component was very small, the structure was not elucidated by NMR.

The effectiveness of herbal extracts has been successfully assessed to date by considering the main components as active and contributing factors. However, we demonstrated that similar to aromatic components, some agonistic components may exert an effect even when only a small amount is present. While limited evidence is currently available to support this, some studies indicated that the aroma emitted during the extraction of Kampo is also effective as a treatment. An assessment of electrophysiological activity is a highly sensitive method that may be used in the future to identify active and stimulatory trace components from novel perspectives. Although the electrophysiology method itself can detect both agonistic and antagonistic effects, when electrophysiology is used as a method for evaluating the active ingredient, the agonist is effective as an evaluation method because it shows a response even in a small amount, but in many cases, it seems that a large amount is needed to consider an antagonistic effect. We believe that the electrophysiological method, which has well sensitivity and is characterized by a dynamic reaction, is suitable for bioassay-like-purification and detection of agonists, and it is thought that the detection and analysis of agonist components will proceed by using this method.

The primary aims of the present study were to identify the active components of HET that exert anti-depressive effects and to elucidate the mechanisms underlying these effects. Although we were unable to directly attribute anti-depressive effects to the “trace component”, we successfully identified the active component that exhibited a strong response even when it was present at a small amount.

The active component appears to directly affect the function of the digestive system, not the brain and is related to another effect of HET, its enhancement of digestive function. The trace molecule identified may stimulate neurons that transmit

activity to the brain. In terms of Kampo medicine, HET is an effective treatment for mild depression, and JTT is more effective than HET when the mood is further depressed. JTT, which is considered to exert stronger anti-depressive effects, did not affect 5-HT2CR in this experimental system. Com5 may contain some components that are active in the brain and reach their target site through absorption and metabolism. This may explain the effects of Kihito in the brain because it also contains Com5[4]. While we are unable to fully elucidate the underlying mechanisms, we previously reported that the expression levels of BNIP-3 mRNA were increased by HET in another experimental system using cultured neuronal cells[37-39]. This is currently being more intensively examined by our group, including the site of expression in the brains of small animals using MRI[40].

The mechanism of action of ghrelin has been attracting increasing attention as the underlying molecular mechanism of Rikkunshito (RKT): Hsiang Sha Lu Chun Tzu Tong, a type of Kampo medicine[41,42]. Ghrelin is a factor involved in appetite and is also associated with the function of 5-HT2CR[43-45]. HET and RKT have similar herbal medicine compositions and exert similar effects on the digestive system. While RKT acts on the symptoms of an upset stomach by activating the stomach and improving digestion, HET functions by resolving malfunctions in the digestive system, such as diarrhea. Neither CR nor Bupleuri Radix (BR) is a component of RKT; however, they are known as a "herb pair" in Kampo medicine and are considered to play a critical role in the effects of HET. CR and BR both constitute Hoc5 and act on the digestive system. They also exert positive systematic effects according to the concept of Kampo medicine. Therefore, they may contribute to the unique effects of HET on qi by acting on the digestive system and subsequently stimulating the nervous system. Although BR alone does not affect 5-HT2CR, it may exert an effect in the presence of CR. In future studies, we will investigate differences in the effects of BR with and without CR, as well as its functions in the digestive system and brain, i.e., by gene expression or magnetic resonance imaging.

In the present study, we used an electrophysiological bioassay method to identify the components responsible for the 5-HT2CR stimulatory effects of HET, and, as a

result, discovered an unknown component with a molecular weight of 283.1393. Although it is unlikely that this component alone is solely responsible for the activation of 5-HT2CR by HET because CM also acts on 5-HT2CR, these results indicate that ultra-trace components, not the main component, are involved in the responses of Kampo medicine. The present study showed that ultra-trace components also have high “biofunctional effects” in Kampo medicine and play a role in the specificity of prescriptions. In the future, the discovery of these “ultra-trace active ingredients” will promote research on Kampo and Wakan-Yaku medicines.

Chapter #4

Clarifying the pharmacological mechanisms of action of Shenfu Decoction on cardiovascular diseases using a network pharmacology approach

4.1 Introduction

Cardiovascular diseases (CVD) are the leading cause of death worldwide[46]. The application of Traditional Chinese Medicine (TCM) to the treatment of COVID-19 has been examined and it is now used in clinical settings in China; however, there is currently insufficient evidence for its global expansion[47]. The use Chinese herbs to prevent various diseases, including CVD, has been investigated[48]. Bioinformatics has become an important tool in the medical field because it effectively reveals relevant knowledge hidden in big data, thereby promoting the discovery of integrated information[49]. The core concepts of TCM and network pharmacology are similar[50], with multicomponent therapy and network targets as the basis for TCM[51] and a molecular network for network pharmacology[52]. Although many methods may be applied in investigations of the mechanisms of action of TCM in the treatment of CVD, network pharmacology is widely accepted and used because it provides a broad perspective[53].

The cardioprotective effects of Shenfu Decoction (SFD) have been demonstrated. It has been shown to inhibit myocardial cell apoptosis in rats with heart failure[54] and protect against myocardial ischemia-reperfusion injury[55]. Metabonomics[56] and proteomics also revealed its protective effects against heart failure. Moreover, the chemome[57] and serum pharmacochemistry[58] of SFD have been characterized.

The rapid development of network pharmacology has contributed to a more detailed understanding of and insights into the mechanisms by which TCM exerts its effects on complex diseases[59]. Therefore, in the present study, network pharmacology was used to elucidate the complex molecular mechanisms of action of SFD in the treatment of CVD. We initially treated cells with the corresponding drugs and then subjected samples to a gene chip analysis. Potential targets were mapped to the corresponding database for a bioinformatic analysis, which provides a bridge for clarifying the mechanisms by which SFD exerts its cardiovascular protective effects.

4.2 Methods and Materials

4.2.1 Preparation of the SFD extract

Two Chinese herbal medicines, ginseng and aconite, were selected at a ratio of 2:1 to prepare SFD. Forty-five grams of Chinese herbal medicine was added to 900 ml of water to prepare SFD. The hot water extract obtained was then freeze-dried. Tochimoto Tenkai-do (Osaka, Japan) provided Panax ginseng CA Meyer (Lot No. 008607037) and Aconitum carmichaeli Debeaux (Lot No. 032017001) for the present study.

4.2.2 Cell culture and treatment

The rat cardiac myoblast cell line H9C2 was purchased from the European Collection of Authenticated Cell Cultures (ECACC: Salisbury, England). According to the information provided in the instructions, the medium selected was complete DMEM containing 10% fetal bovine serum and culture conditions were 37°C in a 10% CO_2 humidification box. Three groups were included in the present study: 1) Control group; 2) Model group; 3) SFD treatment group. Doxorubicin (DXR: Sandoz, Yamagata, Japan: Lot No. HY8542)-mediated H9C2 cytotoxicity was induced as previously described[60]. Following a treatment with SFD or vehicle for 24 hours, cells were incubated with or without DXR (2 μM) for another 24 h to induce cardiotoxicity.

4.2.3 RNA extraction

Total RNA was extracted from H9C2 cells using TRIsure (Bioline, Luckenwale, Germany), and genomic DNA was removed by DNase I (TaKaRa, Ohtsu, Japan), according to the manufacturers' instructions. The quantity and quality of RNA were assessed using a 2100 biological analyzer (Agilent, CA, USA). High-quality RNA samples (OD260/280 = 1.8–2.0 RIN ≥7) were used to construct sequencing libraries.

4.2.4 Microarray data

Three samples each from the Control, Model, and SFD treatment groups were hybridized with an SurePrint G3 Mouse Gene Expression v2 8×60K Microarray at 65℃ for 14 h to analyze expression levels using microarray methods.

4.2.5 Identification of differentially expressed genes (DEG)

DEG among Control, Model, and SFD treatment group samples were screened using Venn diagrams. |log2FC|≥ 1 was considered to be significant.

4.2.6 Protein-protein interaction (PPI) network construction and a module analysis

As a classic PPI network construction tool, the STRING database[61] was employed in the present study, and the standard for significance was a combined score >0.4. In the module analysis after network construction, Cytoscape's plug-in Molecular Complex Detection (MCODE) was selected[62]. The selection of key hub genes relied on the following three characteristics: "degree", "intermediateness", and "intimacy". The criterion selected in the present study was that these three characteristics were higher than the corresponding median values.

4.2.7 Enrichment analyses of candidate genes

WebGestalt is a functional enrichment analysis web tool[63]. The WebGestalt online database, as a popular biological analysis database, facilitates analyses of the functions of DEG. The standard for statistical selection is $P<0.05$. WebGestalt's over-representation enrichment analysis method is used to identify and analyze potential targets. As a gene annotation tool, a gene ontology analysis involves a functional analysis that includes molecular function, biological pathway, and cell component analyses[64]. The Kyoto Encyclopedia of Genes and Genomes (KEGG) is a well-known path analysis tool[65].

4.2.8 Co-expression analysis

GeneMANIA is a user friendly and flexible web server that is used to generate hypotheses about gene functions, analyze gene lists, and assess gene priority for a functional analysis[66]. The database comprises many functions, such as a physical interaction analysis, co-expression predictions, co-localization, and a genetic interaction analysis. These functions were used in the present study to construct the SFD gene network.

4.3 Results and discussion

4.3.1 Identification of DEG

Gene expression datasets were obtained [SET01: Control group vs Model group, SET02: Model group vs SFD treatment group]. After standardizing microarray results, DEG were identified. The overlap between the two data sets contained 1,134 genes, as shown in the Venn diagram (Fig. 12). Forty-six genes were upregulated in the model group compared with the blank group and were further upregulated after drug treatment. Sixty genes were down-regulated in the model group compared with the blank group, but were upregulated after drug treatment. Twenty-eight genes were down-regulated in the model group compared with the blank group, and further down-regulated after drug treatment. A total of 1000 genes were up-regulated in the model group compared with the blank group, but were down-regulated after drug treatment.

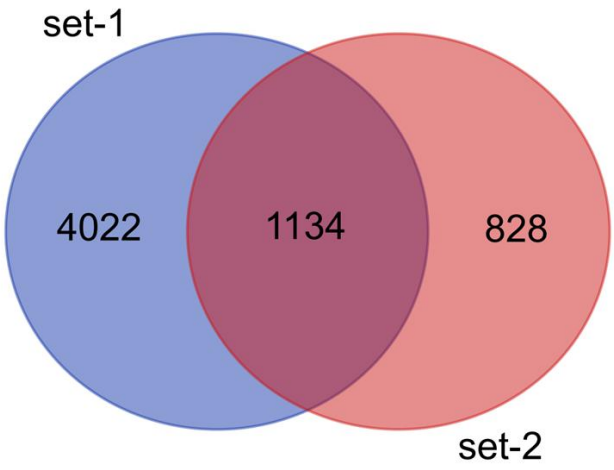

Fig. 12. Venn diagram of the number of genes showing treatment-induced changes in expression.

Differentially expressed genes with a fold change ≥2 in microarray data were selected among mRNA expression profiling set-1 (control vs DXR) and set-2 (DXR vs SFD + DXR). The two data sets show the overlap of 1134 genes.

4.3.2 Prediction analysis of pharmacological mechanisms based on network pharmacology and module identification

Based on the STRING database, a PPI network was constructed with a combined score >0.4 (Fig. 13A), with 908 nodes and 1822 edges together forming a large biological network (Table S2). The network module (cluster or community) is the sub-network that is generally defined. The characteristic of the sub-network is that connections between its nodes are more reliable and firmer than the loose connections in the remainder of the network. In other words, a module is a collection of many nodes with a high degree of correlation. Module identification is important because the amount of crucial information extracted from the network is limited, and it facilitates the discovery of vital information by researchers that may be hidden in the network. Network modules have been utilized in network pharmacology-based TCM studies to reveal the combination rule of TCM herbal formulae[67], chemical modules with similar structures[68], and proteins with equivalent functions[69]. Multi-component and multi-objective analyses have always been a difficult and hot issue in TCM research. Network modularity is based on the "Law of Similarity Attraction" analysis method, which is a precise and powerful method to describe the complexity of TCM. Figure 13B shows the PPI network of the 293 nodes and 1083 edges obtained with a degree of between 5 and 42 inclusive. Although the scope of Figure 13B is smaller than that of Figure 13A, it is also difficult to identify target molecules. Therefore, as shown in Figure 13C, we established a novel network to identify target molecules more accurately. In Figure 13D, the heat map illustrating the differentially expressed genes in three groups.

Through the plug-in MCODE, the most significant module was obtained from the PPI network with 9 nodes -36 edges. The names, abbreviations, and functions of these hub genes are shown in Table S3. We then calculated three topological features ("degree", "intermediateness", and "compactness") of the candidate molecules. According to the screening criteria described above, three candidate molecules were identified ("degree" > 9, "betweenness" > 0.000111031, and "closeness" >

0.27027027), as shown in Table S4. All 9 genes were associated with the functions of the ubiquitin-proteasome system (UPS), which is important in the etiology of CVD.

UPS plays an essential role in the many mechanisms involved in mediating the degradation of intracellular proteins[70]. Ubiquitination and proteasome-mediated degradation are the two main steps of UPS-mediated proteolysis. In other words, ubiquitination is a series of enzymatic reactions in cells[71]. Dysfunctional UPS has been implicated in the development of many CVD (such as atherosclerosis, myocardial ischemia, hypertrophy, and heart failure)[72].

One of the main factors restricting the use of anthracycline antibiotics (such as DXR) in clinical settings is cardiotoxicity[73]. DXR-induced cardiotoxicity may increase the activity of UPS[74]. Sishi et al. also demonstrated that chymotrypsin-like activity in the heart was inhibited by DXR, while the ubiquitination of proteins was simultaneously increased[75]. Dysfunctions in the ubiquitin-proteasome pathway (UPP) have also been shown to play an important role in CVD[76]. The overactivation of UPP has been identified as a contributing factor to the development of acute cardiotoxicity as an adverse event of the administration of anthracyclines.

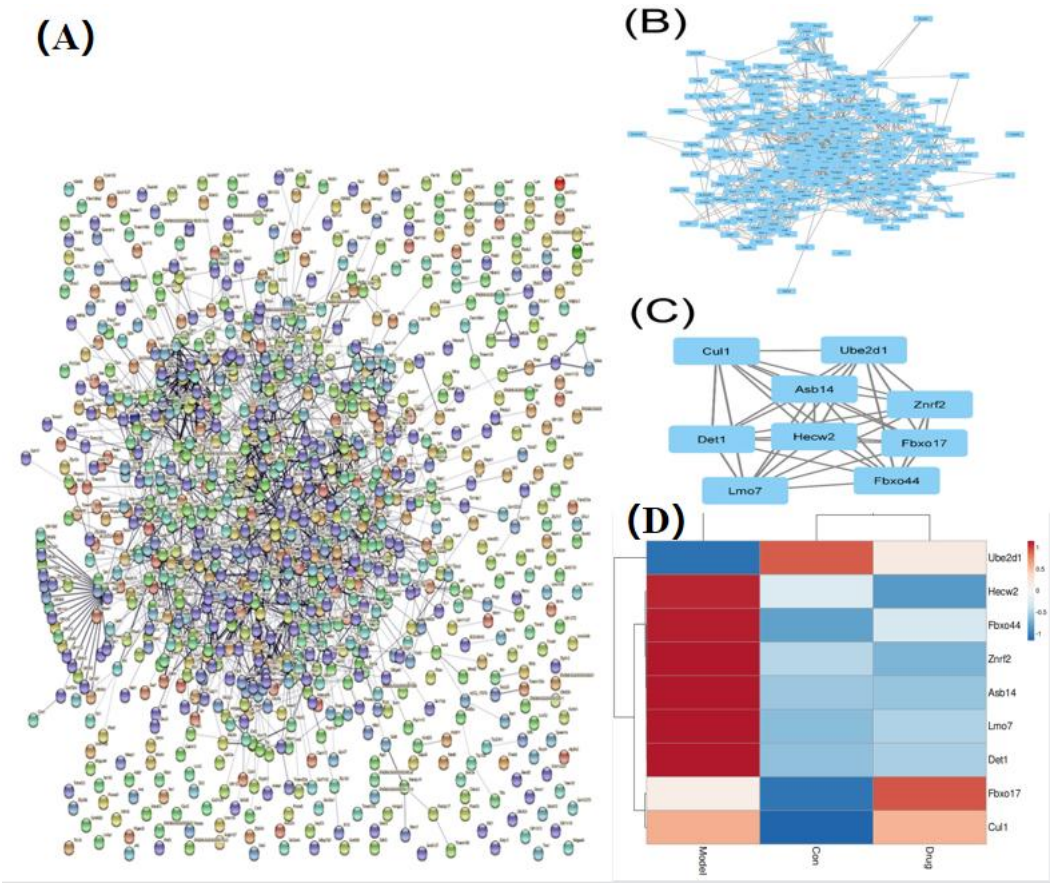

Fig. 13. PPI network structure and module identification

(A) PPI network of differentially expressed genes (DEG). (B) The PPI network of DEG was constructed using Cytoscape. (C) The most significant module with 9 nodes and 36 edges was obtained from the PPI network. (D)The heat map illustrating the differentially expressed genes in three groups.

4.3.3 Enrichment analyses of hub genes

The biological process, cellular composition, molecular function, and pathway of the target protein were analyzed by the WebGestalt database. The results obtained (Fig. 14A) indicated that hub genes were significantly involved in a number of biological processes, including metabolic processes, biological regulation, cellular component organization, multicellular organismal processes, developmental processes, localization, cell communication, responses to stimuli, cell proliferation, and multi-organism processes. According to the classification of cellular components, the protein was located in a protein-containing complex, the nucleus, and endomembrane system. The molecular function of the target protein involved transferase activity and protein binding. To further confirm that the biological processes involved in the treatment of myocardial injury by SFD play a role in the corresponding pathological events in the course of disease progression, we used the KEGG database for a pathway enrichment analysis. Seven important signal pathways were obtained ($p < 0.05$). These results (Fig. 14B) indicated that the protective effects of SFD against myocardial injury involve seven signaling pathways. Previous studies demonstrated that SFD exerted cardiotonic effects by regulating the TNF signaling pathway[77], apoptosis[78], the PI3K-Akt signaling pathway[79], TGF-β/Smads signaling pathway[80], and Akt/eNOS signaling pathway[81]. Ubiquitination[82] and neddylation[83] were also shown to play a role in myocardial injury; however, the relationships between SFD and these pathways need to be confirmed in further studies. Therefore, SFD appears to exert protective effects against myocardial injury by regulating 7 pathways and 10 biological processes. In addition, previous studies demonstrated that SFD may cure heart failure by regulating the TGF-β/Smads signaling pathway, apoptosis, and the PI3K-Akt, Akt/eNOS, and TNF signaling pathways. In summary, regarding myocardial injury, a number of proteins and pathways in the biological network may be regulated by SFD, which ultimately controls the occurrence and development of CVD.

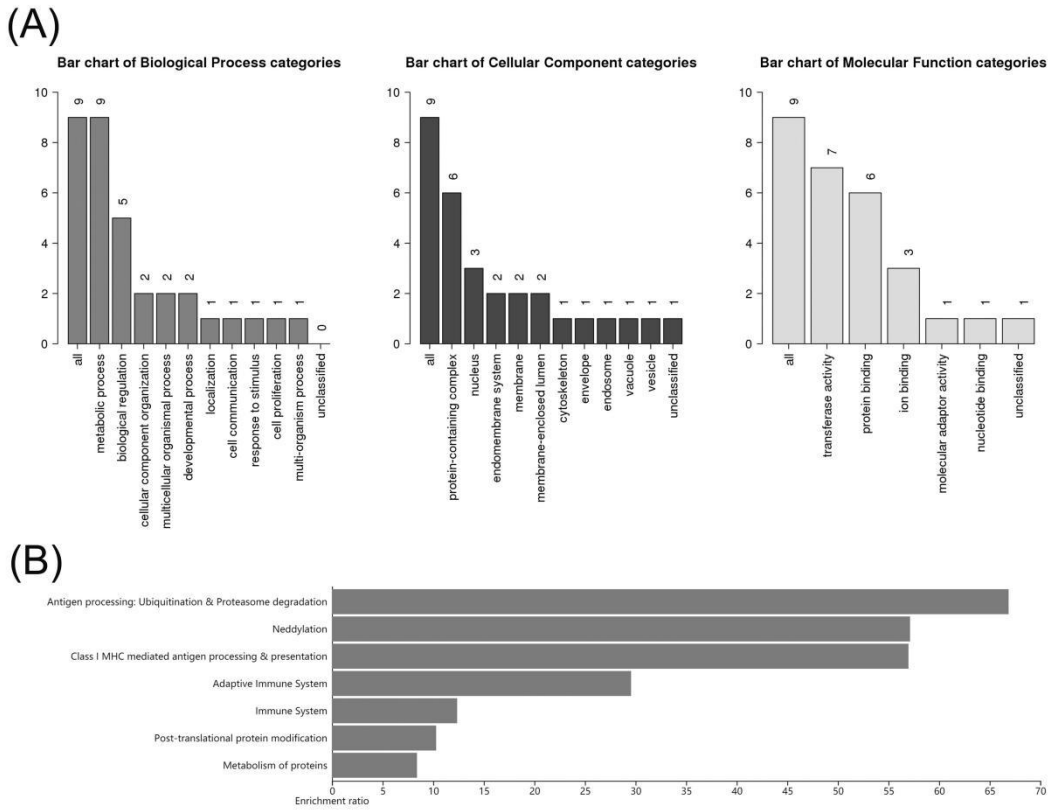

Fig. 14. Enrichment analyses of nine hub genes

(A) An enrichment analysis through the WebGestalt database. (B) A KEGG pathway analysis of nine hub genes.

4.3.4 GeneMANIA analysis

The GeneMANIA database was selected to further analyze the interaction network among hub genes (Fig. 15). The 9 central nodes representing hub genes were surrounded by 20 nodes representing genes that strongly correlated with the hub genes in terms of physical interactions (85.09%), shared protein domains (12.85%), pathways (1.8%), and genetic interactions (0.26%). The top five genes displaying the strongest correlations with hub genes included S-phase kinase-associated protein 1 (SKP1), ETS variant 1 (ETV1), F-box and leucine rich repeat protein 15 (FBXL15), ETV5, and ATPase Na^+/K^+ transporting subunit alpha 2 (ATP1A2), among which SKP1 correlated with cullin 1 (CUL1), ubiquitin-conjugating enzyme E2D 1 (UBE2D1), F-box protein 17 (FBXO17), and FBXO44 in terms of physical interactions. ETV1 correlated with de-etiolated homolog 1 (DET1) in terms of physical interactions and with LIM domain only protein 7 (LMO7) and HECT with C2 and WW domain containing E3 ubiquitin protein ligase 2 (HECW2) in terms of genetic interactions. FBXL15 correlated with CUL1 and HECW2 in terms of physical interactions and with FBXO44 and FBXO17 in terms of shared protein domains. ETV5 correlated with DET1 in terms of physical interactions and with zinc and ring finger 2 (ZNRF2) and UBE2D1 in terms of genetic interactions. In addition, ATP1A2 correlated with ZNRF2 in terms of physical interactions. Further functional analyses revealed that these proteins showed the strongest correlation with ubiquitin-protein ligase activity (FDR = 4.45E-09). Additionally, these proteins correlated with small conjugating protein ligase activity, acid-amino acid ligase activity, ligase activity, the formation of carbon-nitrogen bonds, the Skp, Cullin, F-box containing complex (SCF) ubiquitin ligase complex, ubiquitin ligase complex, and cullin-RING ubiquitin ligase complex.

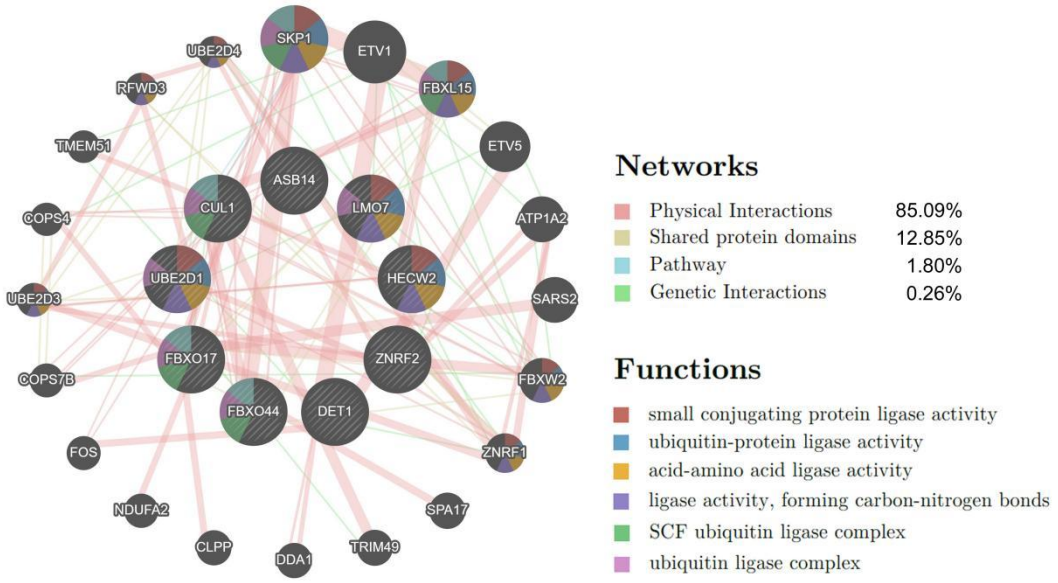

Fig. 15. Gene-gene interaction network among hub genes.

A gene is represented by a node. The strength of the interaction is expressed by the size of the node. Inter-node connection lines represent the types of gene-gene interactions, while the line color shows the types of interactions. The possible function of each gene is represented by the color of the node.

To simultaneously identify the target genes of SFD for protection against heart failure in the present study, the bioinformatic analysis method, including the identification of DEG, and a functional enrichment analysis were extensively used. A total of 1134 DEG were identified using the STRING website. A module analysis showed that nine hub genes exhibited ubiquitin-protein ligase activity. In summary, the hub genes and related pathways discovered in the present study will provide a more detailed understanding of the mechanisms by which SFD protects the myocardium, which will lead to novel research concepts for SFD. Since the safety of drug treatments and the importance of communication with patients are increasing[84], the preventative and therapeutic effects of SFD on heart failure increase the safety of anticancer drug treatments and will also lead to peace of mind for patients.

Conclusion

Until now, analytical methods based mainly on Western element reductionism have been used as research methods for applying the effectiveness of Traditional Chinese Medicine (TCM) to modern medicine. In other words, we have provided evidence of its effectiveness by determining the active ingredient and analyzing its effects on individual factors related to the disease. However, the method is far from elucidating the essence of the treatment concept of TCM, which treats by acting systemically by combining crude drugs. Therefore, in this doctoral dissertation, we conducted four chapters of research with the aim of opening the door to essential research that makes the most of the individuality of TCM. As a result, he obtained the following findings.

In Chapter 1, we first obtained fingerprints of component analysis by 3D-HPLC, which is the information base, for 120 kinds of crude drugs that are the basis of prescription. This information can be freely post-hoc analyzed as needed in the future. Furthermore, for all of the 120 crude drug extracts, two cells, the neurological system and the glial system, were treated at two concentrations to obtain information on morphological changes, RNA was extracted from them, and subsequent genes were extracted. A cDNA library was created for use in expression analysis. Furthermore, as an example of its use, changes in mRNA expression of BNIP-3, which has been suggested to be related to antidepressant effects, were primarily analyzed by real-time PCR for all 120 crude drugs, and based on the results, effective crude drugs were obtained. A secondary analysis was performed by selecting. In this way, the information data and gene library of 120 kinds of crude drug extracts can be easily used for various analyzes starting from here, and the basic information for examining the effect of the combination of crude drugs. It also became an important asset with great potential (detailed below).

In Chapter 2, we proved an example of the idea that the basis of TCM is not a single-flavored herbal medicine, but a combination of two-flavored herbal medicines. This underlying finding is information on cell morphological changes associated with

individual herbal medicines in Chapter 1. It was found that Coptis chinensis and Rhubarb each show strong cytotoxicity alone, but the effect is significantly diminished when both are extracted together. When the two individual extracts were combined in vitro, a large amount of precipitate was formed, but there was no strong association between the formation of this precipitate and the disappearance of toxicity. Although the details of the mechanism need to be further investigated in the future, the value of this result is high as an example of the significant change in action due to extraction together, that is, pairing as a drug. The combination of Coptis chinensis and Rhubarb can be seen in Sanko Shashinto （三黄写心湯）. Sankoshashinto（三黄写心湯） is a prescription that suppresses abnormal rise in qi, but on the other hand, both Coptis chinensis and Rhubarb have an effect on the digestive system, which can be a side effect. It is thought that it contributes to increasing the number of side effects. As shown here, a lot of knowledge about TCM is vaguely known about anti-drugs, but since the starting point in previous studies is a simple crude drug, what has been scientifically elucidated is The reality is that there is almost no information on the drug, and on the contrary, the information on the drug itself is not organized. This research is important as an example showing the importance of the concept of antidrugs, and will also stimulate future research development.

In Chapter 3, we conducted an experiment showing an example based on the hypothesis that the essential main reaction of TCM is caused by the active components contained. Many pure drugs currently on the market are inhibitors. In most cases, even drugs that seem to be promoters are promoted by suppressing the inhibitory mechanism. The pharmacological effect of the pure drug is basically based on the law of metric pharmacology, and the difference in efficacy in the dose-response curve with side effects is defined as safety, and therefore safety is ensured by increasing the dose. It's difficult. In order to obtain high drug efficacy (suppressive effect), the amount of drug tends to be excessive. On the other hand, the dose of TCM may be very small because it stimulates a biological reaction so that the living body reacts naturally when the living body notices it. For example, it is easy to

understand if you think that the smell corresponds to it. If you notice the odor, the living body will have pleasure feelings and will take actions that detect danger. On the other hand, in order to prevent the odor, it is necessary to completely block the odor, and there is a risk of suffocation. In Chapter 3, it was shown that a very small amount of components in the hemp in Hochuekkito has a strong serotonin receptor stimulating effect. The actual situation has not been clarified yet, and other herbal medicines that control it have not been clarified. Future research is essential. However, here, the action of TCM does not necessarily follow the general law of lightweight pharmacology, and even a very small amount of TCM only needs to be noticed and reacted by the living body, while whether or not the living body itself has reactivity. In other words, it seems to show that the idea of "证" is important. So to speak, it is important to think in line with the principles of TCM, but modern science does not have that perspective, so the promotion of research from this perspective has produced epoch-making results that overturned conventional wisdom. It is full of possibilities.

In Chapter 4, the starting point of the idea is that TCM acts systemically, and the partner acting from various related in vivo factors and its action network are analyzed based on the array analysis result of gene expression change. The experimental results that tried to elucidate by the method are shown. Originally, we think that the action of TCM can suppress the heart disease that occurs as a side effect, and develop a new prescription from the viewpoint of systemic action aiming at safe treatment of anticancer drugs through it. This is a study aimed at. At this time, the systemic effect has not been clearly shown, but the drug effect on heart disease-related target factors is ambiguous to both the target and the drug, rather than being targeted and studied from the beginning of the study. The idea is to start research while leaving the gap, discover and evaluate potential factors that utilize the action of TCM, and develop new prescriptions that act on them. There are still many possible related factors, including the one discovered this time. For example, ion channels, water channels, and effects on the kidney may be future targets. Natural medicine, which has the purpose of preventing heart disease through systemic control, is often found in some

folk medicines in Japan, but it provides a scientific basis based on the idea of TCM, and detailed reports based on it. By advancing the analysis, it will be possible to discover more effective and safe preventive and therapeutic agents according to the medical condition, etc. from the viewpoint of systemic action one after another.

As mentioned above, in this thesis, the first chapter is the information related to the individual crude drug information that constitutes the basis of Chinese medicine, the second chapter is based on the research on the concept of medicine, the third chapter is about the research on the trace ingredients, and the fourth chapter is Research on network pharmacology of Chinese medicine.

As described above, by considering the theory of TCM first and using modern analysis methods, it is possible to discover new microagonists and therapeutic concepts that could not be obtained until now. Thought. We hope that this research will be the starting point for the widespread use of this idea.

References

1. Tohda, M., Hayashi, H., Sukma, M. & Tanaka, K. BNIP-3: a novel candidate for an intrinsic depression-related factor found in NG108-15 cells treated with Hochu-ekki-to, a traditional oriental medicine, or typical antidepressants. *Neurosci Res* **62**, 1–8 (2008).
2. Tohda, M., Mingmalairak, S., Murakami, Y. & Matsumoto, K. Enhanced expression of BCL2/adenovirus EIB 19-kDa-interacting protein 3 mRNA, a candidate for intrinsic depression-related factor, and effects of imipramine in the frontal cortex of stressed mice. *Biol Pharm Bull* **33**, 53–57 (2010).
3. Tohda, M. MRI detection of the activated region in the rat brain by Hochuekki-to, a traditional oriental medicine, and the related expression of BNIP-3 mRNA, a candidate of depression-related factor. *J Med Therap* **2**, (2018).
4. Tohda, M. & Mingmalairak, S. Evidence of Antidepressive Effects of a Wakan-yaku, Hochuekkito, in Depression Model Mice with Learned-Helplessness Behavior. *Evid Based Complement Alternat Med* **2013**, 319073 (2013).
5. Tohda, M. Changes in the expression of BNIP-3 and other neuronal factors during the cultivation period of primary cultured rat cerebral cortical neurons and an assessment of each factor's functions. *Cell signalling and Trafficking* **2**, 1 (2014).
6. Dodson, M., Darley-Usmar, V. & Zhang, J. Cellular metabolic and autophagic pathways: traffic control by redox signaling. *Free Radic Biol Med* **63**, 207–221 (2013).
7. Bellot, G. *et al.* Hypoxia-induced autophagy is mediated through hypoxia-inducible factor induction of BNIP3 and BNIP3L via their BH3 domains. *Mol Cell Biol* **29**, 2570–2581 (2009).
8. Zhang, J. & Ney, P. A. Role of BNIP3 and NIX in cell death, autophagy, and mitophagy. *Cell Death Differ* **16**, 939–946 (2009).
9. Jia, F., Mou, L. & Ge, H. Protective effects of ginsenoside Rb1 on H2O2-induced oxidative injury in human endothelial cell line (EA.hy926) via miR-210. *Int J Immunopathol Pharmacol* **33**, 2058738419866021 (2019).
10. Tohda, M., Imaizumi, R., Sekiya, A., Itoh, N. & Nomura, Y. Studies on the activation mechanisms of guanylyl cyclase by serotonin, probably through a novel subtype of serotonin receptor (5-HTGC). *Biol Pharm Bull* **18**, 1072–1075 (1995).
11. Yang, B., Qin, J., Nie, Y., Li, Y. & Chen, Q. Brain-derived neurotrophic factor propeptide inhibits proliferation and induces apoptosis in C6 glioma cells. *Neuroreport* **28**, 726–730 (2017).
12. Chen, Y.-D. *et al.* Hyperthermia with different temperatures inhibits proliferation

and promotes apoptosis through the EGFR/STAT3 pathway in C6 rat glioma cells. *Mol Med Rep* **16**, 9401–9408 (2017).

13. Yin, B., Sheng, H., Lin, J., Zhou, H. & Zhang, N. The cell death of C6 astrocytoma cells induced by oridonin and its mechanism. *Int J Clin Exp Pathol* **5**, 562–568 (2012).
14. Zhang, Z. *et al.* MicroRNA-124 inhibits the proliferation of C6 glioma cells by targeting Smad4. *Int J Mol Med* **40**, 1226–1234 (2017).
15. Bawari, S. *et al.* Targeting BDNF signaling by natural products: Novel synaptic repair therapeutics for neurodegeneration and behavior disorders. *Pharmacological Research* **148**, 104458 (2019).
16. Sakai, H. *et al.* Plag1 regulates neuronal gene expression and neuronal differentiation of neocortical neural progenitor cells. *Genes Cells* **24**, 650–666 (2019).
17. Pandey, A. *et al.* Critical role of the miR-200 family in regulating differentiation and proliferation of neurons. *Journal of Neurochemistry* **133**, 640–652 (2015).
18. Tohda, M. & Watanabe, H. The Wakan-yaku Universe: A Useful Authorized Traditional Concept for Developing Novel Therapeutic Categories and Medicinal Drugs. *Biological and Pharmaceutical Bulletin* **41**, 1627–1631 (2018).
19. Srivastava, A. *et al.* Secretome of Differentiated PC12 Cells Enhances Neuronal Differentiation in Human Mesenchymal Stem Cells Via NGF-Like Mechanism. *Mol Neurobiol* **55**, 8293–8305 (2018).
20. Protective effects of ginsenoside Rb1 on H2O2-induced oxidative injury in human endothelial cell line (EA.hy926) via miR-210 - Fubao Jia, Lei Mou, Hanming Ge, 2019. https://journals.sagepub.com/doi/10.1177/2058738419866021.
21. Kubli, D. A., Quinsay, M. N., Huang, C., Lee, Y. & Gustafsson, A. B. Bnip3 functions as a mitochondrial sensor of oxidative stress during myocardial ischemia and reperfusion. *Am J Physiol Heart Circ Physiol* **295**, H2025-2031 (2008).
22. Dhingra, R. *et al.* Bidirectional regulation of nuclear factor-κB and mammalian target of rapamycin signaling functionally links Bnip3 gene repression and cell survival of ventricular myocytes. *Circ Heart Fail* **6**, 335–343 (2013).
23. Tohda, M. & Watanabe, H. The Wakan-yaku Universe: A Useful Authorized Traditional Concept for Developing Novel Therapeutic Categories and Medicinal Drugs. Biological and Pharmaceutical Bulletin 41, 1627–1631 (2018).
24. Profiling of 120 types of herbal extracts and their effects on morphology in cultured neuronal or glial cell lines, followed by RNA extraction for a cDNA library: Consideration for use in studies based on Kampo theories - Tohda - 2021 - Traditional & Kampo Medicine - Wiley Online Library. https://onlinelibrary.wiley.com/doi/full/10.1002/tkm2.1274.

25. Tohda, M., Imaizumi, R., Sekiya, A., Itoh, N. & Nomura, Y. Studies on the activation mechanisms of guanylyl cyclase by serotonin, probably through a novel subtype of serotonin receptor (5-HTGC). Biol Pharm Bull 18, 1072–1075 (1995).
26. Kobashi, K., Nishimura, T., Kusaka, M., Hattori, M. & Namba, T. Metabolism of sennosides by human intestinal bacteria. Planta Med 40, 225–236 (1980).
27. Fukuchi, M. et al. Screening inducers of neuronal BDNF gene transcription using primary cortical cell cultures from BDNF-luciferase transgenic mice. Sci Rep 9, 11833 (2019).
28. Tohda, M. & Watanabe, H. The Wakan-yaku Universe: A Useful Authorized Traditional Concept for Developing Novel Therapeutic Categories and Medicinal Drugs. Biological and Pharmaceutical Bulletin 41, 1627–1631 (2018).
29. Tohda, M. & Mingmalairak, S. Evidence of Antidepressive Effects of a Wakan-yaku, Hochuekkito, in Depression Model Mice with Learned-Helplessness Behavior. Evid Based Complement Alternat Med 2013, 319073 (2013).
30. Watari, H., Shimada, Y., Matsui, M. & Tohda, C. Kihito, a Traditional Japanese Kampo Medicine, Improves Cognitive Function in Alzheimer's Disease Patients. Evid Based Complement Alternat Med 2019, 4086749 (2019).
31. M, T., M, A.-F. a.-F., S, N. & H, W. Effects of Hochu-ekki-to (Bu-Zhong-Yi-Qi-Tang), a Kampo medicine, on serotonin 2C subtype receptor-evoked current response and the receptor mRNA expression. Journal of Traditional Medicines 17, 34–40 (2000).
32. Tohda, M., Takasu, T. & Nomura, Y. Effects of antidepressants on serotonin-evoked current in Xenopus oocytes injected with rat brain mRNA. Eur J Pharmacol 166, 57–63 (1989).
33. Tohda, M. & Watanabe, H. Imipramine-induced increase in 5-HT2C receptor mRNA level in the rat brain. Neurosci Res 24, 189–193 (1996).
34. Nomura, Y., Kaneko, S., Kato, K., Yamagishi, S. & Sugiyama, H. Inositol phosphate formation and chloride current responses induced by acetylcholine and serotonin through GTP-binding proteins in Xenopus oocyte after injection of rat brain messenger RNA. Brain Res 388, 113–123 (1987).
35. Arellano, R. O., Garay, E. & Miledi, R. Muscarinic receptor heterogeneity in follicle-enclosed Xenopus oocytes. J Physiol 521 Pt 2, 409–419 (1999).
36. Lübbert, H. et al. cDNA cloning of a serotonin 5-HT1C receptor by electrophysiological assays of mRNA-injected Xenopus oocytes. Proc Natl Acad Sci U S A 84, 4332–4336 (1987).
37. Tohda, M., Hayashi, H., Sukma, M. & Tanaka, K. BNIP-3: a novel candidate for an intrinsic depression-related factor found in NG108-15 cells treated with Hochu-ekki-to, a traditional oriental medicine, or typical antidepressants. Neurosci

Res 62, 1–8 (2008).
38. Tohda, M., Mingmalairak, S., Murakami, Y. & Matsumoto, K. Enhanced expression of BCL2/adenovirus EIB 19-kDa-interacting protein 3 mRNA, a candidate for intrinsic depression-related factor, and effects of imipramine in the frontal cortex of stressed mice. Biol Pharm Bull 33, 53–57 (2010).
39. Tohda, M. Changes in the expression of BNIP-3 and other neuronal factors during the cultivation period of primary cultured rat cerebral cortical neurons and an assessment of each factor's functions. Cell signalling and Trafficking 2, 1 (2014).
40. Tohda, M. MRI detection of the activated region in the rat brain by Hochuekki-to, a traditional oriental medicine, and the related expression of BNIP-3 mRNA, a candidate of depression-related factor. J Med Therap 2, (2018).
41. Yoshiya, T. et al. Prospective, randomized, cross-over pilot study of the effects of Rikkunshito, a Japanese traditional herbal medicine, on anorexia and plasma-acylated ghrelin levels in lung cancer patients undergoing cisplatin-based chemotherapy. Invest New Drugs 38, 485–492 (2020).
42. Matsumoto, C. et al. Psychological stress in aged female mice causes acute hypophagia independent of central serotonin 2C receptor activation. PLoS One 12, e0187937 (2017).
43. Schellekens, H. et al. Ghrelin's Orexigenic Effect Is Modulated via a Serotonin 2C Receptor Interaction. ACS Chem Neurosci 6, 1186–1197 (2015).
44. Howell, E. et al. Glucagon-Like Peptide-1 (GLP-1) and 5-Hydroxytryptamine 2c (5-HT2c) Receptor Agonists in the Ventral Tegmental Area (VTA) Inhibit Ghrelin-Stimulated Appetitive Reward. Int J Mol Sci 20, E889 (2019).
45. Wang, S. et al. Compatibility art of traditional Chinese medicine: from the perspective of herb pairs. J Ethnopharmacol 143, 412–423 (2012).
46. Lloyd-Jones DM, Leip EP, Larson MG, d'Agostino RB, Beiser A, Wilson PW, Wolf PA, Levy D. Prediction of lifetime risk for cardiovascular disease by risk factor burden at 50 years of age. Circulation. 2006; 113:791-798.
47. Wang J, Qi F. Traditional Chinese medicine to treat COVID-19: the importance of evidence-based research. Drug Discov Ther. 2020; 14:149-150.
48. Kitazawa T, Park CH, Hiratani K, Choi JS, Yokozawa T. Efficacy of Chinese prescription Kangen-karyu for patient with metabolic syndrome. Drug Discov Ther. 2020; 14:54-57.
49. Gu P, Chen H. Modern bioinformatics meets traditional Chinese medicine. Brief Bioinform. 2014; 15:984-1003.
50. Zhao J, Yang J, Tian S, Zhang W. A survey of web resources and tools for the study of TCM network pharmacology. Quantitative Biology. 2019; 7:17-29.
51. Fang J, Wang L, Wu T, Yang C, Gao L, Cai H, Liu J, Fang S, Chen Y, Tan W,

Wang Q. Network pharmacology-based study on the mechanism of action for herbal medicines in Alzheimer treatment. J Ethnopharmacol. 2017; 196:281-292.
52. Zhao J, Jiang P, Zhang W. Molecular networks for the study of TCM pharmacology. Brief Bioinform. 2010; 11:417-430.
53. Li B, Xu X, Wang X, Yu H, Li X, Tao W, Wang Y, Yang L. A systems biology approach to understanding the mechanisms of action of chinese herbs for treatment of cardiovascular disease. Int J Mol Sci. 2012; 13:13501-13520.
54. Yan X, Wu H, Ren J, Liu Y, Wang S, Yang J, Qin S, Wu D. Shenfu Formula reduces cardiomyocyte apoptosis in heart failure rats by regulating microRNAs. J Ethnopharmacol. 2018; 227:105-112.
55. Zheng SY, Sun J, Zhao X, Xu JG. Protective effect of shen-fu on myocardial ischemia-reperfusion injury in rats. Am J Chin Med. 2004; 32:209-220.
56. Yang D, Wang X, Wu Y, Lu B, Yuan A, Leon C, Guo N. Urinary Metabolomic Profiling Reveals the Effect of Shenfu Decoction on Chronic Heart Failure in Rats. Molecules. 2015; 20:11915-11929.
57. Chen Y, Yu R, Jiang L, Zhang Q, Li B, Liu H, Xu G. A Comprehensive and Rapid Quality Evaluation Method of Traditional Chinese Medicine Decoction by Integrating UPLC-QTOF-MS and UFLC-QQQ-MS and its Application. Molecules. 2019; 24.
58. He JL, Zhao JW, Ma ZC, Wang YG, Liang QD, Tan HL, Xiao CR, Tang XL, Gao Y. Serum Pharmacochemistry Analysis Using UPLC-Q-TOF/MS after Oral Administration to Rats of Shenfu Decoction. Evid Based Complement Alternat
59. Berger SI, Iyengar R. Network analyses in systems pharmacology. Bioinformatics. 2009; 25:2466-2472.
60. Zhou F, Hao G, Zhang J, Zheng Y, Wu X, Hao K, Niu F, Luo D, Sun Y, Wu L, Ye W, Wang G. Protective effect of 23-hydroxybetulinic acid on doxorubicin-induced cardiotoxicity: a correlation with the inhibition of carbonyl reductase-mediated metabolism. Br J Pharmacol. 2015; 172:5690-5703.
61. Szklarczyk D, Morris JH, Cook H, Kuhn M, Wyder S, Simonovic M, Santos A, Doncheva NT, Roth A, Bork P, Jensen LJ, von Mering C. The STRING database in 2017: quality-controlled protein-protein association networks, made broadly accessible. Nucleic Acids Res. 2017; 45:D362-D368.
62. Bader GD, Hogue CW. An automated method for finding molecular complexes in large protein interaction networks. BMC Bioinformatics. 2003; 4:2.
63. Liao Y, Wang J, Jaehnig EJ, Shi Z, Zhang B. WebGestalt 2019: gene set analysis toolkit with revamped UIs and APIs. Nucleic Acids Res. 2019; 47:W199-W205.
64. The Gene Ontology C. Expansion of the Gene Ontology knowledgebase and resources. Nucleic Acids Res. 2017; 45:D331-D338.

65. Kanehisa M, Furumichi M, Tanabe M, Sato Y, Morishima K. KEGG: new perspectives on genomes, pathways, diseases and drugs. Nucleic Acids Res. 2017; 45:D353-D361.
66. Warde-Farley D, Donaldson SL, Comes O, et al. The GeneMANIA prediction server: biological network integration for gene prioritization and predicting gene function. Nucleic Acids Res. 2010; 38:W214-220.
67. Li S, Zhang B, Jiang D, Wei Y, Zhang N. Herb network construction and co-module analysis for uncovering the combination rule of traditional Chinese herbal formulae. BMC Bioinformatics. 2010; 11 Suppl 11:S6.
68. Ding F, Zhang Q, Ung CO, Wang Y, Han Y, Hu Y, Qi J. An analysis of chemical ingredients network of Chinese herbal formulae for the treatment of coronary heart disease. PLoS One. 2015; 10:e0116441.
69. Guimera R, Nunes Amaral LA. Functional cartography of complex metabolic networks. Nature. 2005; 433:895-900.
70. Wang X, Robbins J. Proteasomal and lysosomal protein degradation and heart disease. J Mol Cell Cardiol. 2014; 71:16-24.
71. Powell SR, Herrmann J, Lerman A, Patterson C, Wang X. The ubiquitin-proteasome system and cardiovascular disease. Prog Mol Biol Transl Sci. 2012; 109:295-346.
72. Li YF, Wang X. The role of the proteasome in heart disease. Biochim Biophys Acta. 2011; 1809:141-149.
73. Minotti G, Menna P, Salvatorelli E, Cairo G, Gianni L. Anthracyclines: molecular advances and pharmacologic developments in antitumor activity and cardiotoxicity. Pharmacol Rev. 2004; 56:185-229.
74. Ranek MJ, Wang X. Activation of the ubiquitin-proteasome system in doxorubicin cardiomyopathy. Curr Hypertens Rep. 2009; 11:389-395.
75. Sishi BJ, Loos B, van Rooyen J, Engelbrecht AM. Doxorubicin induces protein ubiquitination and inhibits proteasome activity during cardiotoxicity. Toxicology. 2013; 309:23-29.
76. Bulteau AL, Lundberg KC, Humphries KM, Sadek HA, Szweda PA, Friguet B, Szweda LI. Oxidative modification and inactivation of the proteasome during coronary occlusion/reperfusion. J Biol Chem. 2001; 276:30057-30063.
77. Yu M, Ye L, Bian J, Ma L, Zheng C, Guo H. Effect of Jiawei Shenfu decoction on tumor necrosis factor-alpha and nuclear factor-kappa B in patients who have chronic heart failure with syndromes of deficiency of heart Yang. J Tradit Chin Med. 2019; 39:418-424.
78. Chen RJ, Rui QL, Wang Q, Tian F, Wu J, Kong XQ. Shenfu injection attenuates lipopolysaccharide-induced myocardial inflammation and apoptosis in rats. Chin J

Nat Med. 2020; 18:226-233.
79. Zhu J, Song W, Xu S, Ma Y, Wei B, Wang H, Hua S. Shenfu Injection Promotes Vasodilation by Enhancing eNOS Activity Through the PI3K/Akt Signaling Pathway In Vitro. Front Pharmacol. 2020; 11:121.
80. Ni J, Shi Y, Li L, Chen J, Li L, Li M, Zhu J, Zhu Y, Fan G. Cardioprotection against Heart Failure by Shenfu Injection via TGF-beta/Smads Signaling Pathway. Evid Based Complement Alternat Med. 2017; 2017:7083016.
81. Wang YY, Li YY, Li L, Yang DL, Zhou K, Li YH. Protective Effects of Shenfu Injection against Myocardial Ischemia-Reperfusion Injury via Activation of eNOS in Rats. Biol Pharm Bull. 2018; 41:1406-1413.
82. Willis MS, Townley-Tilson WH, Kang EY, Homeister JW, Patterson C. Sent to destroy: the ubiquitin proteasome system regulates cell signaling and protein quality control in cardiovascular development and disease. Circ Res. 2010; 106:463-478.
83. Zou J, Ma W, Li J, Littlejohn R, Zhou H, Kim IM, Fulton DJR, Chen W, Weintraub NL, Zhou J, Su H. Neddylation mediates ventricular chamber maturation through repression of Hippo signaling. Proc Natl Acad Sci U S A. 2018; 115:E4101-E4110.
84. Yaguchi-Saito A, Yamamoto K, Sengoku T, Suka M, Sato T, Hinata M, Nakamura T, Nakayama T, Yamamoto M. Evaluation of rapid drug safety communication materials for patients in Japan. Drug Discov Ther. 2021; 15:101-107.

SUPPORTING INFORMATION

Table S1 3D-HPLC data shown in “All data on profiling of 120 herbal extracts”

Profiling of 120 types of herbal extracts by 3D-HPLC, their effects on the morphology of cultured neuronal or glial cell lines, and RNA extraction. (Top) 3D-HPLC chart, (Middle) RNA concentration as percentage of vehicle-treated sample, (Bottom) morphological images. RNA was extracted from 35-mm dishes using the acidic phenol method. Control values (100% value) of RNA concentrations in each sample are show

001 Clematidis Radix
イレイセン（威霊仙）

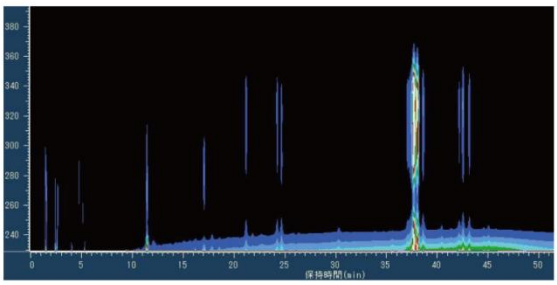

No.001		RNA concentration	
		conc (mg/ml)	% of cont
C6	10 μg/ml	6.35	115.32
	100 μg/ml	4.33	78.63
N18	10 μg/ml	2.91	88.99
	100 μg/ml	2.33	69.83

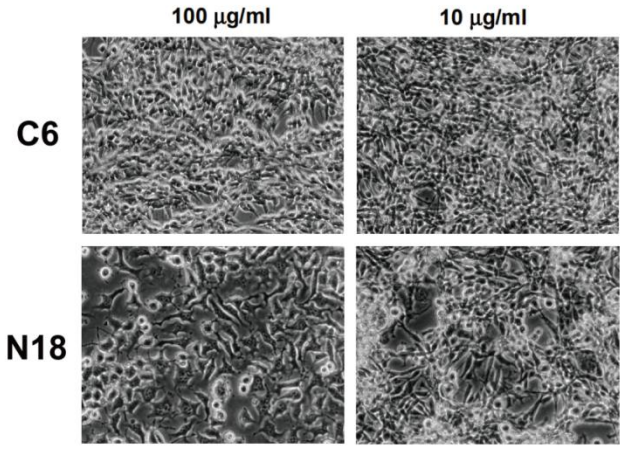

002 Artemisiae Capillari Flos
インチンコウ（茵陳蒿）

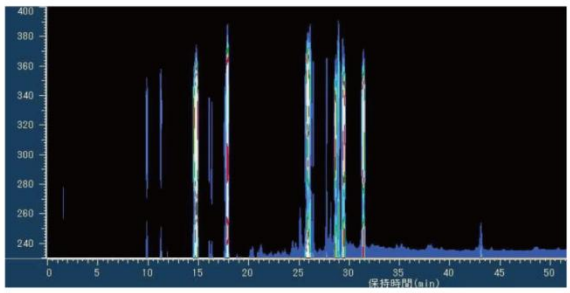

No.002		RNA concentration	
		conc (mg/ml)	% of cont
C6	10 μg/ml	5.73	104.06
	100 μg/ml	2.77	50.30
N18	10 μg/ml	1.73	52.91
	100 μg/ml	ND	ND

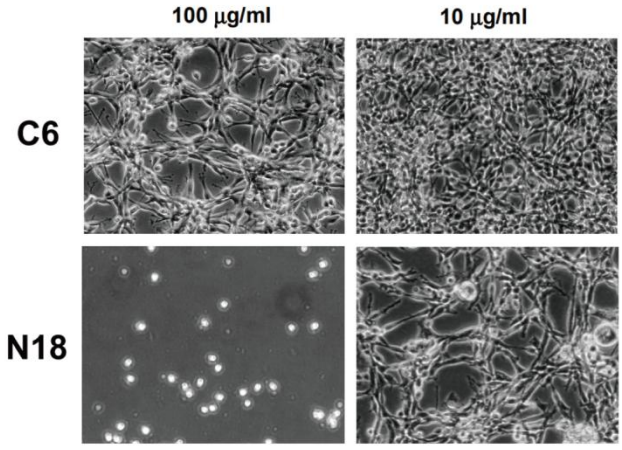

003 Curcumae Rhizoma
ウコン（鬱金）

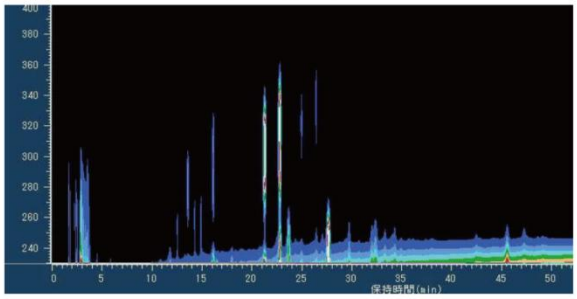

No.003		RNA concentration	
		conc (mg/ml)	% of cont
C6	10 μg/ml	6.88	124.93
	100 μg/ml	4.57	82.99
N18	10 μg/ml	2.90	88.68
	100 μg/ml	2.12	63.54

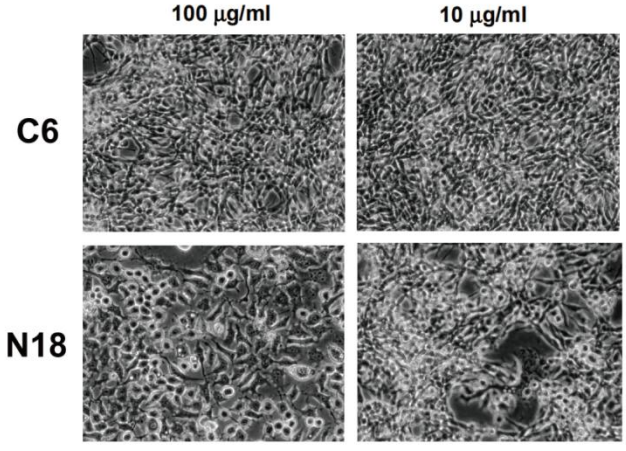

004 Linderae Radix
ウヤク（烏薬）

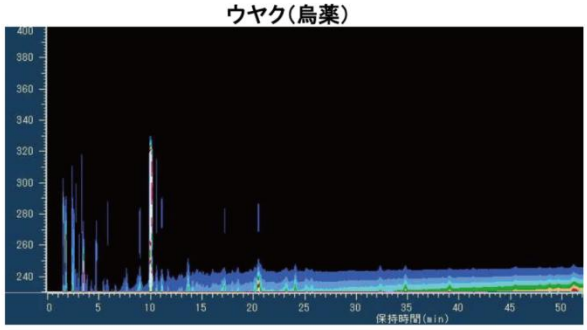

No.004		RNA concentration	
		conc (mg/ml)	% of cont
C6	10 μg/ml	6.29	114.23
	100 μg/ml	4.19	76.09
N18	10 μg/ml	2.05	62.69
	100 μg/ml	3.06	91.70

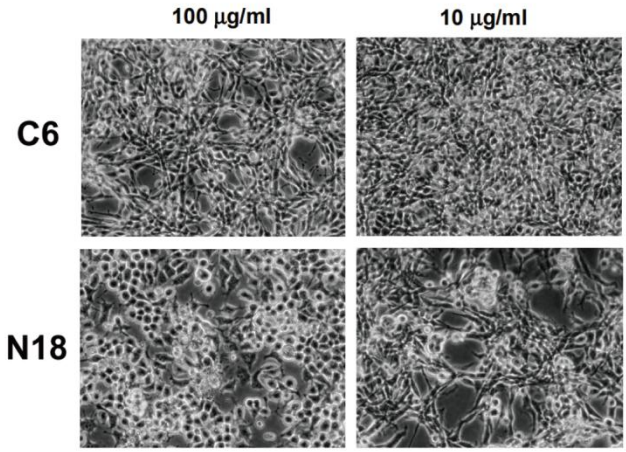

005 Corydalis Tuber
エンゴサク(延胡索)

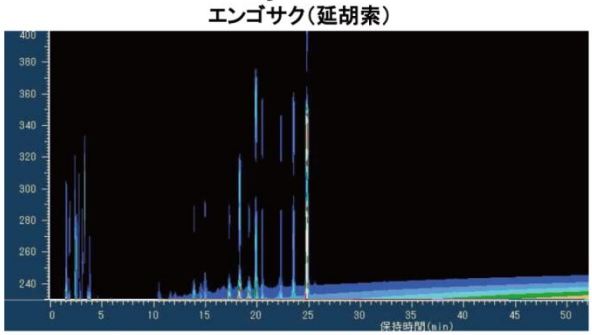

No.005		RNA concentration	
		conc (mg/ml)	% of cont
C6	10 μg/ml	6.3	114.41
	100 μg/ml	3.76	68.28
N18	10 μg/ml	2.82	86.24
	100 μg/ml	3.00	89.91

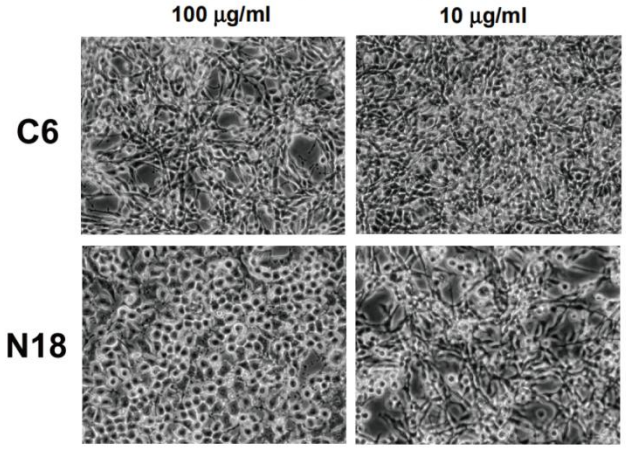

006 Astragali Radix
オウギ(黄耆)

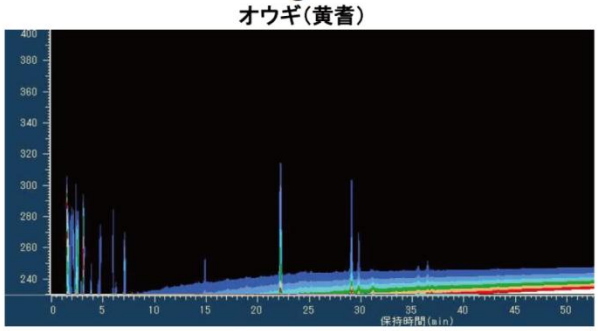

No.006		RNA concentration	
		conc (mg/ml)	% of cont
C6	10 μg/ml	6.85	124.39
	100 μg/ml	5.19	94.25
N18	10 μg/ml	3.07	93.88
	100 μg/ml	3.96	118.67

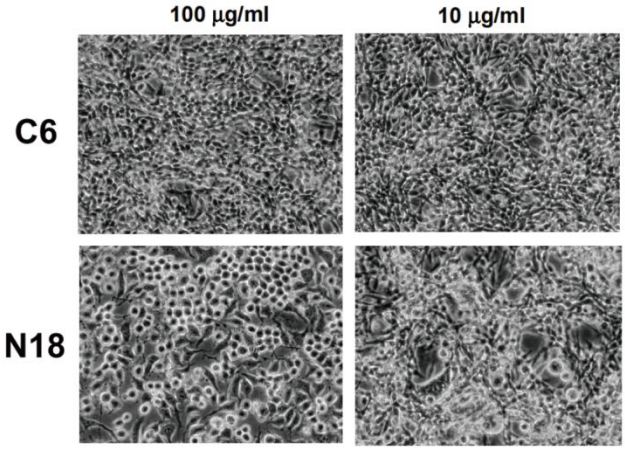

007 Scutellariae Radix
オウゴン(黄芩)

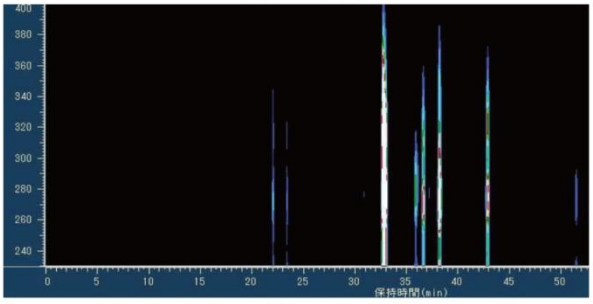

No.007		RNA concentration	
		conc (mg/ml)	% of cont
C6	10 μg/ml	5.28	95.88
	100 μg/ml	ND	ND
N18	10 μg/ml	0.73	11.31
	100 μg/ml	ND	ND

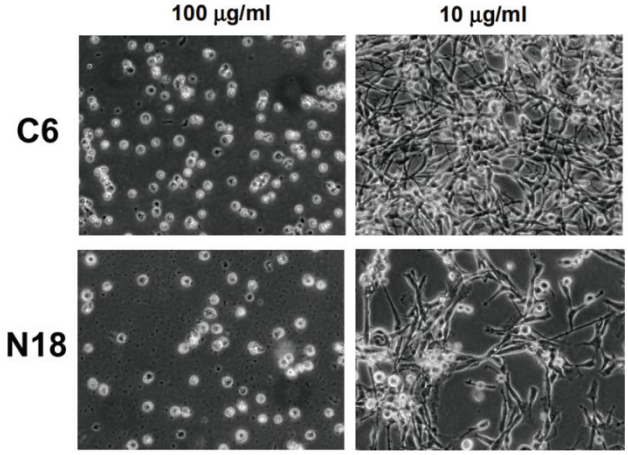

008 Phellodendri Cortex
オウバク(黄柏)

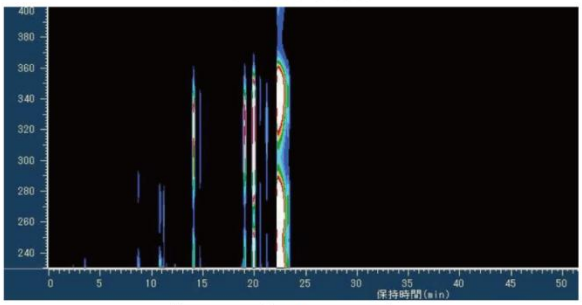

No.008		RNA concentration	
		conc (mg/ml)	% of cont
C6	10 μg/ml	5.21	94.61
	100 μg/ml	2.59	47.03
N18	10 μg/ml	1.39	42.51
	100 μg/ml	ND	ND

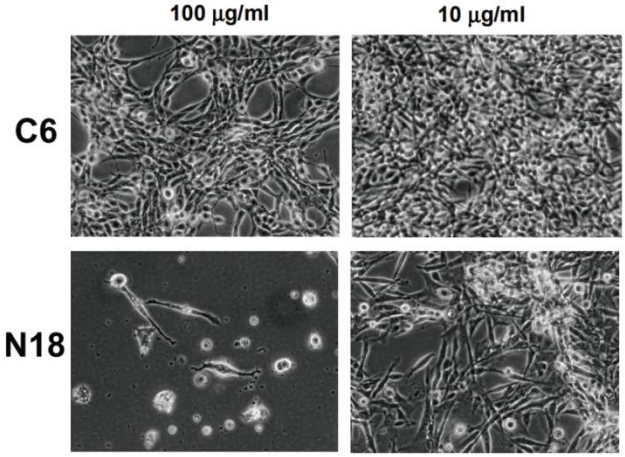

009 Pruni Cortex
オウヒ(桜皮)

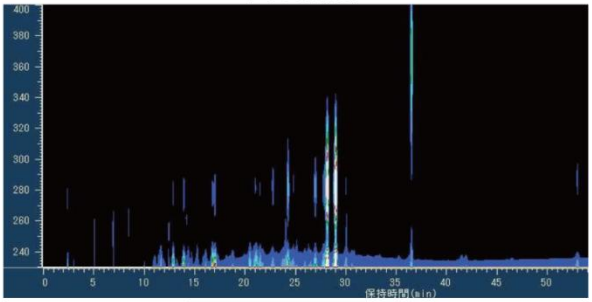

No.009		RNA concentration	
		conc (mg/ml)	% of cont.
C6	10 μg/ml	4.74	86.08
	100 μg/ml	1.83	33.23
N18	10 μg/ml	0.93	28.44
	100 μg/ml	ND	ND

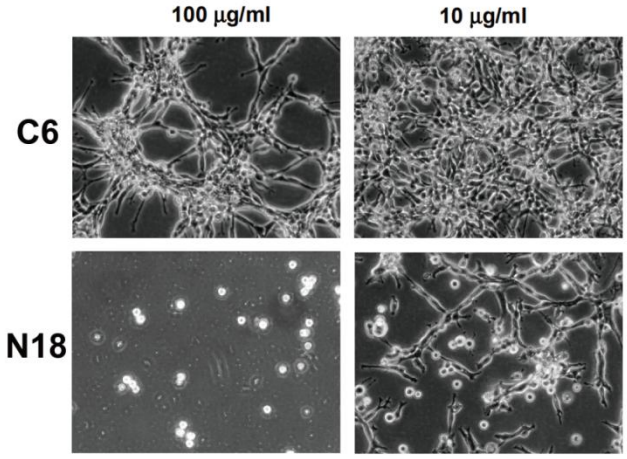

010 Coptidis Rhizoma
オウレン(黄連))

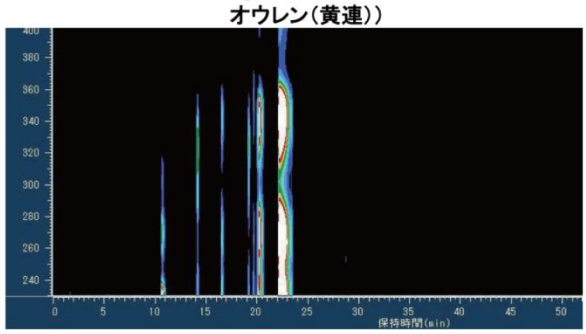

No.010		RNA concentration	
		conc (mg/ml)	% of cont.
C6	10 μg/ml	4.62	83.90
	100 μg/ml	1.57	28.51
N18	10 μg/ml	1.00	30.58
	100 μg/ml	ND	ND

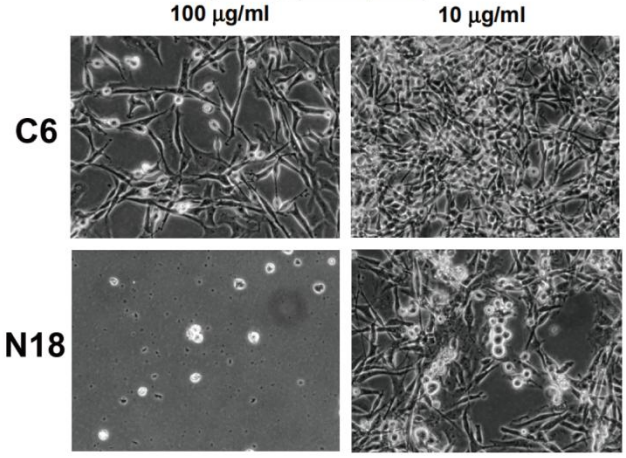

011 Polygalae Radix
オンジ(遠志)

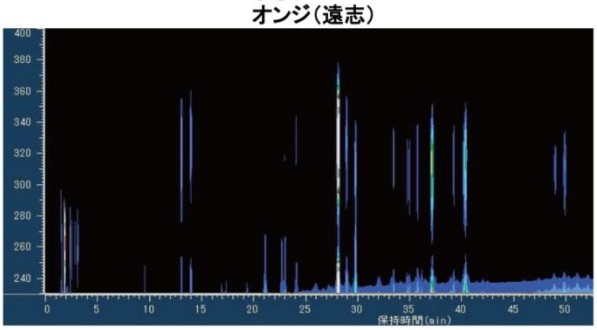

No.011		RNA concentration	
		conc (mg/ml)	% of cont.
C6	10 μg/ml	6.04	109.69
	100 μg/ml	3.72	67.55
N18	10 μg/ml	2.00	61.16
	100 μg/ml	2.26	67.73

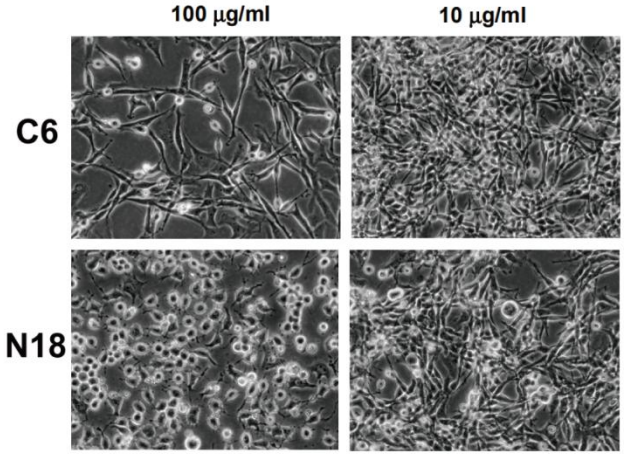

012 Artemisiae Folium
ガイヨウ(艾葉)

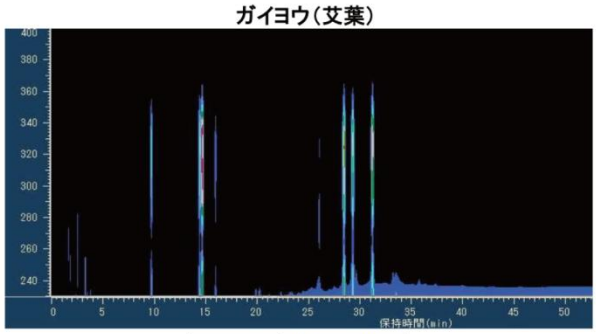

No.012		RNA concentration	
		conc (mg/ml)	% of cont.
C6	10 μg/ml	4.42	80.27
	100 μg/ml	1.26	22.88
N18	10 μg/ml	0.89	27.22
	100 μg/ml	ND	ND

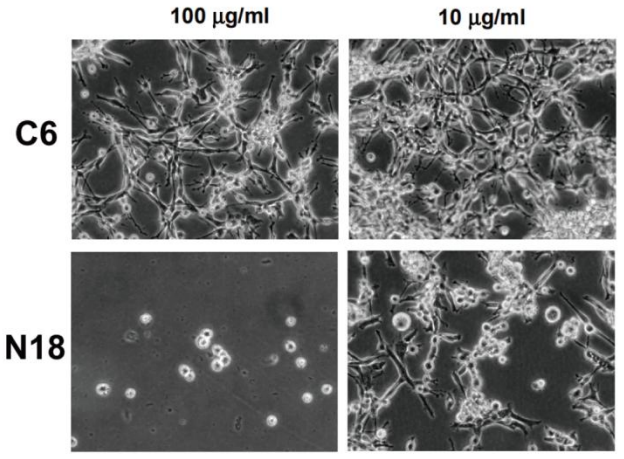

013 Polygoni Multiflori Radix
カシュウ（何首烏）

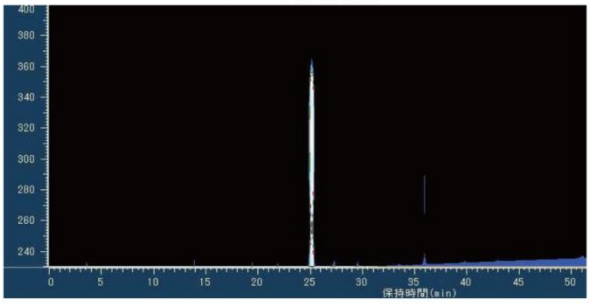

No.013		RNA concentration	
		conc (mg/ml)	% of cont
C6	10 μg/ml	4.72	85.72
	100 μg/ml	2.09	37.95
N18	10 μg/ml	1.18	36.86
	100 μg/ml	ND	ND

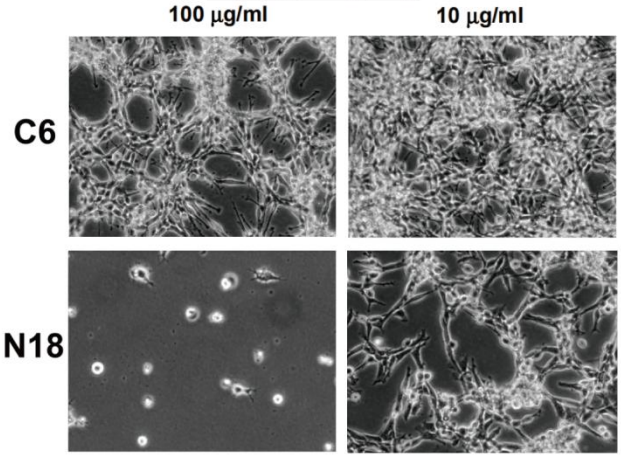

014 Zedoariae Rhizoma
ガジュツ（莪朮）

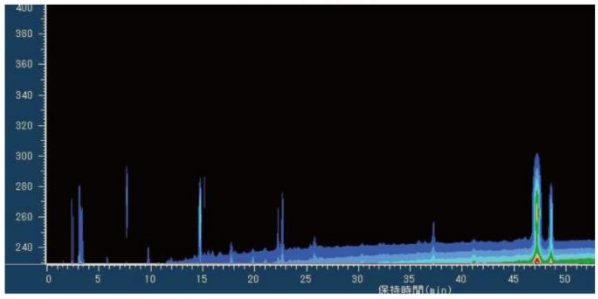

No.014		RNA concentration	
		conc (mg/ml)	% of cont
C6	10 μg/ml	6.76	122.76
	100 μg/ml	4.99	90.62
N18	10 μg/ml	2.85	87.16
	100 μg/ml	2.80	83.92

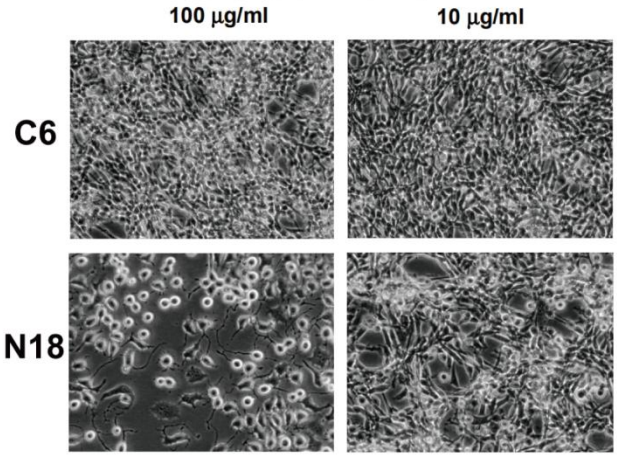

015 Puerariae Radix
カッコン（葛根）

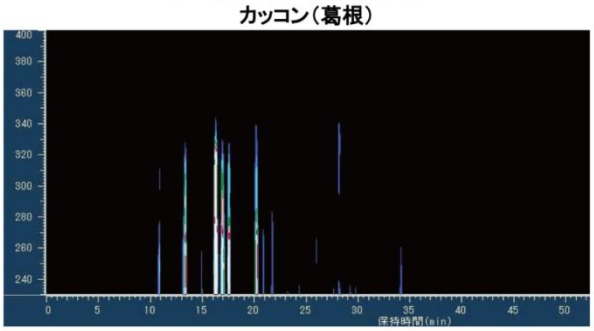

No.015		RNA concentration	
		conc (mg/ml)	% of cont
C6	10 μg/ml	6.61	120.04
	100 μg/ml	5.01	90.99
N18	10 μg/ml	2.30	70.34
	100 μg/ml	2.92	87.51

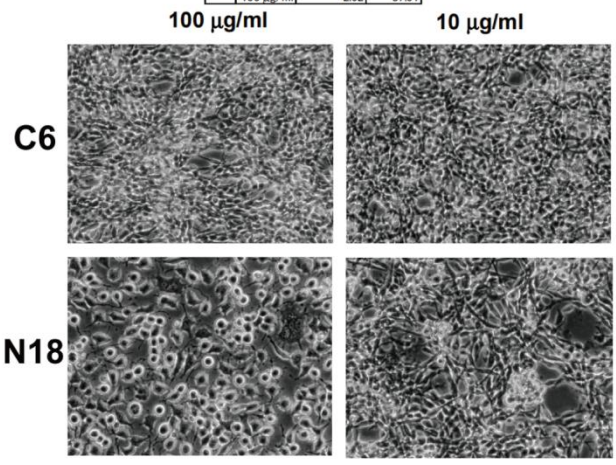

016 Trichosanthis Radix
カロコン（栝楼根）

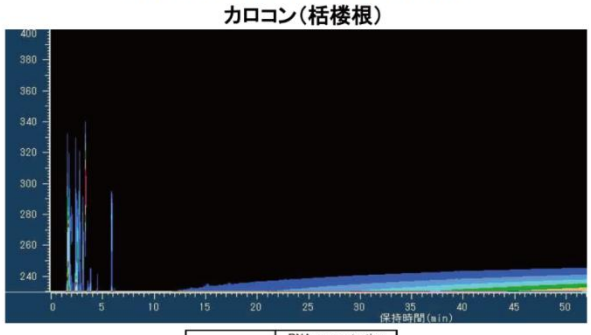

No.016		RNA concentration	
		conc (mg/ml)	% of cont
C6	10 μg/ml	6.61	120.04
	100 μg/ml	5.92	107.51
N18	10 μg/ml	2.61	79.82
	100 μg/ml	2.63	78.82

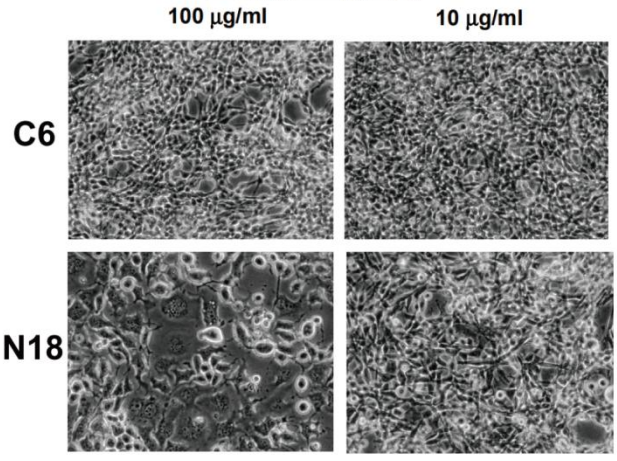

017 Zingiberis Siccatum Rhizoma
カンキョウ（乾姜）

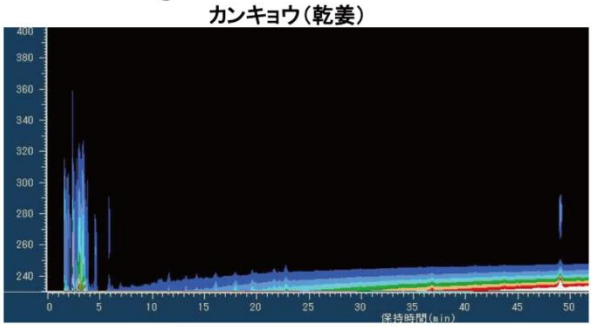

No.017		RNA concentration	
		conc (mg/ml)	% of cont
C6	10 μg/ml	6.44	116.95
	100 μg/ml	5.15	93.52
N18	10 μg/ml	2.28	69.72
	100 μg/ml	2.58	77.62

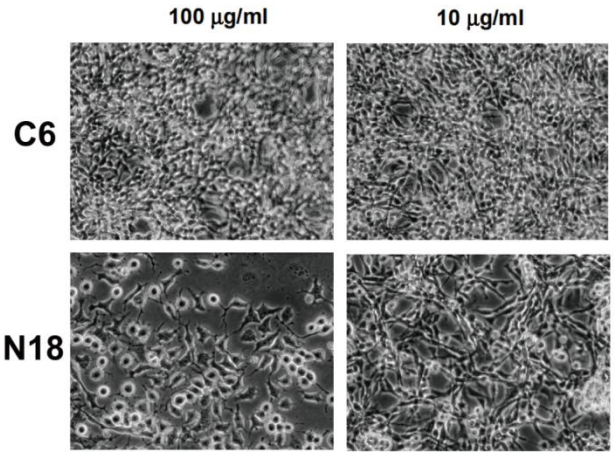

018 Glycyrrhizae Radix
カンゾウ（甘草）

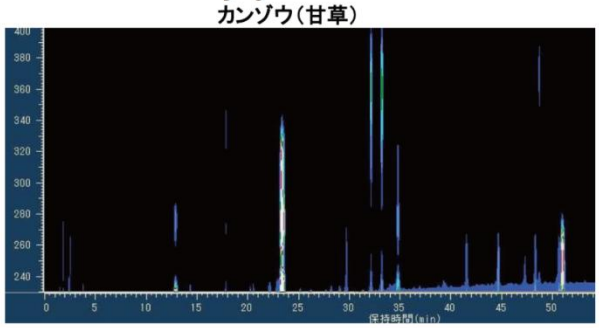

No.018		RNA concentration	
		conc (mg/ml)	% of cont
C6	10 μg/ml	6.47	117.50
	100 μg/ml	5.21	94.61
N18	10 μg/ml	2.52	77.06
	100 μg/ml	2.78	83.32

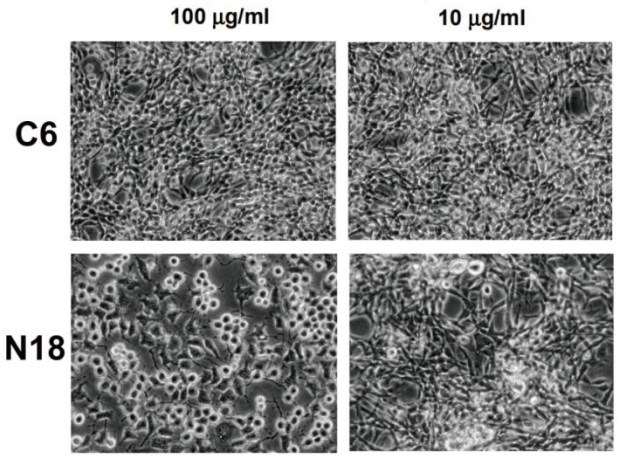

019 Platycodi Radix
キキョウ（桔梗）

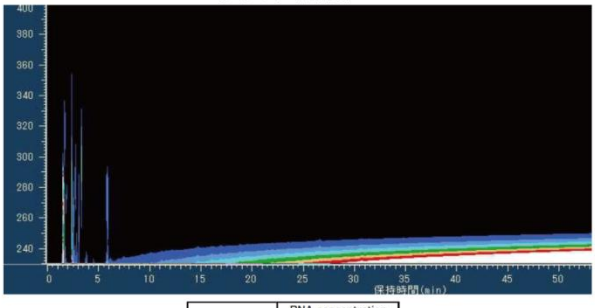

No.019		RNA concentration	
		conc (mg/ml)	% of cont
C6	10 μg/ml	5.83	105.87
	100 μg/ml	5.52	100.24
N18	10 μg/ml	2.53	77.37
	100 μg/ml	3.07	92.01

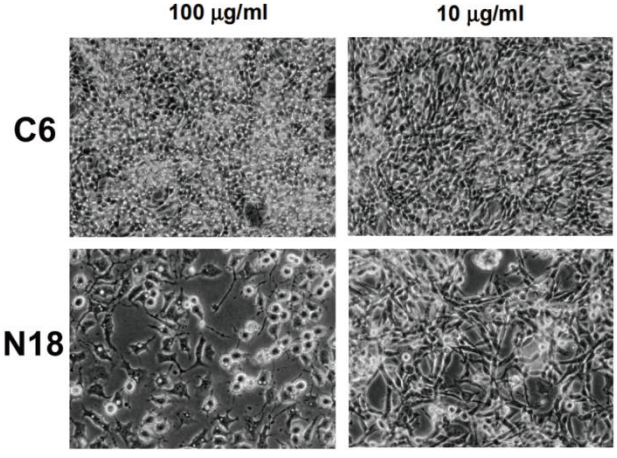

020 Chrysanthemi Flos
キクカ（菊花）

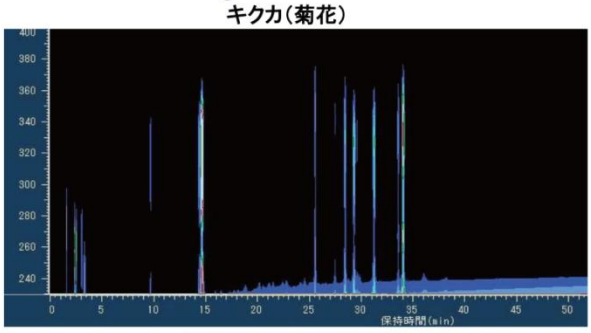

No.020		RNA concentration	
		conc (mg/ml)	% of cont
C6	10 μg/ml	*3.87	93.71
	100 μg/ml	5.32	96.61
N18	10 μg/ml	2.08	63.61
	100 μg/ml	2.04	61.14

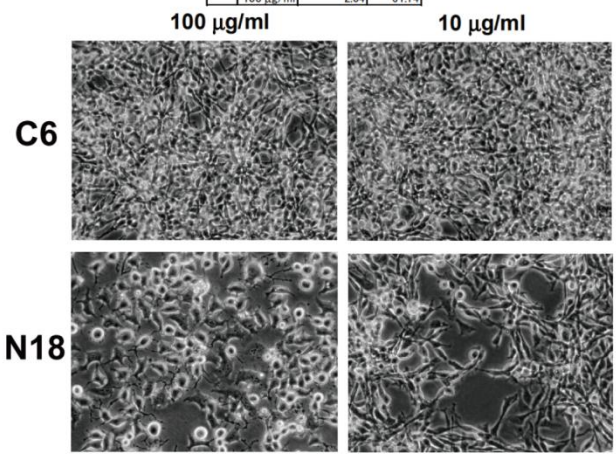

021 Aurantii Fructus Immaturus
キジツ(枳実)

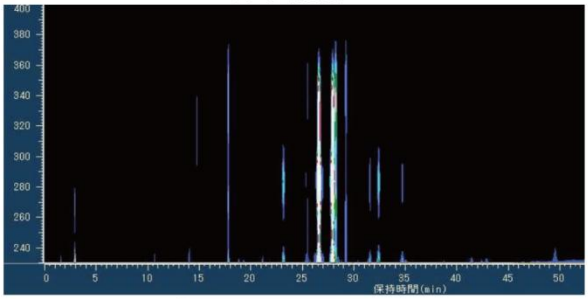

No.021		RNA concentration	
		conc (mg/ml)	% of cont
C6	10 μg/ml	*3.60	87.68
	100 μg/ml	2.53	45.95
N18	10 μg/ml	2.83	86.54
	100 μg/ml	2.27	68.03

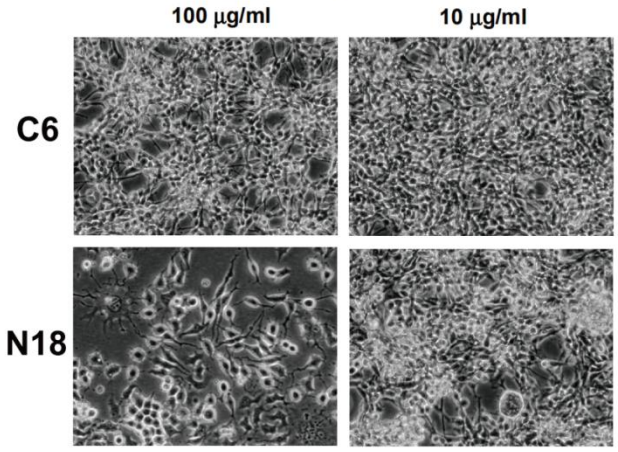

022 Notopterygii Rhizoma
キョウカツ(羌活)

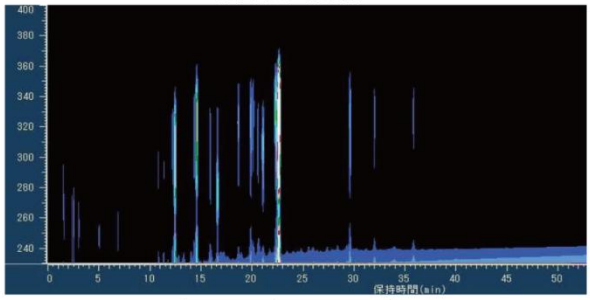

No.022		RNA concentration	
		conc (mg/ml)	% of cont
C6	10 μg/ml	*3.69	89.35
	100 μg/ml	4.65	84.44
N18	10 μg/ml	2.74	83.79
	100 μg/ml	3.09	92.61

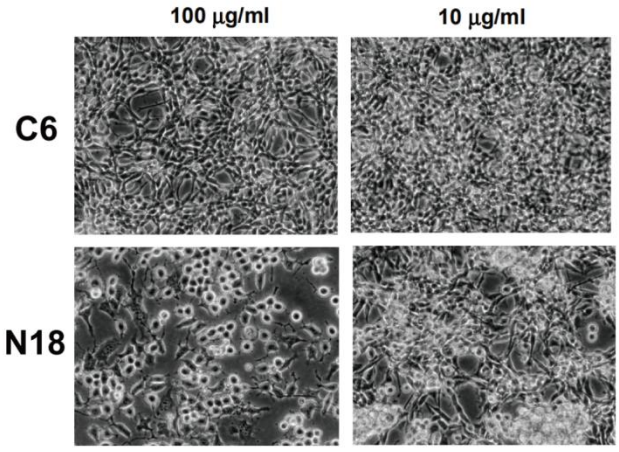

023 Armeniacae Semen
キョウニン(杏仁)

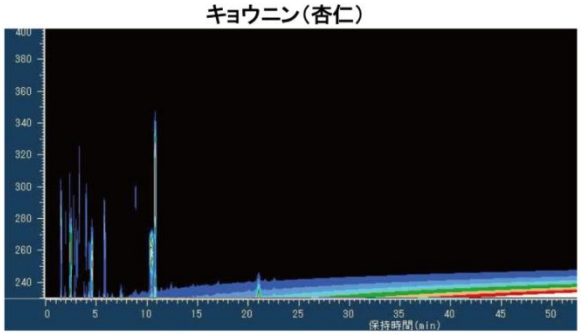

No.023		RNA concentration	
		conc (mg/ml)	% of cont
C6	10 μg/ml	*3.96	95.88
	100 μg/ml	4.81	87.35
N18	10 μg/ml	3.24	99.08
	100 μg/ml	3.27	98.00

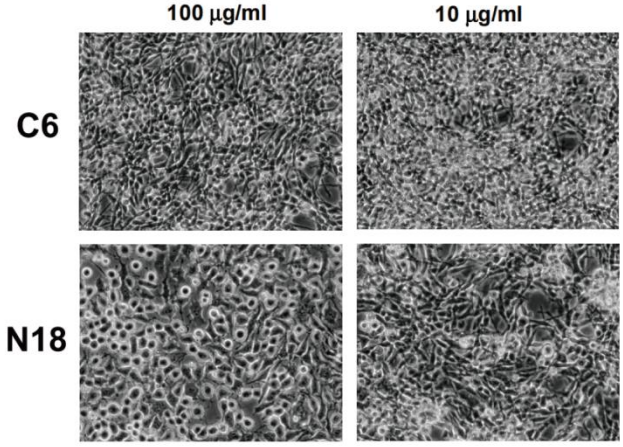

024 Sophorae Radix
クジン(苦参)

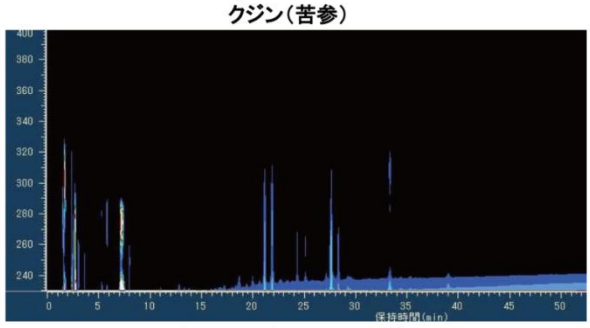

No.024		RNA concentration	
		conc (mg/ml)	% of cont
C6	10 μg/ml	*3.83	92.74
	100 μg/ml	5.39	97.88
N18	10 μg/ml	3.04	92.97
	100 μg/ml	2.47	74.03

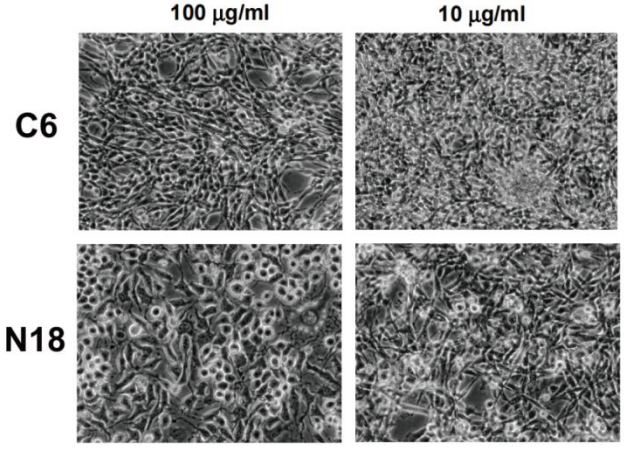

025 Sasa Folium
クマザサ（隈笹）

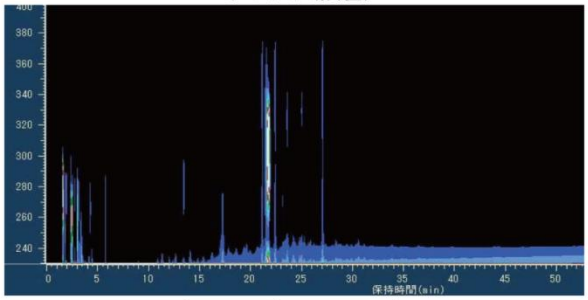

No.025		RNA concentration	
		conc (mg/ml)	% of cont
C6	10 μg/ml	*3.88	93.95
	100 μg/ml	4.18	75.91
N18	10 μg/ml	2.38	72.78
	100 μg/ml	2.15	64.43

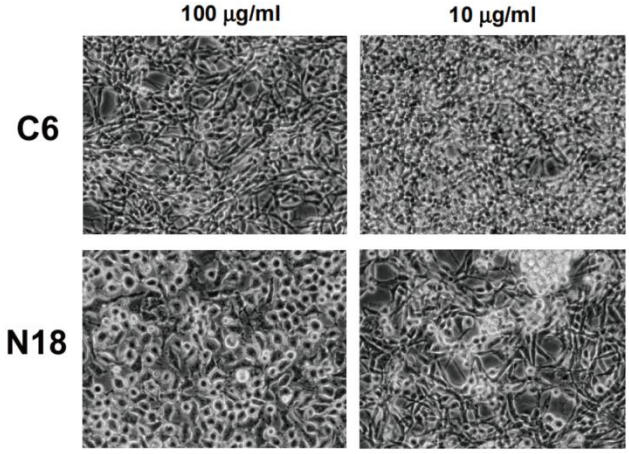

026 Schizonepetae Spica
ケイガイ（荊芥）

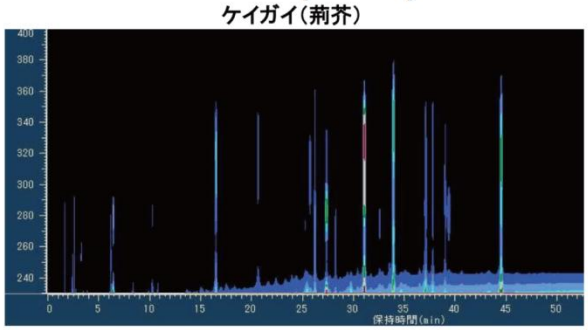

No.026		RNA concentration	
		conc (mg/ml)	% of cont
C6	10 μg/ml	*5.10	123.49
	100 μg/ml	3.22	58.47
N18	10 μg/ml	1.63	49.85
	100 μg/ml	0.28	8.39

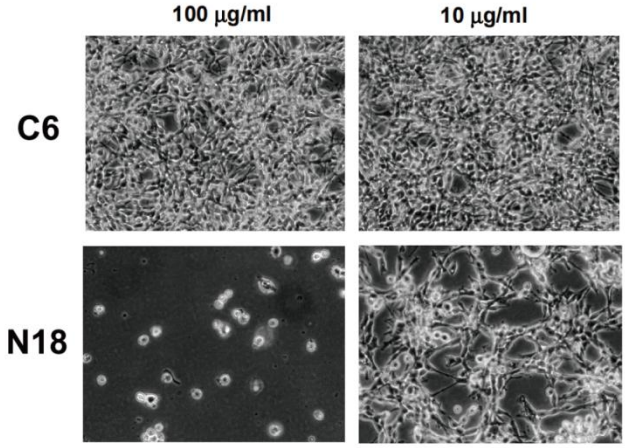

027 Spatholobi Caulis
ケイケットウ（鶏血藤）

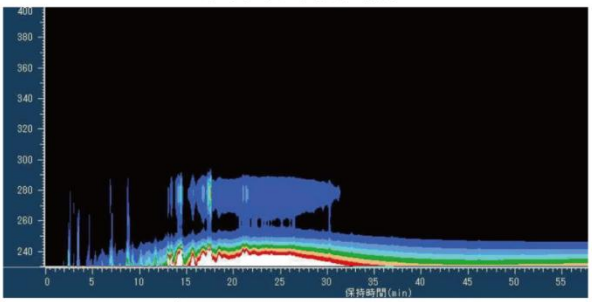

No.027		RNA concentration	
		conc (mg/ml)	% of cont
C6	10 μg/ml	*1.41	34.14
	100 μg/ml	0.79	14.35
N18	10 μg/ml	0.49	14.98
	100 μg/ml	ND	ND

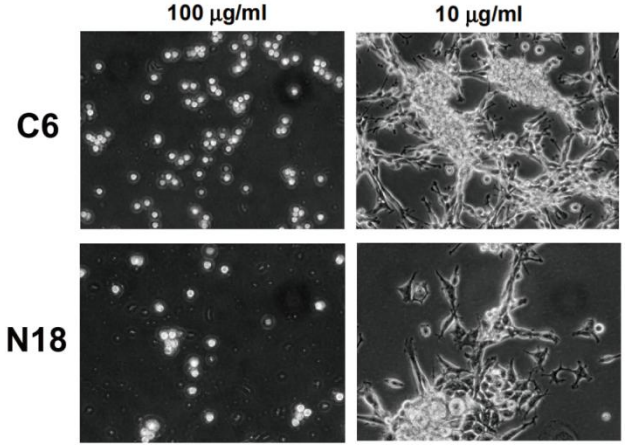

028 Cinnamomi Cortex
ケイヒ（桂皮）

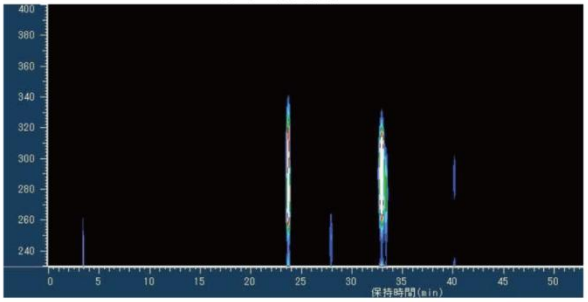

No.028		RNA concentration	
		conc (mg/ml)	% of cont
C6	10 μg/ml	*3.13	75.59
	100 μg/ml	1.91	34.69
N18	10 μg/ml	1.61	49.24
	100 μg/ml	ND	ND

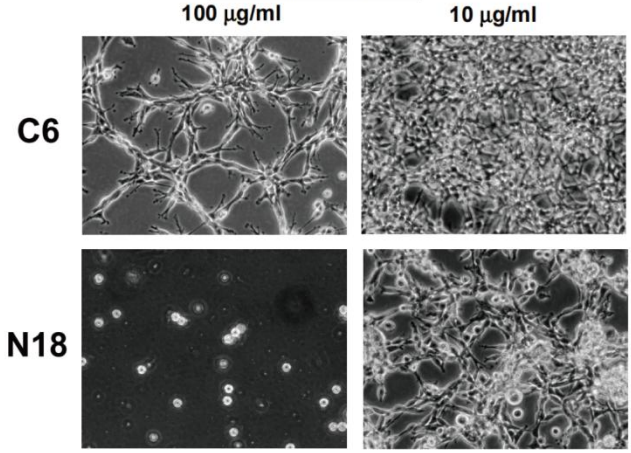

029 Scrophulariae Radix
ゲンジン（玄参）

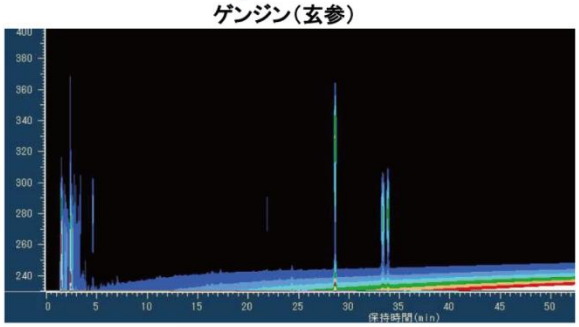

No.029		RNA concentration	
		conc (mg/ml)	% of cont
C6	10 μg/ml	*3.98	96.37
	100 μg/ml	4.83	87.71
N18	10 μg/ml	3.22	98.47
	100 μg/ml	3.35	100.40

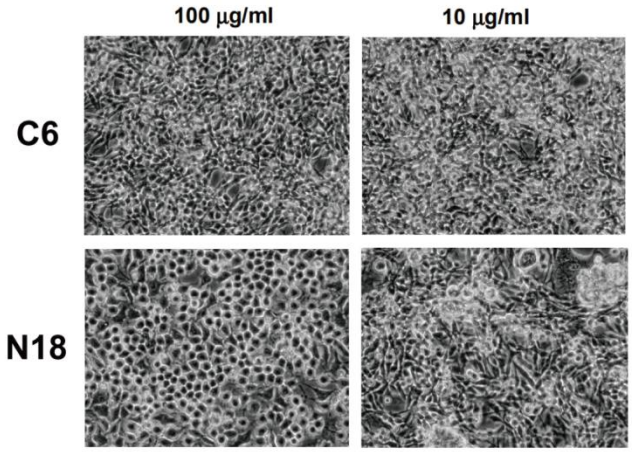

030 Carthami Flos
コウカ（紅花）

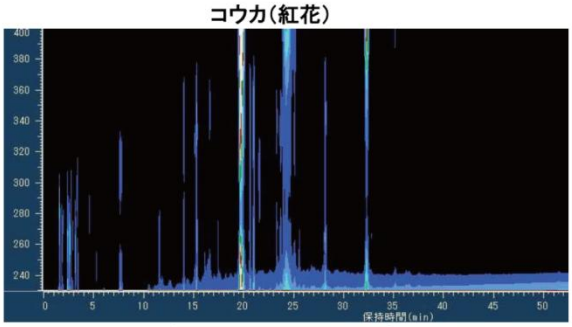

No.030		RNA concentration	
		conc (mg/ml)	% of cont
C6	10 μg/ml	*3.90	94.43
	100 μg/ml	5.18	94.07
N18	10 μg/ml	3.13	95.72
	100 μg/ml	2.32	69.53

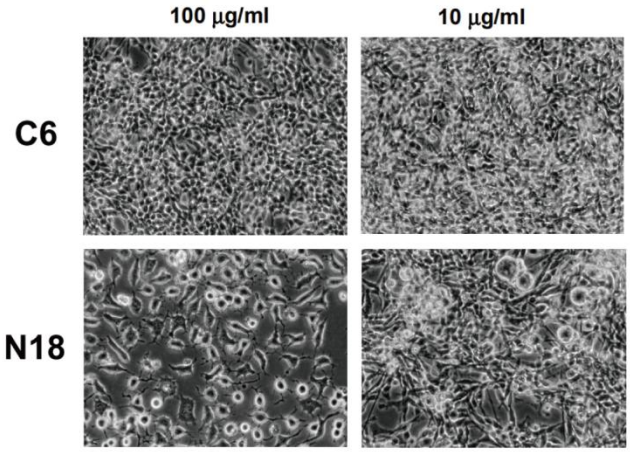

031 Albizziae Cortex
ゴウカンヒ（合歓皮）

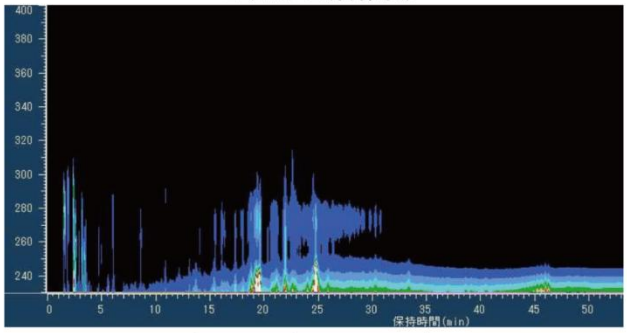

No.031		RNA concentration	
		conc (mg/ml)	% of cont
C6	10 μg/ml	3.01	80.12
	100 μg/ml	0.535	12.21
N18	10 μg/ml	1.94	85.09
	100 μg/ml	ND	ND

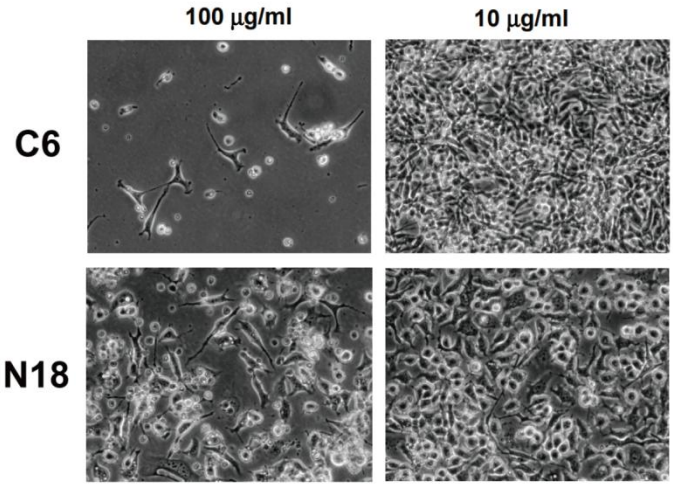

032 Ginseng Radix Rubra
コウジン（紅参）

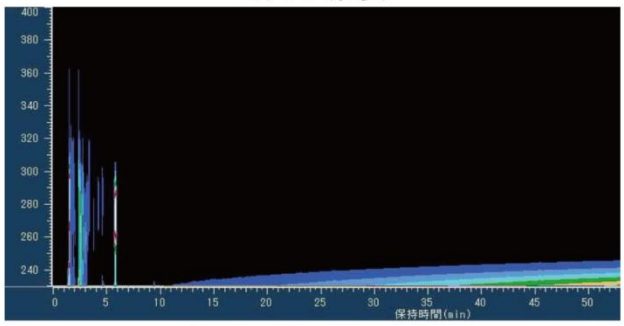

No.032		RNA concentration	
		conc (mg/ml)	% of cont
C6	10 μg/ml	3.22	85.71
	100 μg/ml	5.73	130.82
N18	10 μg/ml	2.63	115.35
	100 μg/ml	2.33	77.07

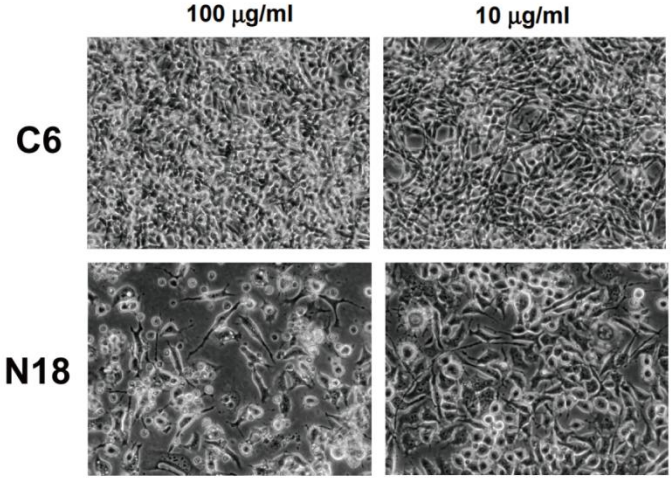

033 Cyperi Rhizoma
コウブシ（香附子）

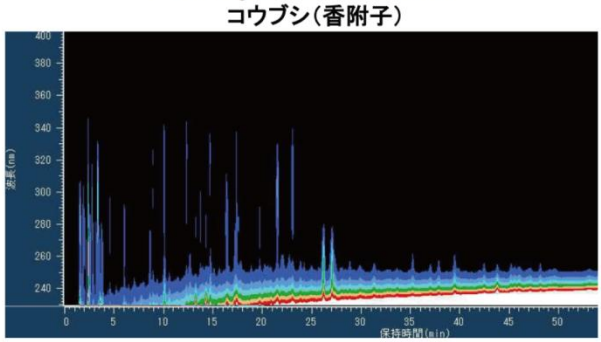

No.033		RNA concentration	
		conc (mg/ml)	% of cont
C6	10 μg/ml	3.47	92.53
	100 μg/ml	4.72	107.76
N18	10 μg/ml	2.44	107.02
	100 μg/ml	1.93	63.84

100 μg/ml　10 μg/ml

C6

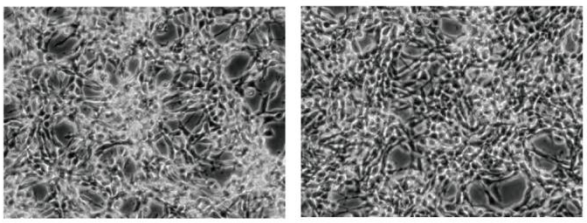

N18

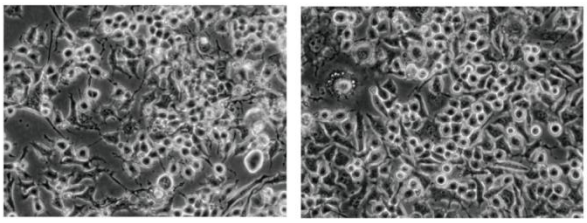

034 Magnoliae Cortex
コウボク（厚朴）

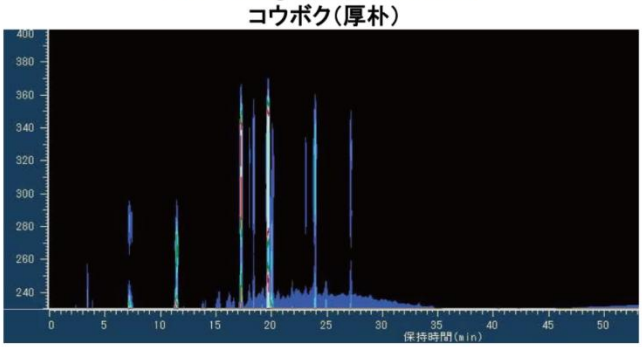

No.034		RNA concentration	
		conc (mg/ml)	% of cont
C6	10 μg/ml	3.14	83.58
	100 μg/ml	ND	ND
N18	10 μg/ml	ND	ND
	100 μg/ml	ND	ND

100 μg/ml　10 μg/ml

C6

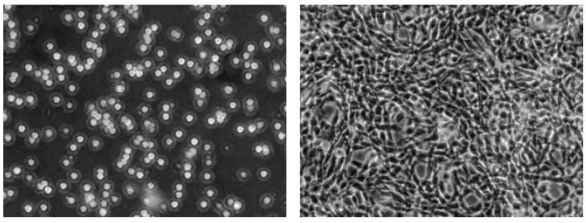

N18

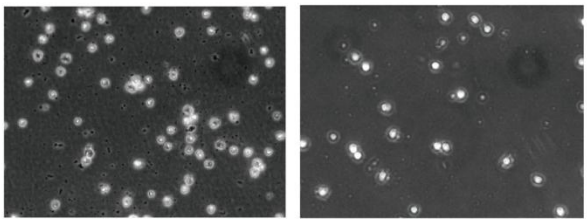

035 Achyranthis Radix
ゴシツ（牛膝）

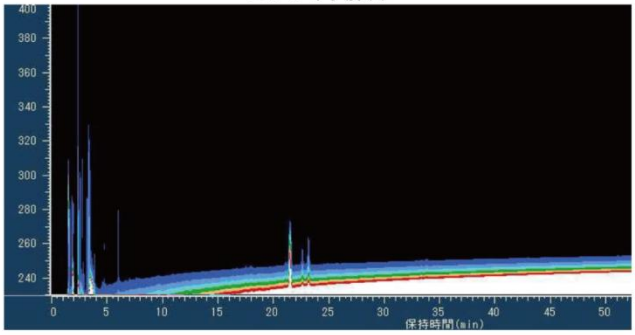

No.035		RNA concentration	
		conc (mg/ml)	% of cont
C6	10 μg/ml	3.50	93.17
	100 μg/ml	6.10	139.27
N18	10 μg/ml	0.79	34.65
	100 μg/ml	3.08	101.85

100 μg/ml　10 μg/ml

C6

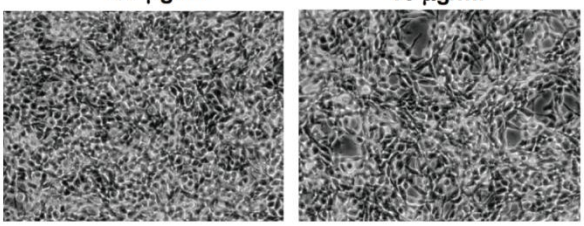

N18

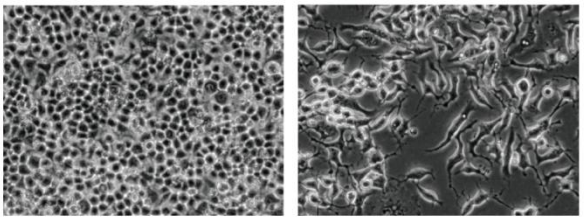

036 Evodiae Fructus
ゴシュユ（呉茱萸）

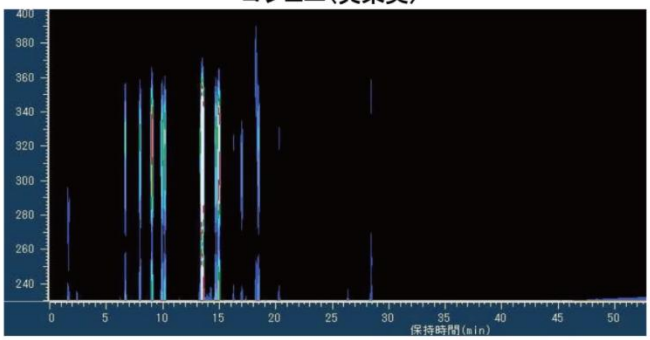

No.036		RNA concentration	
		conc (mg/ml)	% of cont
C6	10 μg/ml	2.64	70.27
	100 μg/ml	ND	ND
N18	10 μg/ml	0.816	35.79
	100 μg/ml	ND	ND

100 μg/ml　10 μg/ml

C6

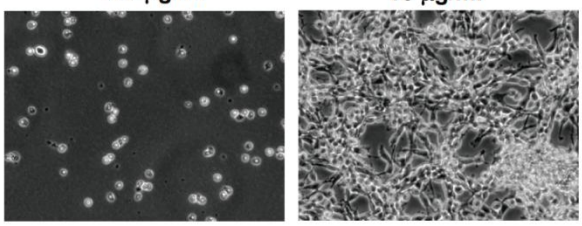

N18

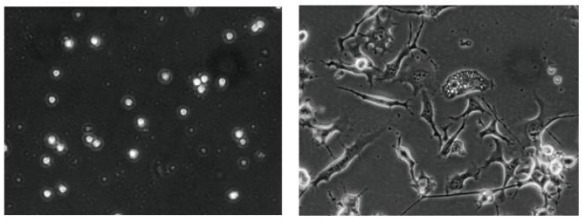

037 Arctii Fructus
ゴボウシ（牛蒡子）

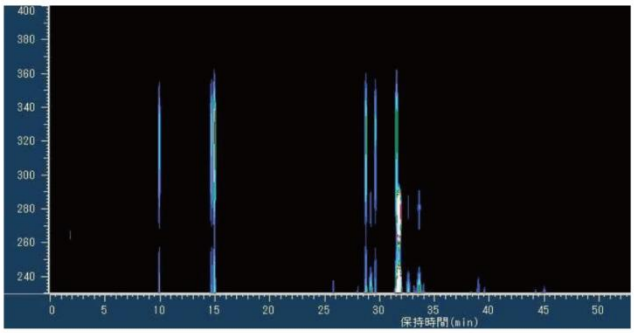

No.037		RNA concentration	
		conc (mg/ml)	% of cont
C6	10 μg/ml	4.31	114.73
	100 μg/ml	2.99	68.26
N18	10 μg/ml	1.75	76.75
	100 μg/ml	0.88	29.11

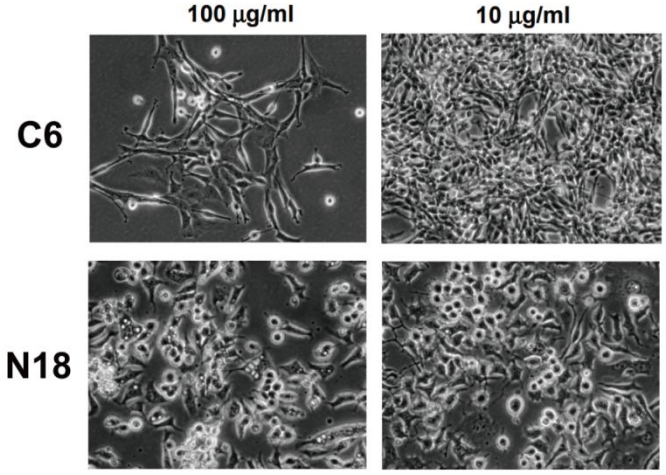

038 Sesami Semen
ゴマ（胡麻）

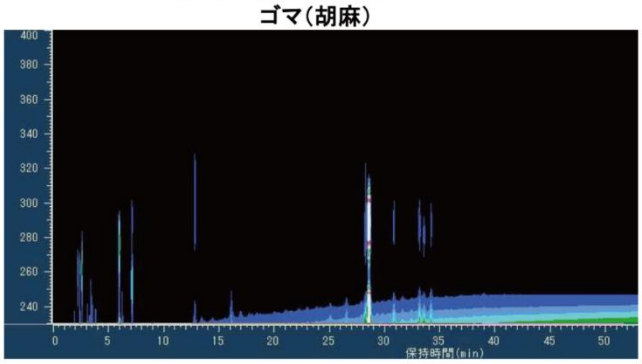

No.038		RNA concentration	
		conc (mg/ml)	% of cont
C6	10 μg/ml	2.87	76.40
	100 μg/ml	1.44	32.88
N18	10 μg/ml	2.23	97.81
	100 μg/ml	1.36	45.00

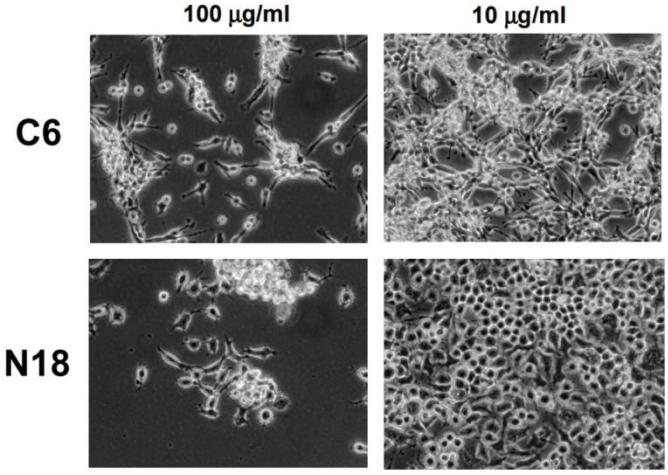

039 Schisandrae Fructus
ゴミシ（五味子）

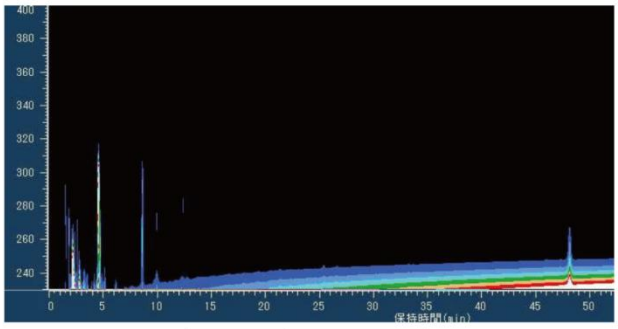

No.039		RNA concentration	
		conc (mg/ml)	% of cont
C6	10 μg/ml	4.38	116.59
	100 μg/ml	5.49	125.34
N18	10 μg/ml	1.50	65.79
	100 μg/ml	2.54	84.01

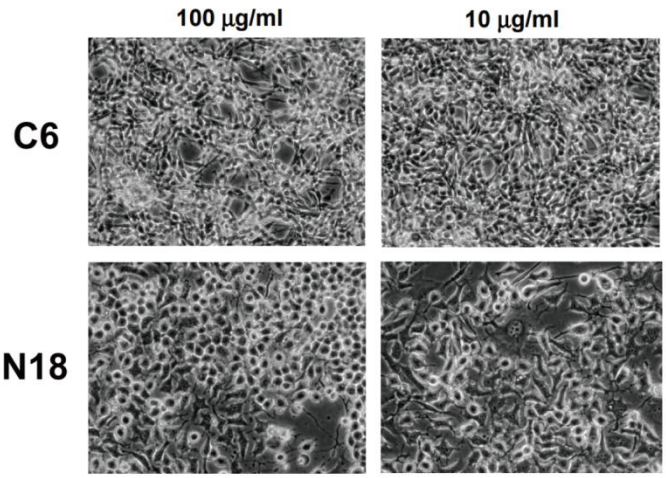

040 Bupleuri Radix
サイコ（柴胡）

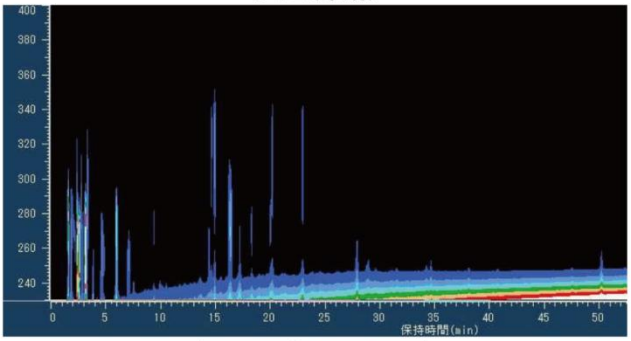

No.040		RNA concentration	
		conc (mg/ml)	% of cont
C6	10 μg/ml	3.65	97.16
	100 μg/ml	6.62	151.14
N18	10 μg/ml	1.11	48.68
	100 μg/ml	2.92	96.58

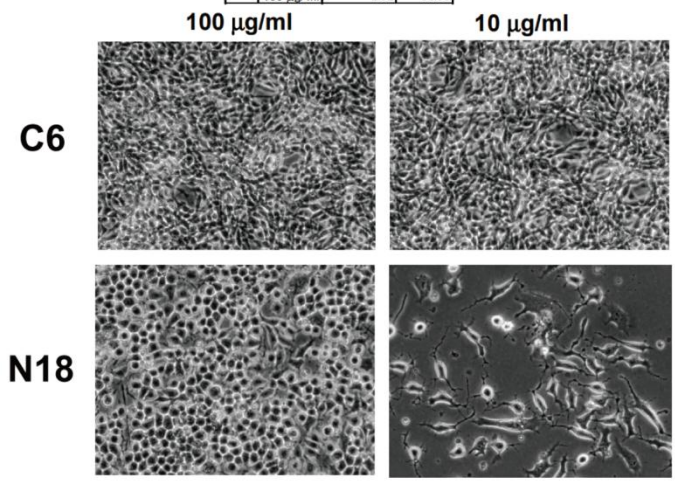

041 Asiasari Radix
サイシン（細辛）

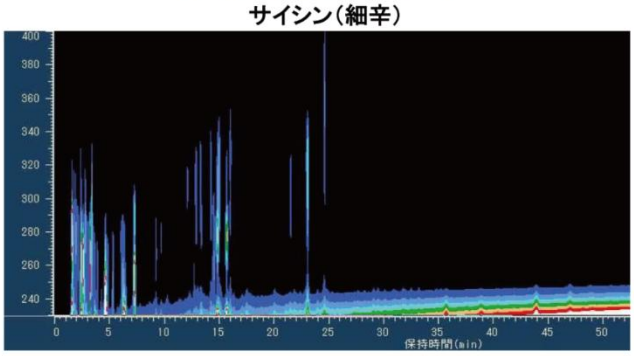

No.041		RNA concentration	
		conc (mg/ml)	% of cont
C6	10 μg/ml	3.42	91.04
	100 μg/ml	5.18	118.26
N18	10 μg/ml	2.25	98.68
	100 μg/ml	0.93	30.76

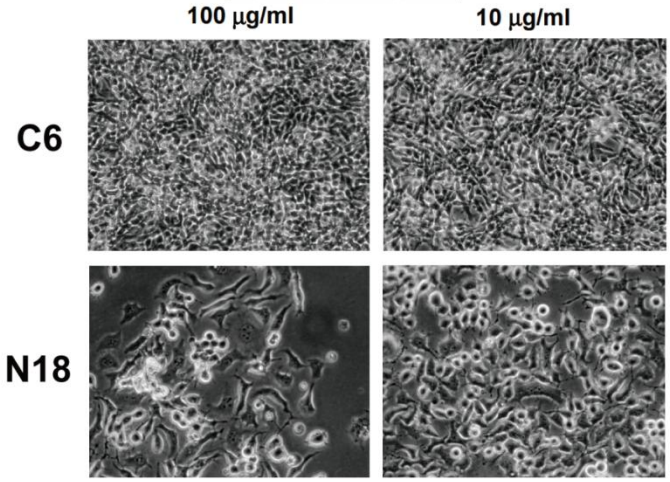

042 Crocus
サフラン

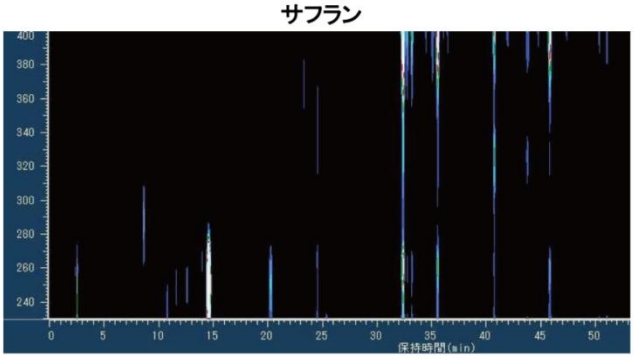

No.042		RNA concentration	
		conc (mg/ml)	% of cont
C6	10 μg/ml	3.06	81.45
	100 μg/ml	5.26	120.09
N18	10 μg/ml	2.62	114.91
	100 μg/ml	2.74	90.63

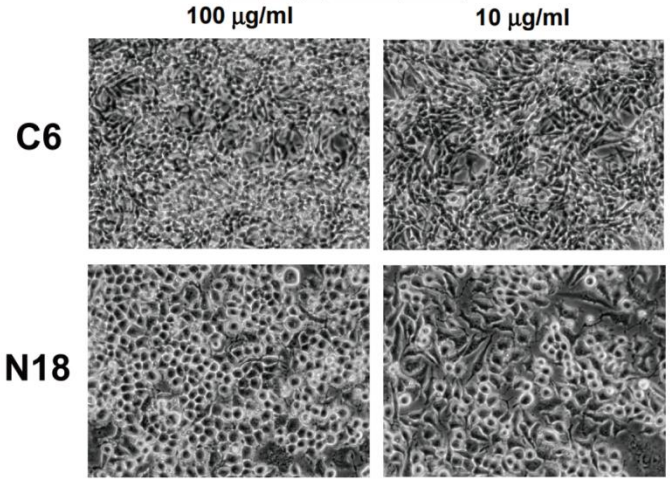

043 Smilacis Rhizoma
サンキライ（山帰来）

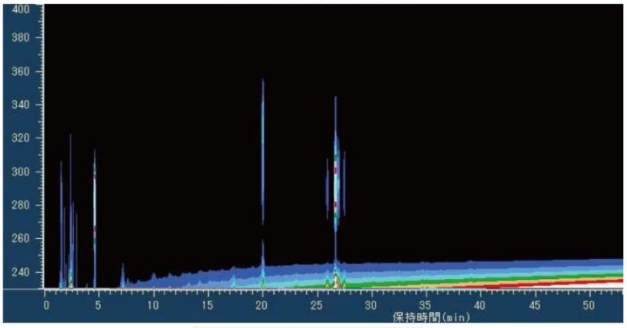

No.043		RNA concentration	
		conc (mg/ml)	% of cont
C6	10 μg/ml	3.02	80.39
	100 μg/ml	4.50	102.74
N18	10 μg/ml	3.15	138.16
	100 μg/ml	2.22	73.43

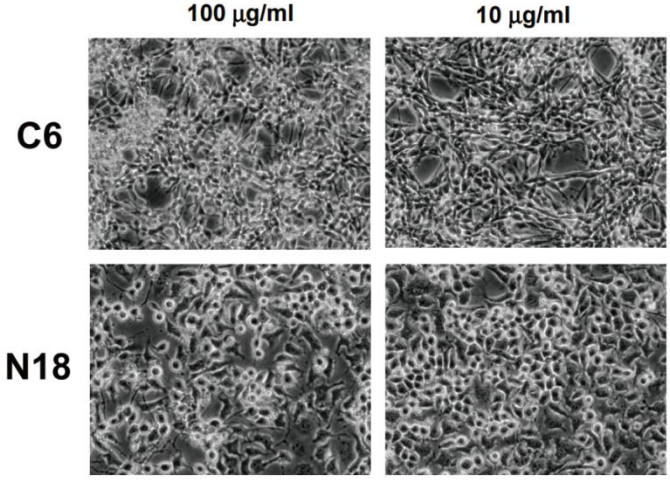

044 Gardeniae Fructus
サンシシ（山梔子）

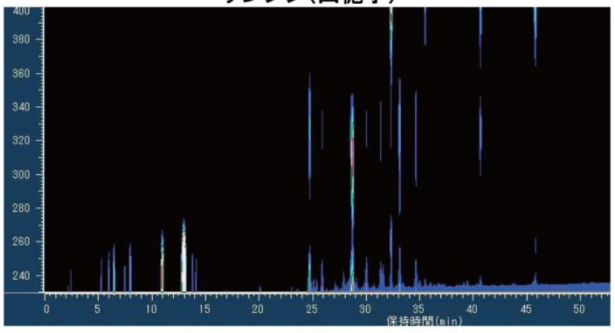

No.044		RNA concentration	
		conc (mg/ml)	% of cont
C6	10 μg/ml	3.41	90.77
	100 μg/ml	5.01	114.38
N18	10 μg/ml	2.78	121.93
	100 μg/ml	2.36	78.60

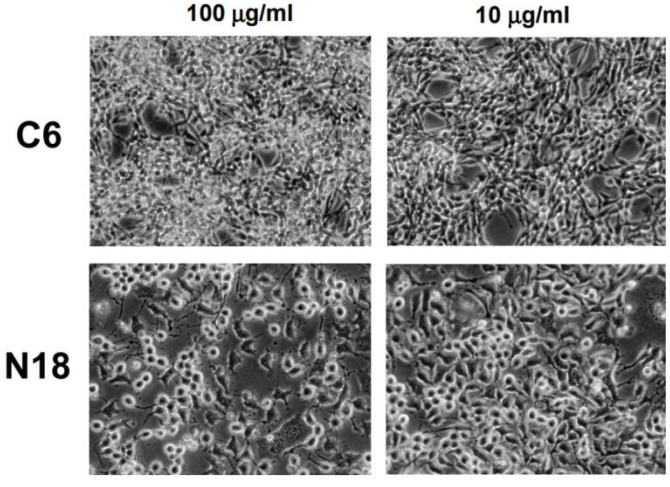

045 Panax Pseudoginseng
サンシチニンジン（三七人参）

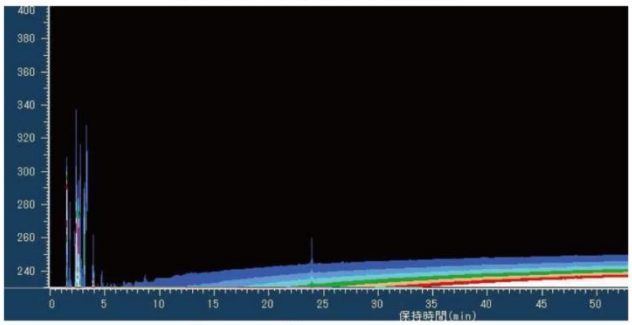

No.045		RNA concentration	
		conc (mg/ml)	% of cont
C6	10 μg/ml	3.55	94.50
	100 μg/ml	5.36	122.37
N18	10 μg/ml	2.61	114.47
	100 μg/ml	2.86	94.60

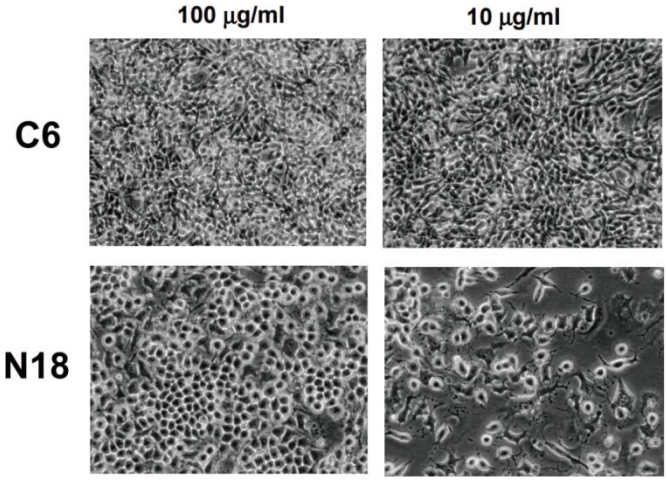

046 Corni Fructus
サンシュユ（山茱萸）

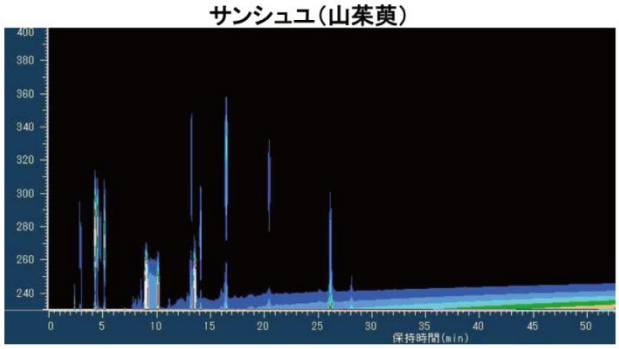

No.046		RNA concentration	
		conc (mg/ml)	% of cont
C6	10 μg/ml	2.37	63.09
	100 μg/ml	2.09	47.72
N18	10 μg/ml	3.01	132.02
	100 μg/ml	0.45	14.88

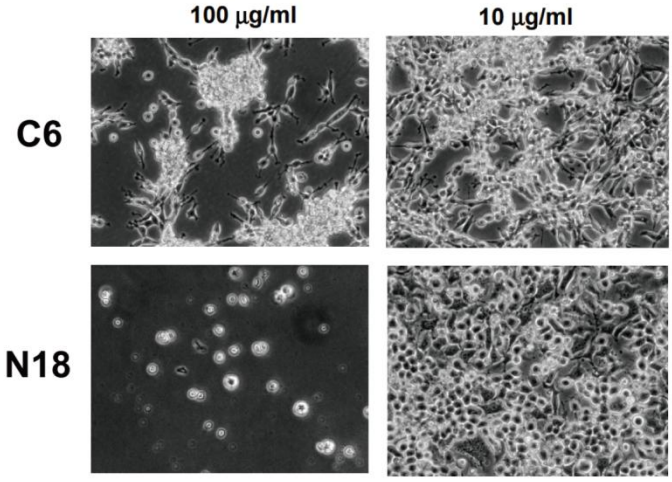

047 Zanthoxyli Fructus
サンショウ（山椒）

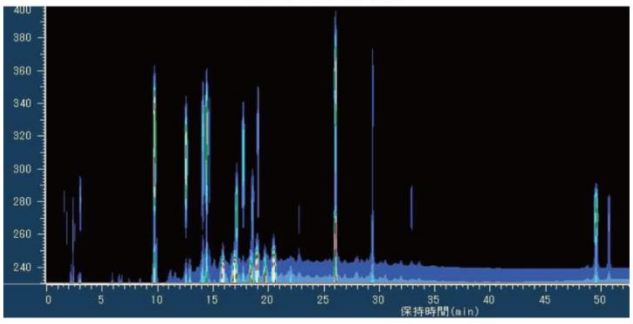

No.047		RNA concentration	
		conc (mg/ml)	% of cont
C6	10 μg/ml	2.02	53.78
	100 μg/ml	2.10	47.95
N18	10 μg/ml	2.46	107.89
	100 μg/ml	ND	ND

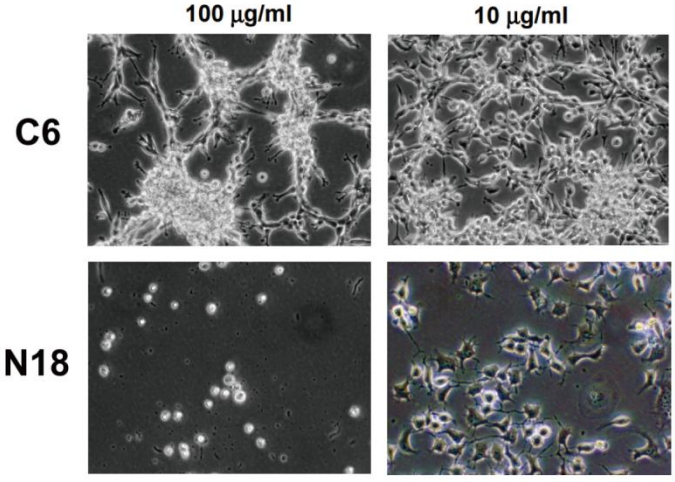

048 Zizyphi Spinosi Semen
サンソウニン（酸棗仁）

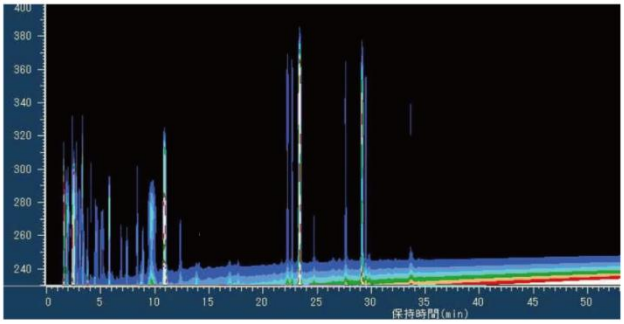

No.048		RNA concentration	
		conc (mg/ml)	% of cont
C6	10 μg/ml	3.23	85.98
	100 μg/ml	5.49	125.34
N18	10 μg/ml	2.83	124.12
	100 μg/ml	2.30	76.08

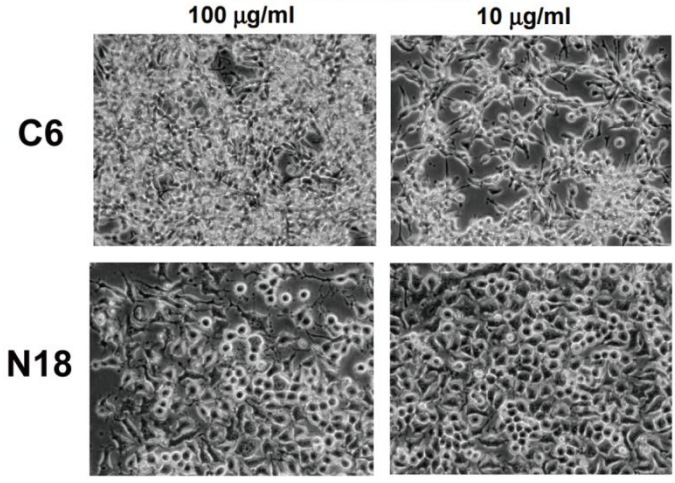

049 Dioscoreae Rhizoma

サンヤク（山薬）

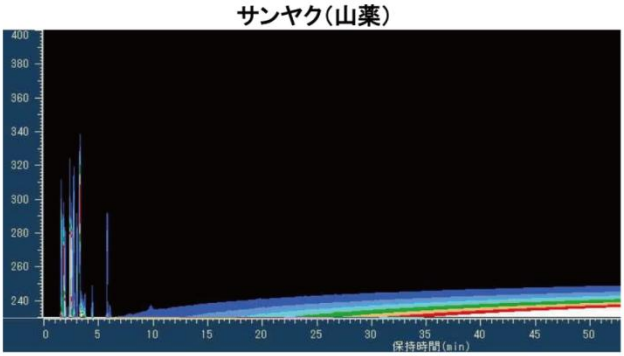

No.049		RNA concentration	
		conc (mg/ml)	% of cont
C6	10 μg/ml	3.02	80.39
	100 μg/ml	5.77	131.74
N18	10 μg/ml	2.80	122.81
	100 μg/ml	3.01	99.56

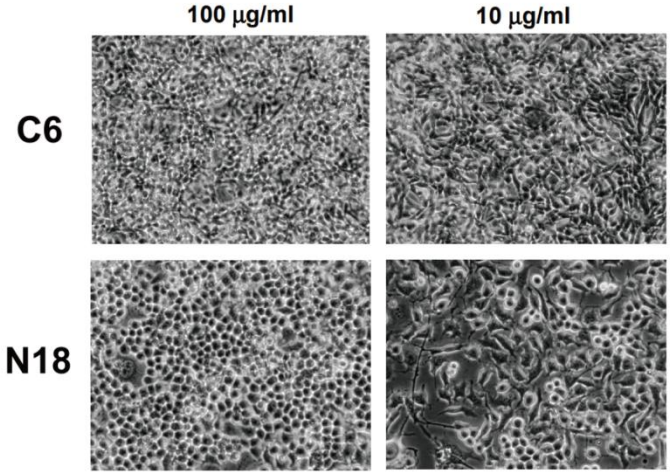

050 Acidum Contentus

サンリョウ（三稜）

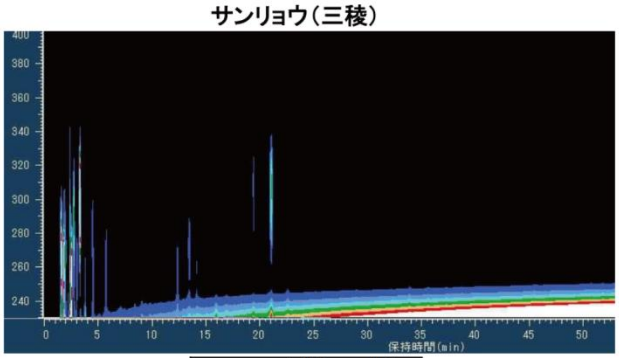

No.050		RNA concentration	
		conc (mg/ml)	% of cont
C6	10 μg/ml	2.63	70.00
	100 μg/ml	5.64	128.77
N18	10 μg/ml	2.02	88.60
	100 μg/ml	2.89	95.59

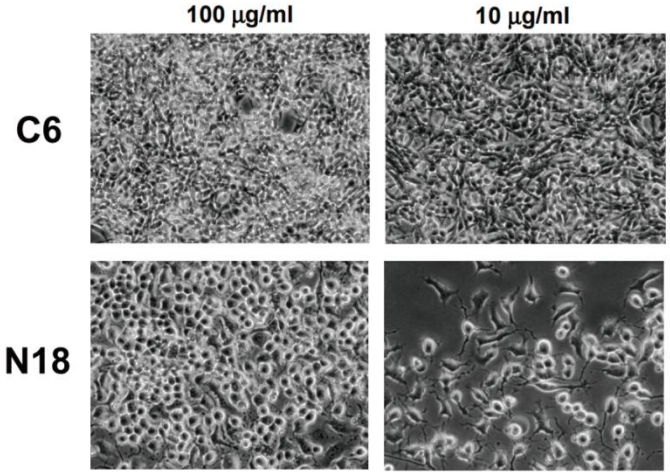

051 Rehmanniae Radix

ジオウ（地黄）

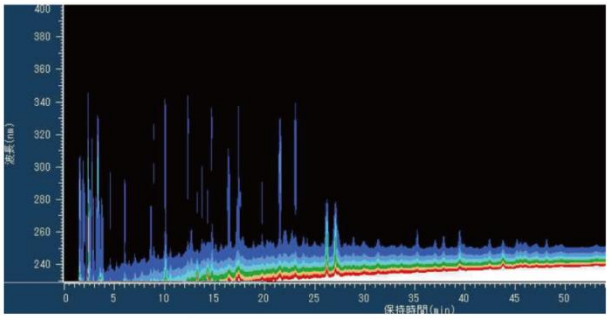

No.051		RNA concentration	
		conc (mg/ml)	% of cont
C6	10 μg/ml	3.21	85.45
	100 μg/ml	4.67	106.62
N18	10 μg/ml	2.80	122.81
	100 μg/ml	2.26	74.75

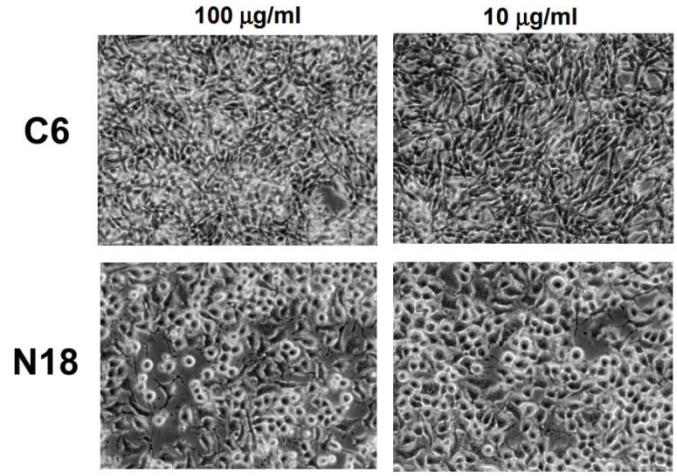

052 Eleutherococci Senticosi Rhizoma

シゴカ（刺五加：エゾウコギ）

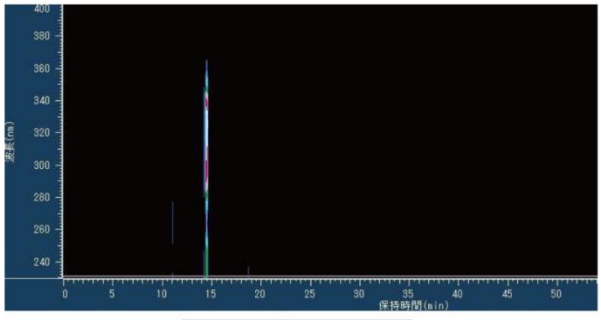

No.052		RNA concentration	
		conc (mg/ml)	% of cont
C6	10 μg/ml	2.94	78.26
	100 μg/ml	4.35	99.32
N18	10 μg/ml	2.82	123.68
	100 μg/ml	1.54	50.94

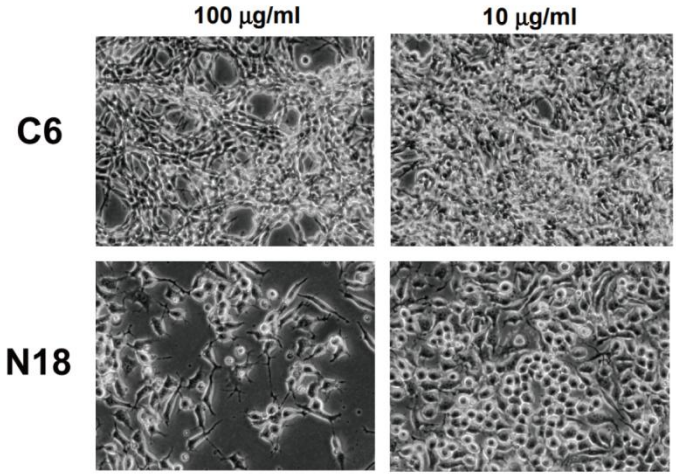

053 Lycii Cortex

ジコッピ（地骨皮）

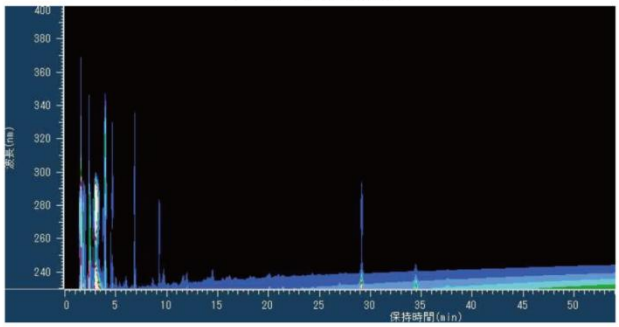

No.053		RNA concentration	
		conc (mg/ml)	% of cont
C6	10 μg/ml	3.31	88.11
	100 μg/ml	0.27	6.16
N18	10 μg/ml	1.51	66.23
	100 μg/ml	ND	ND

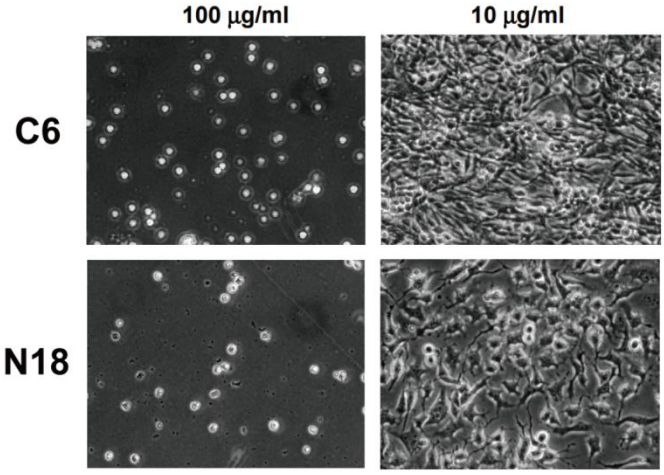

054 Tribuli Fructus

シツリシ（蒺藜子）

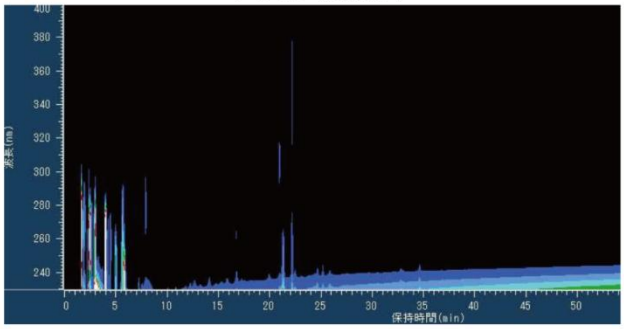

No.054		RNA concentration	
		conc (mg/ml)	% of cont
C6	10 μg/ml	3.31	71.34
	100 μg/ml	5.23	119.41
N18	10 μg/ml	2.51	110.09
	100 μg/ml	2.36	78.06

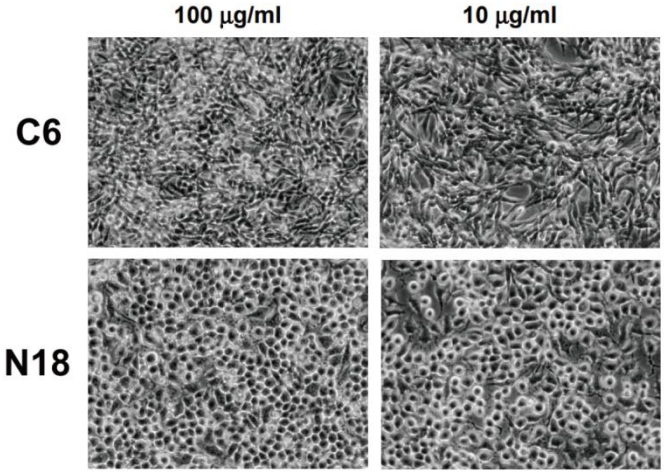

055 Paeoniae Radix

シャクヤク（芍薬）

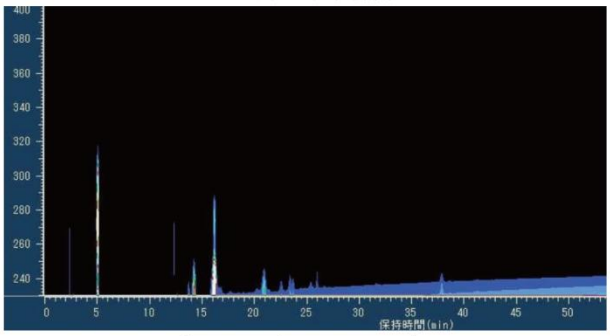

No.055		RNA concentration	
		conc (mg/ml)	% of cont
C6	10 μg/ml	3.27	87.04
	100 μg/ml	2.82	64.38
N18	10 μg/ml	2.25	98.68
	100 μg/ml	0.89	29.43

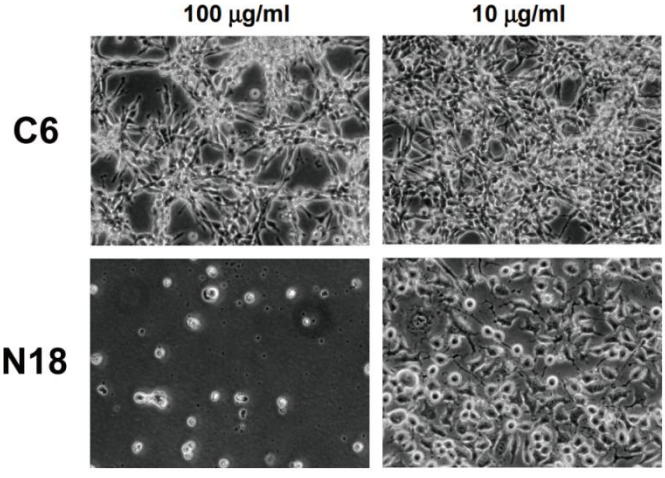

056 Plantaginis Semen

シャゼンシ（車前子）

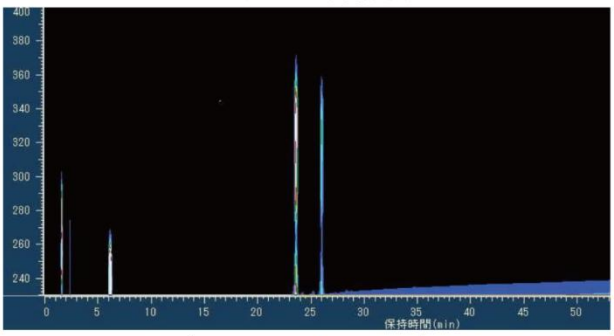

No.056		RNA concentration	
		conc (mg/ml)	% of cont
C6	10 μg/ml	2.57	68.40
	100 μg/ml	4.17	95.21
N18	10 μg/ml	2.68	117.54
	100 μg/ml	1.41	46.64

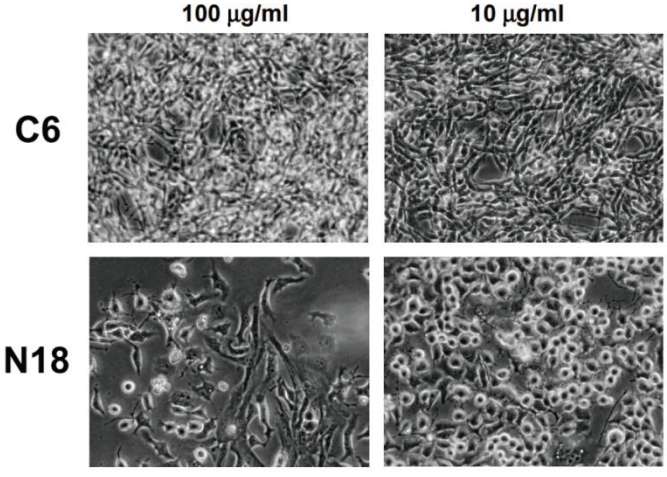

057 Rehmanniae Radix

ジュクジオウ（熟地黄）

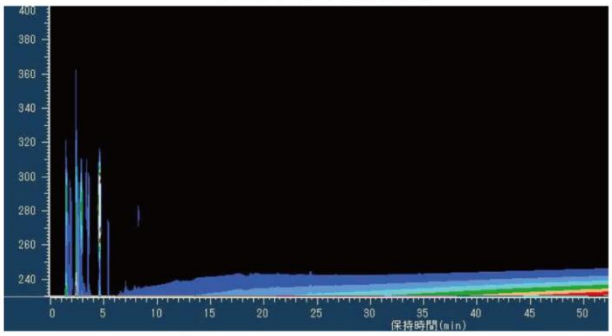

No.057		RNA concentration	
		conc (mg/ml)	% of cont
C6	10 μg/ml	3.24	86.25
	100 μg/ml	5.21	118.95
N18	10 μg/ml	1.83	80.26
	100 μg/ml	2.43	80.38

100 μg/ml　　10 μg/ml

C6

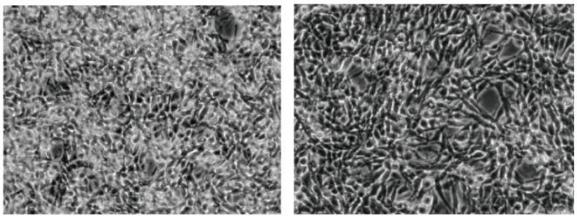

N18

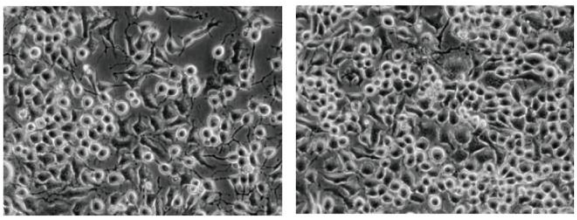

058 Amomi Semen

シュクシャ（縮砂）

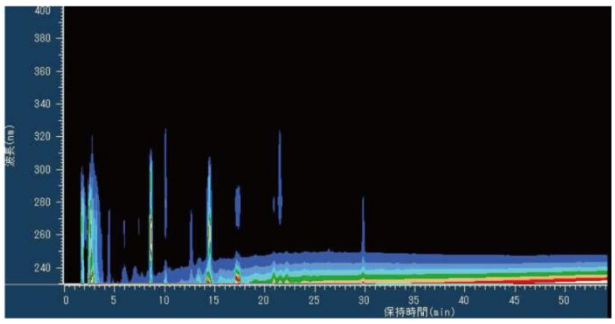

No.058		RNA concentration	
		conc (mg/ml)	% of cont
C6	10 μg/ml	1.58	42.06
	100 μg/ml	5.57	127.17
N18	10 μg/ml	1.81	79.39
	100 μg/ml	0.48	15.88

100 μg/ml　　10 μg/ml

C6

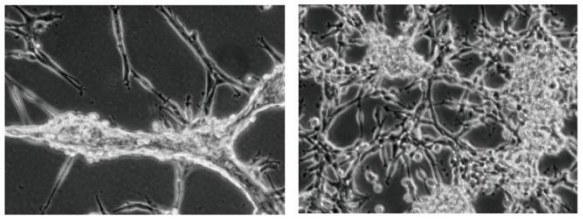

N18

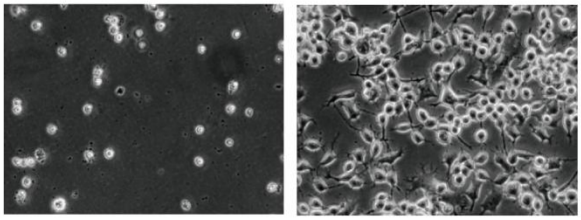

059 Zingiberis Rhizoma

ショウキョウ（生姜）

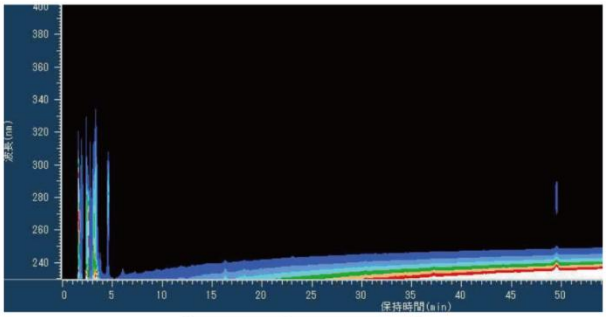

No.059		RNA concentration	
		conc (mg/ml)	% of cont
C6	10 μg/ml	3.23	86.00
	100 μg/ml	5.42	123.74
N18	10 μg/ml	2.44	107.02
	100 μg/ml	2.02	66.81

100 μg/ml　　10 μg/ml

C6

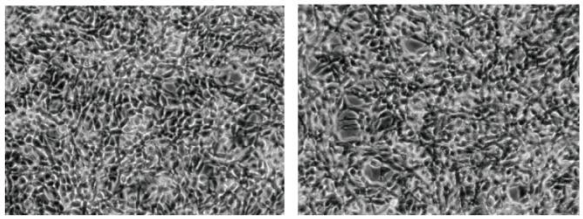

N18

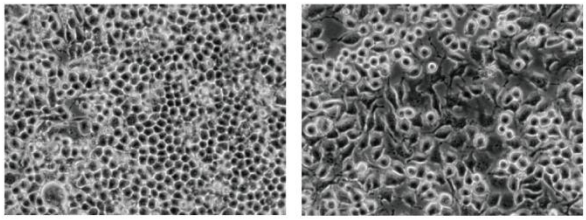

060 Cimicifugae Rhizoma

ショウマ（升麻）

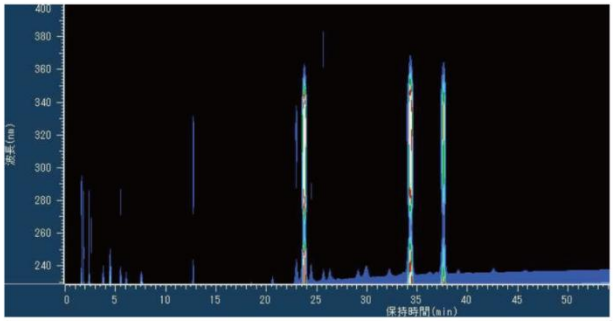

No.060		RNA concentration	
		conc (mg/ml)	% of cont
C6	10 μg/ml	2.80	74.53
	100 μg/ml	3.39	77.4
N18	10 μg/ml	2.00	87.72
	100 μg/ml	0.41	13.56

100 μg/ml　　10 μg/ml

C6

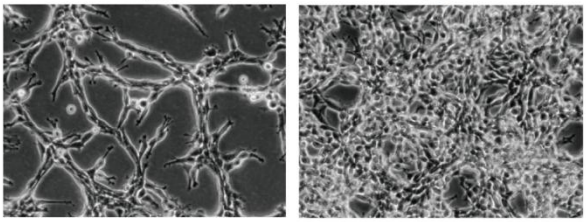

N18

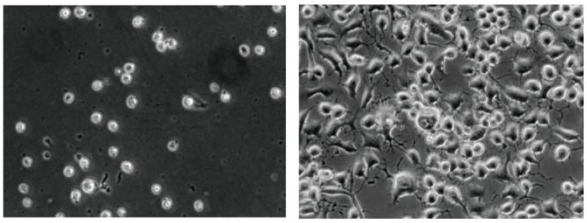

061 Magnoliae Flos
シンイ（辛夷）

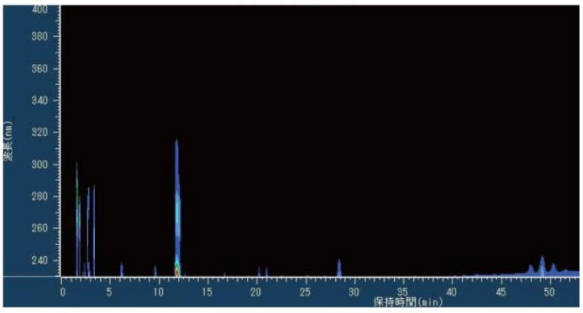

No.061		RNA concentration	
		conc (mg/ml)	% of cont
C6	10 μg/ml	3.17	84.31
	100 μg/ml	3.20	71.59
N18	10 μg/ml	2.34	58.11
	100 μg/ml	0.79	20.21

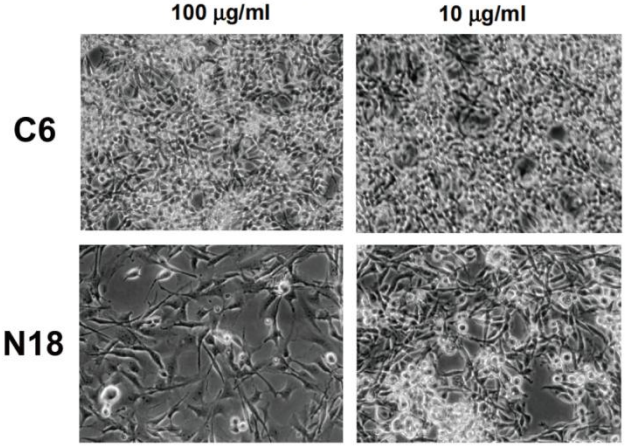

062 Gentianae Macrophyllae Radix
ジンギョウ（秦艽）

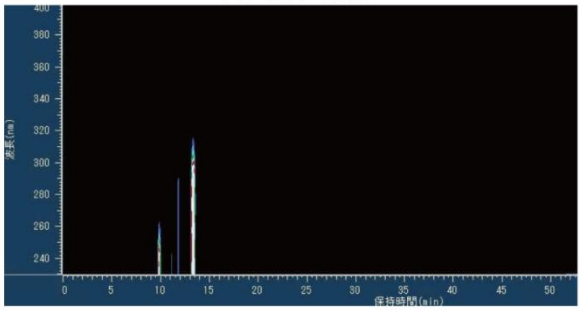

No.062		RNA concentration	
		conc (mg/ml)	% of cont
C6	10 μg/ml	3.43	91.22
	100 μg/ml	4.50	100.67
N18	10 μg/ml	3.37	83.69
	100 μg/ml	3.30	84.40

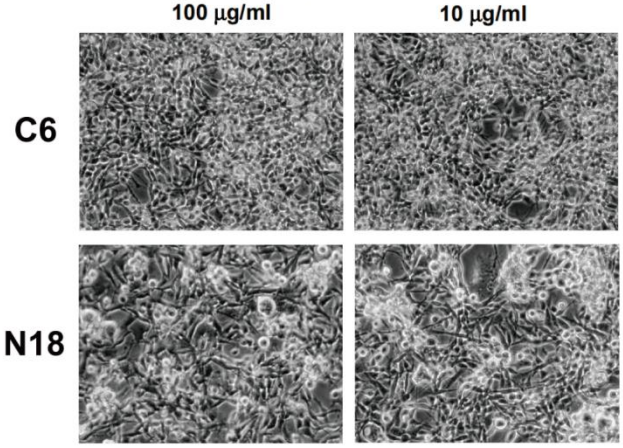

063 Paeoniae Radix Rubra
セキシャク（赤芍）

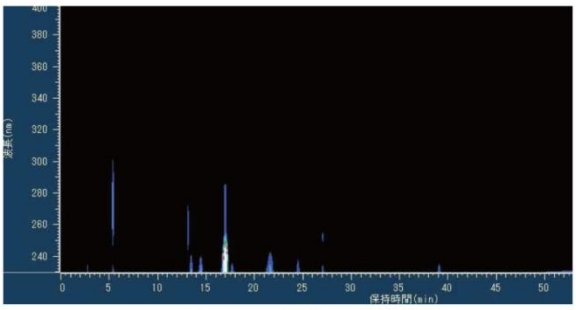

No.063		RNA concentration	
		conc (mg/ml)	% of cont
C6	10 μg/ml	1.96	52.13
	100 μg/ml	1.61	36.02
N18	10 μg/ml	1.02	25.33
	100 μg/ml	ND	ND

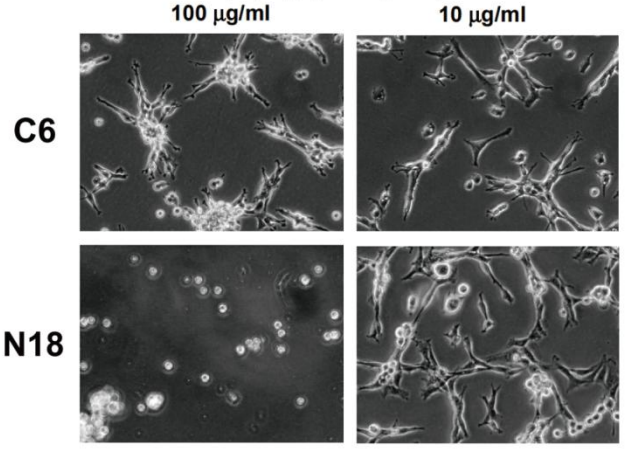

064 Cnidii Rhizoma
センキュウ（川芎）

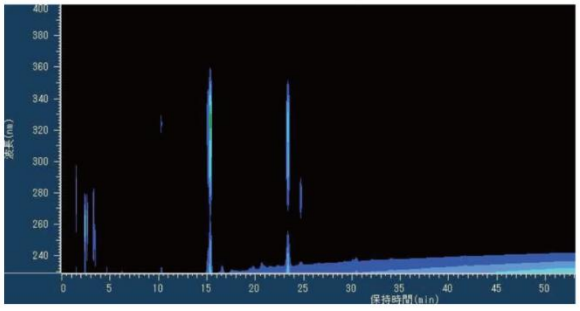

No.064		RNA concentration	
		conc (mg/ml)	% of cont
C6	10 μg/ml	1.92	51.06
	100 μg/ml	4.33	96.87
N18	10 μg/ml	2.55	63.32
	100 μg/ml	3.55	90.79

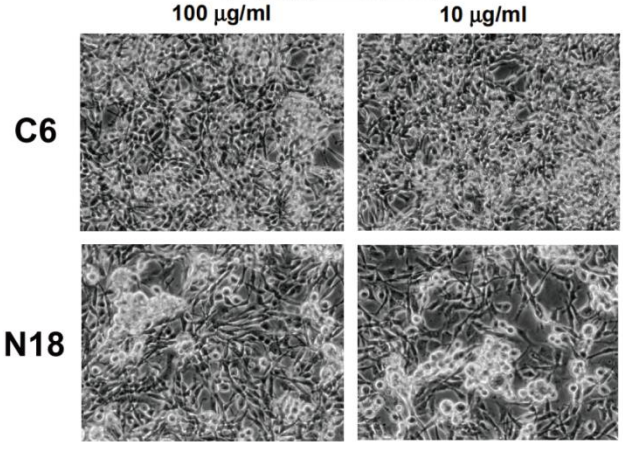

065 (Ginseng Radix)
キボシニンジン（生干人参）

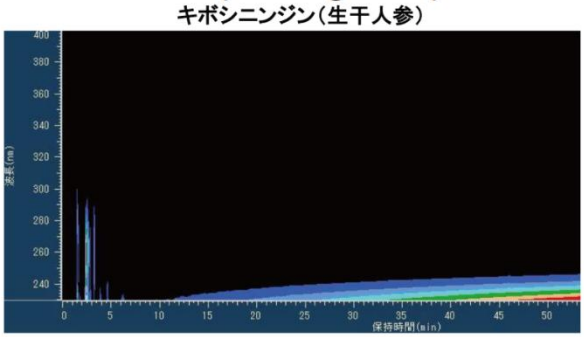

No.065		RNA concentration	
		conc (mg/ml)	% of cont
C6	10 μg/ml	3.15	83.78
	100 μg/ml	5.15	115.21
N18	10 μg/ml	1.91	47.43
	100 μg/ml	3.93	100.51

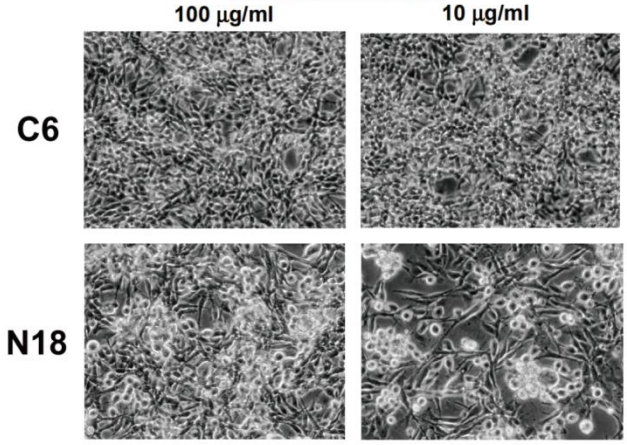

066 Atractylodis Lanceae
ソウジュツ（蒼朮）

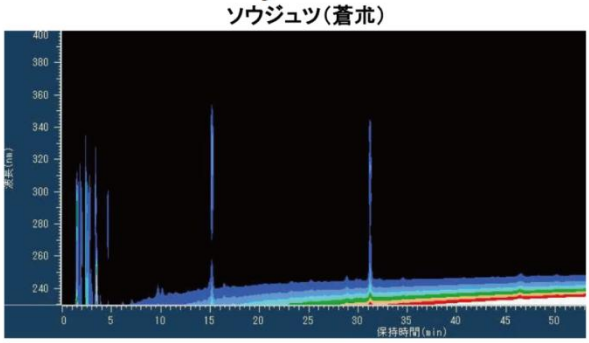

No.066		RNA concentration	
		conc (mg/ml)	% of cont
C6	10 μg/ml	2.79	74.20
	100 μg/ml	4.25	95.08
N18	10 μg/ml	3.66	90.89
	100 μg/ml	3.31	84.65

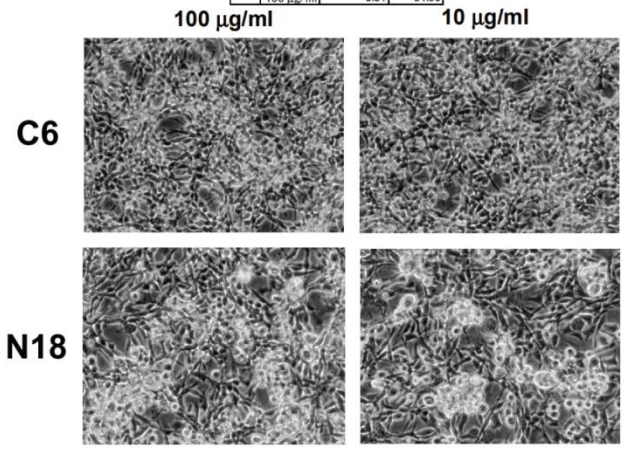

067 Mori Cortex
ソウハクヒ（桑白皮）

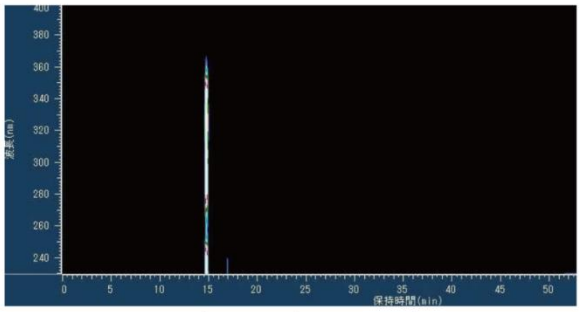

No.067		RNA concentration	
		conc (mg/ml)	% of cont
C6	10 μg/ml	2.86	76.06
	100 μg/ml	5.14	115.00
N18	10 μg/ml	2.29	56.87
	100 μg/ml	2.88	73.66

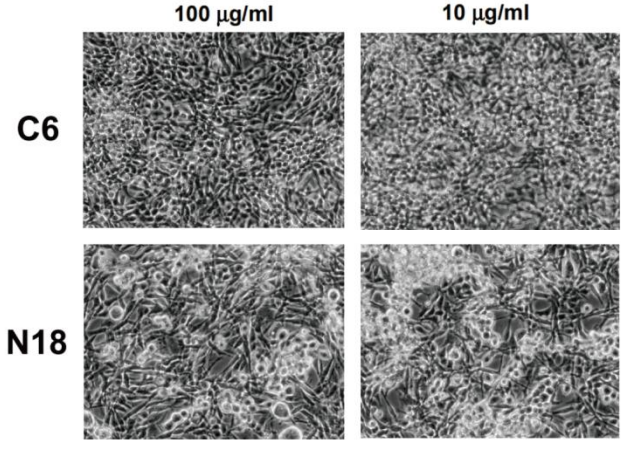

068 Perilla Herba
ソウヨウ（桑葉）

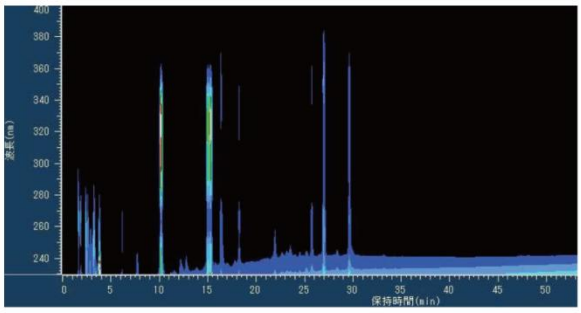

No.068		RNA concentration	
		conc (mg/ml)	% of cont
C6	10 μg/ml	3.08	81.91
	100 μg/ml	4.14	92.62
N18	10 μg/ml	2.41	59.85
	100 μg/ml	1.73	44.25

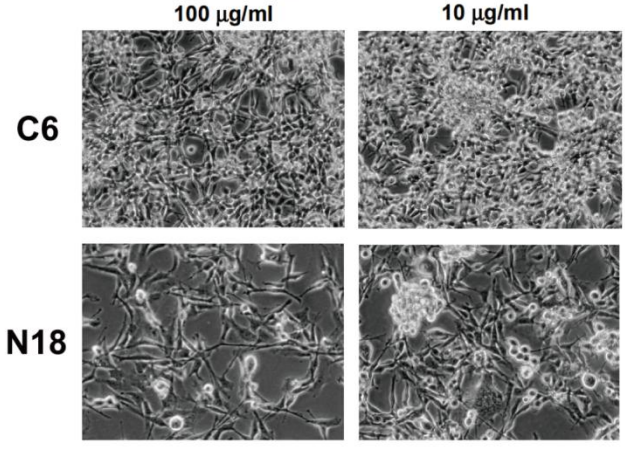

069 Dipsaci Radix
ゾクダン（続断）

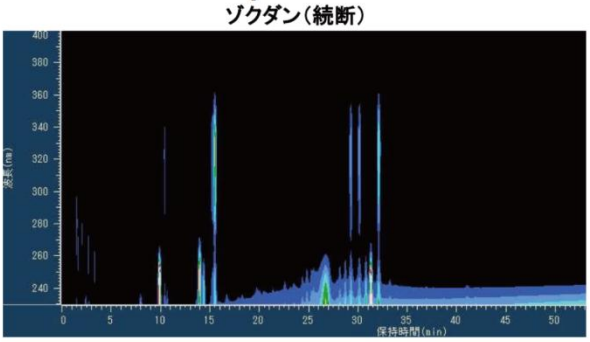

No.069		RNA concentration	
		conc (mg/ml)	% of cont
C6	10 μg/ml	3.00	79.79
	100 μg/ml	3.88	86.80
N18	10 μg/ml	2.40	60.00
	100 μg/ml	3.38	86.45

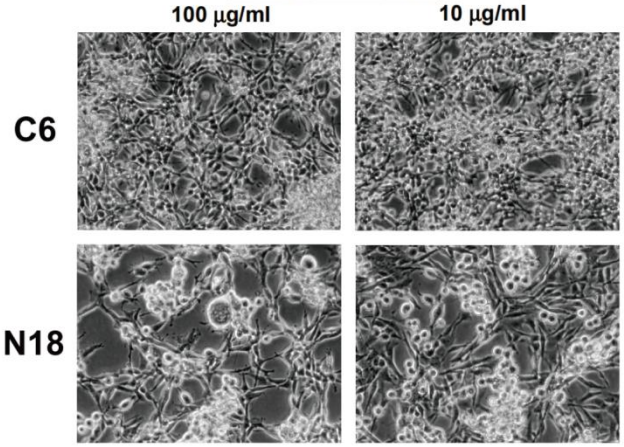

070 Perillae Herba
ソヨウ（蘇葉）

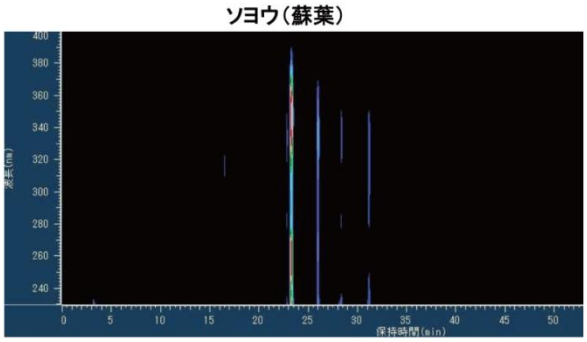

No.070		RNA concentration	
		conc (mg/ml)	% of cont
C6	10 μg/ml	2.87	76.33
	100 μg/ml	3.40	76.06
N18	10 μg/ml	1.43	35.51
	100 μg/ml	0.58	14.83

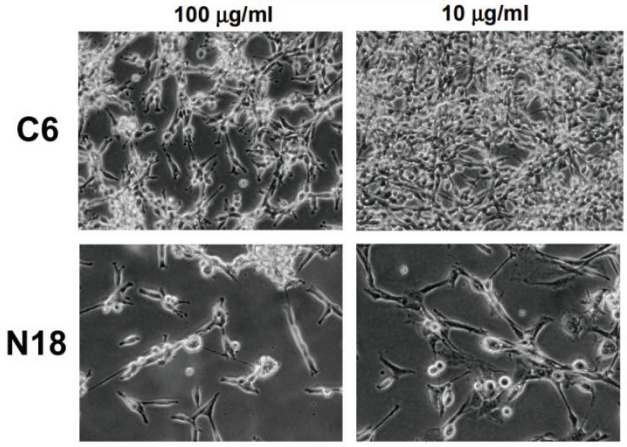

071 Rhei Rhizoma
ダイオウ（大黄）

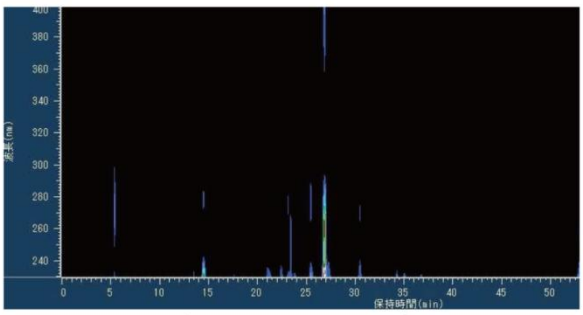

No.071		RNA concentration	
		conc (mg/ml)	% of cont
C6	10 μg/ml	1.28	34.07
	100 μg/ml	0.49	8.90
N18	10 μg/ml	1.13	28.06
	100 μg/ml	ND	ND

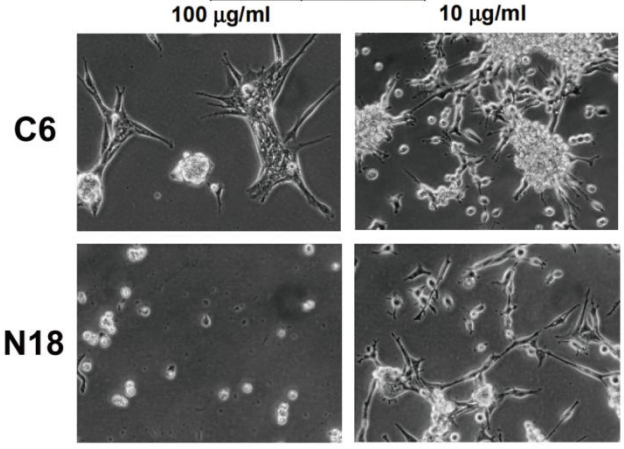

072 Zizyphi Fructus
タイソウ（大棗）

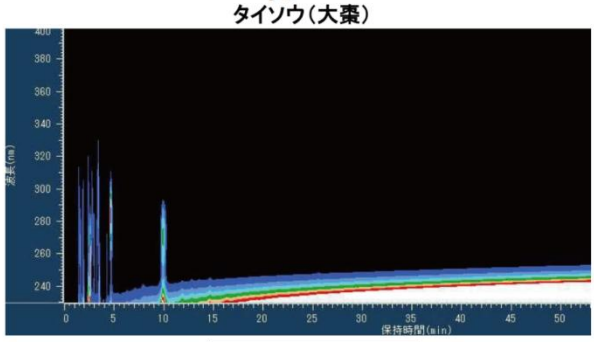

No.072		RNA concentration	
		conc (mg/ml)	% of cont
C6	10 μg/ml	3.26	86.77
	100 μg/ml	3.67	82.18
N18	10 μg/ml	3.75	93.12
	100 μg/ml	2.82	72.12

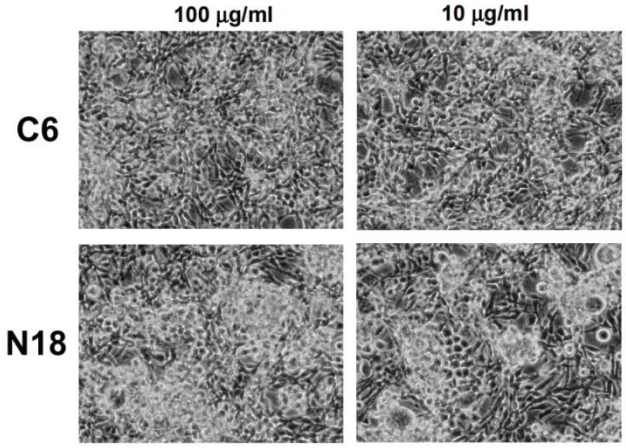

073 Alismatis Rhizoma
タクシャ（沢瀉）

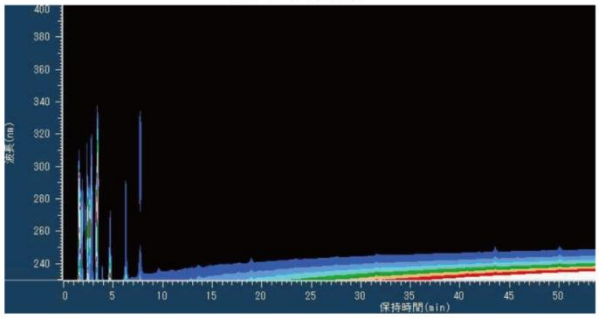

No.073		RNA concentration	
		conc (mg/ml)	% of cont
C6	10 μg/ml	3.28	87.30
	100 μg/ml	4.67	104.57
N18	10 μg/ml	4.31	107.28
	100 μg/ml	3.32	84.91

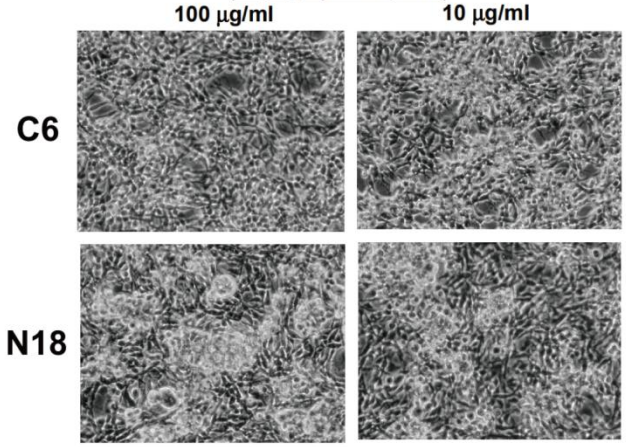

074 Salviae Miltiorhizae Radix
タンジン（丹参）

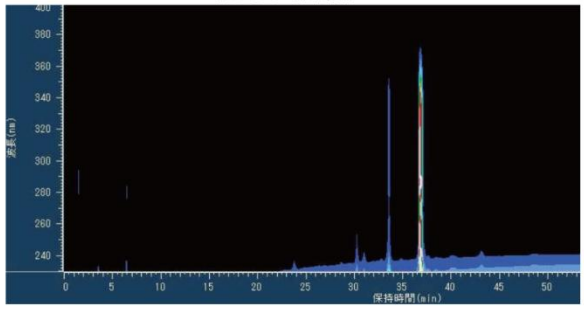

No.074		RNA concentration	
		conc (mg/ml)	% of cont
C6	10 μg/ml	3.00	79.85
	100 μg/ml	3.12	69.86
N18	10 μg/ml	2.14	53.14
	100 μg/ml	0.47	12.02

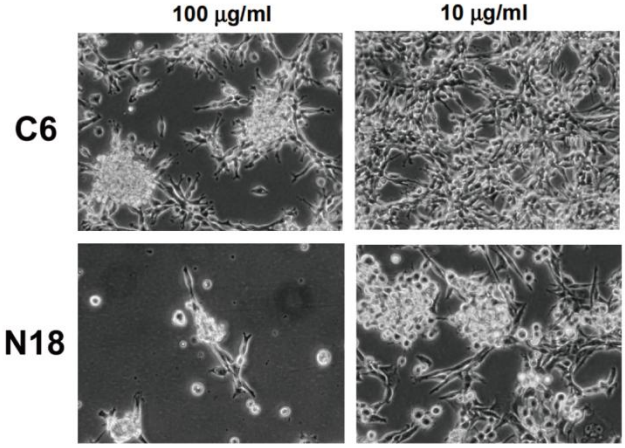

075 Bambusae Caulis
チクジョ（竹茹）

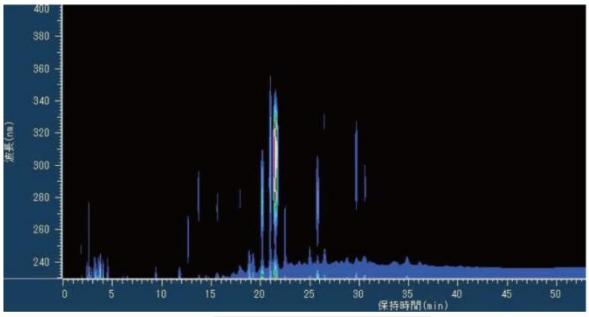

No.075		RNA concentration	
		conc (mg/ml)	% of cont
C6	10 μg/ml	3.04	80.92
	100 μg/ml	4.58	102.55
N18	10 μg/ml	1.75	43.46
	100 μg/ml	0.73	18.67

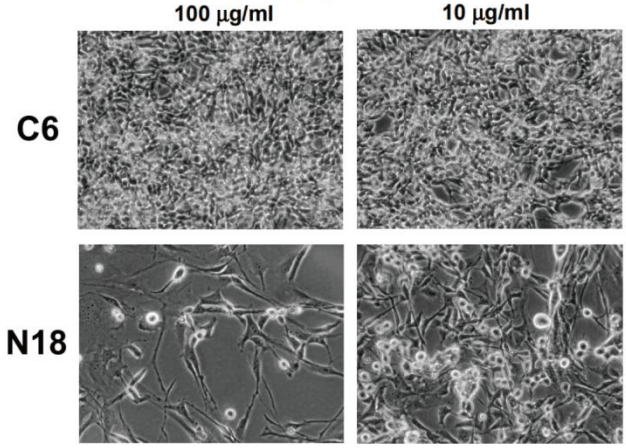

076 Panacis Japonici Rhizoma
チクセツニンジン（竹節人参）

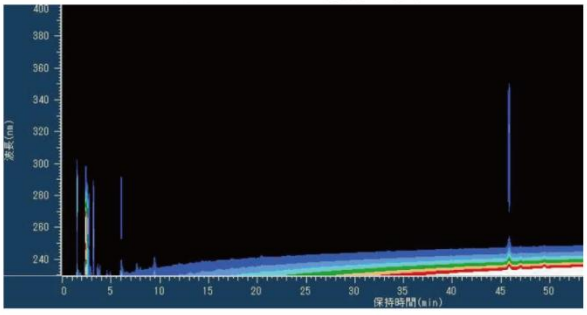

No.076		RNA concentration	
		conc (mg/ml)	% of cont
C6	10 μg/ml	2.90	77.19
	100 μg/ml	5.45	122.03
N18	10 μg/ml	4.28	106.28
	100 μg/ml	3.59	91.82

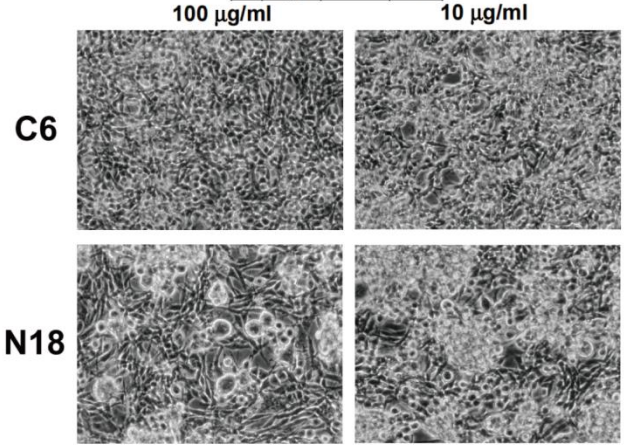

077 Anemarrhenae Rhizoma
チモ（知母）

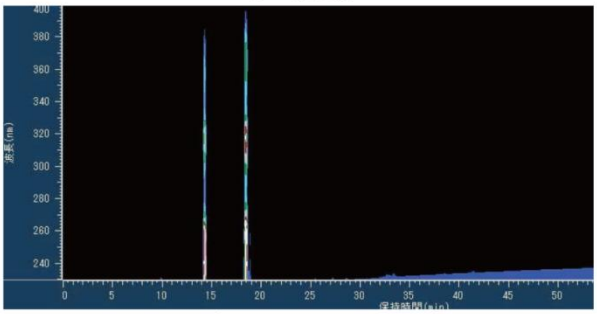

No.077		RNA concentration	
		conc (mg/ml)	% of cont
C6	10 μg/ml	2.94	78.25
	100 μg/ml	4.53	101.43
N18	10 μg/ml	4.14	102.81
	100 μg/ml	3.50	89.51

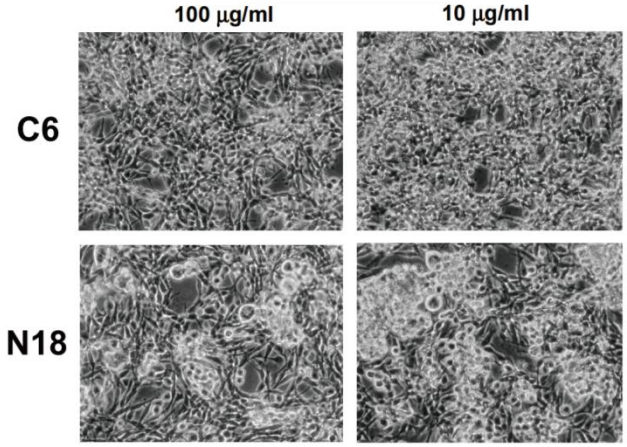

078 Caryophylli Flos
チョウジ（丁子）

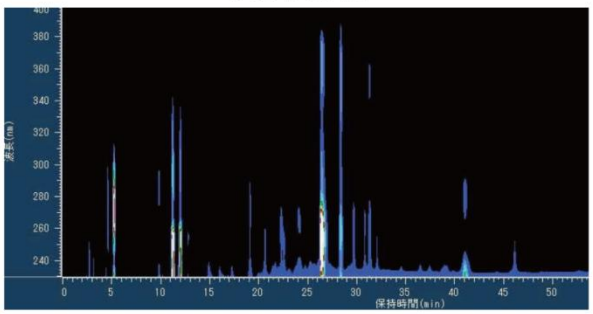

No.078		RNA concentration	
		conc (mg/ml)	% of cont
C6	10 μg/ml	1.27	33.80
	100 μg/ml	ND	ND
N18	10 μg/ml	0.38	9.44
	100 μg/ml	ND	ND

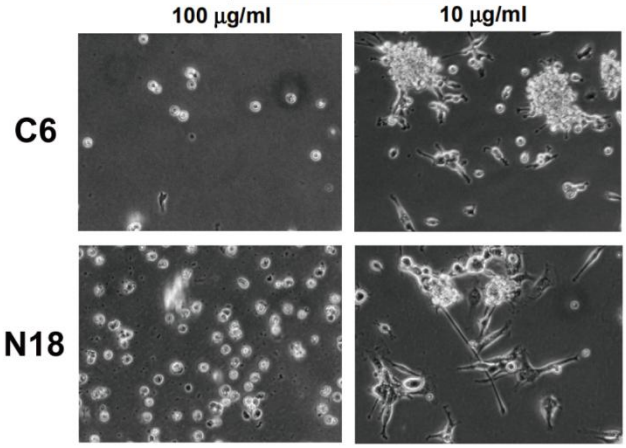

079 Uncariae Uncis Cum Ramulus
チョウトウコウ（釣藤鉤）

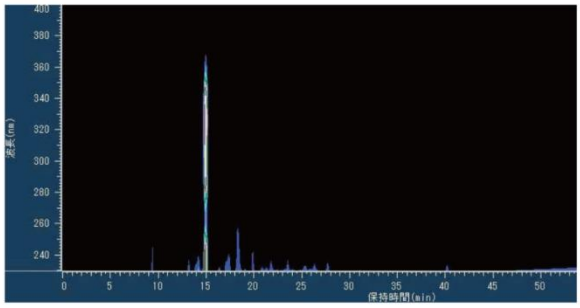

No.079		RNA concentration	
		conc (mg/ml)	% of cont
C6	10 μg/ml	2.44	64.95
	100 μg/ml	2.82	63.14
N18	10 μg/ml	1.76	43.70
	100 μg/ml	0.56	14.32

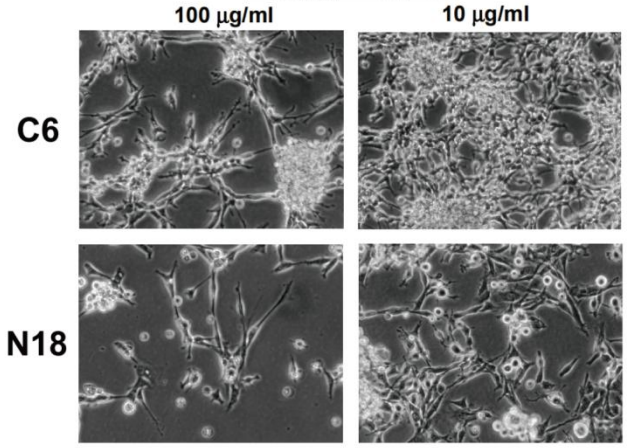

080 Polyporus
チョレイ（猪苓）

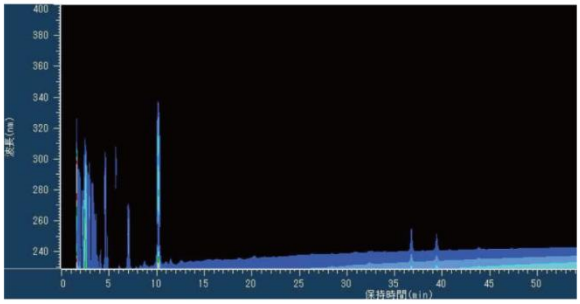

No.080		RNA concentration	
		conc (mg/ml)	% of cont
C6	10 μg/ml	3.45	91.83
	100 μg/ml	4.88	109.27
N18	10 μg/ml	3.37	83.69
	100 μg/ml	3.20	81.84

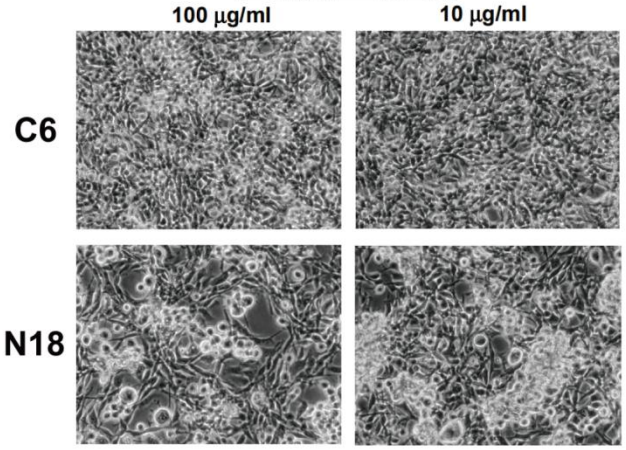

081 Aurantii Nobilis Pericarpium
チンピ（陳皮）

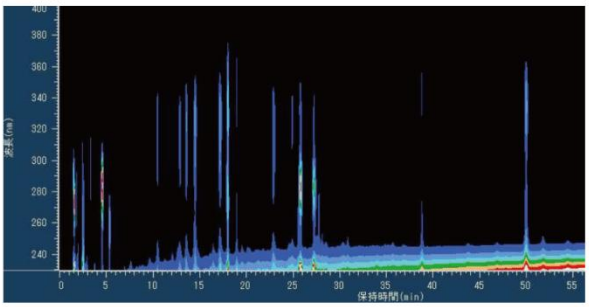

No.081		RNA concentration	
		conc (mg/ml)	% of cont
C6	10 μg/ml	3.04	80.92
	100 μg/ml	3.89	87.10
N18	10 μg/ml	3.43	85.18
	100 μg/ml	3.63	92.84

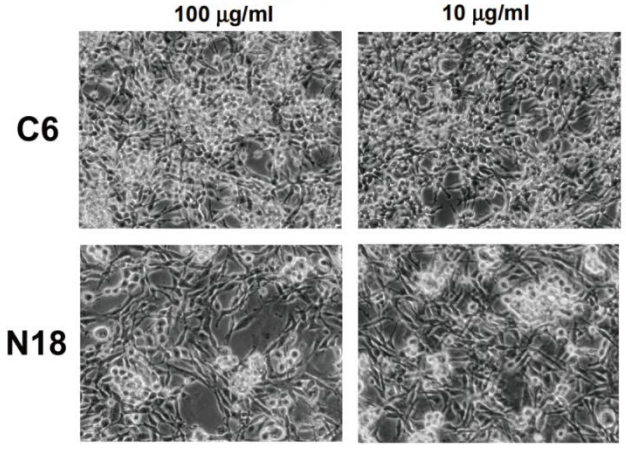

082 Gastrodiae Rhizoma
テンマ（天麻）

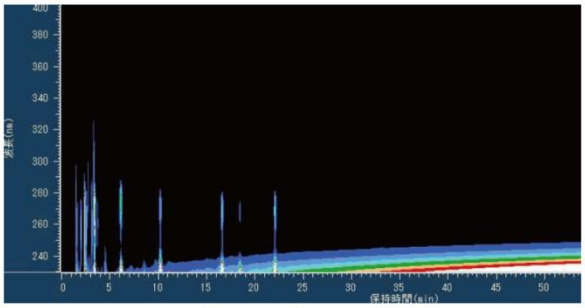

No.082		RNA concentration	
		conc (mg/ml)	% of cont
C6	10 μg/ml	3.16	84.04
	100 μg/ml	5.06	113.20
N18	10 μg/ml	3.75	93.28
	100 μg/ml	3.07	78.52

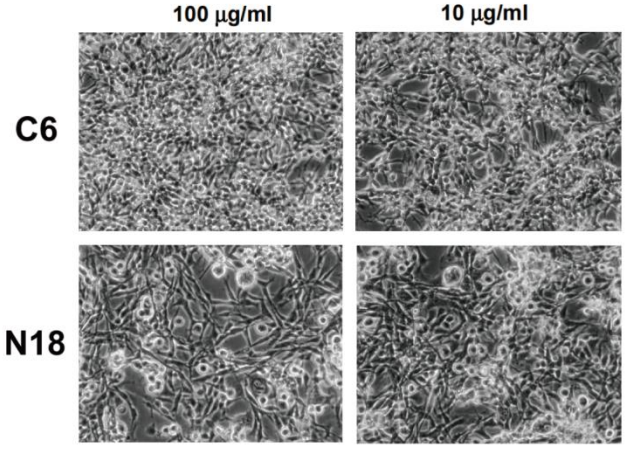

083 Asparagi Radix
テンモンドウ（天門冬）

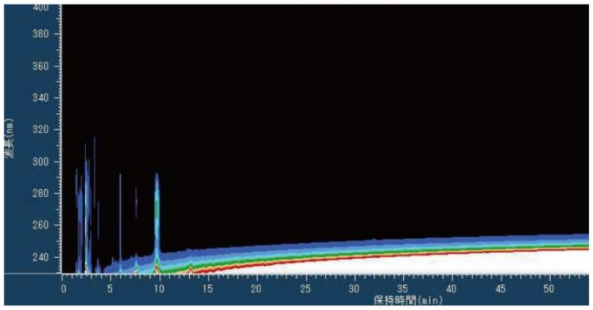

No.083		RNA concentration	
		conc (mg/ml)	% of cont
C6	10 μg/ml	2.68	71.33
	100 μg/ml	4.99	111.73
N18	10 μg/ml	3.90	96.85
	100 μg/ml	2.79	71.36

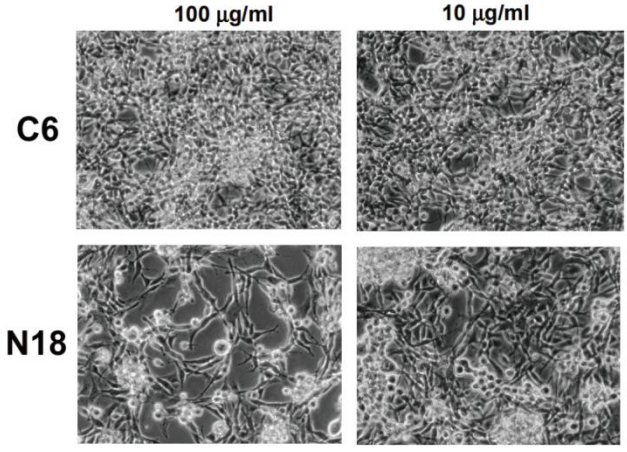

084 Benincasae Semen
トウガシ（冬瓜子）

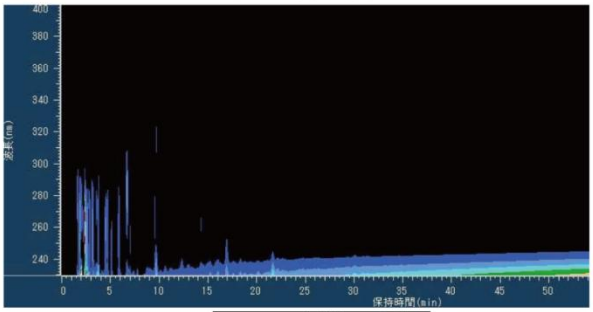

No.084		RNA concentration	
		conc (mg/ml)	% of cont
C6	10 μg/ml	3.08	81.98
	100 μg/ml	4.86	108.82
N18	10 μg/ml	3.75	93.12
	100 μg/ml	2.74	70.08

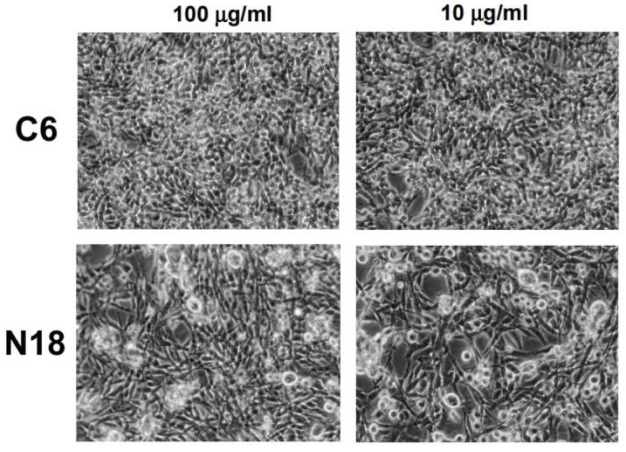

085 Angelicae Radix

トウキ（当帰）

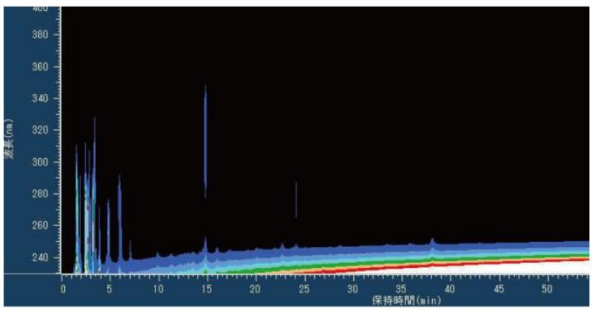

No.085		RNA concentration	
		conc (mg/ml)	% of cont
C6	10 μg/ml	3.20	85.17
	100 μg/ml	5.40	120.91
N18	10 μg/ml	3.68	91.38
	100 μg/ml	3.08	78.77

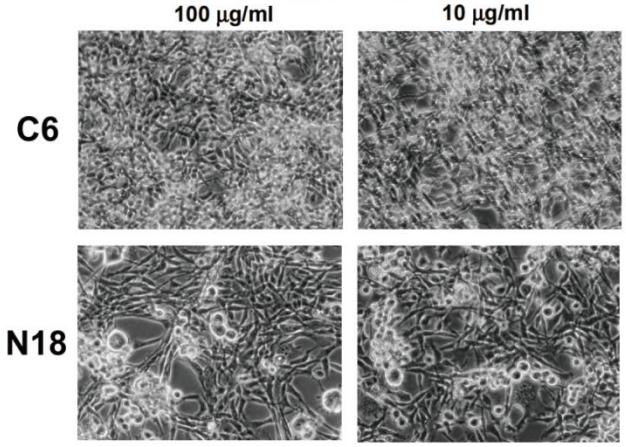

086 Codonopsitis Radix

トウジン（党参）

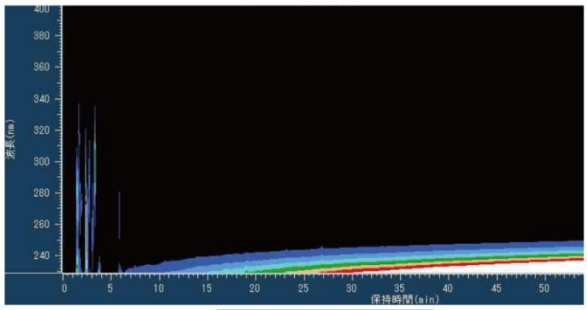

No.086		RNA concentration	
		conc (mg/ml)	% of cont
C6	10 μg/ml	2.90	77.19
	100 μg/ml	5.01	112.18
N18	10 μg/ml	3.50	86.91
	100 μg/ml	3.32	84.91

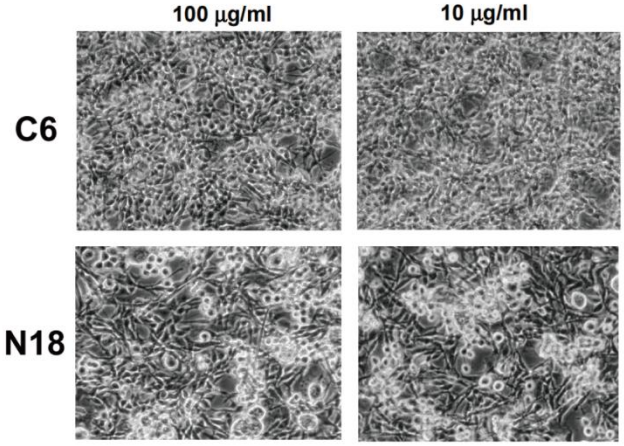

087 Persicae Semen

トウニン（桃仁）

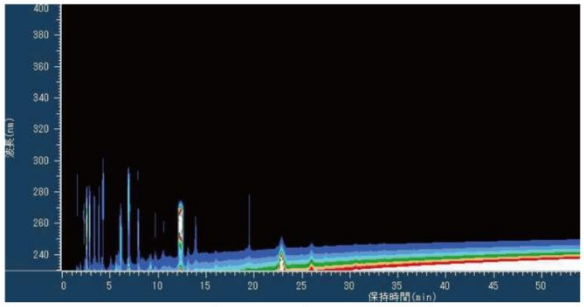

No.087		RNA concentration	
		conc (mg/ml)	% of cont
C6	10 μg/ml	3.36	89.94
	100 μg/ml	4.28	95.84
N18	10 μg/ml	3.44	85.42
	100 μg/ml	2.35	60.10

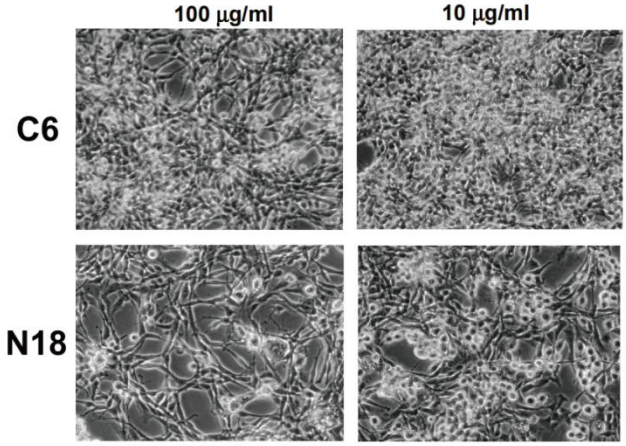

088 Araliae Cordatae Rhizoma

ドクカツ（独活）

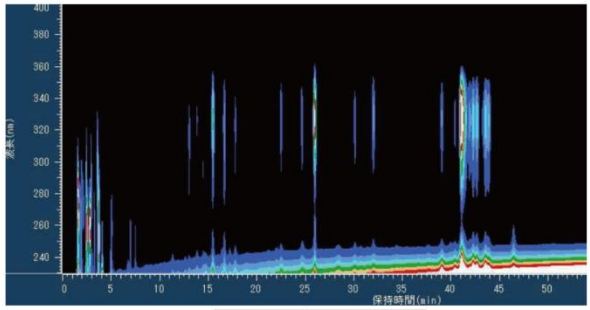

No.088		RNA concentration	
		conc (mg/ml)	% of cont
C6	10 μg/ml	2.87	76.39
	100 μg/ml	4.84	108.37
N18	10 μg/ml	3.31	82.20
	100 μg/ml	3.01	76.98

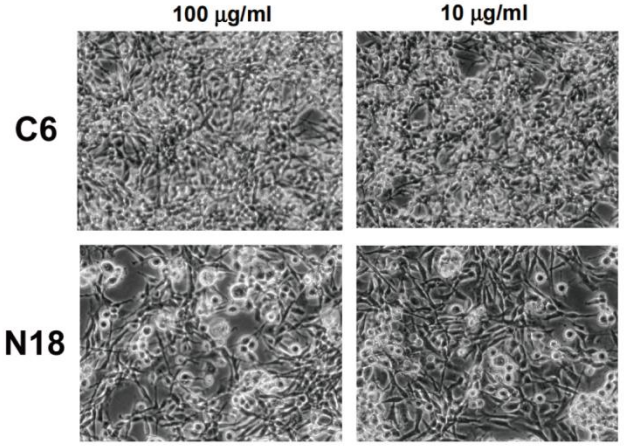

089 Eucommiae Cortex

トチュウ（杜仲）

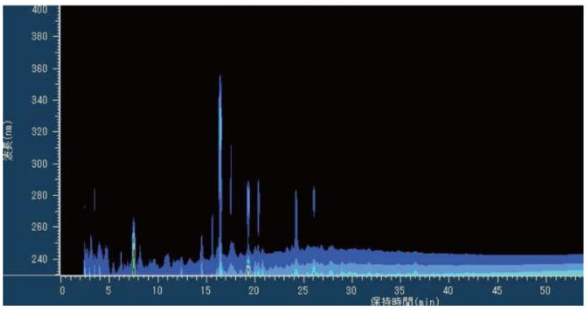

No.089		RNA concentration	
		conc (mg/ml)	% of cont
C6	10 μg/ml	3.43	91.30
	100 μg/ml	4.53	101.43
N18	10 μg/ml	3.01	74.75
	100 μg/ml	2.37	60.61

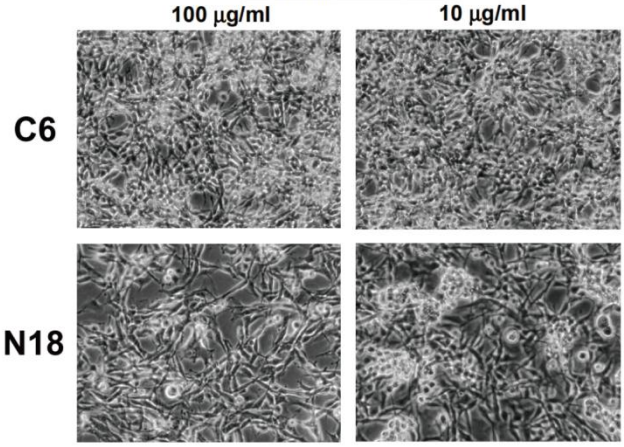

090 Cistanchis Herba

ニクジュウヨウ（肉蓯蓉）

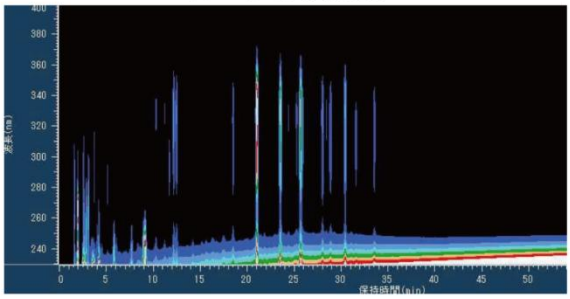

No.090		RNA concentration	
		conc (mg/ml)	% of cont
C6	10 μg/ml	2.49	66.22
	100 μg/ml	4.39	98.21
N18	10 μg/ml	3.38	83.93
	100 μg/ml	2.65	67.78

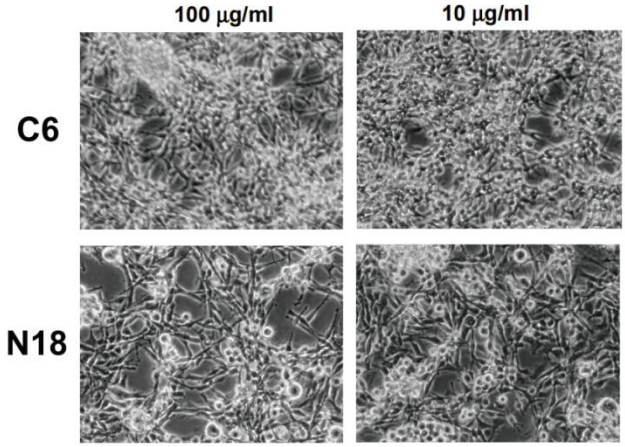

091 Panacis Ginseng Radix

ニンジン（人参）

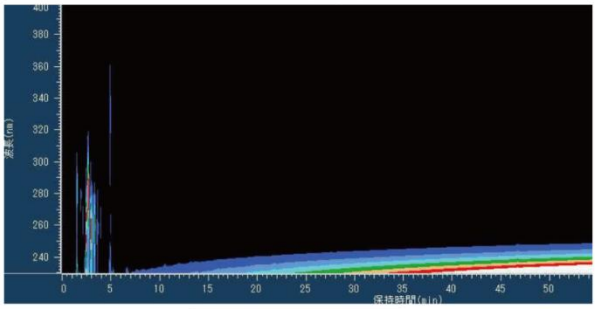

No.091		RNA concentration	
		conc (mg/ml)	% of cont
C6	10 μg/ml	4.52	112.72
	100 μg/ml	6.01	101.74
N18	10 μg/ml	2.11	75.28
	100 μg/ml	3.72	116.50

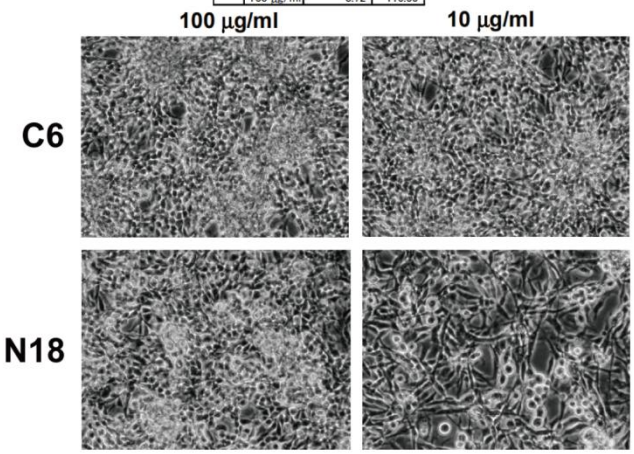

092 Pulsatilla chinensis

バイモ（貝母）

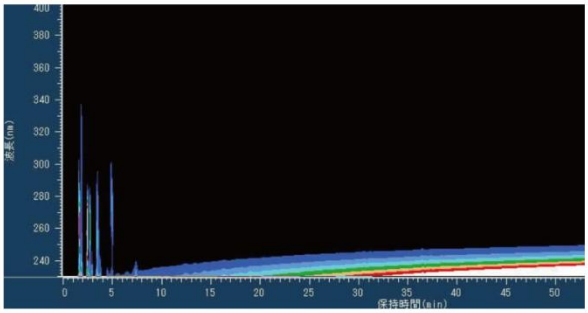

No.092		RNA concentration	
		conc (mg/ml)	% of cont
C6	10 μg/ml	4.51	112.47
	100 μg/ml	6.94	117.49
N18	10 μg/ml	3.43	122.37
	100 μg/ml	4.21	131.85

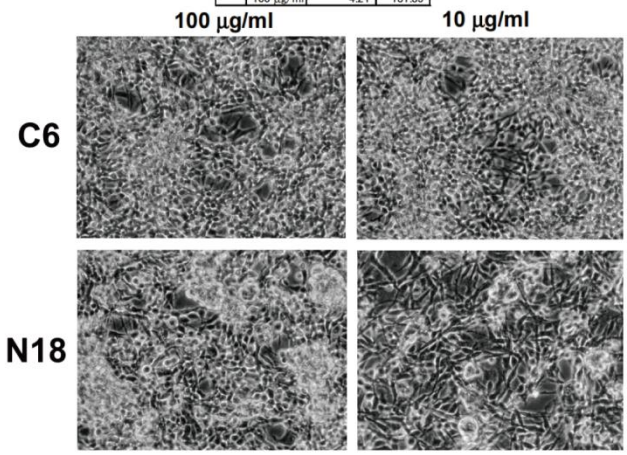

093 Dictamni Radicis Cortex

ハクセンピ（白鮮皮

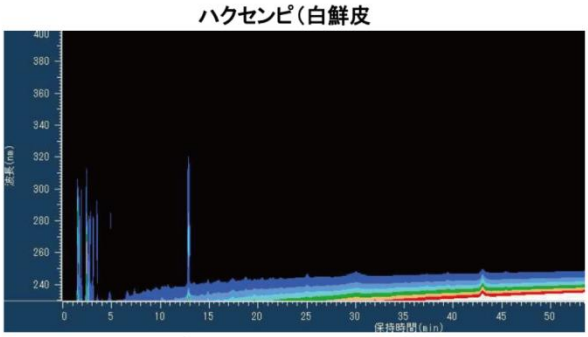

No.093		RNA concentration	
		conc (mg/ml)	% of cont
C6	10 μg/ml	5.48	136.66
	100 μg/ml	6.43	108.85
N18	10 μg/ml	3.68	131.29
	100 μg/ml	3.89	121.83

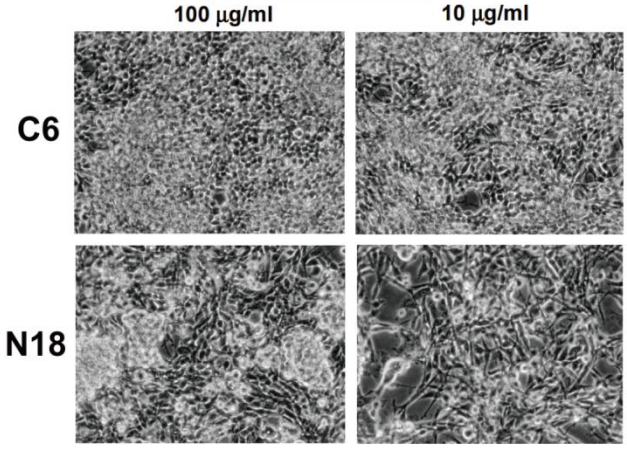

094 Ophiopogonis Tuber

バクモンドウ（麦門冬）

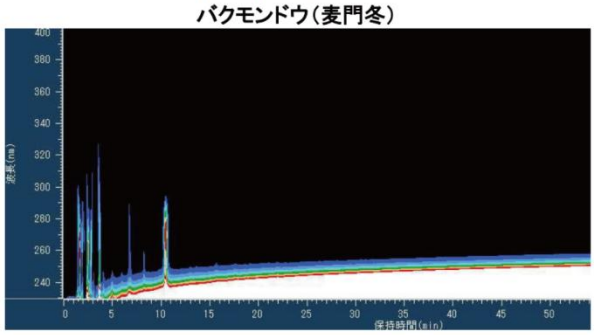

No.094		RNA concentration	
		conc (mg/ml)	% of cont
C6	10 μg/ml	4.69	116.96
	100 μg/ml	7.17	121.38
N18	10 μg/ml	2.74	97.75
	100 μg/ml	3.99	124.96

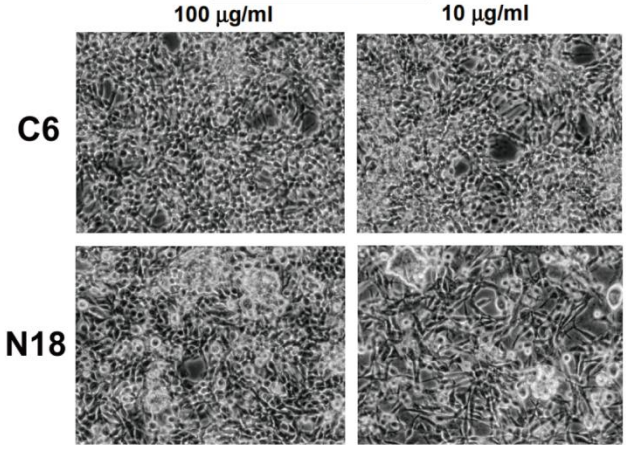

095 Menthae Herba

ハッカ（薄荷）

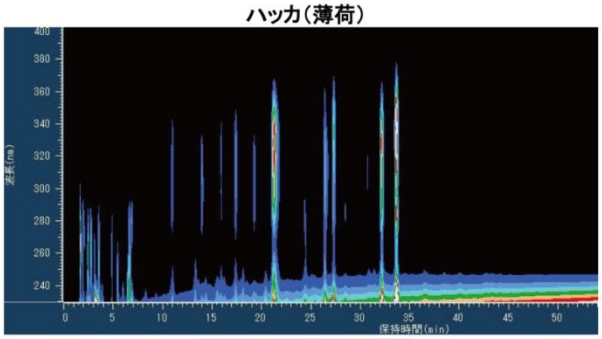

No.095		RNA concentration	
		conc (mg/ml)	% of cont
C6	10 μg/ml	3.47	86.53
	100 μg/ml	4.34	73.47
N18	10 μg/ml	1.47	52.44
	100 μg/ml	2.35	73.60

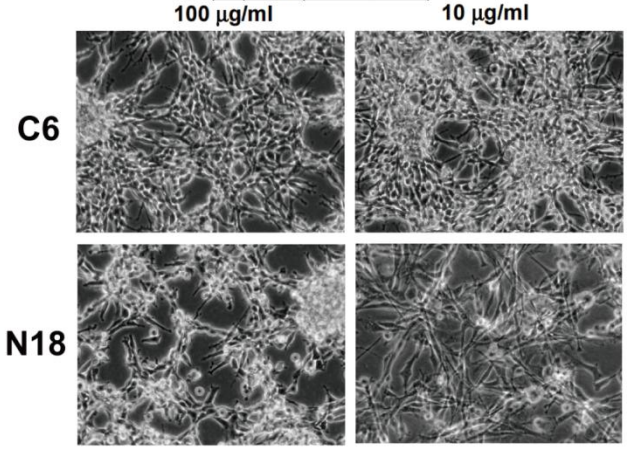

096 Pinelliae Tuber

ハンゲ（半夏）

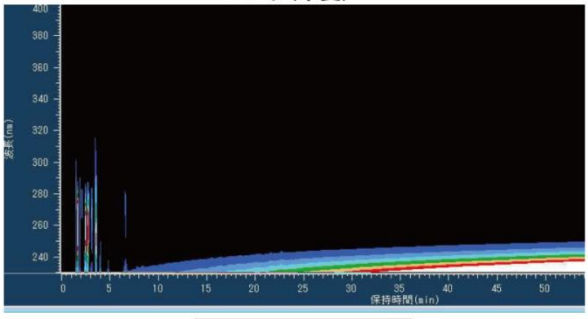

No.096		RNA concentration	
		conc (mg/ml)	% of cont
C6	10 μg/ml	4.81	119.95
	100 μg/ml	7.25	122.74
N18	10 μg/ml	2.32	82.77
	100 μg/ml	3.95	123.71

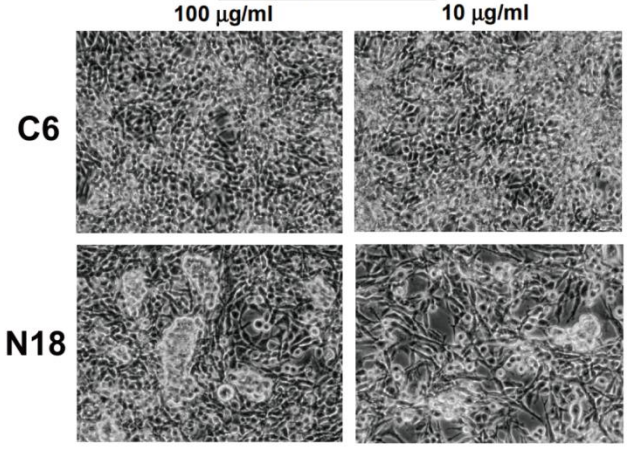

097 Angelicae Dahuricae Rhizoma

ビャクシ（白芷）

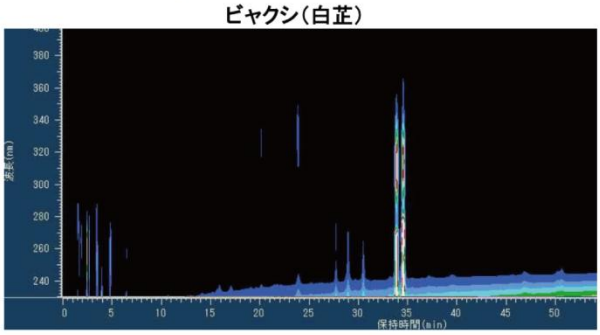

No.097		RNA concentration	
		conc (mg/ml)	% of cont
C6	10 μg/ml	4.20	104.74
	100 μg/ml	6.37	107.84
N18	10 μg/ml	2.99	106.67
	100 μg/ml	4.13	129.35

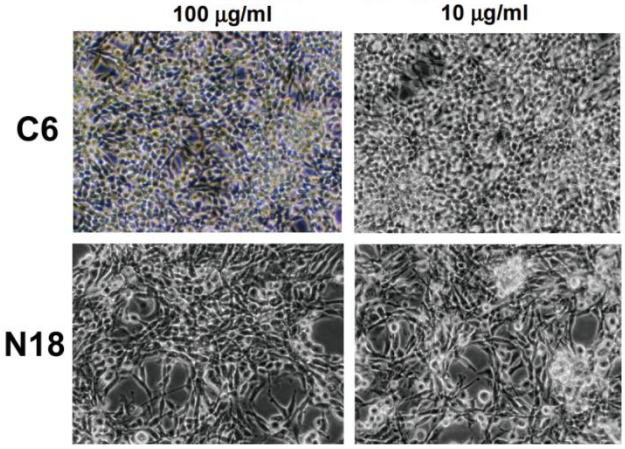

098 Atractylodis Rhizoma

ビャクジュツ（白朮）

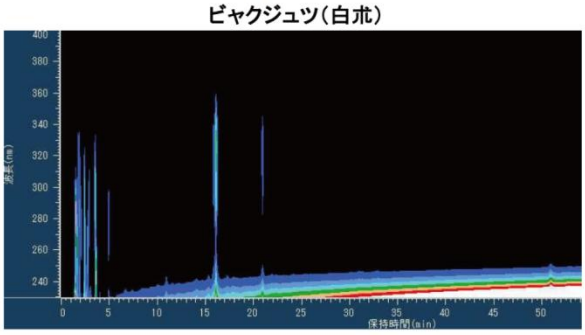

No.098		RNA concentration	
		conc (mg/ml)	% of cont
C6	10 μg/ml	4.12	102.74
	100 μg/ml	6.72	113.76
N18	10 μg/ml	2.50	89.19
	100 μg/ml	4.04	126.53

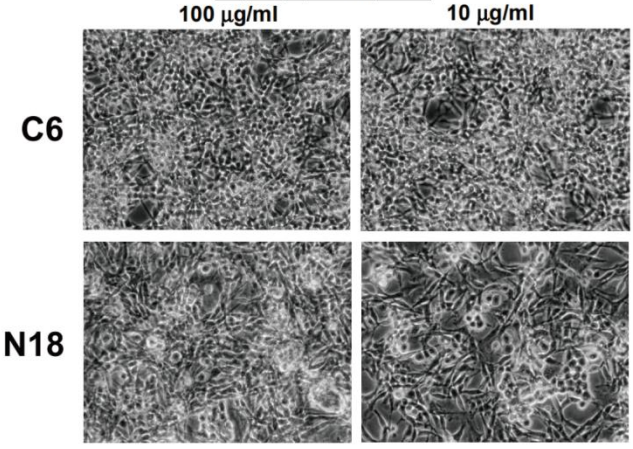

099 Eriobotryae Folium

ビワヨウ（枇杷葉）

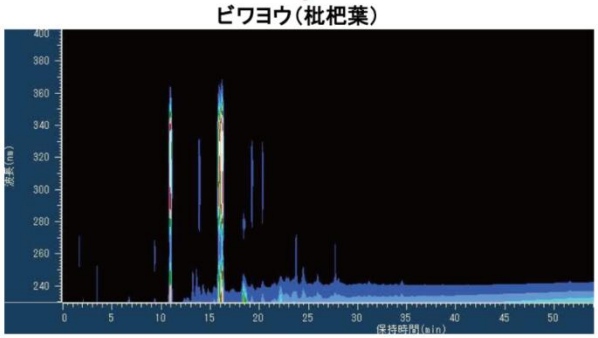

No.099		RNA concentration	
		conc (mg/ml)	% of cont
C6	10 μg/ml	3.26	81.30
	100 μg/ml	3.98	67.38
N18	10 μg/ml	1.17	41.74
	100 μg/ml	1.92	60.13

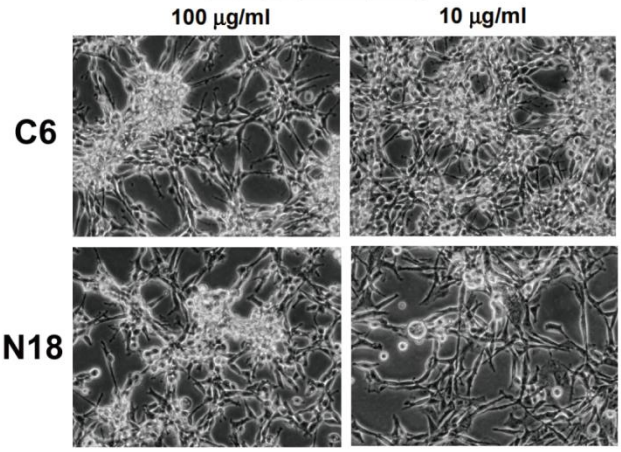

100 Arecae Semen

ビンロウジ（檳榔子）

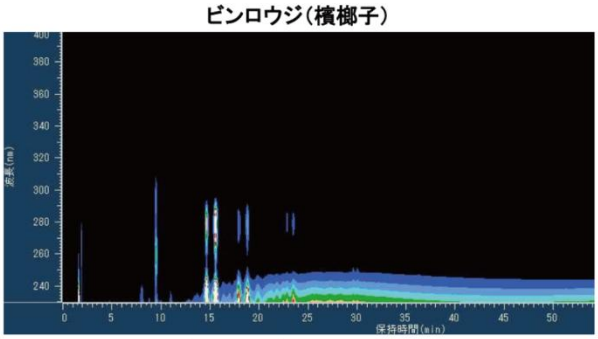

No.100		RNA concentration	
		conc (mg/ml)	% of cont
C6	10 μg/ml	1.72	42.89
	100 μg/ml	0.764	12.93
N18	10 μg/ml	0.383	13.66
	100 μg/ml	0.150	4.70

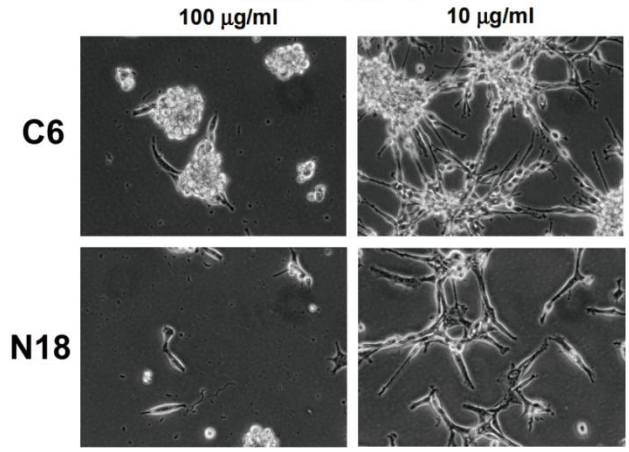

101 Hoelen

ブクリョウ（茯苓）

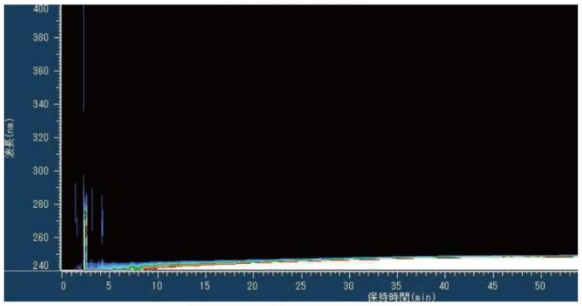

No.101		RNA concentration	
		conc (mg/ml)	% of cont
C6	10 μg/ml	4.57	113.97
	100 μg/ml	5.89	99.71
N18	10 μg/ml	1.84	65.64
	100 μg/ml	3.94	123.39

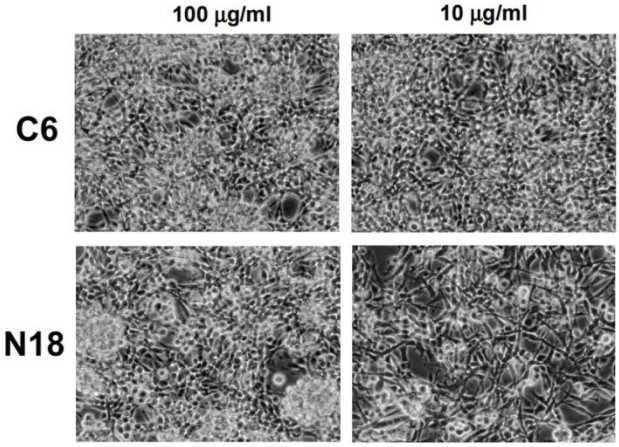

102 Sinomeni Caulis et Rhizoma

ボウイ（防已）

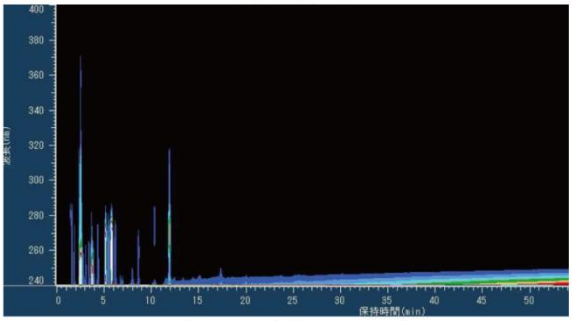

No.102		RNA concentration	
		conc (mg/ml)	% of cont
C6	10 μg/ml	4.94	123.19
	100 μg/ml	5.85	99.04
N18	10 μg/ml	1.38	49.23
	100 μg/ml	3.99	124.96

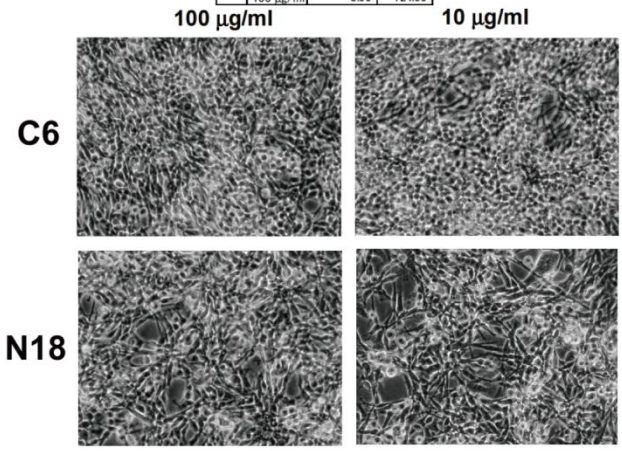

103 Imperatae Rhizoma

ボウコン（茅根）

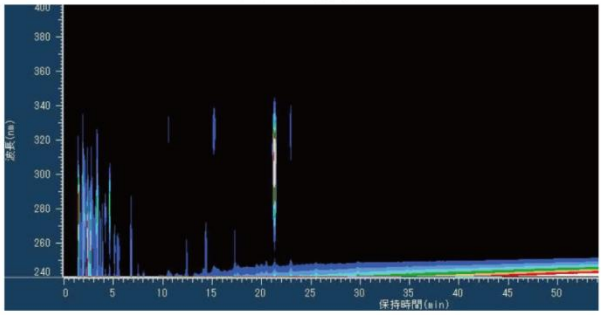

No.103		RNA concentration	
		conc (mg/ml)	% of cont
C6	10 μg/ml	4.24	105.74
	100 μg/ml	6.53	110.55
N18	10 μg/ml	2.43	86.69
	100 μg/ml	4.10	128.41

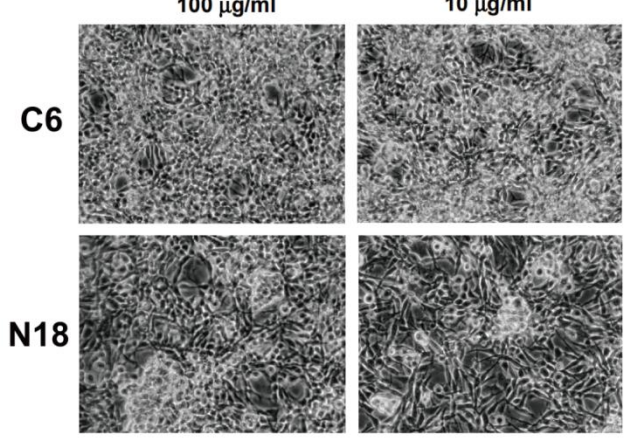

104 Glehniae Radix cum Rhizoma

ボウフウ（防風）

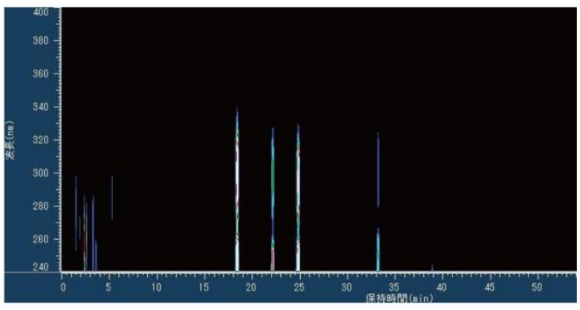

No.104		RNA concentration	
		conc (mg/ml)	% of cont
C6	10 μg/ml	4.75	118.45
	100 μg/ml	6.94	117.49
N18	10 μg/ml	2.13	75.99
	100 μg/ml	4.27	133.73

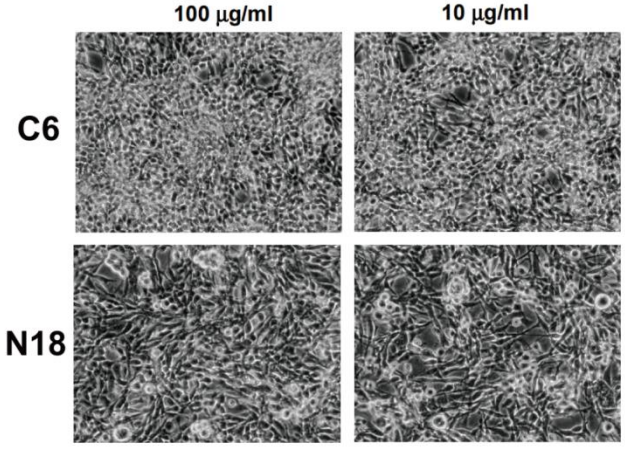

105 Aconiti Tuber Radix

ホウブシ（炮附子）

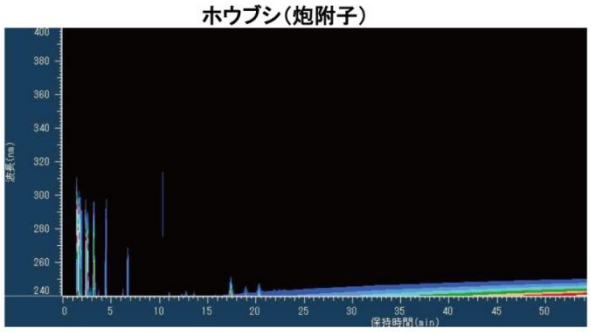

No.105		RNA concentration	
		conc (mg/ml)	% of cont
C6	10 μg/ml	4.08	101.75
	100 μg/ml	6.64	112.41
N18	10 μg/ml	1.91	68.14
	100 μg/ml	4.34	135.92

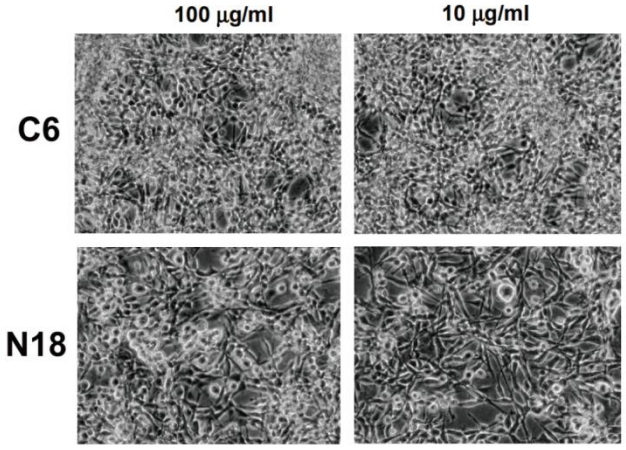

106 Quercus Cortex

ボクソク（樸楸）

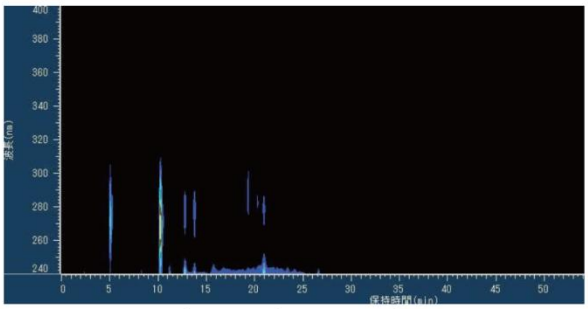

No.106		RNA concentration	
		conc (mg/ml)	% of cont
C6	10 μg/ml	0.70	17.46
	100 μg/ml	0.073	1.23
N18	10 μg/ml	0.286	10.20
	100 μg/ml	0.054	1.69

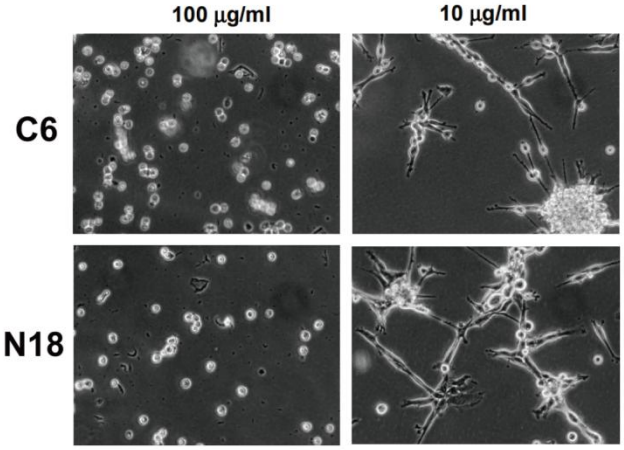

107 Psoraleae Semen

ホコツシ（補骨脂）

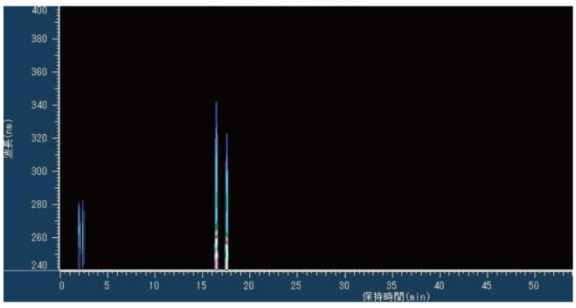

No.107		RNA concentration	
		conc (mg/ml)	% of cont
C6	10 μg/ml	4.18	104.24
	100 μg/ml	2.26	38.26
N18	10 μg/ml	1.74	62.08
	100 μg/ml	1.97	61.97

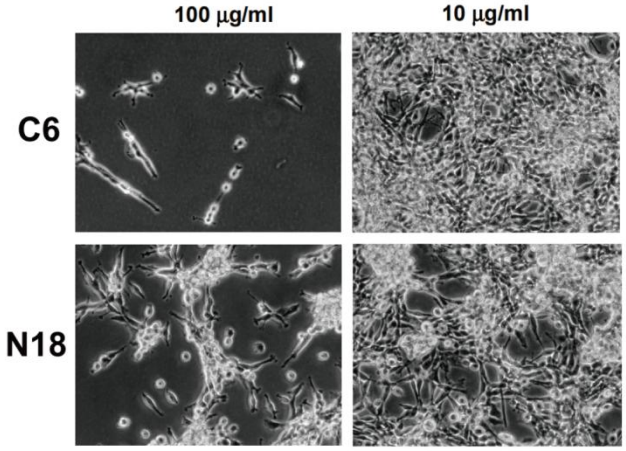

108 Paeoniae Moutan Cortex

ボタンピ（牡丹皮）

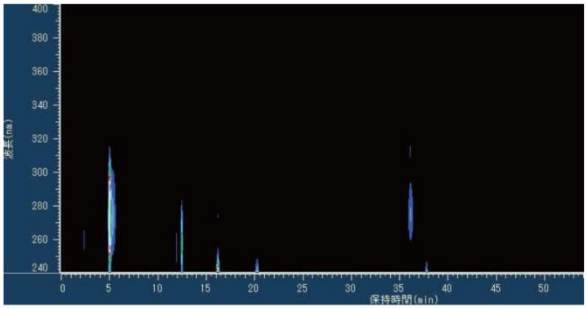

No.108		RNA concentration	
		conc (mg/ml)	% of cont
C6	10 μg/ml	3.14	78.30
	100 μg/ml	1.81	30.64
N18	10 μg/ml	1.05	37.46
	100 μg/ml	0.19	5.95

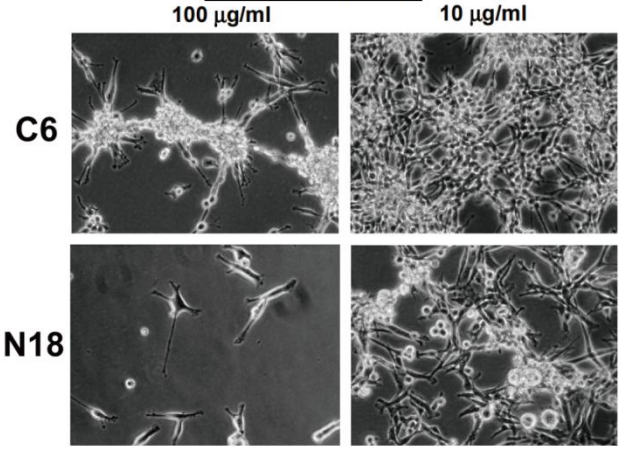

109 Ephedrae Herba

マオウ（麻黄）

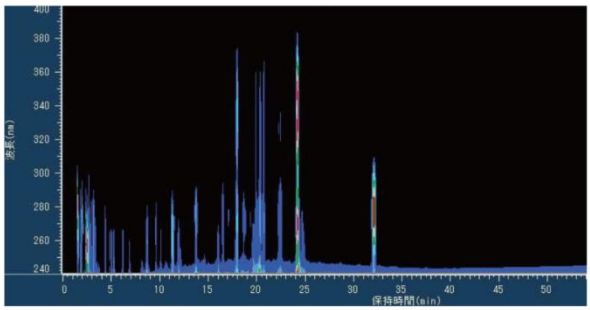

No.109		RNA concentration	
		conc (mg/ml)	% of cont
C6	10 μg/ml	1.76	43.89
	100 μg/ml	0.96	16.25
N18	10 μg/ml	0.57	20.34
	100 μg/ml	ND	ND

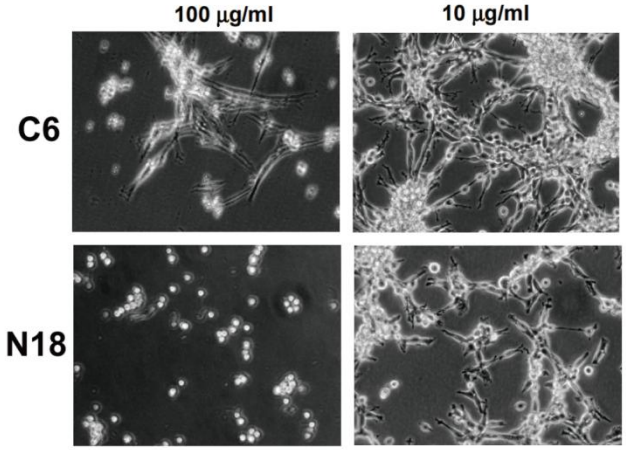

110 Cannabis Fructus

マシニン（麻子仁）

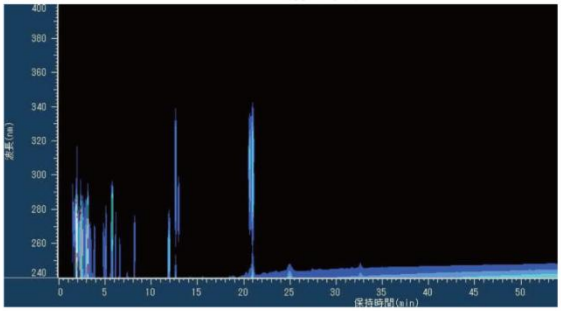

No.110		RNA concentration	
		conc (mg/ml)	% of cont
C6	10 μg/ml	4.72	117.71
	100 μg/ml	4.97	84.14
N18	10 μg/ml	1.82	64.93
	100 μg/ml	2.76	86.44

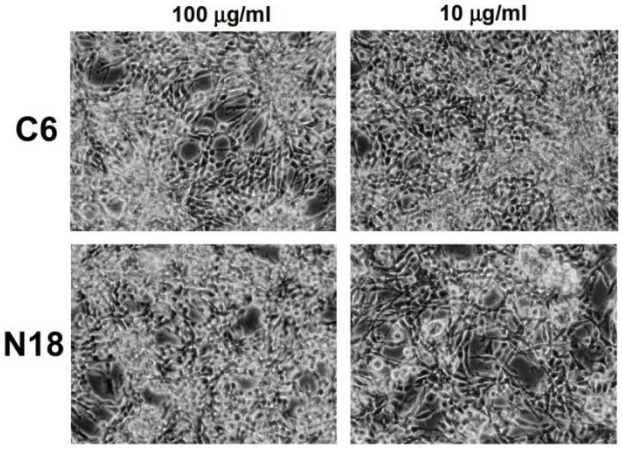

111 Viticis Fructus

マンケイシ（蔓荊子）

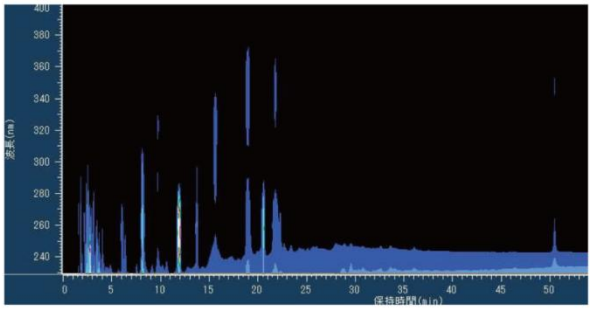

No.111		RNA concentration	
		conc (mg/ml)	% of cont
C6	10 μg/ml	2.59	64.59
	100 μg/ml	1.72	29.12
N18	10 μg/ml	1.11	39.60
	100 μg/ml	0.22	6.89

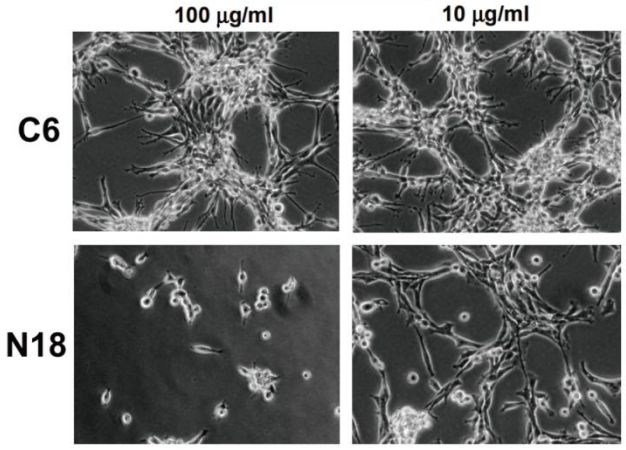

112 Saussureae Radix

モッコウ（木香）

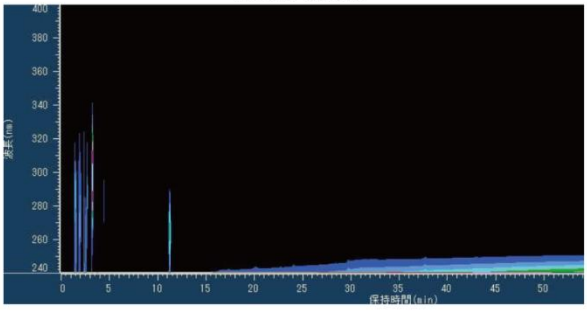

No.112		RNA concentration	
		conc (mg/ml)	% of cont
C6	10 μg/ml	4.30	107.23
	100 μg/ml	5.190	87.86
N18	10 μg/ml	2.230	79.56
	100 μg/ml	3.530	110.55

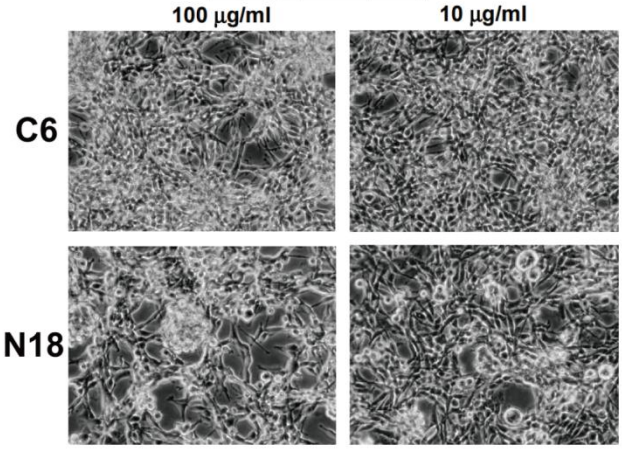

113 Myrrha

モツヤク（没薬）

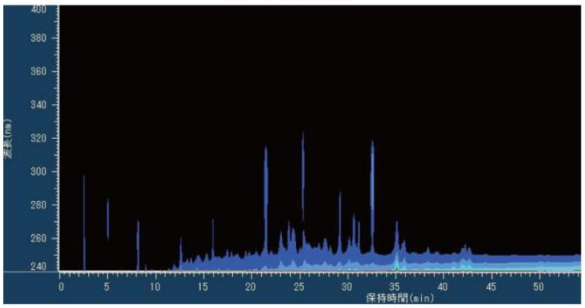

No.113		RNA concentration	
		conc (mg/ml)	% of cont
C6	10 μg/ml	3.64	90.77
	100 μg/ml	1.96	33.12
N18	10 μg/ml	2.12	75.63
	100 μg/ml	0.95	29.75

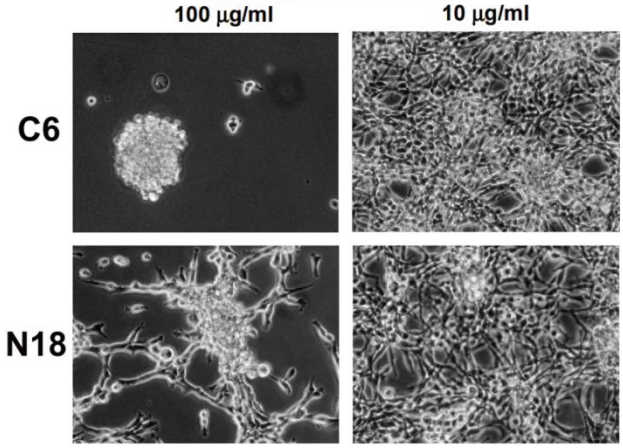

114 Alpiniae Fructus

ヤクチ（益智）

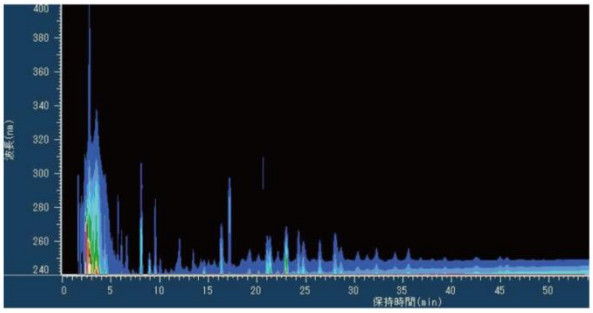

No.114		RNA concentration	
		conc (mg/ml)	% of cont
C6	10 μg/ml	3.68	91.77
	100 μg/ml	1.67	28.27
N18	10 μg/ml	2.24	79.91
	100 μg/ml	1.09	34.14

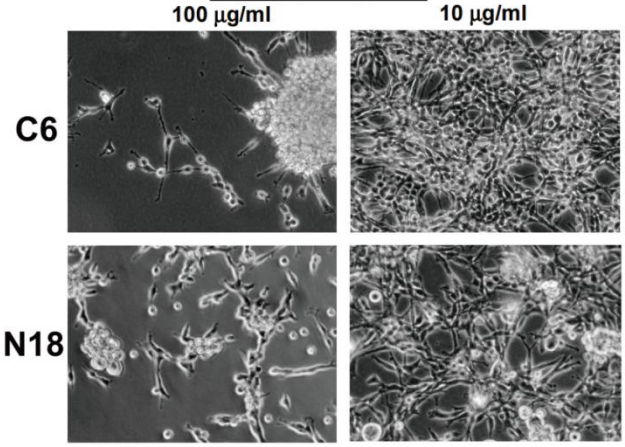

115 Leonuri Herba

ヤクモソウ（益母草）

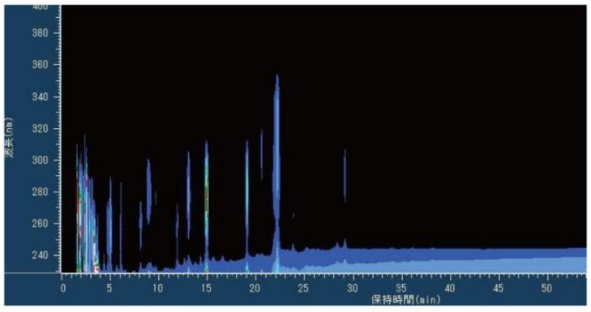

No.115		RNA concentration	
		conc (mg/ml)	% of cont
C6	10 μg/ml	4.11	102.49
	100 μg/ml	5.06	85.66
N18	10 μg/ml	2.60	92.76
	100 μg/ml	3.05	95.52

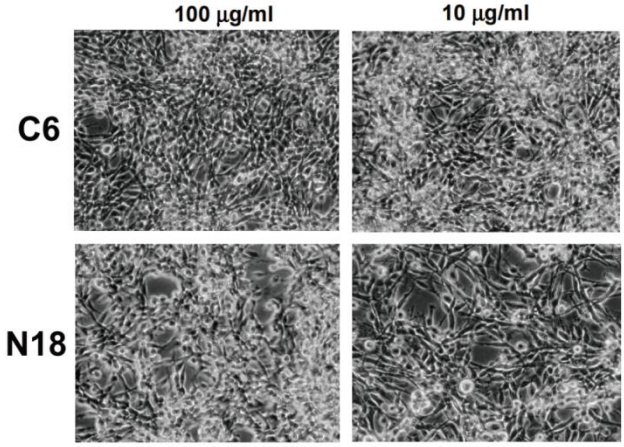

116 Coicis Semen

ヨクイニン（薏苡仁）

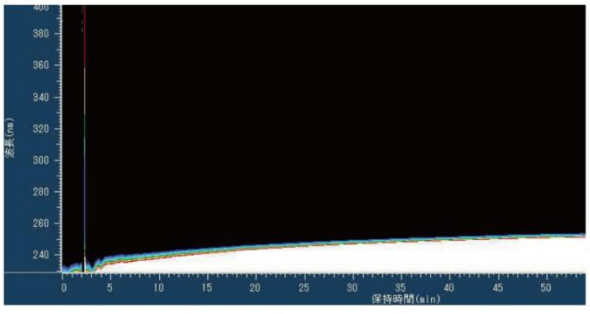

No.116		RNA concentration	
		conc (mg/ml)	% of cont
C6	10 μg/ml	4.53	112.97
	100 μg/ml	6.63	112.24
N18	10 μg/ml	2.57	91.69
	100 μg/ml	4.20	131.54

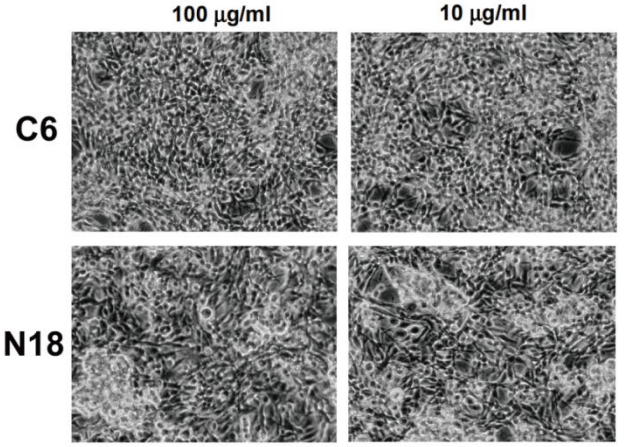

117 Gentianae Scabrae Radix

リュウタン（竜胆）

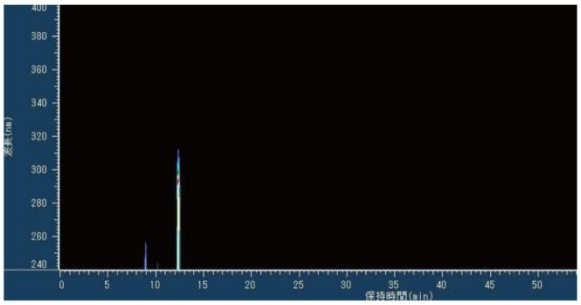

No.117		RNA concentration	
		conc (mg/ml)	% of cont
C6	10 μg/ml	4.26	106.23
	100 μg/ml	7.36	124.60
N18	10 μg/ml	2.77	98.82
	100 μg/ml	3.53	110.55

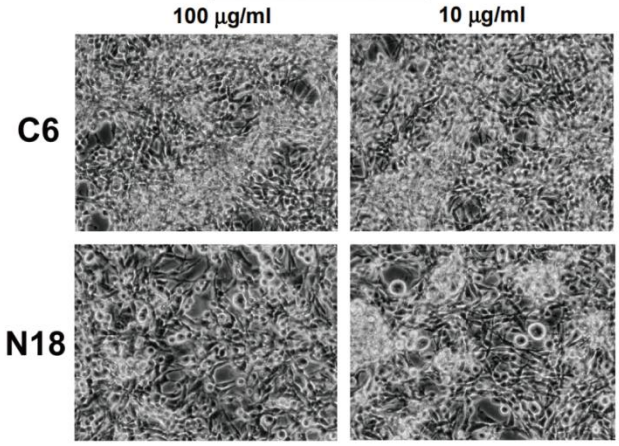

118 Alpiniae Officinari Rhizoma

リョウキョウ（良姜）

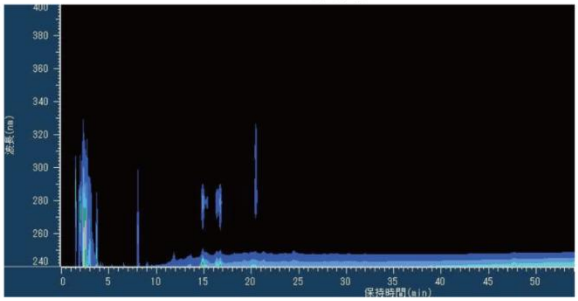

No.118		RNA concentration	
		conc (mg/ml)	% of cont
C6	10 μg/ml	2.74	68.33
	100 μg/ml	1.78	30.13
N18	10 μg/ml	1.24	44.24
	100 μg/ml	0.53	16.60

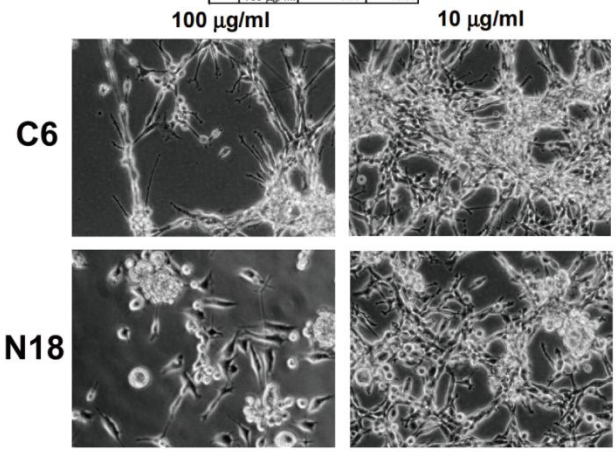

119 Ganoderma

レイシ（霊芝）

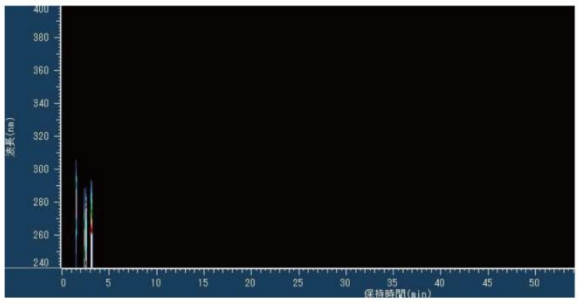

No.119		RNA concentration	
		conc (mg/ml)	% of cont
C6	10 μg/ml	3.97	99.00
	100 μg/ml	5.46	92.43
N18	10 μg/ml	2.23	79.56
	100 μg/ml	2.43	76.10

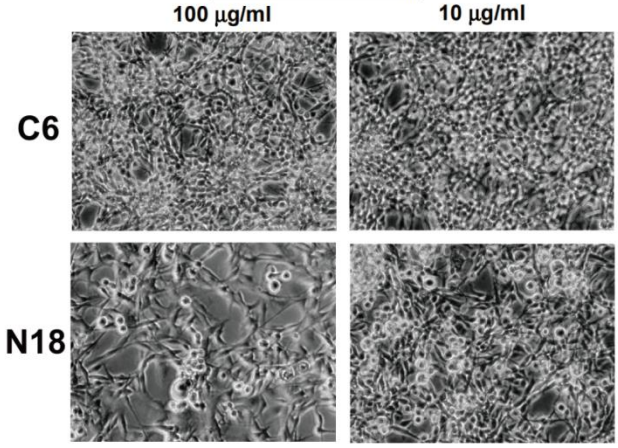

120 Forsythiae Fructus

レンギョウ（連翹）

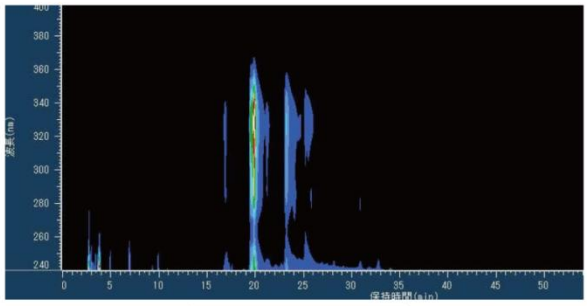

No.120		RNA concentration	
		conc (mg/ml)	% of cont
C6	10 μg/ml	2.75	68.58
	100 μg/ml	0.96	16.25
N18	10 μg/ml	1.70	60.65
	100 μg/ml	ND	ND

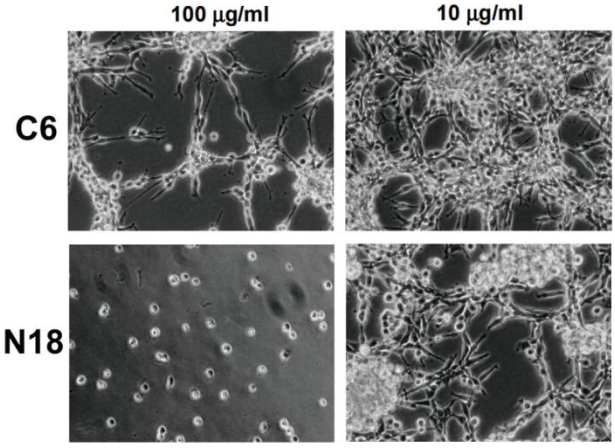

Table S2 Interactions between differentially expressed genes

Nodes represent proteins. Combined score indicates the support of the data

Table S2 Interactions between differentially expressed genes			
Node1	**Node2**	**Combined score**	**Node**
Birc3	Map3k7	0.999	Birc3
Snap25	Syt1	0.999	Snap25
Ap2b1	Ldlrap1	0.997	Ap2b1
Gabrb2	Gabrg2	0.997	Gabrb2
Gemin2	Gemin6	0.997	Gemin2
Ppih	Prpf31	0.997	Ppih
Arnt	Hif1a	0.994	Arnt
Mdm2	Mdm4	0.994	Mdm2
Scn3a	Scn9a	0.994	Scn3a
Aqr	Cdc40	0.993	Aqr
Mrvi1	Prkg1	0.993	Mrvi1
Brcc3	Fam175a	0.992	Brcc3
Ldlr	Ldlrap1	0.992	Ldlr
Phc2	Ring1	0.992	Phc2
Phc2	Rnf2	0.992	Phc2
Cops4	Cul1	0.99	Cops4
Birc3	Traf1	0.989	Birc3
Nsf	Scfd1	0.987	Nsf
Birc3	Casp3	0.986	Birc3
Gabra5	Gabrg2	0.984	Gabra5
Ppih	Snrnp40	0.984	Ppih
Prpf31	Snrnp40	0.984	Prpf31
Mrvi1	Prkg2	0.983	Mrvi1
Scfd1	Sec22a	0.983	Scfd1
Cdc40	Snrnp40	0.982	Cdc40
Nsf	Snap25	0.981	Nsf
Il9	Il9r	0.98	Il9
Dmd	Dtna	0.979	Dmd
Fgf2	Fgfbp1	0.979	Fgf2
Aqr	Snrnp40	0.978	Aqr
Gabra5	Gabrb2	0.978	Gabra5
Cdc40	Srrm2	0.977	Cdc40
Exosc9	Utp6	0.977	Exosc9
H2-K1	Pirb	0.977	H2-K1
Birc3	Ube2d1	0.975	Birc3
Myog	Tcf4	0.975	Myog
Snap25	Syn2	0.974	Snap25
Fam175a	Mdc1	0.972	Fam175a
Itga4	Itgb6	0.972	Itga4

Cops4	Fbxo17	0.971	Cops4
Aqr	Srrm2	0.969	Aqr
Cul1	Ube2d1	0.968	Cul1
Snrnp40	Srrm2	0.965	Snrnp40
Defb26	Defb30	0.963	Defb26
Rad51ap1	Rfc4	0.961	Rad51ap1
Inpp4b	Inpp5j	0.96	Inpp4b
Rad51	Rad51ap1	0.96	Rad51
Ap2b1	Slc2a8	0.959	Ap2b1
Ly6h	Lypd4	0.959	Ly6h
Ccl28	Ccr10	0.958	Ccl28
Rgs7bp	Rgs9	0.958	Rgs7bp
Syt1	Syt11	0.958	Syt1
Aqr	Ppih	0.954	Aqr
Cd80	Cd86	0.953	Cd80
Ctss	Mpeg1	0.953	Ctss
Ap5m1	Ap5s1	0.95	Ap5m1
Ring1	Rnf2	0.95	Ring1
Afp	Serpina1a	0.949	Afp
Ccl25	Ccl28	0.949	Ccl25
Kif1a	Kif1b	0.949	Kif1a
Nsf	Sec22a	0.949	Nsf
Cul1	Det1	0.947	Cul1
Pex12	Ube2d1	0.946	Pex12
Ube2d1	Znrf2	0.946	Ube2d1
Agrn	Gpc5	0.945	Agrn
Tcf7	Tle4	0.945	Tcf7
Gnpat	Pex12	0.944	Gnpat
Afp	Trf	0.943	Afp
Cul1	Fbxo17	0.943	Cul1
Cul1	Fbxo44	0.943	Cul1
Ddx39b	Nudt21	0.943	Ddx39b
Ddx39b	Upf3b	0.943	Ddx39b
Ctss	Mmp9	0.942	Ctss
Dao	Gnpat	0.942	Dao
Dnm3	Syt1	0.941	Dnm3
Gabrb2	Gabrg3	0.941	Gabrb2
Serpina1a	Trf	0.94	Serpina1a
Ap2b1	Dnm3	0.939	Ap2b1
Cdc40	Prpf31	0.939	Cdc40
Irak2	Map3k7	0.939	Irak2
Ccl25	Ccr10	0.938	Ccl25
Crkl	Kidins220	0.938	Crkl

Ppfibp2	Ptprd	0.938	Ppfibp2
Dnm3	Syt11	0.937	Dnm3
Tgoln1	Trf	0.937	Tgoln1
Cdc40	Ppih	0.936	Cdc40
Lrrk2	Rab29	0.936	Lrrk2
Polr3e	Snapc3	0.936	Polr3e
Acss2	Aldh1b1	0.935	Acss2
Det1	Ube2d1	0.935	Det1
Tfap2c	Wwox	0.935	Tfap2c
Acot4	Gnpat	0.934	Acot4
Apc	Tcf7	0.933	Apc
Lama3	Ntn4	0.933	Lama3
Adra1d	Oxt	0.932	Adra1d
Aqr	Upf3b	0.932	Aqr
Cops4	Fbxo44	0.932	Cops4
Hecw2	Ube2d1	0.932	Hecw2
Nudt21	Ppih	0.932	Nudt21
Rgs6	Rgs7bp	0.932	Rgs6
Snrnp40	Upf3b	0.93	Snrnp40
Apc	Casp3	0.929	Apc
Cntn4	Opcml	0.929	Cntn4
Lox	Loxl2	0.929	Lox
Oxt	Trhr	0.929	Oxt
Syt1	Tgoln1	0.928	Syt1
Cdc40	Ddx39b	0.927	Cdc40
Acot1	Gnpat	0.926	Acot1
Det1	Znrf2	0.926	Det1
Itga1	Itgb6	0.926	Itga1
Nudt21	Ybx1	0.926	Nudt21
Defb30	Defb47	0.925	Defb30
Rfc4	Rrm1	0.925	Rfc4
Aqr	Prpf31	0.924	Aqr
Dmd	Tmod1	0.924	Dmd
Mdm2	Sgk1	0.924	Mdm2
Ppih	Srrm2	0.924	Ppih
Dnmt3b	Mat2b	0.923	Dnmt3b
Akap9	Tubgcp4	0.922	Akap9
Hrh1	Ptafr	0.922	Hrh1
Ldlrap1	Trf	0.922	Ldlrap1
Nsf	Tgoln1	0.922	Nsf
Ttc21b	Ttc30b	0.922	Ttc21b
Acsf3	Aldh9a1	0.921	Acsf3
Bub1b	Diap2	0.921	Bub1b

Nudt21	Snrnp40	0.921	Nudt21
Asb14	Lmo7	0.92	Asb14
Cdc40	Upf3b	0.92	Cdc40
Cdh18	Cdh6	0.92	Cdh18
Hif1a	Lrrk2	0.92	Hif1a
Map3k7	Mapk12	0.92	Map3k7
Clu	Serpina1a	0.919	Clu
Ldlr	Trf	0.919	Ldlr
Pex12	Pex5l	0.919	Pex12
Ppih	Ybx1	0.919	Ppih
Cntn4	Ntng2	0.918	Cntn4
Ly6h	Opcml	0.918	Ly6h
Myl6b	Mylpf	0.918	Myl6b
Srrm2	Ybx1	0.918	Srrm2
Tk1	Tk2	0.918	Tk1
Btk	Itk	0.917	Btk
Bub1b	Ube2d1	0.917	Bub1b
Kif16b	Kif1a	0.917	Kif16b
Pde6b	Rgs9	0.917	Pde6b
Rgs6	Rgs9	0.917	Rgs6
Acot1	Acot4	0.916	Acot1
Ap2b1	Tgoln1	0.916	Ap2b1
Asb14	Cul1	0.916	Asb14
Defb26	Defb47	0.916	Defb26
St3gal1	St8sia1	0.916	St3gal1
Acsf3	Aldh1b1	0.915	Acsf3
Adamts2	Adamts6	0.915	Adamts2
Adra2a	Sstr3	0.915	Adra2a
Gabra5	Gabrg3	0.915	Gabra5
Ldlr	Tgoln1	0.915	Ldlr
Prpf31	Srrm2	0.915	Prpf31
Aldh1b1	Gatm	0.914	Aldh1b1
Dhfr	Th	0.914	Dhfr
Kif12	Kif1a	0.914	Kif12
Ap2b1	Syt1	0.913	Ap2b1
Ap2b1	Syt11	0.913	Ap2b1
Asb14	Ube2d1	0.913	Asb14
Dao	Ddo	0.913	Dao
Ddo	Gnpat	0.913	Ddo
Grm2	Sstr3	0.913	Grm2
Inpp4b	Pik3r6	0.913	Inpp4b
Acot4	Ddo	0.912	Acot4
Adamts2	Col11a2	0.912	Adamts2

Akap9	Cc2d2a	0.912	Akap9
Dhfr	Tph1	0.912	Dhfr
Dsc1	Dsc3	0.912	Dsc1
Hif1a	Ube2d1	0.912	Hif1a
Hrh1	Oxt	0.912	Hrh1
Kif16b	Kif1b	0.912	Kif16b
Mapk12	Myog	0.912	Mapk12
Nudt21	Prpf31	0.912	Nudt21
Adra1d	Hrh1	0.911	Adra1d
Apc	Tle4	0.911	Apc
Asb14	Cops4	0.911	Asb14
Fgf2	Fgf6	0.911	Fgf2
Gm28040	Hcrtr2	0.911	Gm28040
Hecw2	Znrf2	0.911	Hecw2
Pirb	Ptafr	0.911	Pirb
Adam8	Clec5a	0.91	Adam8
B3galt4	St3gal1	0.91	B3galt4
Dnm3	Slc2a8	0.91	Dnm3
Dnm3	Ldlrap1	0.91	Dnm3
Fbxo17	Fbxo44	0.91	Fbxo17
Hcrtr2	Oxt	0.91	Hcrtr2
Hcrtr2	Trhr	0.91	Hcrtr2
Hrh1	Trhr	0.91	Hrh1
Aldh1b1	Gadl1	0.909	Aldh1b1
Aldh9a1	Gadl1	0.909	Aldh9a1
Apc	Cul1	0.909	Apc
Clec5a	Ptafr	0.909	Clec5a
Cul1	Hecw2	0.909	Cul1
Adra2a	Grm2	0.908	Adra2a
Aldh9a1	Gatm	0.908	Aldh9a1
Aldoc	Mmp9	0.908	Aldoc
Cntn4	Ly6h	0.908	Cntn4
Cul1	Lmo7	0.908	Cul1
Cul1	Znrf2	0.908	Cul1
Dnm3	Ldlr	0.908	Dnm3
Gm5150	Pirb	0.908	Gm5150
Grik2	Ncald	0.908	Grik2
Adam8	Ptafr	0.907	Adam8
Akap9	Cep78	0.907	Akap9
Ap2b1	Trf	0.907	Ap2b1
Asns	Aspa	0.907	Asns
Ccl28	Tas2r106	0.907	Ccl28
Cdc73	Tcf7	0.907	Cdc73

Cyp2a12	Cyp2j6	0.907	Cyp2a12
Dao	Pex12	0.907	Dao
Hcrtr2	Hrh1	0.907	Hcrtr2
Hecw2	Lmo7	0.907	Hecw2
Kif12	Kif1b	0.907	Kif12
Ldlr	Slc2a8	0.907	Ldlr
Ldlr	Syt1	0.907	Ldlr
Lrrtm4	Vwc2l	0.907	Lrrtm4
Prdx6	Serpina3j	0.907	Prdx6
Prkcb	Prkcg	0.907	Prkcb
Ap2b1	Ldlr	0.906	Ap2b1
Ccl28	Sstr3	0.906	Ccl28
Cdc73	Tle4	0.906	Cdc73
Det1	Hecw2	0.906	Det1
Inpp4b	Pik3ip1	0.906	Inpp4b
Kif12	Kif16b	0.906	Kif12
Kri1	Utp6	0.906	Kri1
Oxt	Ptafr	0.906	Oxt
P2ry10	Ptafr	0.906	P2ry10
Ptafr	Trhr	0.906	Ptafr
Acot4	Dao	0.905	Acot4
Aqr	Nudt21	0.905	Aqr
Cdc40	Nudt21	0.905	Cdc40
Dnm3	Trf	0.905	Dnm3
Fbn2	Itgb6	0.905	Fbn2
Ntng2	Opcml	0.905	Ntng2
Serpina1a	Serpina3j	0.905	Serpina1a
Srrm2	Upf3b	0.905	Srrm2
Syt11	Tgoln1	0.905	Syt11
Acsf3	Aox4	0.904	Acsf3
Akap9	Rasgrf2	0.904	Akap9
Aldoc	Ctss	0.904	Aldoc
Asb14	Hecw2	0.904	Asb14
Clec5a	Gm5150	0.904	Clec5a
Cul1	Prlr	0.904	Cul1
Fbxo17	Ube2d1	0.904	Fbxo17
Gm5150	Ptafr	0.904	Gm5150
H2-K1	Ptafr	0.904	H2-K1
Mapk12	Tcf4	0.904	Mapk12
Snrnp40	Ybx1	0.904	Snrnp40
Upf3b	Ybx1	0.904	Upf3b
Acot1	Ddo	0.903	Acot1
Acot1	Dao	0.903	Acot1

Adra1d	P2ry10	0.903	Adra1d
Adra2a	Ccl28	0.903	Adra2a
Asb14	Znrf2	0.903	Asb14
BC018507	Snapc3	0.903	BC018507
Cc2d2a	Cep78	0.903	Cc2d2a
Clec5a	Snap25	0.903	Clec5a
Cpm	Ulbp1	0.903	Cpm
Dao	Ube2d1	0.903	Dao
Ddo	Ube2d1	0.903	Ddo
Gm28040	Ptafr	0.903	Gm28040
Gnpat	Ube2d1	0.903	Gnpat
Lmo7	Ube2d1	0.903	Lmo7
Mecom	Rnf2	0.903	Mecom
Prpf31	Ybx1	0.903	Prpf31
Syt1	Trf	0.903	Syt1
Syt11	Trf	0.903	Syt11
Acot1	Ube2d1	0.902	Acot1
Acot4	Ube2d1	0.902	Acot4
Adam8	Tmc6	0.902	Adam8
Adam8	Gm5150	0.902	Adam8
Adamts2	Sema5a	0.902	Adamts2
Adra1d	Arhgef1	0.902	Adra1d
Akap9	Fgfr1op	0.902	Akap9
Aqr	Rfc4	0.902	Aqr
Cdc40	Ybx1	0.902	Cdc40
Cep78	Tubgcp4	0.902	Cep78
Dao	Gatm	0.902	Dao
Det1	Fbxo44	0.902	Det1
Det1	Lmo7	0.902	Det1
Dnm3	Tgoln1	0.902	Dnm3
Itga1	Myl6b	0.902	Itga1
Itga1	Mylpf	0.902	Itga1
Ldlr	Syt11	0.902	Ldlr
Ly6h	Ntng2	0.902	Ly6h
Nudt21	Upf3b	0.902	Nudt21
Nudt21	Srrm2	0.902	Nudt21
Sec22a	Serpina1a	0.902	Sec22a
Snrnp48	Ybx1	0.902	Snrnp48
Adra1d	Hcrtr2	0.901	Adra1d
Adra2a	Ccl25	0.901	Adra2a
Afp	Tgoln1	0.901	Afp
Asb14	Fbxo17	0.901	Asb14
Asb14	Det1	0.901	Asb14

Asb14	Fbxo44	0.901	Asb14
BC018507	Vwa9	0.901	BC018507
Bcl2l11	Casp3	0.901	Bcl2l11
Ccl25	Sstr3	0.901	Ccl25
Cd68	Lpcat1	0.901	Cd68
Cep78	Fgfr1op	0.901	Cep78
Cntn4	Cpm	0.901	Cntn4
Cntn4	Lypd4	0.901	Cntn4
Cpm	Ly6h	0.901	Cpm
Ddo	Pex12	0.901	Ddo
Fbxo44	Ube2d1	0.901	Fbxo44
Gm28040	Hrh1	0.901	Gm28040
Gm5150	H2-K1	0.901	Gm5150
Hcrtr2	Ptafr	0.901	Hcrtr2
Hrh1	P2ry10	0.901	Hrh1
Mecom	Phc2	0.901	Mecom
Prelp	St3gal4	0.901	Prelp
Prelp	St3gal1	0.901	Prelp
Slc2a8	Syt11	0.901	Slc2a8
Snapc3	Vwa9	0.901	Snapc3
Snrnp40	Snrnp48	0.901	Snrnp40
Acot1	Pex12	0.9	Acot1
Acot4	Pex12	0.9	Acot4
Adam8	Snap25	0.9	Adam8
Adamts6	Sema5a	0.9	Adamts6
Adra1d	Trhr	0.9	Adra1d
Adra1d	Ptafr	0.9	Adra1d
Adra1d	Gm28040	0.9	Adra1d
Adra2a	Tas2r106	0.9	Adra2a
Adra2a	Ccr10	0.9	Adra2a
Ap2b1	Prkcb	0.9	Ap2b1
Ap2b1	Prkcg	0.9	Ap2b1
Aqr	Ybx1	0.9	Aqr
Art3	Cpm	0.9	Art3
Art3	Tectb	0.9	Art3
Art3	Ntng2	0.9	Art3
Art3	Lypd4	0.9	Art3
Art3	Cntn4	0.9	Art3
Art3	Plet1	0.9	Art3
Art3	Opcml	0.9	Art3
Art3	Ulbp1	0.9	Art3
Art3	Ly6h	0.9	Art3
Cc2d2a	Fgfr1op	0.9	Cc2d2a

Ccl25	Grm2	0.9	Ccl25
Ccl25	Tas2r106	0.9	Ccl25
Ccl28	Grm2	0.9	Ccl28
Ccr10	Grm2	0.9	Ccr10
Ccr10	Sstr3	0.9	Ccr10
Ccr10	Tas2r106	0.9	Ccr10
Cdc73	Eaf2	0.9	Cdc73
Clec5a	Tmc6	0.9	Clec5a
Clu	Serpina3j	0.9	Clu
Cntn4	Tectb	0.9	Cntn4
Cntn4	Plet1	0.9	Cntn4
Cntn4	Ulbp1	0.9	Cntn4
Cops4	Lmo7	0.9	Cops4
Cpm	Lypd4	0.9	Cpm
Cpm	Plet1	0.9	Cpm
Cpm	Ntng2	0.9	Cpm
Cpm	Tectb	0.9	Cpm
Cpm	Opcml	0.9	Cpm
Det1	Fbxo17	0.9	Det1
Fbxo17	Znrf2	0.9	Fbxo17
Fbxo17	Hecw2	0.9	Fbxo17
Fbxo17	Lmo7	0.9	Fbxo17
Fbxo44	Znrf2	0.9	Fbxo44
Fbxo44	Hecw2	0.9	Fbxo44
Fbxo44	Lmo7	0.9	Fbxo44
Fgfr1op	Tubgcp4	0.9	Fgfr1op
Gm10081	Reep5	0.9	Gm10081
Gm28040	Oxt	0.9	Gm28040
Gm28040	Trhr	0.9	Gm28040
Gm28040	P2ry10	0.9	Gm28040
Gm5150	Tmc6	0.9	Gm5150
Gm5150	Snap25	0.9	Gm5150
Grm2	Tas2r106	0.9	Grm2
Hcrtr2	P2ry10	0.9	Hcrtr2
Ldlrap1	Slc2a8	0.9	Ldlrap1
Ldlrap1	Tgoln1	0.9	Ldlrap1
Ldlrap1	Syt1	0.9	Ldlrap1
Ldlrap1	Syt11	0.9	Ldlrap1
Lmo7	Znrf2	0.9	Lmo7
Ly6h	Tectb	0.9	Ly6h
Ly6h	Plet1	0.9	Ly6h
Ly6h	Ulbp1	0.9	Ly6h
Lypd4	Tectb	0.9	Lypd4

Lypd4	Ntng2	0.9	Lypd4
Lypd4	Plet1	0.9	Lypd4
Lypd4	Opcml	0.9	Lypd4
Lypd4	Ulbp1	0.9	Lypd4
Mecom	Ring1	0.9	Mecom
Nsf	Serpina1a	0.9	Nsf
Ntng2	Tectb	0.9	Ntng2
Ntng2	Plet1	0.9	Ntng2
Ntng2	Ulbp1	0.9	Ntng2
Olfr1080	Reep5	0.9	Olfr1080
Olfr1097	Reep5	0.9	Olfr1097
Olfr1152	Reep5	0.9	Olfr1152
Olfr1164	Reep5	0.9	Olfr1164
Olfr1195	Reep5	0.9	Olfr1195
Olfr228	Reep5	0.9	Olfr228
Olfr314	Reep5	0.9	Olfr314
Olfr384	Reep5	0.9	Olfr384
Olfr487	Reep5	0.9	Olfr487
Olfr512	Reep5	0.9	Olfr512
Olfr583	Reep5	0.9	Olfr583
Olfr584	Reep5	0.9	Olfr584
Olfr688	Reep5	0.9	Olfr688
Olfr869	Reep5	0.9	Olfr869
Olfr945	Reep5	0.9	Olfr945
Olfr981	Reep5	0.9	Olfr981
Opcml	Tectb	0.9	Opcml
Opcml	Plet1	0.9	Opcml
Opcml	Ulbp1	0.9	Opcml
Oxt	P2ry10	0.9	Oxt
P2ry10	Trhr	0.9	P2ry10
Plet1	Tectb	0.9	Plet1
Plet1	Ulbp1	0.9	Plet1
Prdx6	Sdcbp	0.9	Prdx6
Ptafr	Tmc6	0.9	Ptafr
Ptafr	Snap25	0.9	Ptafr
Scfd1	Serpina1a	0.9	Scfd1
Sdcbp	Serpina3j	0.9	Sdcbp
Serpina1a	Tgoln1	0.9	Serpina1a
Slc2a8	Trf	0.9	Slc2a8
Slc2a8	Tgoln1	0.9	Slc2a8
Slc2a8	Syt1	0.9	Slc2a8
Snap25	Tmc6	0.9	Snap25
Sstr3	Tas2r106	0.9	Sstr3

Tectb	Ulbp1	0.9	Tectb
Enpp2	Gdpd1	0.899	Enpp2
Clu	Pon1	0.897	Clu
Mdm2	Ube2d1	0.894	Mdm2
Sv2b	Syt1	0.893	Sv2b
Atp13a2	Lrrk2	0.891	Atp13a2
Lpcat1	Pla2g7	0.891	Lpcat1
Cps1	Sirt5	0.888	Cps1
Polr1b	Utp6	0.886	Polr1b
Dao	Srr	0.884	Dao
Map3k7	Mapk10	0.882	Map3k7
Ap2b1	Ap5m1	0.881	Ap2b1
Cbfa2t3	Tcf4	0.879	Cbfa2t3
Pla2g7	Pon1	0.879	Pla2g7
Invs	Rpgr	0.876	Invs
Pif1	Rad51	0.874	Pif1
Chat	Th	0.864	Chat
Cln3	Ppt1	0.862	Cln3
Gid8	Ranbp10	0.862	Gid8
Dhfr	Mthfr	0.861	Dhfr
Tk1	mCG_22911	0.861	Tk1
Cdh1	Fer	0.856	Cdh1
Usp9y	Uty	0.855	Usp9y
Casp3	Prkcg	0.85	Casp3
Crkl	Mapk10	0.85	Crkl
Casp3	Prkcb	0.849	Casp3
Plcd4	Prkcb	0.847	Plcd4
Fgf2	Mmp9	0.846	Fgf2
Aars	Asns	0.843	Aars
Prpf31	Rpp38	0.843	Prpf31
Cd80	Itga4	0.838	Cd80
Msh3	Xrcc4	0.838	Msh3
Casp3	Mdm2	0.836	Casp3
Mdc1	Rad51	0.836	Mdc1
Apc	Cdh1	0.835	Apc
Arhgef1	Arhgef6	0.832	Arhgef1
Ncf2	Prkcb	0.831	Ncf2
Pparg	Scd1	0.831	Pparg
Bub1b	Rrm1	0.83	Bub1b
Cdh1	Mmp9	0.83	Cdh1
Reep5	Rtn1	0.83	Reep5
Syn2	Syt1	0.829	Syn2
Aldh1b1	Aldh9a1	0.827	Aldh1b1

Snap25	Stxbp5l	0.827	Snap25
Aars	Nars2	0.826	Aars
Mapk12	Prkg1	0.824	Mapk12
Mapk12	Prkg2	0.824	Mapk12
Bub1b	Rad51ap1	0.823	Bub1b
Hdac9	Phf12	0.821	Hdac9
Plcd4	Prkcg	0.821	Plcd4
Bub1b	Rfc4	0.819	Bub1b
Pla2g7	Ptafr	0.819	Pla2g7
Plcz1	Prkcb	0.819	Plcz1
Plcz1	Prkcg	0.819	Plcz1
Cngb3	Pde6b	0.818	Cngb3
Dhfr	Tk1	0.818	Dhfr
Il3	Il9	0.818	Il3
Cd80	H2-K1	0.816	Cd80
Ctsl	Ctss	0.816	Ctsl
Aldh1b1	Aox4	0.813	Aldh1b1
Aldh9a1	Aox4	0.813	Aldh9a1
Asns	Gadl1	0.813	Asns
Dmd	Krt19	0.813	Dmd
Aldob	Tktl2	0.812	Aldob
Camk4	Prm2	0.812	Camk4
Itgb6	Lama3	0.812	Itgb6
Ica	Trf	0.811	Ica
Mak16	Utp6	0.811	Mak16
Atp2b4	Prkg2	0.81	Atp2b4
Mak16	Polr1b	0.81	Mak16
Rnf165	Ube2d1	0.81	Rnf165
Atp2b4	Prkg1	0.809	Atp2b4
Prkg1	Prkg2	0.807	Prkg1
Acss2	Aox4	0.806	Acss2
Cdh1	Fgf2	0.805	Cdh1
Kri1	Mak16	0.805	Kri1
Mak16	Nol12	0.805	Mak16
Mdm4	Ube2d1	0.804	Mdm4
Aldoc	Tktl2	0.803	Aldoc
Aspa	Gadl1	0.803	Aspa
Brcc3	Rnf2	0.803	Brcc3
Mapk10	Mecom	0.803	Mapk10
Tk2	mCG_22911	0.803	Tk2
Mak16	Wdr18	0.802	Mak16
Cd86	H2-K1	0.8	Cd86
Polr1b	Wdr18	0.8	Polr1b

Cyp2a12	Cyp4a14	0.799	Cyp2a12
Kri1	Polr1b	0.797	Kri1
Itga1	Itga4	0.794	Itga1
Ppih	Rpp38	0.794	Ppih
Utp6	Wdr18	0.794	Utp6
Tcf4	Tle4	0.791	Tcf4
Rpp38	Utp6	0.788	Rpp38
Ncf2	Pirb	0.786	Ncf2
Nsf	Syt1	0.785	Nsf
Grik2	Scn3a	0.784	Grik2
Junb	Mapk10	0.784	Junb
Afp	Krt19	0.783	Afp
Dmd	Myog	0.783	Dmd
Fgf2	Prom1	0.783	Fgf2
Grik2	Scn9a	0.783	Grik2
Aldob	Ldhc	0.781	Aldob
Dnah17	Dnal1	0.779	Dnah17
Sec22a	Snap25	0.778	Sec22a
Itga4	Lama3	0.777	Itga4
Clu	Pla2g7	0.776	Clu
Acss2	Aldh9a1	0.774	Acss2
Bub1b	Kif14	0.774	Bub1b
Srek1ip1	mCG_22911	0.773	Srek1ip1
Batf3	Junb	0.772	Batf3
Casp3	Cdh1	0.77	Casp3
Casp3	Mapk10	0.77	Casp3
Lama3	Sv2b	0.77	Lama3
Snap25	Syt11	0.77	Snap25
Ak4	Pde4d	0.769	Ak4
Brcc3	Ring1	0.768	Brcc3
Cngb3	Rgs7bp	0.768	Cngb3
Apobec3	Trim5	0.767	Apobec3
Sycp2l	Tmem150b	0.766	Sycp2l
Aplf	Xrcc4	0.761	Aplf
Polr1b	Polr3e	0.761	Polr1b
Ddx39b	Gm4312	0.76	Ddx39b
Prpf31	Utp6	0.759	Prpf31
Hdac9	Nrip1	0.758	Hdac9
Ccdc33	Gramd2	0.756	Ccdc33
Ferd3l	Snx13	0.756	Ferd3l
Atp5d	Uty	0.755	Atp5d
Cd80	Itga1	0.754	Cd80
G3bp1	Ybx1	0.752	G3bp1

Grik2	Lrrtm4	0.751	Grik2
Bub1b	Rad51	0.75	Bub1b
Itga1	Lama3	0.75	Itga1
Cops4	Det1	0.749	Cops4
Kirrel3	Xpr1	0.749	Kirrel3
Aldoc	Ldhc	0.748	Aldoc
Cyp2j6	Cyp4a14	0.747	Cyp2j6
Dhfr	Rrm1	0.747	Dhfr
Mmp9	Ncf2	0.747	Mmp9
Odf1	Prm2	0.747	Odf1
Ldlr	Pon1	0.746	Ldlr
Fads2	Scd1	0.745	Fads2
Aplf	Etaa1	0.744	Aplf
Cd86	Serpinb9f	0.743	Cd86
Grik2	Vwc2l	0.743	Grik2
Clu	Ldlr	0.742	Clu
Rpp38	Snrnp40	0.741	Rpp38
Cd80	Itgb6	0.74	Cd80
Lrrk2	Th	0.739	Lrrk2
Gabrg2	Nsf	0.738	Gabrg2
Prps1l3	Tktl2	0.738	Prps1l3
Cdc40	Luc7l	0.737	Cdc40
Dgkg	Gnpat	0.737	Dgkg
ENSMUSG00000029620	Vmn1r58	0.737	ENSMUSG00000029620
Apobec3	Fv1	0.736	Apobec3
Rrm1	Tk1	0.736	Rrm1
Agrn	Dmd	0.734	Agrn
Cdh1	Prom1	0.734	Cdh1
Reep5	Rtn2	0.734	Reep5
Als2	ENSMUSG00000028300	0.732	Als2
Trpm1	Trpv3	0.732	Trpm1
Cdh1	Krt19	0.731	Cdh1
Amot	Wwc1	0.73	Amot
Casp3	Mmp9	0.729	Casp3
Strc	Tectb	0.729	Strc
Dhx34	Upf3b	0.728	Dhx34
Btaf1	Taf2	0.727	Btaf1
Brcc3	Phc2	0.726	Brcc3
Prpf31	Rnf2	0.726	Prpf31
Gnl1	Utp6	0.724	Gnl1
Kidins220	Xpr1	0.724	Kidins220

Msh3	Rad51	0.724	Msh3
Brcc3	Mdc1	0.723	Brcc3
Crp	Mmp9	0.723	Crp
Dgkg	Plcd4	0.723	Dgkg
Rad51	Rfc4	0.723	Rad51
Atf7	Junb	0.722	Atf7
Bub1b	Fignl1	0.722	Bub1b
Cd80	Serpinb9f	0.721	Cd80
Ap2b1	Ap5s1	0.72	Ap2b1
Dtna	Krt19	0.72	Dtna
Nrip1	Phf12	0.72	Nrip1
Pde4d	Tex40	0.72	Pde4d
Dgkg	Plcz1	0.719	Dgkg
Gabra5	Opcml	0.719	Gabra5
Amot	Mpdz	0.718	Amot
Baz2b	Setdb2	0.718	Baz2b
Fignl1	Rad51	0.718	Fignl1
Fv1	Trim5	0.718	Fv1
Fgf2	Hif1a	0.717	Fgf2
Itgb1bp2	Smpx	0.716	Itgb1bp2
Cenpw	Rad51ap1	0.714	Cenpw
H2-K1	Serpinb9f	0.714	H2-K1
Mylpf	Myot	0.714	Mylpf
Ccdc171	Snapc3	0.712	Ccdc171
Gnl1	Mak16	0.712	Gnl1
Cd80	Tnfsf9	0.71	Cd80
Clu	Mmp9	0.71	Clu
Cd68	Ctss	0.708	Cd68
Ldhc	Prm2	0.708	Ldhc
Mfsd11	Sv2b	0.707	Mfsd11
Cdkn2b	Mdm2	0.706	Cdkn2b
Atad2	Btaf1	0.705	Atad2
Cd86	Ly6c1	0.705	Cd86
Snap25	Zdhhc3	0.705	Snap25
Brcc3	Def6	0.704	Brcc3
Ddo	Srr	0.704	Ddo
Krt19	Prom1	0.704	Krt19
Ak4	Rrm1	0.703	Ak4
Ak7	Rrm1	0.703	Ak7
Ldhc	Tktl2	0.703	Ldhc
Otp	Oxt	0.703	Otp
Ric3	St5	0.703	Ric3
Kiaa1211	Polr1b	0.702	Kiaa1211

Bcl2l11	Mapk10	0.698	Bcl2l11
Ctnnd2	ENSMUSG00000056004	0.698	Ctnnd2
Gnl1	Polr1b	0.698	Gnl1
Otol1	Tectb	0.698	Otol1
Snap25	Syt12	0.695	Snap25
Casp3	Fgf2	0.693	Casp3
Fam189a1	Tmem130	0.693	Fam189a1
Ferd3l	Tcf4	0.693	Ferd3l
Inpp5j	Plcd4	0.692	Inpp5j
Nrip1	Pparg	0.692	Nrip1
Ccr10	Grk6	0.691	Ccr10
Cd68	Cd86	0.691	Cd68
Atp5d	Ppa1	0.69	Atp5d
Dgke	Gnpat	0.69	Dgke
Inpp5j	Plcz1	0.689	Inpp5j
Ncf2	Xdh	0.689	Ncf2
Adra1d	Lrrtm4	0.686	Adra1d
BC018507	Smim23	0.686	BC018507
Cd80	Ly6c1	0.686	Cd80
Kri1	Prpf31	0.685	Kri1
Pif1	Rrm1	0.684	Pif1
Dgke	Plcd4	0.683	Dgke
Cd86	Tnfsf9	0.682	Cd86
Il22ra1	Il9	0.682	Il22ra1
Gabrb2	Nsf	0.681	Gabrb2
Il3	Il9r	0.681	Il3
Aldh1b1	Cyp4a14	0.68	Aldh1b1
ENSMUSG00000029620	Ttc30b	0.68	ENSMUSG00000029620
Lrrk2	Nsf	0.68	Lrrk2
Snap25	Sv2b	0.679	Snap25
Aldh9a1	Cyp4a14	0.678	Aldh9a1
Bub1b	Tk1	0.676	Bub1b
Cdh1	Loxl2	0.675	Cdh1
Cdh1	Clmp	0.675	Cdh1
Ak7	mCG_22911	0.674	Ak7
Cc2d2a	Ttc21b	0.674	Cc2d2a
Junb	Mapk12	0.673	Junb
Cd68	Mmp9	0.672	Cd68
Cytip	Traf3ip3	0.672	Cytip
Plcd4	Plcz1	0.672	Plcd4
Brinp2	Zfp37	0.671	Brinp2

Il3	Prlr	0.67	Il3
Ak4	mCG_22911	0.668	Ak4
Dao	Tnik	0.668	Dao
Fgf2	Sox1	0.667	Fgf2
Mapk12	Ncf2	0.667	Mapk12
Ak7	Pde4d	0.666	Ak7
Dgke	Plcz1	0.666	Dgke
Gabra5	Nsf	0.666	Gabra5
Gap43	Snap25	0.666	Gap43
Ldlr	Scd1	0.666	Ldlr
Fads2	Plb1	0.665	Fads2
Arhgap31	Dock6	0.664	Arhgap31
Btk	Lcp1	0.664	Btk
Dmd	Iqsec3	0.664	Dmd
Gnl1	Wdr18	0.664	Gnl1
Inpp4b	Mtmr1	0.664	Inpp4b
Mtmr1	Tmem55a	0.664	Mtmr1
Peak1	Scaper	0.664	Peak1
Aox4	Cyp4a14	0.663	Aox4
Dnmt3b	Lin28a	0.663	Dnmt3b
Eif4e1b	Patl2	0.663	Eif4e1b
Rad51	Rrm1	0.663	Rad51
Asns	Nars2	0.662	Asns
Dlgap1	Epb4.1l3	0.662	Dlgap1
Mecom	Prdm11	0.662	Mecom
Nacc1	Ranbp10	0.662	Nacc1
Ube2d1	Usp9y	0.662	Ube2d1
Rps6ka2	Ybx1	0.661	Rps6ka2
Atad2	Rad51ap1	0.66	Atad2
Gdpd1	Plb1	0.66	Gdpd1
Peak1	Tk2	0.66	Peak1
Pla2g7	Plb1	0.66	Pla2g7
Cspp1	Ttc21b	0.659	Cspp1
Enpp2	Plb1	0.659	Enpp2
Crkl	Itgb6	0.658	Crkl
Erlin1	Rnf170	0.658	Erlin1
Timm10b	Tmem208	0.658	Timm10b
Mtmr1	Plcd4	0.657	Mtmr1
Adamts2	Phykpl	0.656	Adamts2
Pex5l	Scp2d1	0.655	Pex5l
Birc3	Ctss	0.653	Birc3
Aox4	Cyp2a12	0.652	Aox4
Camk4	Pparg	0.652	Camk4

Fgf2	Lin28a	0.652	Fgf2
Lpcat1	Plb1	0.652	Lpcat1
Afp	Sox1	0.651	Afp
Cps1	Gm28040	0.651	Cps1
Fgf13	Scn9a	0.651	Fgf13
Ttc30b	Vmn1r58	0.651	Ttc30b
Cyp2j6	Plb1	0.65	Cyp2j6
Cyp4a14	Plb1	0.65	Cyp4a14
Mtmr1	Plcz1	0.65	Mtmr1
Pde4d	mCG_22911	0.65	Pde4d
Pde6b	mCG_22911	0.65	Pde6b
Adam8	Mmp9	0.649	Adam8
Apc	Bub1b	0.649	Apc
Phactr1	Taz	0.647	Phactr1
Samsn1	Scfd1	0.647	Samsn1
Aldob	Tmod1	0.646	Aldob
Ipo9	Tnpo3	0.646	Ipo9
Mdc1	Xrcc4	0.646	Mdc1
Crkl	Eif4e1b	0.644	Crkl
Scly	Slc36a1	0.644	Scly
B3galt4	St8sia1	0.643	B3galt4
Btk	Cd81	0.643	Btk
Scube2	St5	0.643	Scube2
Casp3	Hspb3	0.642	Casp3
Myot	Smpx	0.641	Myot
Brcc3	Ube2d1	0.64	Brcc3
Cd68	Ly6c1	0.64	Cd68
Rad51	Xrcc4	0.64	Rad51
Camk4	Pde4d	0.639	Camk4
Mpdz	Sstr3	0.639	Mpdz
Afp	Fgf2	0.638	Afp
Cdk14	Znrf2	0.638	Cdk14
Cngb3	Rpgr	0.637	Cngb3
Rad51	Tk1	0.637	Rad51
Pon1	Pparg	0.636	Pon1
Fgf2	Mmp17	0.635	Fgf2
Gc	Serpina1a	0.635	Gc
Ispd	Large	0.635	Ispd
Mapk10	Mapk12	0.635	Mapk10
Susd2	Tmem72	0.635	Susd2
Mrvi1	Scly	0.634	Mrvi1
Aldh9a1	St5	0.633	Aldh9a1
Crkl	Itga4	0.633	Crkl

Pkd2l2	Trpm1	0.633	Pkd2l2
Atp13a2	Syt11	0.632	Atp13a2
Rfc4	Tk1	0.631	Rfc4
Ano5	Mmd2	0.63	Ano5
Fignl1	Rad51ap1	0.63	Fignl1
Fsd2	Hspb3	0.63	Fsd2
H2-K1	Ulbp1	0.63	H2-K1
Lingo2	Unc13c	0.63	Lingo2
Arl15	Vwc2l	0.629	Arl15
Atp13a2	Prrt3	0.629	Atp13a2
Birc3	Ctsl	0.629	Birc3
Casp3	Th	0.629	Casp3
Crp	Pon1	0.629	Crp
Depdc1b	Rad51ap1	0.629	Depdc1b
Gabrg3	Nsf	0.629	Gabrg3
Mdm2	Rgs7bp	0.629	Mdm2
Phf12	Spag16	0.629	Phf12
Adam7	Cped1	0.628	Adam7
Dlgap1	Sv2b	0.628	Dlgap1
Btaf1	Mms19	0.627	Btaf1
Cd81	Sdcbp	0.627	Cd81
Ica	Ulbp1	0.627	Ica
Ldhc	Odf1	0.627	Ldhc
Mmp16	Spock3	0.627	Mmp16
Brcc3	Rad51	0.626	Brcc3
ENSMUSG00000024209	Ppt1	0.625	ENSMUSG00000024209
Gm10530	Tor1aip1	0.625	Gm10530
Afp	Prom1	0.624	Afp
Dennd4a	Vwa9	0.624	Dennd4a
Patl2	Vmn1r58	0.624	Patl2
Cntfr	Il3	0.623	Cntfr
Klhl30	Smpx	0.622	Klhl30
Lca5	Rpgr	0.622	Lca5
Cc2d2a	Rpgr	0.62	Cc2d2a
Crkl	Itga1	0.62	Crkl
Ppt1	Zdhhc3	0.62	Ppt1
Adam8	Lcp1	0.619	Adam8
Fgf2	Myog	0.619	Fgf2
Lox	Matn2	0.619	Lox
Brd8	Phip	0.618	Brd8
Ctss	Ly9	0.617	Ctss
Ddx39b	Prpf31	0.617	Ddx39b

Mapk10	Nfat5	0.617	Mapk10
Srp54b	Xrcc4	0.615	Srp54b
Aldob	Aldoc	0.614	Aldob
Casp3	Cd68	0.614	Casp3
Cd68	Lcp1	0.614	Cd68
Gabrg2	Syt1	0.613	Gabrg2
Grip2	Tubgcp4	0.613	Grip2
Ifit1	Ifit3b	0.613	Ifit1
Kri1	Nol12	0.613	Kri1
Acot4	Fads2	0.612	Acot4
Acot4	Cyp4a14	0.612	Acot4
H2-K1	Mr1	0.612	H2-K1
Itk	Rasgrp1	0.612	Itk
Apobec3	Atp5d	0.611	Apobec3
Cd86	Il3	0.611	Cd86
Cdh1	Mdm2	0.611	Cdh1
Gabrg2	Scn9a	0.611	Gabrg2
Raly	Vps13d	0.611	Raly
St6gal2	Wdr64	0.611	St6gal2
Brinp2	Gpc5	0.609	Brinp2
Bub1b	Cenpw	0.609	Bub1b
Ctnnd2	Pdzd2	0.609	Ctnnd2
Snx13	Ube2d1	0.609	Snx13
Atp1b4	Prkg1	0.608	Atp1b4
Atp1b4	Prkg2	0.608	Atp1b4
ENSMUSG00000028300	Lingo2	0.608	ENSMUSG00000028300
Kirrel2	Xpr1	0.608	Kirrel2
Ldlr	Pla2g7	0.608	Ldlr
Nsf	Syn2	0.606	Nsf
Cd81	Ldlr	0.605	Cd81
Lox	Mmp9	0.605	Lox
Oxt	Th	0.605	Oxt
Sdcbp	St5	0.605	Sdcbp
Ferd3l	Ube2d1	0.604	Ferd3l
Avil	Scn9a	0.603	Avil
Cngb3	Mdm2	0.603	Cngb3
Dmd	Myot	0.603	Dmd
Lingo2	Ubr3	0.603	Lingo2
Fam214a	Lzts1	0.602	Fam214a
Fgf2	Th	0.602	Fgf2
Fsd2	Perm1	0.602	Fsd2
Il9	Prlr	0.602	Il9

Itgb6	Prkcb	0.602	Itgb6
Itgb6	Prkcg	0.602	Itgb6
Mmp9	Pparg	0.602	Mmp9
Foxd1	Wnt9b	0.601	Foxd1
Cntfr	Il9	0.6	Cntfr
Il22ra1	Il3	0.6	Il22ra1
Acss2	Scd1	0.599	Acss2
Crct1	Gm7664	0.599	Crct1
Cytip	Itk	0.599	Cytip
Fignl1	Rfc4	0.599	Fignl1
Hormad1	Mei1	0.599	Hormad1
Cylc2	Odf1	0.598	Cylc2
Gabrg2	Gabrg3	0.598	Gabrg2
Snap25	Taf2	0.598	Snap25
Syt1	Unc13c	0.598	Syt1
Afp	Cdh1	0.596	Afp
Adamts2	Lox	0.595	Adamts2
Ano5	Myot	0.595	Ano5
Bcl2l11	Birc3	0.595	Bcl2l11
Cd68	Cd80	0.595	Cd68
Ctss	H2-K1	0.595	Ctss
Dnajc10	Hspa12a	0.594	Dnajc10
Dnm3	Samd3	0.593	Dnm3
Gabrg2	Zdhhc3	0.593	Gabrg2
Rasgrp1	Skap1	0.593	Rasgrp1
Dhfr	Rfc4	0.592	Dhfr
Esyt3	Reep5	0.592	Esyt3
Mrvi1	Slc36a1	0.592	Mrvi1
Atf7	Nfe2	0.591	Atf7
Gc	Trf	0.591	Gc
Vps37c	Vps4b	0.591	Vps37c
Acot1	Cyp4a14	0.59	Acot1
Dnajc10	Rrm1	0.59	Dnajc10
Asf1a	Rrm1	0.589	Asf1a
Baz2b	Phip	0.589	Baz2b
Chat	Gc	0.589	Chat
Kif14	Rad51ap1	0.589	Kif14
Bloc1s5	Snrnp48	0.588	Bloc1s5
Fdps	Ldlr	0.588	Fdps
Cdh18	Ctnnd2	0.587	Cdh18
Mzf1	Zfp623	0.587	Mzf1
Atp2b4	Nkiras1	0.586	Atp2b4
Esyt3	Ralgapa1	0.586	Esyt3

Gc	Serpina5	0.586	Gc
Pxdc1	Zmiz1	0.586	Pxdc1
Bcl2l11	Mdm2	0.585	Bcl2l11
Pde6b	Th	0.585	Pde6b
Cd68	Ldlr	0.584	Cd68
Il9	Serpinb9f	0.584	Il9
Kri1	Slc25a36	0.584	Kri1
Raly	Ralyl	0.584	Raly
Chat	Sacs	0.583	Chat
Fv1	Xpr1	0.582	Fv1
Gap43	Syt1	0.582	Gap43
Gpat2	Taz	0.582	Gpat2
Ak4	Ak7	0.581	Ak4
Btk	Dmd	0.581	Btk
Cd68	Crp	0.581	Cd68
Lcp1	Mpeg1	0.581	Lcp1
Abca3	Lzts1	0.58	Abca3
Amot	Wwox	0.579	Amot
Lingo2	Ralyl	0.579	Lingo2
Aanat	Tph1	0.578	Aanat
Btbd11	Cul1	0.578	Btbd11
Cc2d2a	Invs	0.578	Cc2d2a
Cdh1	Pparg	0.578	Cdh1
Afp	Lin28a	0.577	Afp
Gap43	Th	0.577	Gap43
Asns	Nadsyn1	0.576	Asns
Bub1b	Cdk14	0.576	Bub1b
Lmo3	Ssbp2	0.576	Lmo3
Bloc1s5	Lingo2	0.574	Bloc1s5
Kctd11	Kctd20	0.574	Kctd11
Kcnc1	Ldhc	0.573	Kcnc1
Mep1a	Pla2g7	0.573	Mep1a
Prkg1	Rgs9	0.573	Prkg1
Prrg1	Smpx	0.573	Prrg1
Bloc1s5	Dtna	0.572	Bloc1s5
Cdc40	Dhx34	0.572	Cdc40
Rgs7bp	mCG_22911	0.572	Rgs7bp
Kiaa1109	Vps13d	0.571	Kiaa1109
Cytip	Ly9	0.57	Cytip
Hspb3	Perm1	0.57	Hspb3
Ncf2	Prdx6	0.57	Ncf2
Brcc3	Usp11	0.569	Brcc3
Mal	Mobp	0.569	Mal

Crp	Pla2g7	0.568	Crp
Msgn1	Spock3	0.568	Msgn1
Adamts6	mCG_22911	0.567	Adamts6
Cul1	Mdm2	0.567	Cul1
Cbfa2t3	Wwox	0.566	Cbfa2t3
P2rx3	Scn9a	0.566	P2rx3
Prpf31	Rpgr	0.566	Prpf31
Sec22a	Syn2	0.566	Sec22a
Timm10b	Timm21	0.566	Timm10b
Cc2d2a	Upf3b	0.565	Cc2d2a
Cyp4a14	Scd1	0.565	Cyp4a14
Gnl1	Kri1	0.565	Gnl1
Rnf2	Ube2d1	0.565	Rnf2
Rtn1	Scube2	0.565	Rtn1
Afp	Serpina5	0.564	Afp
Invs	Ttc21b	0.564	Invs
Mak16	Prpf31	0.564	Mak16
Clcnkb	Slc5a2	0.563	Clcnkb
Ly9	Traf3ip3	0.563	Ly9
Pparg	Sgk1	0.563	Pparg
Cdh1	Mmp17	0.562	Cdh1
Kif1a	Snap25	0.562	Kif1a
Aplf	Macrod2	0.561	Aplf
Ccdc198	Kif12	0.561	Ccdc198
Fgf6	Fgfbp1	0.561	Fgf6
Hspb3	Klhl30	0.561	Hspb3
Adam26b	Fbxo44	0.56	Adam26b
Adarb1	Grik2	0.56	Adarb1
Itk	Kirrel2	0.56	Itk
Cc2d2a	Lrrc6	0.559	Cc2d2a
Ube2l3	Usp9y	0.559	Ube2l3
Gabrb2	Mark1	0.558	Gabrb2
Nsf	Taf2	0.558	Nsf
Phip	Rfwd3	0.558	Phip
Ranbp17	Tmem190	0.558	Ranbp17
Batf3	Tcf4	0.557	Batf3
Loxhd1	Strc	0.557	Loxhd1
Snap25	Unc13c	0.557	Snap25
Aspa	Trpv3	0.556	Aspa
Crp	Gc	0.556	Crp
Bub1b	Depdc1b	0.555	Bub1b
Cdh1	Dnmt3b	0.555	Cdh1
Agrn	Ldlr	0.554	Agrn

Atp5d	Txn2	0.554	Atp5d
Cd68	Mpeg1	0.554	Cd68
Celf6	Rrm1	0.554	Celf6
Itk	Skap1	0.554	Itk
Clrn1	Strc	0.553	Clrn1
Ldlr	Pparg	0.553	Ldlr
Mylpf	Myog	0.553	Mylpf
Fgf2	Il3	0.552	Fgf2
Casp3	Xdh	0.551	Casp3
Ly6h	Ric3	0.551	Ly6h
Map3k7	Tube1	0.551	Map3k7
Mtl5	Rbl1	0.551	Mtl5
Spag16	Spef2	0.551	Spag16
Acsf3	Sirt5	0.55	Acsf3
Casp3	Traf1	0.55	Casp3
Cdh1	Lox	0.55	Cdh1
Casp3	Mdm4	0.549	Casp3
Casp3	Prom1	0.549	Casp3
Brcc3	Cops4	0.548	Brcc3
Ctnnd2	Sulf1	0.548	Ctnnd2
Gabrg2	Snap25	0.548	Gabrg2
Prkch	Rps6ka2	0.548	Prkch
Clcnkb	Gabrg2	0.547	Clcnkb
Dll4	Mpdz	0.547	Dll4
Gnl1	Snapc3	0.547	Gnl1
Hif1a	Mmp9	0.547	Hif1a
Hif1a	Mdm2	0.547	Hif1a
Mylpf	Smpx	0.547	Mylpf
Piga	Prrg1	0.547	Piga
Birc3	Mdm2	0.546	Birc3
Bloc1s5	Snap25	0.546	Bloc1s5
Casp3	Pidd1	0.546	Casp3
Prlr	Spef2	0.546	Prlr
Ring1	Ube2d1	0.546	Ring1
Aqr	Dcxr	0.545	Aqr
Casp3	Tcf7	0.545	Casp3
Cdh1	Marveld2	0.545	Cdh1
Ddx39b	Dhx34	0.545	Ddx39b
Clcnkb	Gabra5	0.544	Clcnkb
Crp	Serpina5	0.544	Crp
Klhl30	Perm1	0.544	Klhl30
Perm1	Smpx	0.544	Perm1
Fignl1	Rrm1	0.543	Fignl1

Gk5	Ipo9	0.542	Gk5
Hormad1	Rad51	0.542	Hormad1
Irak2	Tnfsf9	0.542	Irak2
Mcoln2	Trpm1	0.542	Mcoln2
Rbm41	Ybx1	0.542	Rbm41
Timm10b	Yme1l1	0.542	Timm10b
Dhfr	Msh3	0.541	Dhfr
Lmbr1	Srek1ip1	0.541	Lmbr1
Btbd11	Fbxo17	0.54	Btbd11
Btbd11	Fbxo44	0.54	Btbd11
Clcnkb	Gabrb2	0.54	Clcnkb
Clcnkb	Gabrg3	0.54	Clcnkb
Prom1	Tcf4	0.54	Prom1
Rbm41	Snrnp48	0.54	Rbm41
Cc2d2a	Cspp1	0.539	Cc2d2a
Cdkn2b	Rbl1	0.539	Cdkn2b
Crp	Slc37a2	0.539	Crp
Gnl1	Nol12	0.539	Gnl1
Mfsd11	Slc25a36	0.539	Mfsd11
Rgs7bp	Srek1ip1	0.539	Rgs7bp
Acss2	Aspa	0.538	Acss2
Itk	P2ry10	0.538	Itk
Phf12	Rsph6a	0.538	Phf12
Casp3	Pparg	0.537	Casp3
Col11a2	Tectb	0.537	Col11a2
Ctss	Ncf2	0.537	Ctss
Gm128	Srek1ip1	0.537	Gm128
Lin28a	Ybx1	0.537	Lin28a
Mdm2	Rbl1	0.537	Mdm2
Pde6b	Rpgr	0.537	Pde6b
Btk	Cd86	0.536	Btk
Crkl	Itk	0.536	Crkl
Lrrc6	Lrrc69	0.536	Lrrc6
Luc7l	Rbm41	0.536	Luc7l
Mfsd11	Slc16a14	0.536	Mfsd11
Pparg	Taz	0.536	Pparg
Sstr3	Ttc21b	0.536	Sstr3
Asf1a	Rad51	0.535	Asf1a
Astn2	Cntn4	0.535	Astn2
Cspp1	ENSMUSG00000029620	0.535	Cspp1
Dhx34	Utp6	0.535	Dhx34
Dlgap1	Grik2	0.535	Dlgap1

Fgf13	Mmp9	0.535	Fgf13
Fsd2	Klhl30	0.535	Fsd2
Mmp9	Prom1	0.535	Mmp9
Scfd1	Snap25	0.535	Scfd1
Tmem208	Zfp280d	0.535	Tmem208
Ak7	Susd2	0.534	Ak7
Tcf4	Tnik	0.534	Tcf4
Afp	Bub1b	0.533	Afp
Dhx34	Srrm2	0.533	Dhx34
Lin28a	Prom1	0.533	Lin28a
Sdcbp	Vps4b	0.533	Sdcbp
Pkd2l2	Trpv3	0.532	Pkd2l2
Adarb1	Syt12	0.531	Adarb1
Btk	Taz	0.531	Btk
Casp3	Hif1a	0.53	Casp3
Ccl25	Itga4	0.53	Ccl25
Hspa12a	Zfp949	0.53	Hspa12a
Msh3	Neil1	0.53	Msh3
Nol12	Utp6	0.53	Nol12
Prps1l3	Zfp185	0.53	Prps1l3
Dmd	Fgf2	0.529	Dmd
Mctp1	Nkain3	0.529	Mctp1
Mdm2	Pidd1	0.529	Mdm2
Cdh1	Epb4.1l3	0.528	Cdh1
ENSMUSG00000024209	Pex5l	0.528	ENSMUSG00000024209
Fbn2	Lox	0.528	Fbn2
Frmd4b	Lrrc69	0.528	Frmd4b
Polr1b	Slc25a36	0.528	Polr1b
Camk1g	Spock3	0.527	Camk1g
Cdh1	Lin28a	0.527	Cdh1
Lmo7	Pdlim5	0.527	Lmo7
Prlr	Wnt9b	0.527	Prlr
Anxa7	Snx13	0.526	Anxa7
P2ry10	Traf3ip3	0.526	P2ry10
Strc	Vmn1r58	0.526	Strc
Adamts6	Srek1ip1	0.525	Adamts6
Cc2d2a	Lca5	0.525	Cc2d2a
Cspp1	Vmn1r58	0.525	Cspp1
Ly6c1	Serpinb9f	0.525	Ly6c1
Nfat5	Sgk1	0.525	Nfat5
Ppt1	Slc2a8	0.525	Ppt1
Ranbp10	Ranbp17	0.525	Ranbp10

Agrn	Fgf2	0.524	Agrn
Ak4	St5	0.524	Ak4
Atad2	Fignl1	0.524	Atad2
Dusp15	Emc8	0.524	Dusp15
ENSMUSG00000027811	Slc25a36	0.524	ENSMUSG00000027811
Hif1a	Prom1	0.524	Hif1a
Btk	Rasgrp1	0.523	Btk
Casp3	Lox	0.523	Casp3
Cd80	Il3	0.523	Cd80
Chat	Pde6b	0.523	Chat
Cpm	Enpp7	0.523	Cpm
Crp	Xdh	0.523	Crp
Fgd6	Syt1	0.523	Fgd6
Pi15	Zfp185	0.523	Pi15
Crp	Pparg	0.522	Crp
Enpp2	P2ry10	0.522	Enpp2
Ppp1r10	St6gal2	0.522	Ppp1r10
Aldob	Cps1	0.521	Aldob
Aspa	Mobp	0.521	Aspa
Cntfr	Rasgrp1	0.521	Cntfr
Crp	Ldlr	0.521	Crp
Gemin6	Ybx1	0.521	Gemin6
Mapk10	Mmp9	0.521	Mapk10
Nsf	Sncb	0.521	Nsf
Olfr740	Ppih	0.521	Olfr740
Oxt	Prlr	0.521	Oxt
Apobec3	Xpr1	0.52	Apobec3
Gc	Pon1	0.52	Gc
Lca5	Prdm15	0.52	Lca5
Il3	Serpinb9f	0.519	Il3
Lca5	Tubgcp4	0.519	Lca5
Ly9	P2ry10	0.519	Ly9
Tk1	Tmc6	0.519	Tk1
Art3	Galnt18	0.517	Art3
Fam175a	Ube2d1	0.517	Fam175a
Gpr35	Wdr64	0.517	Gpr35
Prdm2	Znrf2	0.516	Prdm2
Rgs7bp	Rgs8	0.516	Rgs7bp
Dennd1c	Nav2	0.515	Dennd1c
Gc	Nadsyn1	0.515	Gc
Gm7664	Reep5	0.515	Gm7664
Otp	Th	0.515	Otp

Dlgap1	Iqsec3	0.514	Dlgap1
Reg2	Slc5a2	0.514	Reg2
Aars	Bub1b	0.513	Aars
Adarb1	Scaf4	0.513	Adarb1
Atp2b4	Slc9c1	0.513	Atp2b4
Itga4	Ly6c1	0.513	Itga4
Itga4	Lcp1	0.513	Itga4
Spef2	Wdr64	0.513	Spef2
Cd86	Ctss	0.512	Cd86
Gadl1	Phip	0.51	Gadl1
Mdm2	Usp11	0.51	Mdm2
Mlxip	Vps37c	0.51	Mlxip
Nsf	Stxbp5l	0.51	Nsf
Fgf2	Lox	0.509	Fgf2
Rgs9	Stxbp5l	0.509	Rgs9
Aqr	Dhx34	0.508	Aqr
H2-K1	Lcp1	0.508	H2-K1
Lzts1	Patl2	0.508	Lzts1
Adam7	Ldhc	0.507	Adam7
Polr1b	Rpp38	0.507	Polr1b
Armc9	Clmp	0.506	Armc9
Kri1	Wdr18	0.506	Kri1
Astn2	Phactr1	0.505	Astn2
Gabra5	Syn2	0.505	Gabra5
Txn2	Xdh	0.505	Txn2
Jakmip1	Kif1b	0.504	Jakmip1
Opcml	Syn2	0.504	Opcml
Stxbp5l	Syt1	0.504	Stxbp5l
Cdh1	Cdkn2b	0.503	Cdh1
Cul1	Myog	0.503	Cul1
Dhx34	Nadsyn1	0.503	Dhx34
Gnpat	Pex5l	0.503	Gnpat
Lrrk2	Syt11	0.503	Lrrk2
Atp1b4	Tor1aip1	0.502	Atp1b4
Birc3	Mmp9	0.502	Birc3
Ctnnd2	Srbd1	0.502	Ctnnd2
Kif12	Sstr3	0.502	Kif12
Cdh1	Ctsl	0.501	Cdh1
Gabrg2	Iqsec3	0.501	Gabrg2
Il9	Itk	0.501	Il9
Col11a2	Strc	0.5	Col11a2
Fdps	Scd1	0.5	Fdps
Dhfr	Rbl1	0.499	Dhfr

Masp1	Smpx	0.499	Masp1
Tssk2	Txn2	0.499	Tssk2
Btk	Mmp9	0.498	Btk
L3mbtl3	Phf20l1	0.498	L3mbtl3
Clmp	Stfa2l1	0.497	Clmp
Cps1	Ybx1	0.497	Cps1
Dlgap1	Ptprd	0.497	Dlgap1
Dll4	Fgf2	0.497	Dll4
Lin28a	Sox1	0.497	Lin28a
Prdm15	Ripk4	0.497	Prdm15
Snap25	Sncb	0.497	Snap25
Acsf3	Pik3r6	0.496	Acsf3
Itk	Ly9	0.496	Itk
BC055324	Rfc4	0.495	BC055324
Kif14	Mdm4	0.495	Kif14
Fam175a	Xrcc4	0.494	Fam175a
Ferd3l	Hdac9	0.494	Ferd3l
Kif1a	Syt1	0.494	Kif1a
Ldlr	Mmp9	0.494	Ldlr
Tnfsf9	Traf1	0.494	Tnfsf9
Bub1b	Pidd1	0.493	Bub1b
Casp3	Lcp1	0.493	Casp3
Agrn	Ispd	0.492	Agrn
Dnal1	Gemin2	0.492	Dnal1
Gap43	Prkcg	0.492	Gap43
Mlf1	Myot	0.492	Mlf1
Neurod6	Tcf4	0.492	Neurod6
Aqr	Tbcel	0.491	Aqr
Camta1	Gabrg2	0.491	Camta1
BC018507	Upf3b	0.49	BC018507
Cdh1	Podxl	0.49	Cdh1
Mak16	Pex12	0.49	Mak16
Prom1	Sdcbp	0.49	Prom1
Atp13a2	Cln3	0.489	Atp13a2
Cdkn2b	Dnmt3b	0.489	Cdkn2b
ENSMUSG00000044121	S100a5	0.489	ENSMUSG00000044121
ENSMUSG00000056004	Plb1	0.489	ENSMUSG00000056004
Gjb6	Strc	0.489	Gjb6
Aqr	Prkch	0.488	Aqr
Gm28040	Kcnc1	0.488	Gm28040
Rpgr	Ttc21b	0.488	Rpgr

Slc17a5	Th	0.488	Slc17a5
Cdkl3	ENSMUSG00000027811	0.487	Cdkl3
Clu	Lrrk2	0.487	Clu
Dennd1c	Gnl1	0.487	Dennd1c
Diap2	Vmn1r199	0.487	Diap2
Dnmt3b	Tfap2c	0.487	Dnmt3b
Galnt18	Gramd1b	0.487	Galnt18
Ring1	Ube2l3	0.487	Ring1
Setdb2	Wwox	0.487	Setdb2
Afp	Casp3	0.485	Afp
Cdh1	Snai3	0.485	Cdh1
Prdx6	Txn2	0.485	Prdx6
Rad51ap1	Rrm1	0.485	Rad51ap1
Aldob	Gc	0.484	Aldob
Casp3	Nfat5	0.484	Casp3
ENSMUSG00000028300	Lrrk2	0.484	ENSMUSG00000028300
St5	Ulk4	0.484	St5
Batf3	Cd86	0.483	Batf3
Casp3	Il3	0.483	Casp3
Casp3	Crp	0.483	Casp3
Mak16	Rpp38	0.483	Mak16
Marveld2	Mpdz	0.483	Marveld2
Scaf4	Tk2	0.483	Scaf4
Ap5m1	Pde4d	0.482	Ap5m1
BC055324	Rad51ap1	0.482	BC055324
Baz2b	Phf20l1	0.482	Baz2b
Bub1b	Dsc1	0.482	Bub1b
Cd68	Ncf2	0.482	Cd68
Fgf2	Il9	0.482	Fgf2
Hspb3	Smpx	0.482	Hspb3
Lox	Xdh	0.482	Lox
Ap2b1	Zcchc10	0.481	Ap2b1
H2-K1	Ly6c1	0.481	H2-K1
Mmp9	Serpinb9f	0.481	Mmp9
Nsf	Slc4a8	0.481	Nsf
Nsf	Syt11	0.481	Nsf
Acss2	Gnpat	0.48	Acss2
Adam26b	Gnpda2	0.48	Adam26b
Btbd11	Tmod1	0.48	Btbd11
Ccdc88c	Dgkg	0.48	Ccdc88c
Lingo2	Zfp608	0.48	Lingo2

Acot4	Acsm1	0.479	Acot4
Cul1	Mpeg1	0.479	Cul1
Hif1a	Pparg	0.479	Hif1a
Astn2	Brinp2	0.478	Astn2
Ccdc88c	Mpdz	0.478	Ccdc88c
Dnajc10	Prdx6	0.478	Dnajc10
Gpr35	St6gal2	0.478	Gpr35
Batf3	Ly6c1	0.477	Batf3
Ctss	Lcp1	0.477	Ctss
Gabrg2	Scn3a	0.477	Gabrg2
Hsf3	Pdzd2	0.477	Hsf3
P2rx3	Trpv3	0.477	P2rx3
Atad2	Bub1b	0.476	Atad2
Clcnkb	Slc4a8	0.476	Clcnkb
Ctnnd2	Rtn1	0.476	Ctnnd2
Dnm3	Pik3ip1	0.476	Dnm3
Syn2	Syt11	0.476	Syn2
Abca3	Lpcat1	0.475	Abca3
Cd81	H2-K1	0.475	Cd81
Cps1	Gc	0.475	Cps1
Sox1	Th	0.475	Sox1
Stxbp5l	Unc13c	0.475	Stxbp5l
Ccdc33	Lrrtm4	0.474	Ccdc33
Clu	Gc	0.474	Clu
Dnah17	Kif1a	0.474	Dnah17
Hdac9	Snx13	0.474	Hdac9
Mdc1	Mdm2	0.474	Mdc1
Msgn1	Spef2	0.474	Msgn1
Sv2b	Syn2	0.474	Sv2b
Acvr1b	Mtl5	0.473	Acvr1b
Akap9	Tnik	0.473	Akap9
Anxa7	Cd81	0.473	Anxa7
Casp3	Cdkn2b	0.473	Casp3
Loxhd1	Rnf165	0.473	Loxhd1
Mpeg1	Traf3ip3	0.473	Mpeg1
Spag16	Vwc2l	0.473	Spag16
Bcl2l11	Cdh1	0.472	Bcl2l11
Cd80	Il9	0.472	Cd80
Chat	ENSMUSG00000024209	0.472	Chat
Dnmt3b	Mthfr	0.472	Dnmt3b
Gap43	Rtn1	0.472	Gap43
Masp1	Skap1	0.472	Masp1

Slc17a5	Slc37a2	0.472	Slc17a5
Ak4	Gpr35	0.471	Ak4
Aqr	BC018507	0.471	Aqr
Cdh1	Tcf4	0.471	Cdh1
Cdk14	ENSMUSG00000056004	0.471	Cdk14
Cpm	Ctnnd2	0.471	Cpm
Pirb	Xdh	0.471	Pirb
Prdm11	Setd3	0.471	Prdm11
Adam8	Ctss	0.47	Adam8
Ak7	Polr1b	0.47	Ak7
Junb	Nfat5	0.47	Junb
Ly9	Mpeg1	0.47	Ly9
Acsf3	Emc8	0.469	Acsf3
Asf1a	Sirt5	0.469	Asf1a
Atp13a2	Rab29	0.469	Atp13a2
Avil	Hspb3	0.469	Avil
Brinp2	Tle4	0.469	Brinp2
Casp3	Lrrk2	0.469	Casp3
Kiaa1211	Wdr18	0.469	Kiaa1211
Lpcat1	Scd1	0.469	Lpcat1
Dnal1	Tnpo3	0.468	Dnal1
Lin28a	Tfap2c	0.468	Lin28a
Arhgef6	Camk4	0.467	Arhgef6
Camta1	Kif1b	0.467	Camta1
Gabrb2	Spock3	0.467	Gabrb2
Mfsd11	Slc16a9	0.467	Mfsd11
Mthfr	Pon1	0.467	Mthfr
Rspo3	Wnt9b	0.467	Rspo3
Ube2d1	Xrcc4	0.467	Ube2d1
Dennd4a	Esyt3	0.466	Dennd4a
Gnpat	Lpcat1	0.466	Gnpat
Gnpda2	Snx12	0.466	Gnpda2
Serpina5	Trf	0.466	Serpina5
Slc2a8	Slc5a2	0.466	Slc2a8
Chat	Gap43	0.465	Chat
Invs	Wnt9b	0.465	Invs
Cenpw	Tk1	0.464	Cenpw
Sncb	Syn2	0.464	Sncb
Cd86	Itga4	0.463	Cd86
Ap5m1	Dtna	0.462	Ap5m1
Batf3	H2-K1	0.462	Batf3
Cd68	H2-K1	0.462	Cd68

Cd68	Fgf2	0.462	Cd68
Ddx39b	Raly	0.462	Ddx39b
Kcnc1	Tph1	0.462	Kcnc1
Ppp6r2	Znrf2	0.462	Ppp6r2
Prdm2	Setdb2	0.462	Prdm2
Prkcb	Tnik	0.462	Prkcb
Bcl2l11	Traf1	0.461	Bcl2l11
Fbxo17	Pik3r6	0.461	Fbxo17
Fgf2	Mmp16	0.461	Fgf2
Gm4312	Upf3b	0.461	Gm4312
Invs	Ttll3	0.461	Invs
Asf1a	Rfc4	0.46	Asf1a
Atf7	Det1	0.46	Atf7
BC018507	Pidd1	0.46	BC018507
Batf3	Det1	0.46	Batf3
Cd81	Itga4	0.46	Cd81
Col11a2	Ring1	0.46	Col11a2
Dnm3	Rtn1	0.46	Dnm3
Hspb3	Mmp9	0.46	Hspb3
Ispd	Myot	0.46	Ispd
Casp3	Chat	0.459	Casp3
Cd68	Pparg	0.459	Cd68
Cd86	Il9	0.459	Cd86
Edil3	Ssbp2	0.459	Edil3
Exosc9	Polr1b	0.459	Exosc9
Fignl1	Rtn1	0.459	Fignl1
Gabrg2	Neurod6	0.459	Gabrg2
Hspb3	Taf2	0.459	Hspb3
Mmp9	Serpina5	0.459	Mmp9
Odf1	Olfr157	0.459	Odf1
Prdm15	Setd6	0.459	Prdm15
Prkcb	Rps6ka2	0.459	Prkcb
Casp3	Gap43	0.458	Casp3
Ky	Pstpip2	0.458	Ky
Asns	Cps1	0.457	Asns
Atad2	Rad51	0.457	Atad2
Camta1	Lzic	0.457	Camta1
Cc2d2a	Sstr3	0.457	Cc2d2a
Cd81	Cd86	0.457	Cd81
Cdh1	Hif1a	0.457	Cdh1
H2-K1	Tnfsf9	0.457	H2-K1
Invs	Lrrc6	0.457	Invs
Irak2	Pidd1	0.457	Irak2

Macrod2	Sema5a	0.457	Macrod2
Anxa7	Syn2	0.456	Anxa7
Ap2b1	Tfap2c	0.456	Ap2b1
Capn15	Casp3	0.456	Capn15
Dmd	H2-K1	0.456	Dmd
Dmd	Sacs	0.456	Dmd
Dmd	Large	0.456	Dmd
Etaa1	Rfwd3	0.456	Etaa1
Grhl1	Taf2	0.456	Grhl1
Tcp10b	Tifa	0.456	Tcp10b
Acss2	Sirt5	0.455	Acss2
Dlgap1	Gabrg2	0.455	Dlgap1
Gpr110	Ntng2	0.455	Gpr110
Atp5d	Gid8	0.454	Atp5d
Fgf13	Fgfbp1	0.454	Fgf13
Avil	Sulf1	0.453	Avil
Clu	Trf	0.453	Clu
Itk	Kirrel3	0.453	Itk
Ppih	Rfc4	0.453	Ppih
Acss2	Fdps	0.452	Acss2
Atp13a2	Unc13c	0.452	Atp13a2
Bai1	mCG_17678	0.452	Bai1
Raly	Srrm2	0.452	Raly
Atp13a2	Ppt1	0.451	Atp13a2
Cbfa2t3	Cnbd2	0.451	Cbfa2t3
Cd86	Lcp1	0.451	Cd86
Depdc1b	Macrod2	0.451	Depdc1b
Fam214a	Spef2	0.451	Fam214a
L3mbtl3	Phc2	0.451	L3mbtl3
Lrrc6	Rpgr	0.451	Lrrc6
Nsf	Sv2b	0.451	Nsf
Prkcg	Rps6ka2	0.451	Prkcg
Snap25	Th	0.451	Snap25
Zfp558	Zfp608	0.451	Zfp558
Casp3	Serpinb9f	0.45	Casp3
Csmd2	Ctnnd2	0.45	Csmd2
Gabrg2	Grik2	0.45	Gabrg2
Adam8	Cd68	0.449	Adam8
Atf7	Batf3	0.449	Atf7
Cps1	Cyp2a12	0.449	Cps1
Gabra5	Grik2	0.449	Gabra5
Gabrg2	Rtn1	0.449	Gabrg2
Ano5	Ispd	0.448	Ano5

Cdh1	Fgf13	0.448	Cdh1
Fgf2	Podxl	0.448	Fgf2
Gm7978	Pif1	0.448	Gm7978
Gpat2	Lpcat1	0.448	Gpat2
Phip	Pwwp2a	0.448	Phip
Rtn1	Rtn2	0.448	Rtn1
Casp3	Rps6ka2	0.447	Casp3
Casp3	Pde6b	0.447	Casp3
Ctnnd2	Dlgap1	0.447	Ctnnd2
Nsf	Vps4b	0.447	Nsf
Adh6a	Dcxr	0.446	Adh6a
Cdkn2b	Mdm4	0.446	Cdkn2b
Ctsl	Mmp9	0.446	Ctsl
Dnajc10	Uty	0.446	Dnajc10
Gabrg2	Ralyl	0.446	Gabrg2
Kcnc1	Spock3	0.446	Kcnc1
Gm11437	Mrm1	0.445	Gm11437
Macrod2	Wwox	0.445	Macrod2
Rtkn2	Unc13c	0.445	Rtkn2
Rtn1	Snap25	0.445	Rtn1
Slc17a2	Slc37a2	0.445	Slc17a2
Ano5	mCG_17678	0.444	Ano5
Asrgl1	Tktl2	0.444	Asrgl1
Ccl25	Dll4	0.444	Ccl25
Dhx34	Snrnp40	0.444	Dhx34
Grk6	Rgs9	0.444	Grk6
Hdac9	Kidins220	0.444	Hdac9
Atf7	Mapk12	0.443	Atf7
Kcnc1	Snap25	0.443	Kcnc1
Pdzd2	Scn9a	0.443	Pdzd2
Pdzd2	Ptprd	0.443	Pdzd2
Rnf148	Rnf170	0.443	Rnf148
Rtkn2	Snx13	0.443	Rtkn2
Acsf3	Pex5l	0.442	Acsf3
Fgf2	Ntrk3	0.442	Fgf2
Mdm2	Rnf2	0.442	Mdm2
Rad51ap1	Tk1	0.442	Rad51ap1
Sncb	Th	0.442	Sncb
Aldob	Cyp2a12	0.441	Aldob
Bub1b	Rbl1	0.441	Bub1b
Cbfa2t3	Dennd4a	0.441	Cbfa2t3
Clu	Serpina5	0.441	Clu
Hspa12a	Polr1b	0.441	Hspa12a

Mlf1	Smpx	0.441	Mlf1
Scn9a	Trpv3	0.441	Scn9a
Spef2	Ttll3	0.441	Spef2
Spef2	Spock3	0.441	Spef2
Cntfr	Ntrk3	0.44	Cntfr
Cps1	Gnpda2	0.44	Cps1
ENSMUSG00000091089	Hspb3	0.44	ENSMUSG00000091089
Grik2	Ptprd	0.44	Grik2
Lmo3	Neurod6	0.44	Lmo3
Mmp9	Xdh	0.44	Mmp9
Nsf	Srrm2	0.44	Nsf
Prkcg	Tnik	0.44	Prkcg
Acsf3	Matn2	0.439	Acsf3
Akap9	Cdh1	0.439	Akap9
Astn2	Ctnnd2	0.439	Astn2
BC018507	Serpinb9f	0.439	BC018507
ENSMUSG00000091089	Perm1	0.439	ENSMUSG00000091089
Ggnbp1	Polr3e	0.439	Ggnbp1
Ntrk3	Th	0.439	Ntrk3
Asf1a	Pif1	0.438	Asf1a
Casp3	Clu	0.438	Casp3
Csmd2	Gadl1	0.438	Csmd2
Dmd	Mmp9	0.438	Dmd
Gabrb2	Grik2	0.438	Gabrb2
Ptgds	Serpinb9f	0.438	Ptgds
Rtn1	Tmem208	0.438	Rtn1
Abcb4	Zfp608	0.437	Abcb4
Adra2a	Th	0.437	Adra2a
Agrn	Fgf13	0.437	Agrn
Cd86	Mpeg1	0.437	Cd86
Fignl1	Tk1	0.437	Fignl1
Lcp1	Mmp9	0.437	Lcp1
Abca9	Abcc9	0.436	Abca9
Agbl2	Plcz1	0.436	Agbl2
Anxa7	Dtna	0.436	Anxa7
Aplf	Mdc1	0.436	Aplf
Chat	Fgf2	0.436	Chat
Phip	Zfp280d	0.436	Phip
Rad51ap1	Zfyve9	0.436	Rad51ap1
Rgs6	Rnf2	0.436	Rgs6
Sgk1	Tcf7	0.436	Sgk1

Adarb1	Hormad1	0.435	Adarb1
Btaf1	Chd7	0.435	Btaf1
Cep78	Cspp1	0.435	Cep78
Cspp1	Dennd4a	0.435	Cspp1
Dlgap1	Jph4	0.435	Dlgap1
Dsc3	Grhl1	0.435	Dsc3
Gnl1	Mr1	0.435	Gnl1
Jakmip1	Kirrel3	0.435	Jakmip1
Mpeg1	Ncf2	0.435	Mpeg1
BC055324	Bub1b	0.434	BC055324
Grhl1	Rnf2	0.434	Grhl1
Hdac9	Ube2d1	0.434	Hdac9
Mcoln2	Trpv3	0.434	Mcoln2
Pparg	Xdh	0.434	Pparg
Ppt1	Snap25	0.434	Ppt1
Aplf	Taf2	0.433	Aplf
Arl15	Zmiz1	0.433	Arl15
Casp3	Cul1	0.433	Casp3
Cd86	Mmp9	0.433	Cd86
Cyp2a12	Gc	0.433	Cyp2a12
Gimap6	Pdzd2	0.433	Gimap6
Hecw2	Kiaa1109	0.433	Hecw2
Atad2	Rfc4	0.432	Atad2
BC048546	Nlrp10	0.432	BC048546
Cln3	Mfsd11	0.432	Cln3
Dhfr	Pdf	0.432	Dhfr
Jph4	Lmo3	0.432	Jph4
Kcng4	Pex5l	0.432	Kcng4
Lpcat1	Taz	0.432	Lpcat1
Luc7l	Rrm1	0.432	Luc7l
Abcc9	Akap9	0.431	Abcc9
Asns	Gnpda2	0.431	Asns
Camta1	Prdm2	0.431	Camta1
Cdkl3	Slc25a36	0.431	Cdkl3
Il3	Ly6c1	0.431	Il3
Pdzd2	Scn3a	0.431	Pdzd2
Atp2b4	Sv2b	0.43	Atp2b4
Det1	Mplkip	0.43	Det1
Det1	Gm7102	0.43	Det1
Dhx34	Prpf31	0.43	Dhx34
Fgf2	Tcf4	0.43	Fgf2
Pparg	Syn2	0.43	Pparg
Raph1	Trim67	0.43	Raph1

Bub1b	Tube1	0.429	Bub1b
Gabrg2	Opcml	0.429	Gabrg2
Ispd	Pdf	0.429	Ispd
Prkg2	Rgs9	0.429	Prkg2
Tcf7	Tox	0.429	Tcf7
Casp3	Mmp16	0.428	Casp3
Cdc40	Taf2	0.428	Cdc40
Cep78	Unc13c	0.428	Cep78
Clec2i	Dhfr	0.428	Clec2i
Grhl1	Ripk4	0.428	Grhl1
Rad51	Rfwd3	0.428	Rad51
Ccdc171	Phactr1	0.427	Ccdc171
Dnajc16	Susd2	0.427	Dnajc16
Fgf2	Sulf1	0.427	Fgf2
Aanat	Cpm	0.426	Aanat
Aldob	Rtkn2	0.426	Aldob
Ano5	Faxc	0.426	Ano5
Astn2	Nkiras1	0.426	Astn2
Atf7	Tcf7	0.426	Atf7
Cdh1	Ctnnd2	0.426	Cdh1
Chat	Ntrk3	0.426	Chat
Scly	Tmc6	0.426	Scly
Tnpo3	Trim5	0.426	Tnpo3
Dll4	Prom1	0.425	Dll4
Fignl1	Rbl1	0.425	Fignl1
Frmd4b	Pdzd2	0.425	Frmd4b
Il3	Mcpt8	0.425	Il3
Kcng4	Lrrc6	0.425	Kcng4
Amot	Cdh1	0.424	Amot
Astn2	Prlr	0.424	Astn2
Camk1g	Unc13c	0.424	Camk1g
Casp3	Krt19	0.424	Casp3
Cul1	ENSMUSG00000091089	0.424	Cul1
Depdc1b	Rad51	0.424	Depdc1b
Dhfr	Rad51	0.424	Dhfr
Dnajc10	Nudt21	0.424	Dnajc10
Esyt3	Phf20l1	0.424	Esyt3
Gabra5	Grm2	0.424	Gabra5
Gramd2	Traf3ip3	0.424	Gramd2
Grik2	Mapk10	0.424	Grik2
L3mbtl3	Ring1	0.424	L3mbtl3
Sat2	Scly	0.424	Sat2

Sat2	St3gal4	0.424	Sat2
Casp3	Mmp17	0.423	Casp3
Depdc1b	Kif14	0.423	Depdc1b
Dnah14	Spag16	0.423	Dnah14
Dnah17	Spag16	0.423	Dnah17
Kcng4	Wdr18	0.423	Kcng4
Tom1	Txn2	0.423	Tom1
Acsm1	Aldob	0.422	Acsm1
Atad2	Rrm1	0.422	Atad2
Atp13a2	Syt12	0.422	Atp13a2
Cytip	Tcf4	0.422	Cytip
Dtna	Taz	0.422	Dtna
Fgf2	Krt19	0.422	Fgf2
Kri1	Scaf4	0.422	Kri1
Prm2	Tsn	0.422	Prm2
Rasgrf2	Ssbp2	0.422	Rasgrf2
Snx12	Tnpo3	0.422	Snx12
Afp	Dnmt3b	0.421	Afp
Afp	Crp	0.421	Afp
Dll4	Mmp9	0.421	Dll4
Hif1a	Lox	0.421	Hif1a
Mobp	Syt1	0.421	Mobp
Prkch	Txn2	0.421	Prkch
Raph1	Skap1	0.421	Raph1
Rnf2	Swt1	0.421	Rnf2
Specc1	Vps13d	0.421	Specc1
Asns	Fgd6	0.42	Asns
Crkl	Dock6	0.42	Crkl
Dusp15	Mapk10	0.42	Dusp15
Fgf2	Mapk10	0.42	Fgf2
Gemin6	Prpf31	0.42	Gemin6
Ispd	Tktl2	0.42	Ispd
Lox	Ptgds	0.42	Lox
Ly6c1	Mmp9	0.42	Ly6c1
Sacs	Trhr	0.42	Sacs
BC055324	Rad51	0.419	BC055324
Btaf1	Wdr18	0.419	Btaf1
Cbfa2t3	Zfp106	0.419	Cbfa2t3
Cdh1	Spint2	0.419	Cdh1
Cenpw	Rfc4	0.419	Cenpw
Chd7	Phactr4	0.419	Chd7
Cps1	Pon1	0.419	Cps1
Ctss	Pirb	0.419	Ctss

Fgf2	Gap43	0.419	Fgf2
Mpeg1	Pirb	0.419	Mpeg1
Nbeal1	Phip	0.419	Nbeal1
Nsf	Syt12	0.419	Nsf
Afp	Cps1	0.418	Afp
Akap9	Rfc4	0.418	Akap9
Arhgef1	Il3	0.418	Arhgef1
Arid5a	Tcp10b	0.418	Arid5a
Bcl2l11	Il3	0.418	Bcl2l11
Casp3	Taf2	0.418	Casp3
Depdc1b	Fignl1	0.418	Depdc1b
Frmd4b	Smim3	0.418	Frmd4b
Gabrg2	Snx12	0.418	Gabrg2
Itk	Snapc3	0.418	Itk
Kncn	Prom1	0.418	Kncn
Mdm2	Mmp9	0.418	Mdm2
Myog	Pparg	0.418	Myog
Nadsyn1	Syt12	0.418	Nadsyn1
Pdlim5	Prkch	0.418	Pdlim5
Polr3e	Rnf157	0.418	Polr3e
Prom1	Sox1	0.418	Prom1
Slc25a36	Utp6	0.418	Slc25a36
Aldob	Glyat	0.417	Aldob
Cd68	Dmd	0.417	Cd68
Chd7	Fbn2	0.417	Chd7
Cps1	Ica	0.417	Cps1
Crkl	Samsn1	0.417	Crkl
Ctc1	Pif1	0.417	Ctc1
Mmp9	Sacs	0.417	Mmp9
Oxt	Ptgds	0.417	Oxt
Polr1b	Prpf31	0.417	Polr1b
Acvr1b	Fgf2	0.416	Acvr1b
Asrgl1	Baz2b	0.416	Asrgl1
Cps1	Crp	0.416	Cps1
Gap43	Syn2	0.416	Gap43
Pif1	Plbd1	0.416	Pif1
Ankle1	Lmo7	0.415	Ankle1
Asf1a	Atad2	0.415	Asf1a
Cd68	Th	0.415	Cd68
Diap2	Stxbp5l	0.415	Diap2
Hormad1	Mdc1	0.415	Hormad1
Polr1b	Rad51	0.415	Polr1b
Adra1d	Th	0.414	Adra1d

Apc	Reep5	0.414	Apc
Arhgef1	Rgs6	0.414	Arhgef1
Asf1a	Msh3	0.414	Asf1a
Cdh18	Zfp37	0.414	Cdh18
Cops4	Ube2l3	0.414	Cops4
Cped1	Rspo3	0.414	Cped1
Cul1	Wdr64	0.414	Cul1
Dlgap1	Lrfn1	0.414	Dlgap1
Nav2	Syt1	0.414	Nav2
Nrip1	Taf2	0.414	Nrip1
Ntrk3	Ptprd	0.414	Ntrk3
Pdzd2	Ripk4	0.414	Pdzd2
Prdm11	Setd6	0.414	Prdm11
Cenpw	Cped1	0.413	Cenpw
Csmd2	Tnik	0.413	Csmd2
ENSMUSG00000029559	Tmem130	0.413	ENSMUSG00000029559
Etaa1	Pidd1	0.413	Etaa1
G3bp1	Rrm1	0.413	G3bp1
Btk	Pirb	0.412	Btk
Bub1b	Mdm2	0.412	Bub1b
Cul1	Usp11	0.412	Cul1
Hsf3	Hspa12a	0.412	Hsf3
Phip	Taf2	0.412	Phip
Plcl2	Zfp608	0.412	Plcl2
Agbl2	Crp	0.411	Agbl2
Apc	Crkl	0.411	Apc
Ctnnd2	Fer	0.411	Ctnnd2
Dnm3	Nsf	0.411	Dnm3
Fgf2	Fignl1	0.411	Fgf2
Grhl1	Ring1	0.411	Grhl1
Irak2	Traf1	0.411	Irak2
Arl15	Cobll1	0.41	Arl15
Atad2	Kif14	0.41	Atad2
Crkl	Rasgrp1	0.41	Crkl
Dpy19l3	Rtkn2	0.41	Dpy19l3
Fgf13	Prom1	0.41	Fgf13
Gas2l1	Tnik	0.41	Gas2l1
Setd6	Setdb2	0.41	Setd6
Wdr18	Ybx1	0.41	Wdr18
Cdk14	Rbl1	0.409	Cdk14
Ddx39b	Snrnp40	0.409	Ddx39b
Dnal1	Spag16	0.409	Dnal1

Hdac9	Sirt5	0.409	Hdac9
Myot	Tnpo3	0.409	Myot
Rnf165	Srp54b	0.409	Rnf165
Rrm1	Uty	0.409	Rrm1
Bcl2l11	Prune2	0.408	Bcl2l11
Casp3	Fgf13	0.408	Casp3
Cd80	Mmp9	0.408	Cd80
Clrn1	Rpgr	0.408	Clrn1
Cntn4	Macrod2	0.408	Cntn4
Fgf6	Mmp9	0.408	Fgf6
Galnt10	Mthfr	0.408	Galnt10
Got1l1	Rtn2	0.408	Got1l1
Grk6	Trhr	0.408	Grk6
Hcrtr2	Rpgr	0.408	Hcrtr2
Klf9	Trp53i11	0.408	Klf9
Rad51	Tsn	0.408	Rad51
Agrn	Large	0.407	Agrn
Asf1a	Cdh1	0.407	Asf1a
BC018507	Mdc1	0.407	BC018507
Gemin6	Rfc4	0.407	Gemin6
Ispd	Snx13	0.407	Ispd
Itga4	Prom1	0.407	Itga4
Lox	Ripk4	0.407	Lox
Slc25a36	Yme1l1	0.407	Slc25a36
Actbl2	Lcp1	0.406	Actbl2
Asns	BC018507	0.406	Asns
Baz2b	Tcf4	0.406	Baz2b
Dnajc16	Sacs	0.406	Dnajc16
Dnajc16	Hspa12a	0.406	Dnajc16
Dnm3	Snap25	0.406	Dnm3
Dtna	Kif1b	0.406	Dtna
Il3	Prom1	0.406	Il3
Slc36a1	Slc39a2	0.406	Slc36a1
Acsf3	ENSMUSG00000024209	0.405	Acsf3
Cyp2a12	Pon1	0.405	Cyp2a12
Gnl1	Specc1	0.405	Gnl1
Mat2b	Mthfr	0.405	Mat2b
Pdlim5	Prkcb	0.405	Pdlim5
Rab29	Syt11	0.405	Rab29
Acsm1	Cps1	0.404	Acsm1
Btaf1	Yme1l1	0.404	Btaf1
Cd80	Lcp1	0.404	Cd80

Cd86	Crp	0.404	Cd86
Cdh6	Ctnnd2	0.404	Cdh6
Invs	Sstr3	0.404	Invs
Adra2a	Ptafr	0.403	Adra2a
Birc3	Sdcbp	0.403	Birc3
Camk4	Syn2	0.403	Camk4
Clu	Myot	0.403	Clu
Ctnnd2	Gabrg2	0.403	Ctnnd2
Cyp2a12	Ica	0.403	Cyp2a12
Edrf1	Hdac9	0.403	Edrf1
Gpr27	Gpr35	0.403	Gpr27
Inpp4b	Sh2d5	0.403	Inpp4b
Mpdz	Wwc1	0.403	Mpdz
Pex5l	Srp54b	0.403	Pex5l
Aanat	Luc7l	0.402	Aanat
Cenpw	Rad51	0.402	Cenpw
Cngb3	Lrrc6	0.402	Cngb3
Dnajc10	Sacs	0.402	Dnajc10
Fgf2	Pparg	0.402	Fgf2
Gnpat	Taz	0.402	Gnpat
Lrrc6	Pde6b	0.402	Lrrc6
Phc2	Prdm2	0.402	Phc2
Sec22a	Yme1l1	0.402	Sec22a
Sncb	Zmiz1	0.402	Sncb
Aars	Yme1l1	0.401	Aars
Ak4	Dock6	0.401	Ak4
Bcl2l11	Hspb3	0.401	Bcl2l11
Cd80	Crp	0.401	Cd80
Cd81	Rasgrp1	0.401	Cd81
Dlgap1	Fam172a	0.401	Dlgap1
Gnl1	Prpf31	0.401	Gnl1
Mdm2	Wwox	0.401	Mdm2
Acsm1	Pon1	0.4	Acsm1
Adra1d	Akap9	0.4	Adra1d
BC018507	Snrnp40	0.4	BC018507
Car8	Tox	0.4	Car8
Crp	Cyp2a12	0.4	Crp
Dcbld2	Nudt21	0.4	Dcbld2
ENSMUSG00000027811	Rad51ap1	0.4	ENSMUSG00000027811
Glyat	Serpina1a	0.4	Glyat

Table S3 Hub genes and their functions

Table S3 Hub genes and their functions			
No	**Gene Symbol**	**Full name**	**Gene function**
1	Hecw2	HECT, C2 and WW domain containing E3 ubiquitin protein ligase 2	Hecw2 contributes to ubiquitin protein ligase activity.
2	Asb14	ankyrin repeat and SOCS box-containing 14	Asb14 mediates the ubiquitination and subsequent proteasomal degradation of target proteins.
3	Lmo7	LIM domain only 7	Lmo7 contributes to ubiquitin-protein transferase activity.
4	Fbxo17	F-box protein 17	Fbxo17 contributes to ubiquitin protein ligase activity.
5	Det1	de-etiolated homolog 1	Det1 contributes to ubiquitin protein ligase binding.
6	Ube2d1	ubiquitin-conjugating enzyme E2D 1	Ube2d1 functions in the ubiquitination of the tumor-suppressor protein p53
7	Znrf2	zinc and ring finger 2	Znrf2 contributes to ubiquitin protein ligase activity.
8	Fbxo44	F-box protein 44	Fbxo44 contributes to ubiquitin protein ligase activity.
9	Cul1	cullin 1	Cullin 1 contributes to ubiquitin-protein transferase activity.

Table S4 Major hubs in the network

Degree means number of node connections (edges).

The betweenness of a node reflects the amount of control that this node exerts over the interactions of other nodes in the network.

Closeness is a measure of how fast information spreads from a given node to other reachable nodes in the network.

Table S4 Major hubs in the network			
Major hubs	**Degree**	**Betweenness**	**Closeness**
Hecw2	8	0	0.270018622
Asb14	9	1.11E-04	0.27027027
Lmo7	9	1.11E-04	0.27027027
Fbxo17	9	1.11E-04	0.27027027
Det1	11	0.006252114	0.27938343
Ube2d1	25	0.07613847	0.326576577
Znrf2	8	0	0.270018622
Fbxo44	9	1.11E-04	0.27027027
Cul1	15	0.043067603	0.333333333